# Genetic, cellular and transcriptomic studies of chloroplast development, protein import and inter-organellar communication in Arabidopsis and wheat

**Naresh Loudya**

Thesis submitted for the degree of Doctor of Philosophy

**Royal Holloway, University of London**

November 2018

# Declaration of authorship

I hereby declare that the work presented in this thesis is the original work of the author unless otherwise stated. Original material used in the creation of this thesis has not been previously submitted either in part or whole for a degree of any description from any institution.

_____

**Naresh Loudya**

26.11.2018

# Abstract

The chloroplast, with a small genome, can encode only 2% of its total proteins, while the majority are encoded by the nucleus. The import of thousands of cytosolic proteins is mediated by TOC and TIC (Translocon at the Outer membrane/Translocon at the Inner membrane of Chloroplast) complexes. It has been proposed that a TIC 1MDa complex includes proteins encoded by the nucleus (TIC100, TIC56, and TIC20) and the chloroplast (TIC214). Arabidopsis *cue8* (carrying a mutation in *TIC100*) was originally identified as a virescent mutant, defective in chloroplast development. The current study has revealed activation of a compensatory mechanism by the partial loss of function in *cue8*, to support chloroplast gene expression. This homeostasis mechanism includes elevation of expression of nucleus-encoded plastid RNA polymerase (NEP) genes, maintenance of chloroplast DNA replication in spite of the defect, and modulation of expression of sigma factors. The finding provides an explanation for delayed chloroplast differentiation (virescence) and highlights importance of chloroplast-to-nucleus communication, revealing the fitness advantage it confers. The phenotypic difference in *cue8* plants can be explained by reduction of GLK transcription factors. However, simple overexpression of *GLK1*, *GLK2,* or *FC1*, the known source of a positive chloroplast-to-nucleus signal, fails to rescue the *cue8* defect. A forward genetic screen for suppressors of *cue8* resulted in identification of an intragenic suppressor that demonstrates the role of *TIC100* in translocation of cytosolic proteins across the chloroplast inner membrane, and necessity of the 1MDa TIC complex in the import of both photosynthetic and housekeeping proteins.

A developing wheat leaf (with its white base and its green tip) is a model system to observe and quantify the extent of plastid development in the cells, its individual processes, and the associated gene expression program. A thorough analysis of the greening wheat leaf, through quantitative microscopy and high-throughput gene expression data, has contributed to understanding the sequence of processes occurring during chloroplast biogenesis, including growth, division, chloroplast DNA replication, gene expression, protein import, and greening. The current study distinguishes various phases of chloroplast development and explains how defects in plastid protein import affect a specific phase. The unique combination of investigations in Arabidopsis and wheat has contributed to an overall understanding of plastid biogenesis and extends the scope of search for novel candidate regulators of chloroplast development.

# Acknowledgements

First of all, my heartiest thanks go to my beloved Mom and Dad for having such a pure heart, for your dedication, patience and for always encouraging me on the right path. You are the best, and our conversations double my hope and my positive attitude. I would like to give my most special thanks to Priyanka, for making this journey a joyful and productive one. You are the one who really believed in me and fully encouraged me to give my best, from the first day of my PhD to writing the thesis. I am very grateful to our amazing Mamma, Papa and Jyoti for their love and constant encouragement which made this journey so smooth. You have all made a huge contribution to this achievement.

But, of course, I couldn't be more grateful to my supervisor Dr. Enrique Lopez-Juez, for being such a wonderful person, for your knowledge and passion for science. Thank you very much for your patience and for encouraging me throughout the last four years. I have enjoyed every discussion and am immensely glad to have learned as wonderful ideas took shape. I am very lucky to be your student. My interest in chloroplast biology was initiated by the research of Prof. Paul Jarvis. It is amazing to see your pragmatism, Prof. Jarvis. Thank you very much for introducing me to the beauty of chloroplasts. There is so much to learn from you both, and I feel privileged to be under your expert guidance. You both will always be my SUPER supervisors. I cannot imagine having anything more than what I have gained over time during my PhD. This has been a very satisfying learning experience.

A big thank you to two wonderful people, Profs. Laszlo Bogre and Alessandra Devoto, for the encouragement and happiness you spread around. To Csaba Papdi and Imma Perez Salamo for all your patient help, for sharing your practical experience and for your humour. It is an amazing experience to have met you both during my PhD. To Zaki Ahmad for being such a good friend, for all those interesting discussions and our collaborative work. To Jia He for helping me in the lab and to Sara Farahi Bilooei, and to Stacey Vincent for the lab fun and showing me the R codes.

I am very thankful to most influential people, Dr. Blessymole K. Alex, Dr. Eapen P Koshy, and Prof. George Thomas for inspiring me, always being there and encouraging me to pursue my passion for research. My beloved brothers Dr. Dheeraj Naik and Surya Banoth for all the positive ambiances. You are very important people of my life.

I thank the Ministry of Tribal Affairs, Government of India, for the award of the National Overseas Scholarship, and Royal Holloway University of London for supporting my research.

I thank all those failed experiments for teaching me to develop reason, build patience and try again.

**I dedicate this thesis to my beloved parents**

# Table of contents

# List of Figures

# List of Tables

# Abbreviations

| | |
|---|---|
| ADH | Alcohol dehydrogenase |
| At | *Arabidopsis thaliana* |
| bp | Base pair |
| CIB | Chloroplast isolation buffer |
| cpDNA | Chloroplast DNA |
| *cue8* | *CAB underexpressed* |
| DAPI | 4',6-diamidino-2-phenylindole |
| DMF | Dimethylformamide |
| DNA | Double-stranded deoxyribonucleic acid |
| DTT | Dithiothreitol |
| *E. coli* | *Escherichia coli* |
| EDTA | Ethylenediaminetetraacetic acid |
| EMS | Ethyl methanesulfonate |
| EtBr | Ethidium bromide |
| g | Gram |
| *g* | Standard gravity |
| h | Hour |
| $dH_2O$ | Distilled water |
| HEPES | 4-(2-hydroxyethyl)-1-piperazineethanesulfonic acid |
| HMS | Hepes-mes-sorbitol buffer |
| kbp | Kilo base pair |
| l | Litre |
| LB | Luria-bertani |
| LIN | Lincomycin |
| M | Molarity |
| M Da | Mega dalton |
| min | Minute |
| ml | Millilitre |
| mm | Millimetre |
| MS | Murashige-Skoog |
| NEP | Nucleus-encoded RNA polymerase |
| $^oC$ | Degrees centigrade |

| | |
|---|---|
| OD | Optical density |
| PCR | Polymerase chain reaction |
| PEP | Plastid-encoded RNA polymerase |
| qPCR | Real-time polymerase chain reaction |
| qPCR | Quantitative polymerase chain reaction |
| RNA | Ribonucleic acid |
| SDS | Sodium dodecyl sulfate |
| SEM | Standard error mean |
| TAIR | The arabidopsis information resource |
| TBE | Tris borate EDTA |
| TBS(-Tween) | Tris-buffered saline (with tween-20) |
| TEMED | Tetramethyl ethylenediamine |
| TGS | Tris-glycine-SDS buffer |
| TIC | Translocon at the inner envelope membrane of chloroplasts |
| TOC | Translocon at the outer envelope membrane of chloroplasts |
| Tris | Tris (hydroxymethyl) aminomethane |
| UV | Ultraviolet |
| V | Volt |
| WT | Wild-type |
| β-ME | B- mercaptoethanol |
| µg | Microgram |
| *HO1* | *Heme oxygenase 1* |
| *CHS* | *Chalcone synthase* |
| *KO1* | *Kaurene oxidase 1* |
| *KS* | *Kaurene synthase* |

# Chapter 1

# Introduction

## 1.1 Biogenesis of chloroplasts and other plastids

The chloroplast is a plant cell organelle that converts solar energy into food through the process of photosynthesis and supports life on earth. It is one of the major forms of plastids that are distributed in various tissues to perform a variety of functions in plants (Fig. 1.1). Apart from photosynthesis, the function of plastids includes the synthesis of amino acids, fatty acids, purine and pyrimidine bases, terpenoids, various pigments, hormones, and the performance of key aspects of nitrogen and sulphur assimilation (Neuhaus and Emes, 2000; Lopez-Juez and Pyke, 2005) and plant immune responses (Nomura et al., 2012). Unlike other organelles, plastids have a unique ability to interconvert into other plastid forms in response to developmental and environmental signals. The interconversion of plastids is connected to reorganisation of nucleus-encoded proteins and, as will be discussed later, of the translocon complexes in the membrane (Ling et al., 2012). Chloroplasts contain green pigment and are developed from undifferentiated meristematic proplastids which are also found in reproductive organs (Jarvis and Lopez-Juez, 2013). These proplastids develop into specialized chloroplasts during the process of cellular differentiation (Waters et al., 2009; Chotewutmontri P, 2016).

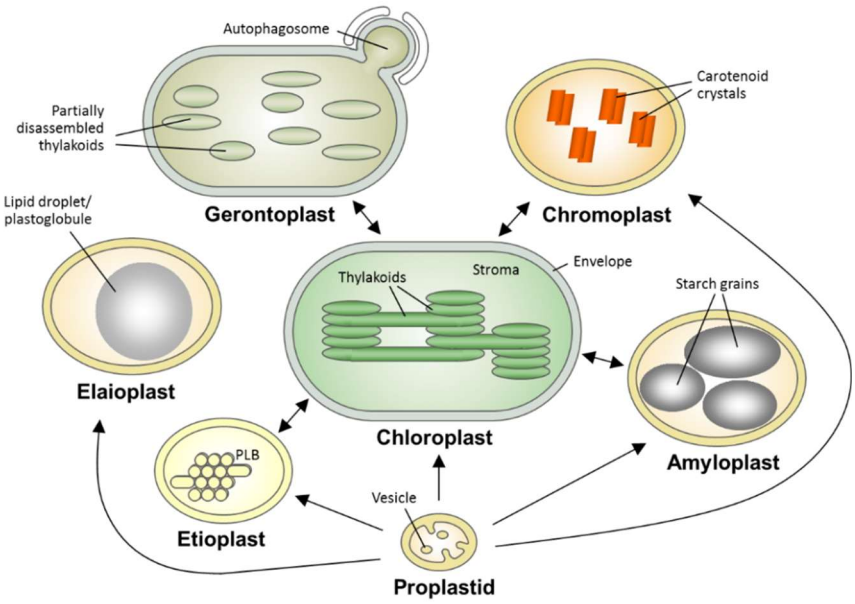


**Figure 1.1** Development of plastids from a proplastid. Plants harbour different types of plastids based on their cellular function. A plastid can interconvert into other forms depending on the developmental signals. The green tissues in plants are filled with chloroplasts which perform photosynthesis. The chloroplasts in the fruits and flower buds turn into chromoplasts, which contain carotenoid pigments, as they ripe or mature. Etioplasts are developed when plants are grown under the absence of light. Non-photosynthetic parts of the plant, like starch-storing organs, contain amyloplasts. Elaioplasts are responsible for storing lipids, while gerontoplasts are formed during the process of senescence (courtesy of Jarvis and Lopez-Juez, 2013).

A proplastid may, if in darkness, transform into an intermediate plastid known as etioplast that possesses a prolamellar body (PLB), constituting a lattice-like membrane structure (Fig. 1.1). Upon light exposure the etioplast converts into a chloroplast (Pogson et al., 2015). The non-photosynthetic plant tissues, like roots and petals, develop leucoplasts while colourful plant parts like flowers and fruits contain chromoplasts, which are enriched with carotenoid pigments (Mullet, 1988; Egea et al., 2010). The tissues of oilseeds develop elaioplast which store lipid generally as plastoglobules (Lopez-Juez and Pyke, 2005).

## 1.2 Endosymbiosis

According to the endosymbiosis theory, a free-living cyanobacterial ancestor gave rise to the present-day chloroplast (Martin et al., 2002). Over time most of the cyanobacterial genes have been transferred to the host nucleus, but many of their polypeptides still appear to function in the plastids. This is not always the case, as many genes of cyanobacterial origin and transferred to the nucleus have acquired new cellular roles. The remaining plastid genome in the organelle encodes about 80 proteins, in land plants, that are necessary for plastid development, the majority of them for photosynthetic function. A typical chloroplast is predicted to contain over 3000 proteins. Therefore, most of the plastid proteins are nucleus-encoded and must be imported from the cytoplasm as part of chloroplast biogenesis (Kessler and Schnell, 2009). The transfer of the early plastid genome to the host nucleus and partition of genetic machinery in a way that plastids still depend on the nucleus brings about a necessity of coordination between the organelle and the nucleus (Sakamoto et al., 2008). The import of nucleus-encoded proteins, maintenance and expression of the plastid genetic machinery and communicating the status to the nucleus must be coordinated to ensure appropriate plastid biogenesis (Inaba and Ito-Inaba, 2010).

## 1.3 Plastid molecular genetics

### 1.3.1 Genetic machinery

The chloroplast genome of land plants exists as a multi-copy DNA known as a ‘Nucleoid’ or ‘Plastome’ which has a single-copy size of ~120-160 kb (Sakamoto et al., 2008). As part of the development processes, the number of plastid DNA copies increases from about 10 in the proplastid (meristematic) to about 50 in a mature chloroplast (Jarvis and Lopez-Juez, 2013). The process of cpDNA replication is governed by two nucleus-encoded organellar DNA

polymerases, POLIA and POL1B, that are dual-targeted to chloroplasts and mitochondria. (Parent et al., 2011; Cupp JD, 2013); however not much is known about the regulation of DNA synthesis. The linear or branched plastid DNA (Bendich, 2013) is probably attached to either the inner membrane or the thylakoids (Sakamoto et al. 2008) with the help of a PEND protein (Sato et al., 1999). There are conflicting observations about the cpDNA degradation during the process of senescence (Golczyk et al., 2014; Kumar et al., 2014). A proper experimental model and techniques are required to address the issue of cpDNA degradation during the process of ageing.

### 1.3.2 Gene expression

The plastid genome is largely organized in operons, and encodes in Arabidopsis 54 proteins for photosynthesis, 31 proteins necessary for its gene expression and 45 transfer RNA as well as ribosomal RNA (Lopez-Juez and Pyke, 2005). There are two types of RNA polymerases responsible for the process of transcription in plastids, shown in figure 1.2 (Shiina et al., 2005). The two RNA polymerases are named according to the site of their synthesis: a nucleus-encoded polymerase (NEP), a single subunit prokaryotic phage-type enzyme, which is similar to that operating in mitochondria and is imported into plastids from the cytoplasm, and a plastid-encoded polymerase (PEP) which is a multi-subunit eubacterial type (Allison, 1996; Hricová et al., 2006). According to the functional destination there are three categories of NEP polymerases in eudicot flowering plants (like Arabidopsis), the RPOTp is targeted to plastids, the RPOTm functions in mitochondria and the RPOTmp is dual targeted to mitochondria and plastids (Baba K, 2004). The NEP is mostly responsible for housekeeping functions of plastids; thus, its expression occurs very early in plastid development (Zhelyazkova et al., 2012). After its import into chloroplasts, the NEP polymerase transcribes, among others, PEP subunit genes (*rpoA, rpoB, rpoC1* and *rpoC2*). Similar to bacterial gene expression, the multi-subunit polymerase requires the assistance of cofactors called sigma factors, which, in contrast with to rest of polymerase subunits, are encoded by the nucleus. There are 6 sigma factors (SIG1-SIG6) that function in the chloroplasts of land plants (Fujiwara et al., 2000). The PEP polymerase transcribes most of the photosynthesis related genes (Hajdukiewicz et al., 1997). In addition, there are several pTAC (transcriptionally active chromosome) proteins that are translocated from the cytoplasm and are involved in plastid gene expression (Pfalz et al., 2006; Börner T, 2015). Therefore, one could conclude that the entire plastid gene expression machinery is ultimately under the

control of the nucleus (López-Juez et al., 2007). The processes of chloroplast protein import, gene expression, chloroplast division and photosynthesis involve protein complexes formed from the products of the nucleus and the chloroplast. A stringent coordination between the nucleus and the chloroplast is maintained to ensure plant growth and development.

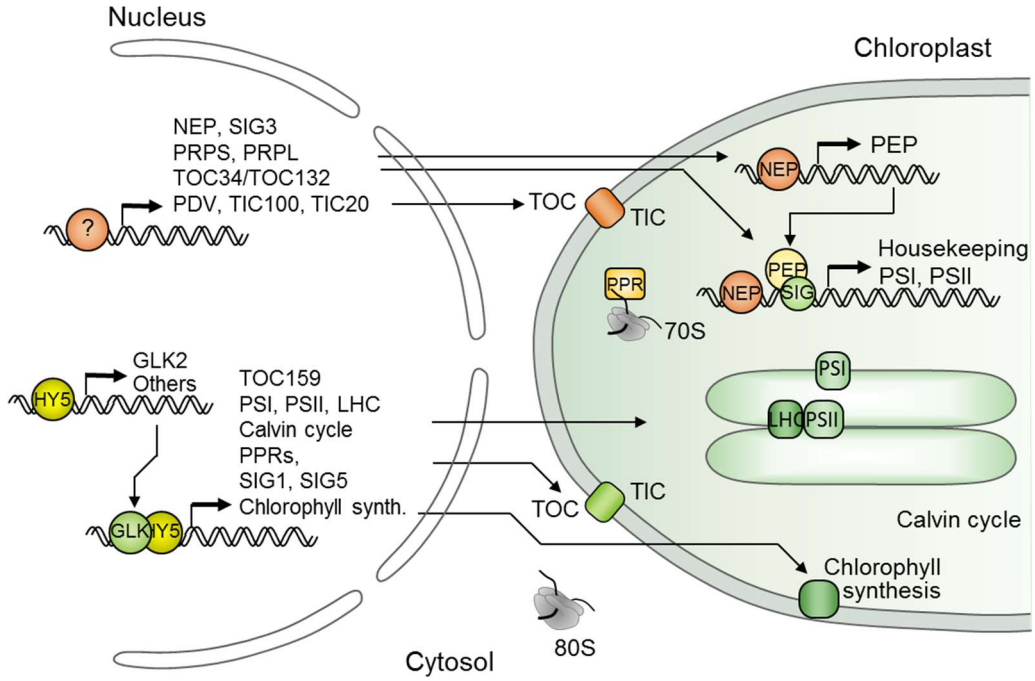


**Figure 1.2** Chloroplast gene expression and nucleus control. The chloroplast has two RNA polymerases based on the location of their synthesis: nucleus-encoded polymerase (NEP) and plastid-encoded polymerase (PEP). The NEP is imported from the cytoplasm through the chloroplast membrane and it recognises the promoters of PEP subunits. The holoenzyme of PEP is formed with the binding of nucleus-encoded sigma factors. Most of the chloroplast genes responsible for plastid division, protein import, gene expression, thylakoid development and photosynthesis are encoded by the nucleus (adapted from Jarvis and Lopez-Juez, 2013).

## 1.4 Plastid division

As an endosymbiont, the chloroplast undergoes division by binary fission. An undifferentiated meristem cell contains only about 10 proplastids, however a mature leaf cell can accommodate 20-100 chloroplasts (Mullet, 1988; Lopez-Juez and Pyke, 2005). Plastid division occurs in parallel to their gene expression and protein import. The number and size of chloroplasts tend to behave according to division and growth of their cells (Boffey SA, 1979). Research on the chloroplast division mechanism has identified different mutants, including 12 *ACCUMULATION AND REPLICATION OF CHLOROPLASTS* (*ARC*) mutants (Pyke and Leech, 1991; Pyke and Leech, 1992, 1994) and two *PLASTID DIVISION* (PD) mutants (Miyagishima et al., 2006). Cells of *arc* mutants show abnormal chloroplasts

throughout plant development, for example a mesophyll cell in *arc6* contains only two chloroplasts, while *arc5* has about 13 chloroplasts per cell, compared to the wild type containing over 50 (Pyke and Leech, 1994; Pyke et al., 1994). Active components of the division machinery are encoded by the nucleus, as well as some in single-cell algae being encoded by the chloroplast itself, hence they function accordingly towards the cytoplasm and plastid stroma (Yoshida et al., 2012). The division apparatus forms a construction of different plastid division (PD) rings. A Z-ring is formed inside the chloroplast membrane with two homologous proteins, FtsZ1 & FtsZ2, tubulin-like GTPases with distinct functions, as shown in figure 1.3 (Miyagishima et al., 2011; Osteryoung and Pyke, 2014). The min system, consisting of ARC3, MCD1, MinD, and MinE, positions this ring by binding at other membrane sites internally and excluding the ring from those sites. An inner PD ring of unknown components is formed between the inner chloroplast membrane and the Z-ring (Chen C, 2018). ARC6 and PARC6 are inner membrane-spanning proteins while PDV1 and PDV2 span the outer membrane of plastids. ARC6 binds to FtsZ2 and stabilises the Z ring (Johnson et al., 2013). Similarly, PARC6 also interacts with FtsZ2 of the Z-ring. On the other hand, PDV1 and PDV2 span the outer membrane and bind to the inter-membrane space c-terminal regions of PARC6 and ARC6 respectively (Glynn et al., 2008; Zhang et al., 2016). Overexpression of PDV proteins results in increased number of smaller chloroplasts (Miyagishima et al., 2006; Okazaki et al., 2009), an observation which is unique among all chloroplast division proteins. The outer PD ring in the red alga *Cyanidioschyzon merolae* is formed with polyglucan filaments (Kuroiwa et al., 2008; Yoshida et al., 2012). It is not known whether these components are conserved in higher plants. Both PDVs recruit discontinuous ARC5, a dynamin related protein 5B (DRP5B) towards the cytosolic region (Miyagishima et al., 2006). It was hypothesized that polyglucan sliding initiates a constriction from outside, which leads to the division of plastids (Yoshida et al., 2012). However, due to lack of information on how conserved outer PD components are, the mechanism of division remains unclear. Interestingly, loss of function of *CRUMPLED LEAF1* (*CRL*), a chloroplast outer membrane protein, results in plastid division defects showing larger plastids and perturbed cell division (Asano T, 2004), while CLUMPED CHLOROPLAST1 (CLMP1) is required for separation and distribution of plastids (Yang et al., 2011). Importantly, overexpression of *GROWTH REGULATING FACTOR5* (*GRF5*) increases chloroplast division and cell division (Vercruyssen et al., 2015). Some of the other proteins targeted to the inner chloroplast membrane are FZL (FZO-Like), similar to mitochondrial FZO protein (Gao et al., 2006) and GIANT CHLOROPLAST 1 (GC1) (Maple

et al., 2004). Defects in *FZL* and *GC1* show impaired chloroplast division and growth. It was identified that *fzl* exhibited a hypersensitive response, which might be due to the production of reactive oxygen species form damaged chloroplast membrane (Landoni et al., 2013). Over-expression of a CYTOKININ-RESONSIVE TRANSCRIPTION FACTOR2 or supplementation of cytokinin had similar chloroplast effects as in PDV1ox and PDV2ox (Okazaki et al., 2009). Many genes were identified to participate in chloroplast division, but how their interaction is achieved, the connection between cell division and chloroplast division and regulatory aspects of the mechanism remain poorly understood.

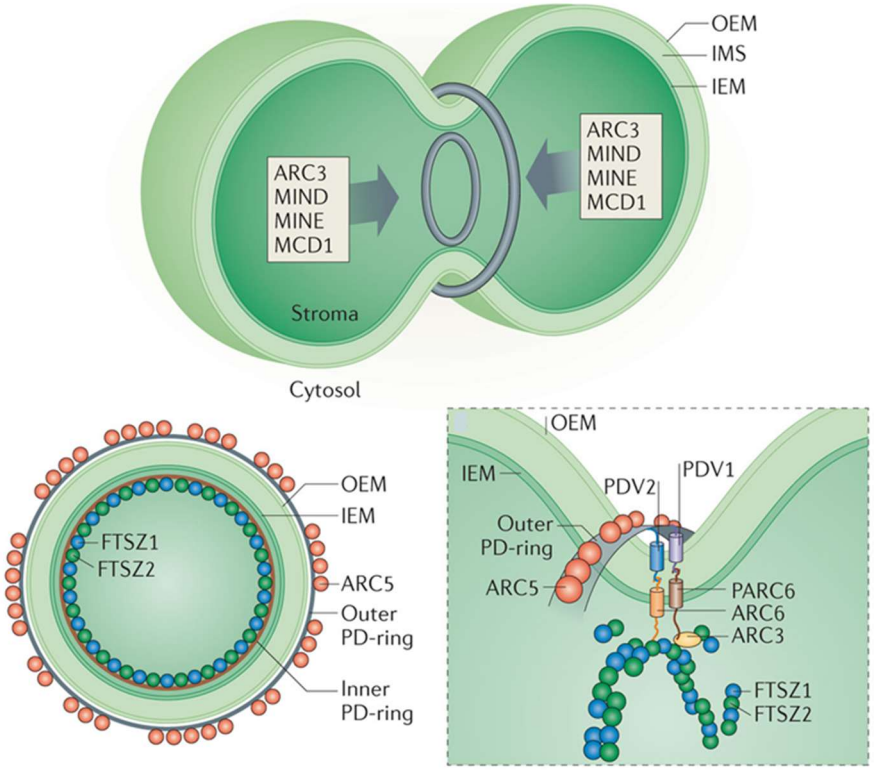


**Figure 1.3** Mechanism of the chloroplast division. Formation of outer and inner PD rings across the chloroplast membranes. FtsZ1 and FtsZ2 form a Z-ring towards the stroma of the dividing plastid which is stabilised by ARC3, MIND, MINE and AMCD1 binding at sites other than the division site. The outer membrane spanning proteins PDV1 and PDV2 interact with PARC6 and ARC6 which binds to the Z-ring. ARC5 is recruited on the outer PD ring (courtesy of Jarvis and Lopez-Juez, 2013).

## 1.5 Plastid protein import

The majority of the proteins responsible for development and function of the chloroplast are translated on 80S cytoplasmic ribosomes. The targeting of cytoplasmic proteins to chloroplasts is possible by a signal at their N-terminus end, called transit peptide (Flores-Pérez and Jarvis, 2013; Lee et al., 2013) that varies greatly in size (~20 to 100 amino acids)

and sequence (Bruce, 2001; Li and Teng, 2013). Most of the cytosolic precursor proteins are translocated through multi protein complexes of plastids embedded in the outer (TOC: Translocon at the Outer envelope membrane of Chloroplasts) and inner membranes (TIC: Translocon at the Inner envelope membrane of Chloroplasts). Mutations in the subunits of TOC/TIC machinery lead to plastid defects and affect plant development (Soll and Schleiff, 2004; Bedard, 2005). Upon successful import of pre-protein into the stroma, the directing transit peptide is cleaved by a stromal processing peptidase and rest of the polypeptide attains a functional conformation or is further directed for import into the thylakoid lumen with a second transit peptide (Keegstra and Cline, 1999; Jarvis and Robinson, 2004).

Arabidopsis research on chloroplast membrane receptors revealed the presence of two distinct routes of preprotein import: one containing the GTPase receptors atTOC159 and atTOC33 while the other is formed of atTOC132/120 and atTOC34 proteins. A common channel of the two routes is atTOC75 (Bauer, 2000). Plastid protein import mutant, *ppi1* (*toc33*) is defective primarily in importing the photosynthetic precursor proteins (Jarvis et al., 1998; Kubis et al., 2003; Gutensohn et al., 2004). On the other hand, a double mutant, *toc132 toc120/+* (heterozygous), is impaired in importing primarily housekeeping proteins. The single mutant *toc132* has no visible phenotype and the double homozygous shows severe defects (Kubis et al., 2004; Kessler and Schnell, 2009). Hence the studies on outer membrane complexes suggest there are separate entry routes for photosynthetic and housekeeping plastid preproteins (Ling and Jarvis, 2015). (Ling et al., 2012) identified SUPRESSOR OF PPI1 (SP1) the first E3 ligase known to be involved in chloroplast biogenesis, which targets chloroplast TOC proteins for degradation. It seems SP1 mediates the reorganisation of TOC complexes depending on developmental signals. For example, interconversion of an etioplast to chloroplast requires the role of SP1.

The inner membrane of the chloroplast also has translocon complexes, TIC110 is highly abundant and considered as a marker protein in the membrane. This was revealed to be a central player of import acting as a channel (Waegemann et al., 1992; Heins et al., 2002; Inaba et al., 2003; Balsera M, 2009). In addition, other proteins like TIC20 and TIC22 were identified as components at the inner membrane. TIC20 was reported as another translocon, as a core TIC protein of the inner membrane, while TIC22 is an inter-membrane space protein (Kouranov et al., 1998). Further, TIC21 (PIC1) was also identified as another potential TIC channel (Teng et al., 2006). Research conducted by Kikuchi et al. (2013) identified a 1MDa Tic complex, with TIC20 as part of it and a main channel. This complex

consists of other nucleus-encoded proteins namely TIC100, TIC56 and a plastid encoded TIC214 protein (Fig. 1.4). Interestingly, except for TIC20, the associates of this complex are absent from grasses, therefore doubts were raised against the existence of the 1MDa complex (Paila et al., 2015; Bolter, 2016). Another recent study showed formation of a super complex involving both TOC and TIC proteins. This complex contained proteins of TOC75, TOC159, TOC34, TIC20, TIC56 and TIC110 (Chen and Li, 2017). The presence of multiple translocon channels in the inner membrane whose loss of function results in severe phenotypes, are aspects of the TIC complex which are intensely debated; also, how preproteins are sorted at the chloroplast inner membrane remains as a subject of controversy.

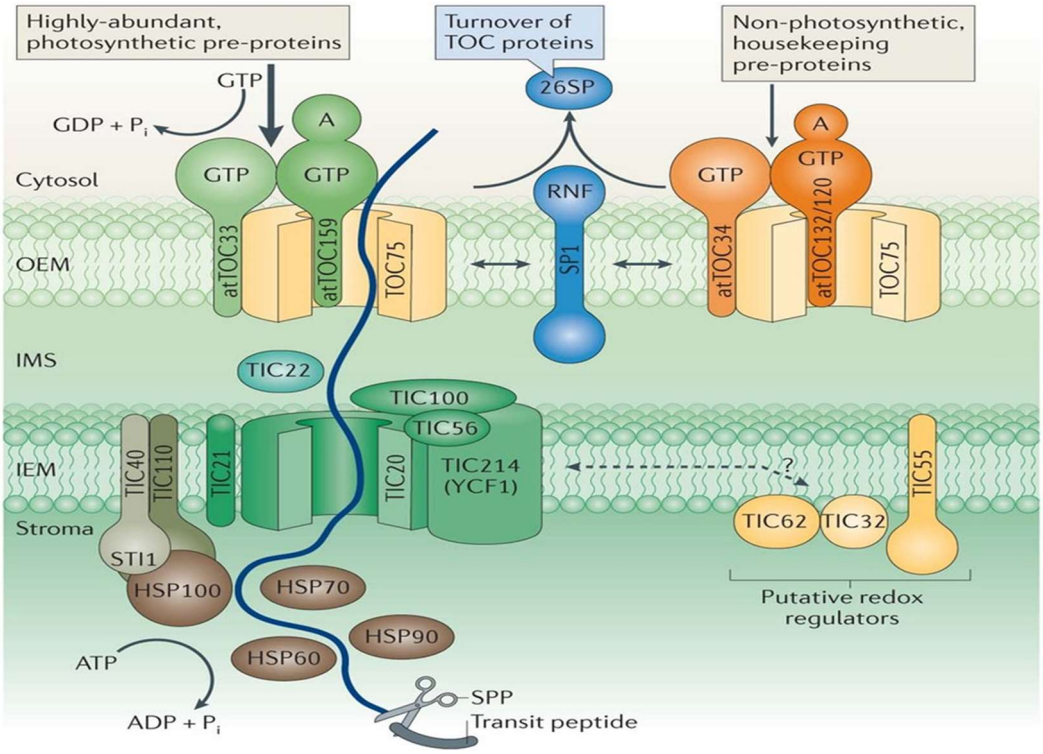


**Figure 1.4** Import of cytosolic preproteins through the chloroplast membrane. The chloroplast outer envelope membrane (OEM) and inner envelope membrane (IEM) contain TOC (translocon at the outer envelope membrane of chloroplasts) and TIC (translocon at the inner envelope membrane of chloroplasts) that facilitate the import of nucleus-encoded proteins. There are specific receptor routes with TOC75 as a translocon channel for the import of photosynthetic (TOC34 and TOC159) and housekeeping (TOC34, TOC132, TOC120) proteins. SP1 (an E3 ligase) in the outer membrane reorganises the TOC components depending on developmental cues. A 1MDa TIC complex shows TIC20 as channel, TIC100, TIC56 and TIC214 associated proteins. The other TIC complex includes TIC110, TIC40 and Heat shock proteins acting in the import of preproteins (courtesy of Jarvis and López-Juez, 2013)

*In vitro* studies reveal the import of cytoplasmic proteins into the chloroplast is an energy dependent process. Molecular chaperones play key roles to maintain the functional

conformation of active proteins (Mayer, 2010). Transport of preproteins to the chloroplast requires various chaperones at different stages - assisting a cytosolic preprotein, passing through the membrane complexes, inside the stroma and thylakoids (Bédard J, 2017). Chaperone HSP70 (Zhang and Glaser, 2002) along with a 14-3-3 protein forms a guidance complex with the preprotein, thereby increasing the import efficiency for some proteins *in vitro* (May and Soll, 2000). HSP90 with HOP (HSP70/HSP90 organising proteins) co-chaperones also guide the preproteins to the chloroplast membrane (Fellerer et al., 2011). Crossing the intermembrane space is another step in the process of protein import. The proposed components include TOC64, TOC12, TIC22 and imsHSP70, but many of these proteins are not widely accepted. In the inner envelope TIC40 and TIC110 are found to mediate the last stage of the import process (Flores-Pérez and Jarvis, 2013). TIC40 is responsible for proper targeting of proteins to the inner envelope and thylakoid membranes. In the absence of a functional TIC40; STIC1 and STIC2 might cause mistargeting of preproteins (Bédard J, 2017). The process of protein import seems more complex, with the multiple membrane components, in the inner chloroplast membrane. Whether there are specific routes also in the inner membrane, similar to what occurs at the TOC machinery, remains elusive.

### 1.6 Chloroplasts as metabolic hubs

In addition to photosynthesis, chloroplasts perform a variety of functions in plant cell. Although they are primarily known for carbon metabolism, their role is even wider, chloroplasts can be described as central metabolic hubs. For example, primary metabolism of sugars, lipids, aminoacids, nucleotides, and also the sources of precursors for most secondary metabolites (Neuhaus and Emes, 2000; Rolland et al., 2012; Rolland et al., 2018). As a result, chloroplasts also play fundamental roles in the synthesis of many plant hormones.

The role of chloroplasts in primary carbon metabolism derives from their photosynthetic function. Following the generation of ATP and NADPH in thylakoids through the photosynthetic light reactions, carbon fixation takes place in the stroma through the action of the enzymes of the Calvin-Benson cycle (Raines, 2003; Smith, 2010), and generates glyceraldehyde 3-phosphate (G3P).

This can be exported to the cytosol and converted to glucose, then used to synthesise sucrose for export outside the cell. Alternatively, G3P can remain in the chloroplast, converted to

glucose and polymerised into storage starch, accumulated during the day in mesophyll cell chloroplasts and degraded to fuel cellular activities at night (Smith, 2010). The activity of Calvin cycle enzymes can also generate phosphoglycolate which is used for photorespiratory process that metabolically links the chloroplasts, mitochondria and the specialised type of plant peroxisome called glyoxisomes (South et al., 2018).

The synthesis of fatty acids from fixed carbon also takes place in chloroplasts which is stored for long-term as lipid or used for membrane biogenesis (Buchanan BB, 2000; Smith, 2010). Fatty acids are synthesised in chloroplasts from photosynthetic outputs or in heterotrophic plastids, like those in storage organs, from imported carbon. Those fatty acids are used for extra-plastidic membrane biogenesis in the endoplasmic reticulum or for the assembly of chloroplast membranes, rich in galactolipids, inside the plastids. An important class of lipids, the isoprenoids, are synthesised in and out of plastids, the plastidic pathway, shared with prokaryotes, being the major source of terpenoids including carotenoids and sterols (Fraser and Bramley, 2004).

Aminoacids, in addition to ultimately deriving their carbon skeletons from products synthesised in chloroplasts, incorporate ammonium generally acquired by plants as nitrate. The bulk of nitrate reduction to an amino group occurs in chloroplasts, and the incorporation of such a group into the first aminoacid takes place in plastids (Smith, 2010). Many other aminoacids are also plastid products (Reyes-Prieto and Moustafa, 2012), with the synthesis of aromatic aminoacids specifically being possible thanks to the stromal shikimate pathway (Smith, 2010). Of the nitrogenous bases of nucleotides, pyrimidines are fully synthesised in plastids. One important primary metabolic pathway which in plants occurs in plastids is the oxidative pentose phosphate pathway (Kruger and von Schaewen, 2003). This is a fundamental pathway which generates the reducing power needed in non-photosynthetic plastids for fatty acid synthesis or nitrogen assimilation. In addition, it produces the sugar moiety of nucleotides and the precursor of the shikimate pathway.

In addition, many metabolites traditionally called “secondary”, although not less important, are synthesised from primary metabolites of plastids. Chloroplasts synthesise their tetrapyrroles (haem and chlorophylls) which, together with carotenoids, constitute the photosynthetic pigments. The products of the shikimate pathway are also used to synthesise in the cytosol all the aromatic secondary metabolites, including the phenyl-propanoid flavonoids (pigments), tannins (defence compounds) and, lignin monomers (for secondary cell wall formation) (Buchanan BB, 2000; Heldt and Heldt, 2005; Smith, 2010).

Furthermore, plastids synthesise most plant hormones or their precursors. This includes auxin (from aromatic aminoacid metabolites), cytokinins (from purines), brassinosteroids and gibberellins (from sterols), abscisic acid (from carotenoids) and jasmonates (from oxidated fatty acids). Overall, the central metabolic role of chloroplasts or heterotrophic plastids in non-photosynthetic cells should not be underestimated.

### 1.7 Chloroplast to nucleus communication

An important discovery in plant science research was understanding that a constant communication is maintained in cells between plastids and the nucleus. The plastids generate signals to inform about their status, a process which is often referred as "retrograde signalling", to distinguish it from the build-up of chloroplasts through the expression of nucleus-encoded genes. Gene expression in the nucleus relies on the chloroplast signals, for example defects in plastids result in reduction of photosynthesis associated nucleus-encoded genes (PhANGs) that are targeted to plastids, this being the basis for the discovery of such retrograde signalling originally in plastid-defective barley mutants (T., 2017). Research on the retrograde signalling mechanisms has frequently been carried out by damaging chloroplasts using norflurazon (NF) a carotenoid biosynthesis inhibitor and lincomycin (LIN) a plastid ribosomal inhibitor. In general, the use of NF or LIN affects the plastid development and represses the expression of PhANGs (Terry and Smith, 2013; Hills et al., 2015). A genetic screen in Arabidopsis, using these experimental approaches, identified six *GENOMES UNCOUPLED (GUN)* mutants where the expression of PhANGs was less repressed, i.e. the mutations hindered the communication between plastid and nucleus (on the assumption that the plastid defect "triggered" the communication using a negative signal). The genes encoded by *GUN2* to *GUN5* are identified as components of the tetrapyrrole biosynthetic (TBP) pathway (Mochizuki et al., 2001; Koussevitzky et al., 2007; Adhikari et al., 2011; Woodson et al., 2011), while GUN1 is a pentatricopeptide repeat protein which acts as an integrator of multiple plastid defects and signalling to the nucleus (Susek et al., 1993; Koussevitzky et al., 2007; Colombo M, 2016). Recent evidence has shown that this is achieved possibly because GUN1 exhibits direct interaction with proteins involved in plastid gene expression, protein import and TBP (Tadini et al., 2016). *GUN2 (HY1)* and *GUN3 (HY2)* encode haem oxygenase and phytochromobilin synthase respectively, which are necessary in plastids for the formation of phytochromobilin from haem (Mochizuki et al., 2001). Meanwhile *GUN4* and *GUN5* encode a regulator of Mg-chelatase and the H-subunit

of Mg-chelatase respectively, these being proteins which direct tetrapyrrole intermediates towards chlorophyll rather than haem synthesis (Larkin et al., 2003). Woodson et al. (2011) reported *gun6-1D*, a dominant mutation, overexpresses an endogenous FC1 (Ferrochelatase I/Heam synthase), implying that haem acts as a positive signal to regulate the photosynthesis associated nuclear genes for chloroplast development. Certainly, these extensive studies reveal an active interoganellar communication with special emphasis on TBP components. Additionally, there are reports on other signal-inducing factors in the plastids, particularly in relation to the photosynthetic function of fully developed chloroplasts. Conceptually, these later factors have been termed "operational signals", to distinguish them from those alluded to first, the "biogenic signals", and are particularly important to cope with stress (Chan et al., 2016). How these various signals are transmitted, or the nature of biogenic signals themselves in particular, remains obscure.

### 1.8 Regulation of plastid biogenesis

During the past decades, much information has been elucidated regarding the individual processes of chloroplast biogenesis, but the understanding of regulatory mechanisms involved in the biogenesis is very limited. A lot of chloroplast defective mutants arrest plant growth at the embryonic stage, suggesting chloroplasts play an important role very early in development (Bryant N, 2011). It has been observed that plastid division begins during the process of cell division, yet very little is known about how meristematic cells share their dividing plastids. Mutation of *CRUMPLED LEAF1*, gene which encodes a protein targeted to the chloroplast outer membrane, inhibited plastid division and showed perturbations in cell division and the process of differentiation (Asano T, 2004). The RNAi-mediated downregulation of prereplication complex proteins AtCDT1a and AtCDT1b was shown to affect both nuclear DNA replication and plastid proliferation. It was reported that AtCDT1a interacts with ARC6, a plastid division protein, and possibly impacts plastid propagation (Raynaud et al., 2005). Attempts have been made to describe the role of different transcriptional factors as positive and negative regulators of chloroplast development. Constitutive expression of *GROWTH REGULATING FACTOR 5* (*GRF5*) extends the duration of cell division and also enhances chloroplast proliferation. Interestingly these plants stayed green for longer and delayed the process of senescence (Vercruyssen et al., 2015). These studies provide evidence for the links between cell division and plastid proliferation.

Cytokinin seems to act as a positive regulator of plastid development. The expression of transcriptional factors – *GATA NITRATE-INDUCIBLE CARBON-METABOLISM-INVOLVED* (*GNC*) and *CYTOKININ-RESPONSIVE GATA1* (*CGA1*) - is regulated by cytokinin. The *gnc cga1* double mutant exhibited defects in overall chloroplast development; these factors are proposed to act downstream of cytokinin and are master regulators of chloroplast development (Chiang YH, 2012). Furthermore, the *CYTOKININ RESPONSE FACTOR2* (*CRF2*) enhances plastid count per cell, possibly by regulating plastid division genes (Rashotte et al., 2006). Chloroplast growth is achieved by import of thousands of nucleus-encoded proteins. As the import proteins are regulated depending on developmental cues, the process of protein import would be expected to occur throughout the period of chloroplast development. Ectopic expression of *CHLOROPLAST IMPORT APPARATUS2* (*CIA2*) upregulates the expression of two genes encoding import-related membrane components (TOC75 and TOC33), thereby promoting plastid protein import. In addition, this also enhances the expression of plastid ribosomal proteins (Sun et al., 2009). Perhaps the best-known chloroplast regulator has been widely observed, and used, across different species. Golden2, and the GOLDEN2-Like1 and GOLDEN2-Like2 (GLK1 and 2) transcription factors participate in chloroplast development (Hall et al., 1998; Waters et al., 2009; Wang et al., 2017). The overexpression of *GLK1* leads to development of green callus in rice (Nakamura et al., 2009) and also promotes the unusual phenomenon of chloroplasts developing in Arabidopsis roots (Kobayashi et al., 2012). Interestingly, the defect in the plastid protein import mutant *ppi2* (*toc159*) is communicated to the nucleus through the action of GUN1, and the subsequent suppression of PhANGs was achieved by repression of GLK factors (Kakizaki et al., 2009). Therefore, coordination between plastid and nuclear gene expression involves the role of GUN1 and GLKs. The *UNIFORM RIPENING* (*U*) gene encodes a GLK2 transcription factor (*SlGLK2*) in tomato. Overexpression of *SIGLK2* upregulated the expression of PhANGs and promoted chloroplast development, which led to greener fruit with increased carbohydrates and carotenoid pigments (Powell et al., 2012). Similarly, the GLK-related factor APRR2, in tomato, acts as positive regulator for chloroplast and chromoplast biogenesis in fruits (Pan et al. 2013). The knowledge of GLK transcriptional factors highlights the importance of candidate regulators of chloroplast development in enhancing food production. The phytochrome interacting factors PIF1 and PIF3 function as repressors of chloroplast development. The *pif* mutants show elevated levels of protochlorophyllide in dark grown seedlings, indicating enhanced etioplast development, which consequently promotes chloroplast development (Stephenson et al., 2009). Recently, a

forward genetic screen in Arabidopsis has led to the identification of *lyn1* as the suppressor of the *hy1* (*gun2*) mutant. *hy1* is defective in haem oxygenase, necessary for phytochromobilin formation, hence the mutation disrupts phytochrome biosynthesis. Interestingly, *lyn1* single mutant shows an improved chloroplast development relative to WT, therefore LYN1 can be considered as a negative regulator of plastid biogenesis (He, 2017). All these studies show that many factors regulate plastid biogenesis in different ways; meanwhile how this is achieved and whether there is any upstream master regulator that tunes their expression is not known.

### 1.9 Arabidopsis virescent mutants

Light is an essential factor that triggers photosynthesis, the life supporting process of the Biosphere. One of the sequential changes from plumule emergence to plant development is the conversion of etioplasts to chloroplasts in green tissues. This process is mediated by the light induction of nuclear and plastid encoded genes. Li et al. (1995) developed a negative genetic selection to understand the mechanism of light-induced nuclear gene expression. A transgene, pOCA108, was constructed and introduced into the *Arabidopsis adh* mutant of the Bensheim ecotype with *CAB3* (*chlorophyll a/b-binding*) gene promoter, of an important antenna protein called LHCB1 (light harvesting chlorophyll binding protein), to express *ADH* (alcohol dehydrogenase) and *UidA* (β-glucoronidase). A forward genetic screen was carried out using pOCA108 line and screening was performed against *ADH* activity which converts allyl alcohol to a toxic aldehyde, acrolein, that ceases plant growth. Therefore, the only plants which survived had reduced levels of ADH activity. A search for seedlings with reduced *CAB3* expression led to identification of various *cue* (chlorophyll a/b-binding gene under expressed) mutants. Investigation of the first mutant found that *CUE1* encodes a plastid inner envelope phosphoenolpyruvate/ phosphate translocator (PPT) necessary for importing substrates of aromatic amino acids and various secondary metabolites in to the chloroplasts (Streatfield et al. 1999). Extension of the screen revealed a series of *cue* mutants with less accumulation of photosynthesis-associated nucleus-encoded genes.

Among different phenotypic types of mutants, one particularly intriguing class shows a pattern of delayed greening, or virescence. These mutants show pigment-deficient pale tissues in the new leaves, which turn to green in mature stages. The screening of *cue* mutants identified *cue3, cue6*, and *cue8* showing gradual greening phenotypes (Lopez-Juez et al.,

1998). Some of the other genes underlying a pale-to-green mutant phenotype encode the following proteins: the sigma factors SIG2 and SIG6, responsible for PEP-associated chloroplast transcription (Hanaoka et al., 2003; Ishizaki et al., 2005), CLPR2, a Clp protease that maintains chloroplast protein homeostasis (Rudella et al., 2006), SLOW GREEN1 (SG1), a tetratricopeptide repeat protein necessary for chloroplast gene expression (Hu et al., 2014), VIR3, a metalloprotease protein (Qi et al., 2016), and DELAYED PALE GREENING1 (DPG1), a predicted chloroplast membrane protein (Liu et al., 2016). A striking feature of most of these genes is that they are involved in chloroplast gene expression or protein homeostasis. It is not clear whether they have any underlining common molecular phenotype. A typical example of a virescent mutant, *cue6*, is shown in figure 1.5. The current research uses one of these virescent mutants (*cue8*) to understand the chloroplast biogenesis mechanism.

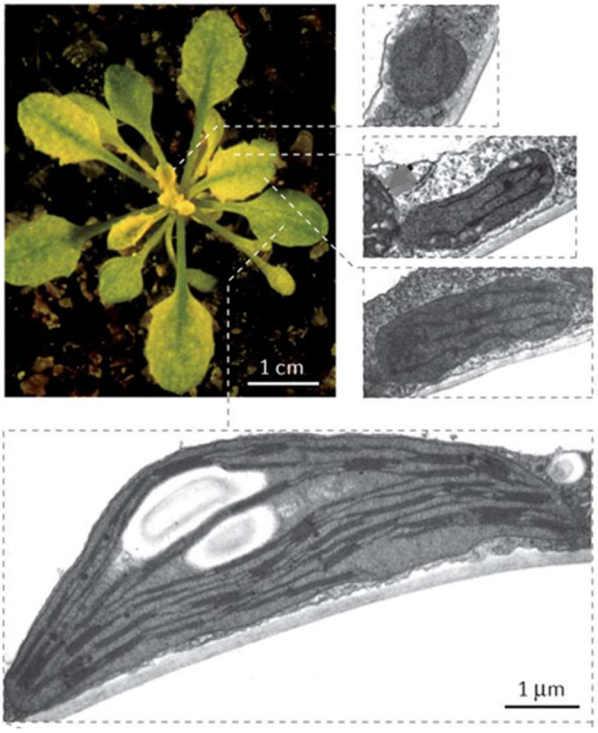


**Figure 1.5.** Arabidopsis virescent mutant (*cue6*) showing delayed chloroplast development. The newly emerging leaves are pale and contain undifferentiated plastids. Transmission electron microscopy images reveal their smaller size and lack of thylakoid structures. As shown in the mature rosette leaves, they manage to develop chloroplasts and green over time (courtesy of Lopez-Juez and Pyke, 2005).

## 1.10 Unravelling the process of chloroplast biogenesis in the developing wheat leaf

Increase in population and climate change presses the necessity of finding ways of improving photosynthetic yield of crops. It is estimated that the world will need an extra 85% of primary production by 2050. Conventional agriculture practises, which also involve overuse of

fertilisers and pesticides, have a direct impact on public health and the environment. The less apparent, global impact is land use change, which is a primary driver of climate change. Increasing those impacts, and expand the land they would require, by 85% could have devastating consequences. Therefore, it is extremely important to identify novel routes to enhance photosynthesis and reduce the reliance on practices which encourage environmental damage. A wide and intense effort is underway across many laboratories to optimise and enhance photosynthesis as a route towards increased plant yield (Long et al., 2015; Ort et al., 2015; Driever et al., 2017; Simkin et al., 2017). However, one of the possible routes (which is least explored) towards such an end is regulating the photosynthetic organelles themselves in the cells.

Plant development is defined, among other parameters, by the proportion of healthy chloroplasts in the cells; therefore, the factors regulating plastid size, number and distribution are crucial to determine plant performance (Boffey SA, 1982). Some of the interesting, fundamental questions, like when do cells decide to fill with chloroplasts and how the plastid biogenesis is regulated, remain elusive. One of the reasons is not finding an appropriate model system. Most of the chloroplast mutations studied so far, which target gene expression, protein import or maintenance of photosynthesis process, result either in premature arrest or lethality of embryo development, which affirms that the initiation of plastid biogenesis occurs at an early stage of plant development. As described above, the individual plastid development processes progress either in close sequence or in parallel to each other. As they are very closely connected, and proplastid-to-chloroplast differentiation occurs very quickly, it is difficult to study the entire mechanism in a dicot plant. Interestingly, monocot seedlings can be used as a model to follow proplastid-to-chloroplast development. For example, the base (near meristem) of the monocot leaf has actively dividing cells. They are pushed towards the leaf tip as new cells, through a combined process of division and early expansion, are accumulated at the base. As they age, cells undergo differentiation and form specialised leaf tissues. This results in a developmental pattern of cells from undifferentiated meristem to fully mature region within the same leaf and at a single time. Therefore, a monocot leaf gives rise to a complete developmental sequence from base to tip (Boffey SA, 1979), which is evidenced by a phenotypic gradient along the developing leaf (Pogson et al., 2015). On the other hand, this system also provides sufficient material to perform quantitative studies on cell division and cell expansion, to understand plant organ growth (Avramova V, 2015). As cell differentiation involves, as one of its components, organellar development, it is possible

to quantify chloroplast development (plastid number, size) in a cereal leaf (Fig. 1.6) and seek to identify the underlying regulators along the leaf gradient (Jarvis and Lopez-Juez, 2013). Previous studies conducted by Boffey et al. (1979) shed light on chloroplast proliferation in wheat leaves, quantifying plastids per mesophyll cell along the gradient. They observed chloroplast division happens up to a specific distance from the leaf base. Recent quantitative work on maize seedlings revealed the build-up of proteins and organelles, cellular biogenesis as well as metabolism along the gradient of the growing leaf (Majeran et al., 2010). Their observations included the leaf blade, from ligule to leaf tip, overlooking the actual early developmental events initiated at the base (close to the undifferentiated meristematic region). A gene expression analysis by high throughput sequencing of RNA was conducted by Li et al. (2010) to understand cellular development and photosynthetic build-up in maize. The samples were prepared from four district region of the leaf taking the ligules of leaf 2 and leaf 3 as reference points for two basal samples. Although a cluster of cell cycle genes was observed in the first sample, that analysis also missed the very early developmental region. Another detailed study on maize leaf development performed a combined analysis of transcriptome, metabolome and enzyme activity covering a series of sections (2 cm each) from tip (at a distance of 20 cm from emergence from the stem) to base, excluding the early stages (Pick et al., 2011). Wang et al. (2014) attempted a comparative analysis of transcriptome and metabolites between maize and rice to identify differences in photosynthesis among $C_4$ and $C_3$ species. Like other studies, there was no sample showing early developmental stage, and the earliest rice sample, of 2 cm in length, was acknowledged to correspond to the second sample isolated from maize. While all the studies show different developmental stages, none of them could help in understanding the initiation and series of plastid biogenesis events, due to lack of early cellular stages and a wide sample section that mixes cells from different developmental stages. Research work exploring plastid division and gene expression was initiated previously, but so far nobody has combined those quantitative cellular development and quantitative gene expression profiles, the closest being the study by Majeran and collaborators (2010), which carried out a TEM-based qualitative organelle analysis. If designed with a proper sampling strategy, this could be a valuable resource to identify novel regulators of plastid growth, division, and cellular development.

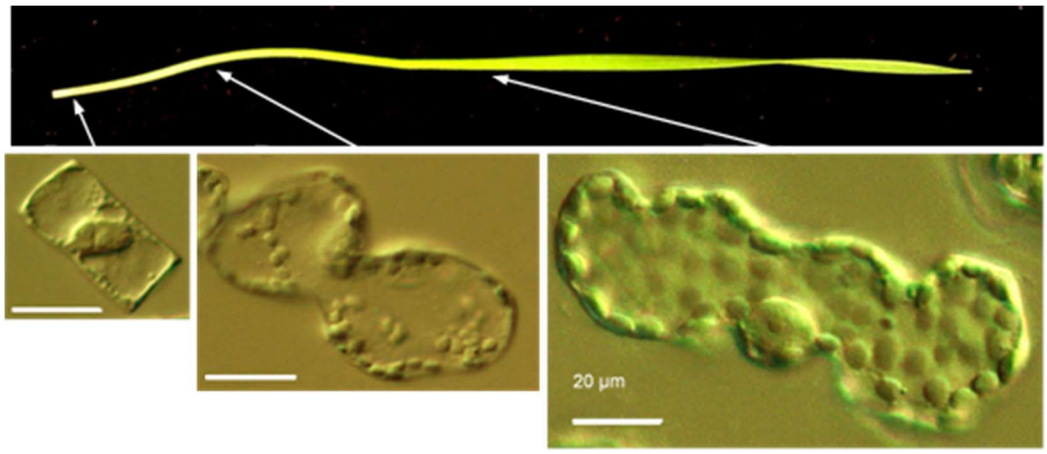


**Figure 1.6** Morphology of wheat seedling showing a phenotypic gradient. The base of the wheat seedlings has newly developed cells with proplastids which eventually develop into differentiated chloroplasts as the cells move towards the mature leaf tip (courtesy of Jarvis and Lopez-Juez, 2013).

### 1.11 Aim and objectives of the research

The aim of the current research is to understand the process of chloroplast biogenesis with special emphasis on chloroplast protein import and gene expression. The objectives of the project are to:

1. **Understand the role of CUE8 in the function of the chloroplast genetic machinery.**

   It has been observed that *CUE8* gene is co-expressed with genes involved in early chloroplast development, including plastid genetic machinery and ribosomal proteins. Therefore, an objective is to understand whether CUE8 plays a role in chloroplast gene expression.

2. **Confirm whether CUE8 is involved in chloroplast protein import.**

   Recent research reveals that TIC100 is part of the novel TIC 1MDa complex in the chloroplast membrane and it is necessary for the import of cytosolic proteins. The *cue8* mutant allows biochemical studies (which could otherwise be difficult in a *tic100* knockout mutant) due to its partial loss of TIC100 function. Hence, the second objective is to confirm whether *cue8* is defective in chloroplast protein import and investigate whether CUE8/TIC100 has a preferential role for importing photosynthetic or housekeeping preproteins.

3. **Identify suppressors of *cue8* using forward genetics to further understand the functional role of CUE8/TIC100.**

   The partial loss of function of CUE8 leads to impaired plastid development and results in the peculiar virescent phenotype. Therefore, the objective of the research is to employ forward genetic screen on *cue8* and identify genetic suppressors to understand the function of CUE8 and how it impacts on the formation of the TIC 1MDa complex and overall chloroplast development.

4. **Decipher the individual processes involved in chloroplast biogenesis along the developing wheat leaf.**

   Chloroplast biogenesis is a complex phenomenon which involves multiple elementary processes. The sequential events occurring during chloroplast development, and how those events interact with each other, is poorly understood. A monocot leaf model shows a developmental pattern with actively dividing cells in the meristem and to a fully photosynthetic stage. The fourth objective is to explore the developmental gradient of a wheat leaf using microscopy and molecular tools to understand the process of chloroplast biogenesis.

5. **Construct a transcriptome dataset along the growing wheat leaf to identify candidate genes involved in the process of chloroplast development and allow the future search for novel regulators.**

   Although many genes have been identified for the individual processes of chloroplast development, how they are regulated is poorly understood. It is not known whether there are multiple regulators for individual processes or the entire mechanism is under the control of a master regulator. Therefore, the fifth objective is to generate whole-genome transcriptome data along the developing wheat leaf in parallel to quantitative chloroplast data, which could be used to identify candidate genes and novel chloroplast regulators.

# Chapter 2

# Materials and Methods

## 2.1 Media preparation

Murashige-Skoog media (MS) (Murashige and Skoog, 1962) was prepared from a commercial ready mix (Duchefa, The Netherlands) with 0.8% (w/v) agar and 1% (w/v) sucrose unless otherwise stated (Table 2.1). The pH of media was adjusted to 5.7 using 1N KOH and autoclaved at 121°C for 20 minutes. Once the bottles were cooled to 50°C, media was poured into 9 cm petri plates to about 5 mm (or 35 - 40 ml) in each plate. Pouring was done in the sterile conditions in a laminar air flow cabinet. Plates were partly covered until solidified to avoid water condensation on the lids. Arabidopsis root growth studies were performed on 12x12 cm square plates, 1.5% (w/v) agar, with different sucrose concentrations (described in results). Square plates were aligned vertically to grow roots on the media surface.

**Table 2.1 Reagents used for the media preparation**

| **Reagents** | **grams/Litre** |
|---|---|
| Phyto-agar (Duchefa) | 8 |
| MS salts with Gamborg's vitamins (Duchefa) | 4.4 |
| MES | 0.5 |
| Sucrose | 10 |
| $dH_2O$ | 1000 ml |

## 2.2 Plant material, sterilisation and plating

Arabidopsis thaliana wild type ecotypes Bensheim, transgenic line pOCA108, (Li et al., 1995), Columbia (Col-0) and mutants: *cue8* (Lopez-Juez et al., 1998), *ppi1*-1 (Jarvis et al., 1998), *toc132 toc120*/+ (Kubis et al., 2004), *cop1*-4 (Deng et al., 1992), *GLK1ox* and *GLK2ox* (Waters et al., 2008), *gun1-1* (Susek et al., 1993), *gun6D-1* (Woodson et al., 2011), and *lyn1-1* (lab stock unpublished), were used in the present study. Seeds up to 1000 (20-25 mg), were sterilised with 95% (v/v) ethanol (1 min) and diluted bleach (1:2) for 10 min. Seeds were washed with sterile $dH_2O$ for 4-5 times in laminar air flow cabinet. Sterilised seeds were vernalized (4$^oC$) in an appropriate volume of 0.1% (w/v) autoclaved agar for 3 days to encourage germination and synchronous growth. Imbibed seeds were evenly distributed on MS media plates. All the consumables in contact with seeds were autoclaved prior to use.

*Triticum aestivum* (Chinese Spring Wheat strain WPGS 6265, L42 line) was obtained from John Innes Centre, Germplasm Resources Unit. Seeds of similar size were surface sterilised

with 90% (v/v) ethanol and rinsed thoroughly with $dH_2O$. Seeds were stratified in sterile water at 4ºC for 3 days before sowing in the soil.

### 2.3 Growth conditions and soil preparation

Petri plates with seeds were sealed with parafilm and transferred to the growth incubator (I-30 Percival Scientific, USA) with a continuous light of 100 µmol $m^{-2}$ $s^{-1}$ (TLD 840, 18 W SYLVANIA, Germany), maintained at 20 - 22°C, with a 60% relative humidity. In some etiolation experiments, a dark incubator (LSM Ltd, UK) with similar conditions was used except for the absence of light. Petri plates were fully wrapped in aluminium foil before they went into the dark incubator.

Soil mixture was prepared with 6-parts Levington M3, 6-parts John Innes number 3, 1-part perlite. Healthy seedlings previously grown on plates were then transferred to soil trays in the growth room maintained for 16h photoperiod (200 µmol $m^{-2}$ $s^{-1}$ light) at 21ºC. Trays with freshly transferred seedlings were covered for 4 - 5 days and lids were opened gradually for acclimatization. Growth was constantly monitored by irrigating trays whenever necessary. Plants with well-developed siliques (yellow/brown) and declining flowers number were enclosed in paper bags and allowed to dry. Seeds were harvested in small paper envelopes to get rid of moisture and stored in Eppendorf tubes for future use.

Wheat seeds were sown at the same depth in soil mixture and covered with 1 cm vermiculite layer to keep the top moist. A constant light (285-395 µmol $m^{-2}$ $s^{-1}$) with a combination of red and blue LED in addition to white fluorescent lamps (TLD 840) was used in the growth room set at 23ºC. Wheat was grown for 14 days with irrigation at regular intervals.

### 2.4 Sample collection

Arabidopsis wild-type (WT) seedlings grown on MS media were collected after 5-days while the slow-growing *cue8* mutants were harvested after 6-days unless otherwise stated. Samples for gene expression studies were prepared from very young juvenile leaves (<4 mm) in length. Chloroplast compartment experiments were performed from seedlings; developed juvenile leaves (1.5 cm) and rosette leaves (3 cm) from 4 weeks old plants. Chloroplast isolation, protein import, and western blot analysis were performed on 13-days old WT and 17-days old *cue8* and *soh1* (see results).

Wheat seedlings were grown for 6-days and harvested when the first leaf was about 170 mm, enclosed by a coleoptile (ca. 35 mm) at the base. A second leaf, approximately 85 mm, was developing inside leaf 1, which had enclosed a newly emerged leaf 3 primordium (around 1.5 mm in length) and an embedded dome-shaped shoot apical meristem. A transparent ligule was barely detectable at ca. 8 mm at the base of the first leaf. Initially, the roots and seed testa were trimmed at the crown region without damaging the base (Fig. 2.1). The coleoptile was removed with the help of fine forceps and scalpel. The laborious task was to open the base of the first leaf and obtain intact shoot apex sample, consisting of the shoot apical meristem and emerging leaf 3 (ca. 1.5 mm). This served as sample 1 and the leaf 1 was carefully sectioned into 13 samples (2 - 14) to achieve various developmental stages from an actively proliferating base to a fully mature stage. Samples 2 to 9 contained consecutive 5 mm sections, while samples 10 to 14 were 10 mm each. Some sections were excluded as their developmental stages were similar to already selected samples. Basal sections were very fragile and easy to cut compared to the later ones. A fully mature sample 15 was collected from mid-point (20 mm) of leaf 1 that was grown for 14 days from the same batch, shortly before the senescence begun to appear at the leaf tip (Fig. 2.1 C). At least three biological samples were prepared for each experiment (flow cytometry, microscopy, spectrophotometry, combined nucleic acid and protein extraction) from the seedlings grown under identical conditions.

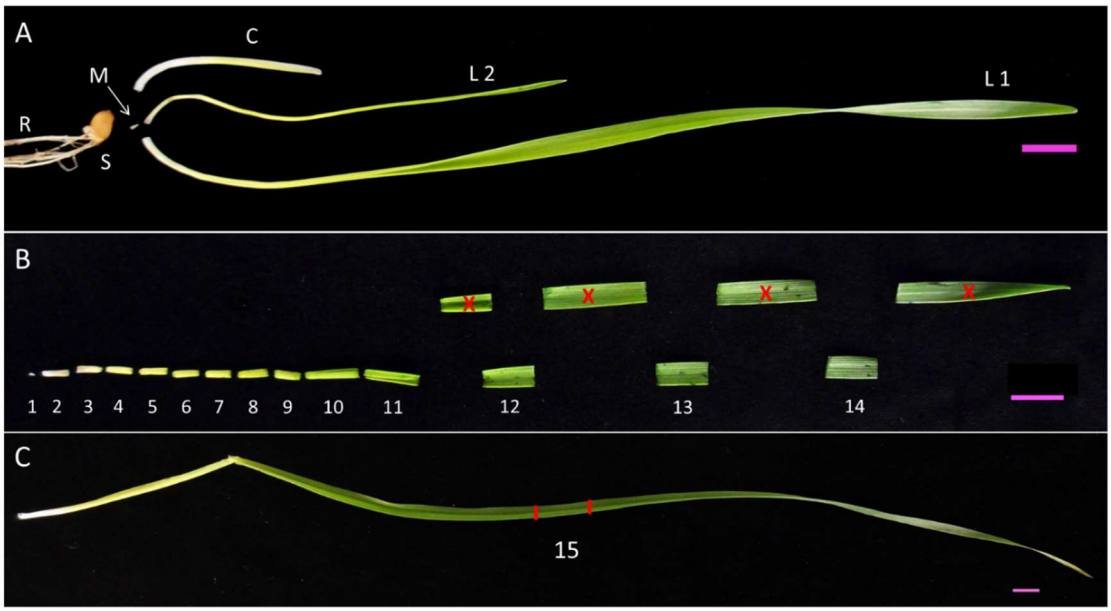


**Figure 2.1** Wheat seedlings dissection and sample collection. (A) The image depicts various parts roots, seed testa, leaf 1, leaf 2 and coleoptile of 6 days old seedling. An arrow indicates the meristem at the leaf base. (B) Dissected meristem and leaf 1 showing dissected samples 1 to 14, excluded parts are shown with cross marks. (C) Section 15 collected from 14 days old leaf 1. Scale bar represents 1 cm.

## 2.5 Cell cycle analysis

Cell cycle analysis by DNA content was measured along the monocot leaf using flow cytometer (Sysmex CyFlow® Space, Sysmex, UK). The flow cytometer fluidics was initially rinsed with a provided cleaning solution and then with double $dH_2O$. To harvest enough material the meristem sample was collected from 4 seedlings. Samples with 5mm sections were collected from 2 seedlings and 10mm samples were prepared from one seedling. Plant tissue was finely chopped with Wilkinson blades by adding an appropriate amount of Partec cystain UV precise P Solution 1 (Sysmex) lysis buffer (ca. 20µl for sections 1 to 9 and 100µl for section 10 to 15 to cover the plant material). Partec cystain UV precise P Solution 2 (Sysmex) DNA-binding 4',6-diamidino-2-phenylindole (DAPI) was added to the samples (2 ml for the section 1 and 1 - 1.5 ml for rest of the samples). The lysis mixture was filtered (20 - 30 µm pore size) and run through the flow cytometer. The station was cleaned with decontaminating and cleaning solution followed by double $dH_2O$ after every sample. DNA content (2C or 4C) was determined by counting a minimum of 10,000 nuclei per biological replicate. Frequency histograms outcome was fit into the cell cycle analysis tool of the instrument's software to obtain percentages of different phases of the cell cycle.

## 2.6 Nomarski and fluorescence microscopy

500 µl of fixative (3.5% (v/v) Glutaraldehyde and 0.05% (v/v) Tween 20, detergent) was placed in eppendorf tubes under the fume cupboard. Arabidopsis seedlings (4 - 5) or leaf samples (1 - 2 per plant) were collected and immersed in the fixative. Tubes were left undisturbed to fix the plant material for 1 hr in relative darkness. Glutaraldehyde was replaced with 500 µl of EDTA solution (100 mM, pH 9) and incubated for 2 hrs at 65°C. The cotyledons/leaves were cut into two halves and the apex portion was placed on a microscope slide with a tiny drop of 50% (v/v) glycerol. A coverslip was placed over the tissue and gently squashed (by tapping with a pencil head) until the material was smudged. Care was taken to avoid any air bubbles and not to break the cell membrane by over tapping. Excess fluid was wiped off and the coverslip sides were sealed with nail varnish. Samples were in triplicates for every experiment, and every replicate produced 4 slides from different plant material. Slides were observed under a Nikon microscope (Eclipse 80i or Optiphot-2) focussed in x10 objective, selected intact cells in x20, and x40 objectives to perform quantitative measurements using Nomarski optics. Data was collected using NIS-Elements

AR 2.30 software calibrated for measurements to 0.26 μm/pixel at x40 magnification and the images were captured using a MicroPublisher 5.0 RTV (QImaging, Canada). Inbuilt software tools like area and count allowed the measurements of the cell, chloroplast area, and organelle count. Total chloroplasts were deduced by live counting on different planes, completely moving out of focus and slowly focussing inwards (until the last plane, losing the focus again) ticking only clearly visible plastids in different planes (Pyke, 2011).

Arabidopsis seedlings of dsRED transgenic line (Haswell and Meyerowitz, 2006) were fixed similarly, and images were captured from partially squeezed leaves and roots showing plastid fluorescence. Chloroplast DNA distribution was visualised also in the fixed samples but mounted with a strong DNA binding dye, DAPI (Sysmex), instead of glycerol. Selected mesophyll cells were visualized under a Nikon H600L Ni-E fluorescence microscope, using a x60 objective, UV excitation and blue emission filters.

Wheat samples were prepared for microscopy as described for Arabidopsis with minor changes. Triplicate samples were prepared with 4 seedlings in each replicate. The 5 mm and 1 cm sections were subjected to 1 hr fixation in the dark and vacuum infiltrated for 5 minutes at 500 mBar in a DNA mini vacuum centrifuge. To encourage penetration of fixative this step was repeated after 30 minutes. The fixative was replaced with EDTA as above, and samples were heated at 65ºC overnight. The following day, tubes were stored at 4ºC for further use. Mature wheat sections were much harder to separate, so the fragments were finely split with forceps while mounting in 50% (v/v) glycerol. To obtain clean data tissue was selected from the midpoint of every section. Fluorescence microscopy was also used to confirm the distribution of chloroplasts in wheat samples mounted with DAPI.

### 2.7 Confocal microscopy for root meristem

Arabidopsis seedlings grown for root studies were collected after 7-days of growth and mounted in propidium iodide (PI) 10μg/ml (from a stock of 1 g/ml in water) on long cover slips (22 x 50 mm, VWR, UK). An Olympus FV 1000 laser scanning confocal microscope was used to analyse the root meristem by focussing on a single plane using a 40x water objective. Samples were excited with the 543 nm laser line and root images in the red channel were processed with the Olympus FV10-ASW software.

## 2.8 Primer designing

Arabidopsis genomic DNA and coding sequences were obtained from The Arabidopsis Information Resource (version TAIR 10: https://www.arabidopsis.org). Primers used for gene expression studies were designed with the online tools Primer3 (http://primer3.ut.ee/) and Quant Prime (http://quantprime.mpimp-golm.mpg.de). Selected primers were aligned by blast against TAIR 10 transcripts. Some of the genotyping primers were retrieved from publications as described in the appendix. PCR primers for chloroplast genome copy number were designed using the Primer3. Genotyping primers for single nucleotide changes were designed using Cleaved Amplified Polymorphic Sequence (CAPS) online tool (http://heimanlab.com/cut2.html) if the SNPs resulted in a restriction site (Konieczny and Ausubel, 1993). In case the mutation was not differentially accessible to restriction endonucleases, modified primers were designed using Derived Cleaved Amplified Polymorphic Sequences (dCAPS), http://helix.wustl.edu/dcaps/dcaps.html (Neff et al., 2002).

Primers for chloroplast genome were designed in the matching sequence of two wheat chloroplast genome submissions found on NCBI with some differences (Ogihara et al., 2002; Middleton et al., 2014).

Techniques were devised to quantify the reverse transcribed cytoplasmic 18S rRNA and chloroplast 16S rRNA in wheat. The 18S rRNA sequence of the three wheat genomes A, B and D (3J5Z_d, AY049040, and AJ272181) and the orthologous rice sequence (Os_17SrRNA) were retrieved from NCBI (https://www.ncbi.nlm.nih.gov/nucleotide/). All the sequences were searched by BLAST against the wheat genome in Ensemble Plants (http://plants.ensembl.org/index.html) to find the homologous sequences. Highly matched A, B and D genome sequences were selected and aligned in Clustal Omega (http://www.ebi.ac.uk/Tools/msa/clustalo/). Common sequences were highlighted and realigned with NCBI 18S rRNA to obtain the final sequence which was then compared with consensus chloroplast 16S rRNA. A primer targeting both 18S rRNA and 16S rRNA shared sequence was designed using Primer3 for reverse transcription. Gene-specific primers were used in the non-homologous region to quantify each ribosomal RNA separately. Modified Primer3 parameters are shown in table 2.2. All primers were supplied by Sigma Aldrich (UK) and stored as 100 µM stocks.

**Table 2.2 Parameters used for primer designing**

| Primer Tm | Old Secondary Structure Alignments |
|---|---|
| Minimum: 57 | Max self-complementarity: 5 |
| Optimum: 60 | Max pair complementarity: 5 |
| Maximum: 63 | Max 3'self-complementarity: 1 |
| Product size range: 70-120 | Max 3' pair complementarity: 1 |

## 2.9 Arabidopsis genotyping

Arabidopsis mutants were genotyped with seedlings on media plates or with a leaf from a healthy growing plant. Genomic DNA was extracted from flash frozen plant material using a published method (Edwards et al., 1991). Tissue was homogenised with cold plastic pestle assembled on a mechanical drill. Edwards buffer (500 µl) was quickly added and vortexed vigorously for 10 seconds to rapidly mix with the ground tissue. The lysate was spun at full speed for 5 minutes and without disturbing the pellet 450µl of the supernatant was mixed into equal volumes of isopropyl alcohol (IPA). Samples were left undisturbed at room temperature for 10 minutes and spun for 7 minutes. The supernatant was poured off and the pellet was washed with 1ml, ice-cold 70% (v/v) ethanol. Extraction carried out from an individual seedling resulted in a thin precipitate over the wall of the tube. Tubes were dried at 65$^{o}$C by opening the lids and the pellet containing DNA was resuspended in 50 µl of TE (50/10). The volume of TE used varied (20 - 50 µl) according to the size of the pellet. 2 µl of DNA sample was used for PCR reaction with sequence-specific primers (Table 2.3). In case of T-DNA insertion (KO mutants) PCR product was subjected to gel electrophoresis whereas, for point mutations, the amplicons were digested with restriction endonuclease before running on a gel.

**Table 2.3 Preparation of reagents for DNA extraction using Edward's method**

| Edward's buffer | | TE buffer | |
|---|---|---|---|
| Tris-base (200 mM, pH 7.5) | 10 ml | Tris-base (50 mM, pH 7.5) | 2.5 ml |
| NaCl (250mM) | 2.5 ml | EDTA (10 Mm) | 1 ml |
| EDTA (25Mm) | 2.5 ml | $dH_2O$ (total) | 50 ml |
| SDS 0.5% (w/v) | 2.5 ml | | |
| $dH_2O$ (total) | 50 ml | | |

## 2.10 Polymerase chain reaction

In vitro DNA fragments provided with specific primers were amplified by Polymerase Chain Reaction (PCR). GoTaq® G2 Flexi DNA Polymerase (Promega UK), GoTaq® Flexi Buffer,

$MgCl_2$, dNTPs mix, forward primer and reverse primer were mixed into nuclease-free water to prepare a master mix as per the number of reactions. Unless otherwise stated, each reaction was prepared for 25 µl with 2 µl template DNA and amplified in the thermal cycler (Eppendorf Master Cycler gradient) using the program settings shown in table 2.4.

**Table 2.4 Reagents and program used for standard PCR reaction**

| Reagents | Per reaction | Final conc. | Programme | | |
|---|---|---|---|---|---|
| Nuclease free Water | added to 25 µl | | Initialisation | 94°C 2’ | |
| GoTaq PCR buffer (5x) | 5 µl | 1x | Denaturation | 94°C 30” | } rep 32 |
| $MgCl_2$ (25 mM stock) | 2.5 µl | 2.5 mM | Primer annealing | 60°C 30” | |
| dNTPs (12.5 mM each) | 0.4 µl | 200 mM | Extension | 72°C 1’ | |
| Primer F/B (20 mM) | 0.25 µl | 5 pmol | Final-extension | 72°C 5’ | |
| Primer R (20 mM) | 0.25 µl | 5 pmol | Hold | 15°C | |
| Taq Polymerase (5u/ µl) | 0.2 µl | | | | |
| DNA sample | 2 µl | | | | |

PCR amplification of *TIC100, cue8* and *soh1* cDNA for cloning-related procedures was carried out using Thermo Scientific™ (UK), Phusion™ High-Fidelity DNA Polymerase kit following manufacturer’s instructions with small modifications. Ingredients and modified 3-step cycling conditions used are shown in table 2.5.

**Table 2.5 Reagents and program used for Phusion PCR reaction**

| Reagents | Per reaction | Final conc. | Programme | | |
|---|---|---|---|---|---|
| Nuclease free Water | added to 50 µl | | Initialisation | 98°C 30” | |
| 5X Phusion HF buffer * | 10 µl | 1x | Denaturation | 98°C 10” | } rep 32 |
| dNTPs (12.5 mM each) | 0.8 µl | 200 mM | Primer annealing | 60°C 30” | |
| Primer F/B (20 mM) | 1.25 µl | 0.5 mM | Extension | 72°C 1:40” | |
| Primer R (20 mM) | 1.25 µl | 0.5 mM | Final-extension | 72°C 6’ | |
| Phusion Polymerase (5 u/µl) | 0.5 µl | 0.02 U/ µl | Hold | 15°C | |
| Template (50-250 ng/50 µl) | x µl | | | | |

* 5X Phusion HF buffer contained 7.5 mM $MgCl_2$ (1.5 mM final concentration)

## 2.11 Gel electrophoresis

Agarose gel electrophoresis was used to determine RNA quality, size of the PCR amplicons, 1.2% (w/v) agarose, and to separate the restriction digested DNA fragments, 2% (w/v) agarose. The agarose (Molecular biology grade, Helena BioSciences, Europe) was dissolved in 1xTBE in a microwave and 2 µl ethidium bromide (10 mg/ml stock) per 40 ml of gel was added before pouring into the casting tray. Once solidified the comb was gently pulled and gel tray was immersed in 1xTBE in the electrophoresis tank. Samples mixed with 6x loading

dye in parallel to a ladder (GeneRuler 1kb DNA Ladder, Thermo Scientific) with a mixture of DNA fragments of known size were loaded in the wells. An electric field of 95 volts was applied and the nucleic acids were run until the dye had reached the bottom of the gel. The gel was visualised under UV light in the Gene Flash Syngene Bioimaging Gel Doc and captured with the inbuilt camera.

**Table 2.6 Preparation of Gel electrophoresis**

| **10x TBE** | | **Gel** | | **Loading** | |
|---|---|---|---|---|---|
| Tris-base | 242 g | 1x TBE | 40 ml | PCR product or | 5 µl |
| Glacial acetic acid | 57.1 ml | Agarose | 480 mg | RNA | 1 µg |
| 0.5M EDTA (pH 8.0) | 100 ml | EtBr (10 mg/ml) | 2 µl | Loading dye | 1 µl |
| $dH_2O$ (total) | 1000 ml | | | Ladder | 2 µl |

## 2.12 Extraction of nucleic acids

Arabidopsis (seedlings/juvenile leaves) grown in the white light (100 µmol $m^{-2}$ $s^{-1}$) were harvested in triplicates and quickly frozen in liquid $N_2$. DNA and RNA were extracted from the same samples using NucleoSpin® RNA/DNA Buffer Set (Macherey Nagel, Germany) with some modifications to the manufacturer's instructions. The frozen wheat sample was ground in two steps with a mechanical drill and IKA Ultra Turax® homogenizer. A mixture of 400 µl of RA1 and β-mercaptoethanol was added before the tissue had melted. To avoid clogging in the shredder filter, the homogenate was spun at 16000 rcf for 2 minutes. The filtrate was mixed with 400 µl of ethanol without disturbing the pellet. Hereafter the centrifuge was used according to the protocol. DNA was eluted in 100 µl elution buffer, the rDNase reaction mixture was applied to the nucleic acid binding column to remove any traces of DNA and after three washes the RNA was eluted in 60 µl RNase-free water.

## 2.13 Quantification of nucleic acids

DNA and RNA extracted from plant tissue were quantified using the NanoDrop™ 1000 Spectrophotometer. The instrument was stabilized with RNase free water, blanked with the respective reagent used for the elution. Concentration (ng/µl) was measured and the purity was confirmed by 260/280 ratio (1.9 to 2.5) and 260/230 (2.0 to 2.23). RNA stored at -80ºC and used more than once was quantified each time before reverse transcription.

## 2.14 Determination of RNA quality using Bioanalyzer

Quality of Wheat RNA samples was confirmed by the RNA integrity number (RIN) using Agilent 2100 Bioanalyzer and Agilent Expert software (Mueller et al., 2004). A volume of 0.5 µl of each RNA solution, before concentration was known, was loaded into the Agilent RNA 6000 Nano chip wells along with 1 µl of RNA ladder. The analysis was made by following instructions in the manufacturer's protocol.

In addition, to maintain the quality before shipment, about 7ug of RNA was dried by gently mixing with the matrix of RNA stable tubes (Sigma Aldrich, UK) and vacuum centrifuged for 2 - 3 hours (depending on the volume) at room temperature. Dry RNA tubes were temporarily stored in a desiccator with silica gel that provides moisture-free environment. High-quality RNA samples in four replicates obtained from developing wheat leaf were sealed in moisture barrier bags (supplied by Sigma Aldrich, UK) and posted for sequencing. During the entire procedure, from the extraction of RNA to drying used tools were constantly cleaned to reduce the risk of RNases.

## 2.15 Reverse transcription

RNA extracted from Arabidopsis seedlings / juvenile leaves was checked for its integrity by gel electrophoresis and reverse-transcribed into cDNA by Qiagen (UK) QuantiTect® Reverse Transcription (RT) protocol following instructions in the kit (Table 2.7). Synthesis of cDNA was done from 1µg RNA using reverse transcriptase with oligo-dT and random primers. Genomic DNA traces were eliminated from the template by adding gDNA wipeout buffer and incubating at 42ºC for 2 mins. Reverse transcription was performed at 42ºC for 16 mins and the enzyme was inactivated at 95ºC for 3 mins. For efficient cDNA synthesis, the kit was supplied with an RNase inhibitor solution. The cDNA was diluted to 10-fold prior to quantitative PCR.

**Table 2.7 Reagents used for reverse transcription**

| Reagents | Per sample | Reaction | Volume |
|---|---|---|---|
| gDNA Wipeout Buffer | 2 µl | RT Primer Mix | 1 µl |
| RNA | 1 µg | 5x RT Buffer ($Mg^{2+}$ and dNTPs) | 4 µl |
| RNase-free water | Up to 14 µl | Reverse Transcriptase | 1 µl |
| | | RNA (dilution) | 14 µl |
| | | Total reaction | 20 µl |

Wheat RNA samples were reverse transcribed using the Thermo Scientific Maxima cDNA synthesis kit, following the manufacturer's instructions. Ribosomal RNA has frequent secondary structure and is abundant compared to other cellular RNA. Therefore, a specific primer (0.1 pM) common to sequences of both 16S rRNA and 18S rRNA, along with provided oligo-dT and random hexamers were used to reverse transcribe 1 ng of RNA template. The 10-fold diluted cDNA was used for qPCR analysis.

### 2.16 Quantitative PCR

Gene expression was quantified in a two-step RT-qPCR reaction. Firstly, mRNA was reverse transcribed to cDNA as described above and quantified through quantitative PCR technique using the SyGreen Mix Lo-ROX (2x qPCRBIO, SyGreen Mix Lo-ROX, PCRBIOSYSTEMS, UK) in the QIAGEN's Rotor-Gene Q real-time PCR cycler. Primer working standard was prepared from stocks (100µM) as recommended by the manufacturer. A typical qPCR program is shown in table 2.8, where the number of cycles (35 – 42) was modified based on the cycle of signal appearance. Relative transcript levels of target genes were analyzed using RotorgeneQ software. Results of each target gene expression was normalized to the expression levels of a reference gene (*UBQ10*) and each mutant relative to the WT was calculated individually ($E^{-Ct_{test}}/E^{-Ct_{control}}$, where E = efficiency and Ct = takeoff value as calculated by RotorgeneQ).

**Table 2.8 Reagents and program used for RT qPCR reaction**

| **Reagents** | **Per sample** | **Program** | | |
|---|---|---|---|---|
| RNase free water | 6.4 µl | Hold | 95°C 2' | |
| 2x SYBR® Mix | 10 µl | Cycling | 95°C 5'' | rep 35 |
| Primers F+R (5 µM each) | 1.6 µl | | 60°C 20'' | |
| Template (DNA/ cDNA) | 2 µl | Melt | 72 °C - 95°C | |
| Total reaction | 20 µl | Channels | Green<br>source: 470<br>detector: 510<br>gain: 10 | |

### 2.17 Chloroplast genome copy number

Chloroplast genome copy number was determined by quantitative PCR analysis of DNA copies using a standard curve. To prepare the standards with known concentration, specific gene sequences of chloroplast genome and nuclear genome were PCR amplified and the

amplicons with confirmed, correct size (gel electrophoresis) were purified using QIAquick kit, Qiagen, following the manufacturer's instructions. Concentration was measured by NanoDrop™ 1000 Spectrophotometer. For each gene, the purified DNA was serially diluted to six standard concentrations from 25 pg/µl to 0.0025 pg/µl. Total DNA extracted from plant tissue as described above were 10-fold diluted for nuclear genes and 100-fold for quantitation of plastid genes. These samples were subjected to qPCR analysis along with their standards of known concentration. Results were normalized by standard curves, prepared for each gene, to calculate the actual amount of cpDNA present with respect to the haploid nuclear genome.

To quantify the ratio of plastid DNA/ genomic DNA in Arabidopsis, a total of five genes were taken in to account, two nuclear single copy genes - *HO1* and *CHS,* and three plastid genes at different regions - *rbcL* (large single copy region)*, ndhG* (small single copy region) and *ycf2* (inverted repeat region) (Fig 2.2).


**Figure 2.2** Structure of Arabidopsis chloroplast genome map. Image showing large single-copy (LSC), small single-copy (SSC) and Inverted repeat regions (IR). Image taken from http://www.ruhr-uni-bochum.de/pcp/JSchweer.html. and details of a publication (Sato et al., 1999).

For wheat genome copy number, primers were designed from three genes, *rbcL* (Large single copy), *ndhD* (small single copy) and *rps7* (inverted repeat) covering three different regions of chloroplast genome (Fig. 2.3). On the other hand, nuclear single copy genes – *KO1* and *KS* (of A, B and D genomes) were selected from NCBI, Ensemble Plants and aligned in Clustal Omega. A final sequence with a perfect match in between A, B and D genomes in both sources was used for selection of primers.

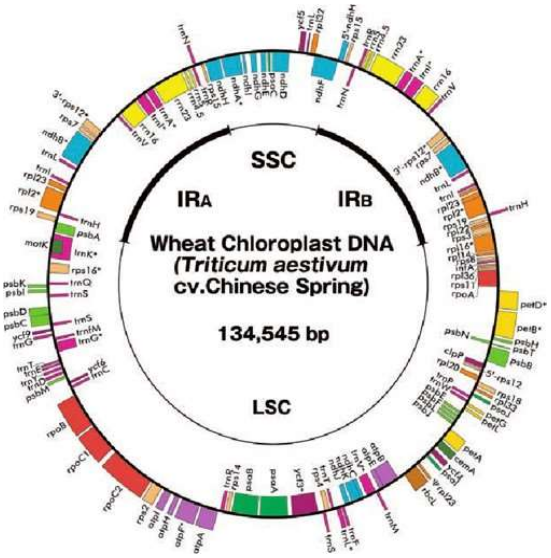


**Figure 2.3** Structure of wheat chloroplast genome map. Image showing three distinct regions, large single-copy (LSC), small single-copy (SSC) and inverted repeat (IR) (Ogihara et al., 2002).

## 2.18 Ribosomal build-up

Reverse transcribed 18S rcDNA and 16S rcDNA along the growing wheat were quantified using quantitative PCR. Specific primers were used for PCR amplification and standard concentrations (25 pg/µl to 0.0025 pg/µl) were prepared using purified PCR product. The absolute amount of cDNA was calculated using a standard curve analysis. From the results, relative amounts of 16S rRNA to 18S rRNA levels were quantified

## 2.19 Ethylmethane sulfonate (EMS) mutagenesis

The *cue8* seeds (ca. 5000; 100 mg) were pre-imbibed overnight, in 0.1% (w/v) potassium chloride. The next day, the experiment was set up in an Atmos bag (Sigma) in a fume hood. The KCl solution was removed and seeds were soaked for 3-5 hrs, in 0.1 M sodium phosphate pH 5.0, 5% (v/v), dimethyl sulfoxide, and 50 mM EMS (Wilson, 2000; López-Juez and Hills, 2011). Seeds were washed twice in 100 mM sodium thiosulfate for 15 min and later in $dH_2O$ for 15 min. Seeds were dried on a 3MM paper overnight. Mutagenized seeds were sterilised, plated on MS medium and M1 seedlings with good germination were transferred to 50 soil trays. Each tray contained about 50 - 80 growing healthy plants (Table 2.9). The Atmos bag was cut into pieces and all the waste solutions were discarded into a beaker with solid sodium thiosulfate, for 24 hrs to destroy the traces of EMS.

**Table 2.9 EMS mutagenesis of Arabidopsis seeds**

| | |
|---|---|
| M1 seeds | 15000 |
| Seedlings transferred to soil | ca. 100 per pool |
| Total M1 plants | 50 pools |
| Plants successfully grown per pool | 50 - 80 |
| M2 seeds per pool | 20000 - 30000 |
| Seeds used for screening | ca. 2000 |

## 2.20 Suppressor screen

Seeds (M2) were harvested from 50 pools and about 2000 seeds (40 mg) from each pool were sterilised and cultured on 10 MS media plates. The seedling phenotype was observed from day 5 and interesting ones with altered greening were marked. The majority of the seedlings in various pools looked no different from *cue8*, while some were albino and seedling lethal. The screen initially aimed to identify enhanced green cotyledons. Greener seedlings compared to unmutagenised *cue8* (control) were considered as putative mutants and allowed to grow in soil. The phenotype of those individual putative mutants was rechecked in the next generation (M3). The M4 seedlings were used to quantify the chlorophyll and protochlorophyllide content. Additionally, candidate putative mutants were confirmed by genotyping for the *cue8* mutation.

## 2.21 Chlorophyll and protochlorophyllide quantitation

The experiment was set up with 3 biological replicates with the respective controls. For example, in the *cue8* suppressor screen, the WT (5-days old) and *cue8* seedlings (6-days old) served as controls. Out of the homogenous population of 5/6-days old seedlings plated on 1% (w/v) sucrose media, 5 seedlings were immersed in 500 µl of N, N-dimethylformamide (DMF) in labelled eppendorf tubes. Samples were covered with aluminium foil and stored at 4$^{o}$C in the dark overnight to 2 days, with occasional mixing to ensure complete extraction of tissue in DMF solution. All the DMF handling was done in the fume cupboard. The contents were vortexed and centrifuged at 13000 g for 15 minutes and the absorption of the supernatant was recorded (Inskeep and Bloom, 1985), using Thermo Scientific Heλios-β Spectrophotometer, and the amount of chlorophyll (nmol) was calculated per seedling (Porra et al., 1989). Chlorophyll quantitation in wheat was performed in triplicate samples collected

from 6 seedlings (two sections per tube). Tissue sections were weighed prior to extraction, and chlorophyll content was measured per gram fresh weight (Table 2.13).

Protochlorophyllide content was measured using LS 50B spectrofluorimeter (Perkin Elmer, UK) and FL Winlab Scan v4.01 software (Vinti et al. 2005). Five Arabidopsis etiolated seedlings (6-days old) were dipped in the 500 µl DMF. This step was carried out under a very dim green light. The actual number of seedlings was confirmed after recording the fluorescence. Measurements were obtained with an excitation of 433 nm, and emission at 635 nm from a spectrum between 620 nm and 650 nm, through 5 nm slits. After confirming in the short spectrum, the presence of an emission peak at 635 nm, the relative fluorescence value at that wavelength per unit seedling, was used as relative protochlorophyllide quantity.

### 2.22 Cross pollination in Arabidopsis

In the inflorescence, very young floral buds, basal siliques and opened flowers were trimmed off and only unopened larger flower buds were selected. In the bud selected as recipient, the sepals, petals and enclosed anthers were removed, leaving the sticky stigma. On the other hand, from the selected as donor plant, fresh flowers with mature pollens were selected by pressing the base of the sepals, which opened the anthers and allowed to brush pollens on the stigma of the female plant. Forceps were cleaned with 90% (v/v) ethanol after the emasculation and pollination. A piece of cling film was wrapped to cover the stigma from any uninvited pollen and also to reduce the draught stress. Successful cross would result in a bulged and elongated gynoecium after 2 - 3 days. The F1 seeds were collected once the siliques were dry and ready.

### 2.23 Mapping strategy to identify the dominant suppressor

The *soh1* mutation was identified by short-read mapping (SHOREmap) (Schneeberger et al., 2009) of a DNA pool from 150 $BC_1F_2$ recombinant *cue8* phenotype confirmed individual plants (F), as well as 100 unmutagenised *cue8* wild types seedlings (P1) and 100 homozygous *soh1* parents (P2). Sequencing was carried out at the Oxford Genomics centre, Wellcome Centre for Human Genetics (http://www.well.ox.ac.uk/ogc/) and mapping-by-sequencing was performed by using (http://bioinfo.mpipz.mpg.de/shoremap/guide.html) the SHOREmap analysis package. To narrow the region, filters were set for quality reads (>100) and indels were included to make sure the polymorphisms of Bensheim are not considered as casual

mutations. Given the dominant nature of the *soh1* mutation (Fig. 4.9), homozygous non-mutant F2 plants were selected as a mapping population. To identify the dominant mutation a mapping strategy was designed to first compare the polymorphisms in the *soh1cue8* parent (P2, test) caused by mutagenesis and absent in the *cue8* parent (P1, reference) which gave list 1 (Fig. 2.4). Secondly, the polymorphisms (induced mutations) in the backcrossed F2 *cue8* population which are absent in P1 resulted in list 2. In the last step, list 1 was used as test and list 2 as a reference to find out the EMS-induced true SNPs.

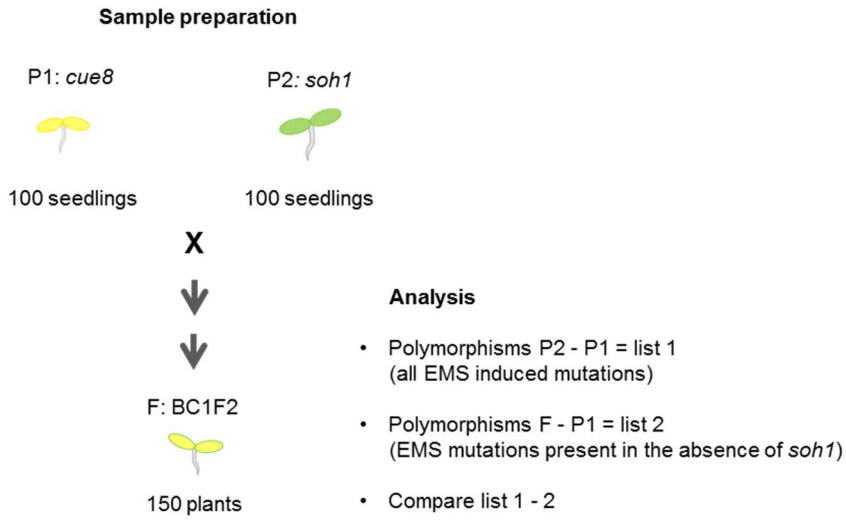


**Figure 2.4** Schematic diagram of mapping by sequencing strategy. DNA samples for sequencing were prepared from unmutagenised *cue8* (P1) and *soh1* (P2) parents as well as *cue8* phenotypes (F) from backcross F2 population. About 100 seedlings from P1 and P2 and newly emerging tender shoots of 150 confirmed F2, *cue8* plants were collected. Analysis of sequencing was done by looking for polymorphisms only in P2 and F (list1 and list2) and the region was narrowed by considering SNPs present in list 1 and absent in list2.

## 2.24 Protein extraction from chloroplasts

Total proteins were extracted from isolated chloroplasts. A freshly prepared, standard Protein Extraction Buffer (PEB) was made (1 ml) by adding 10 µl 1M DTT and 10 µl protease inhibitors (Sigma Aldrich, UK) to 980 µl PEB taken from stock (Table 2.10). About 200 µl of isolated chloroplast suspension (section 2.28.1) was centrifuged (microcentrifuge max. speed) at 4°C and the chloroplast pellet was frozen in a 1.5 ml eppendorf tube with liquid $N_2$. Chloroplast pellet was finely ground placing on ice using a pestle and homogenised by adding 100 µl freshly prepared PEB. The homogenate was centrifuged for 10 min at 4°C and grinding was repeated to dissolve any insoluble material. The supernatant was transferred to a fresh tube and used for protein quantification.

**Table 2.10 Preparation of protein extraction buffer**

| **PEB stock** | |
|---|---|
| Tris-HCl, pH 6.8 | 100 mM |
| Glycerol (v/v) | 10% |
| SDS (w/v) | 0.5% |
| Triton X-100 (v/v) | 0.1% |
| EDTA | 5 mM |

## 2.25 Protein quantitation

Protein concentration was measured using Bradford reagent and standard curve analysis. Dilution series of standard protein concentrations (1, 2, 4, 8 and 10 µl) was prepared from a bovine serum albumin stock (1 mg/ml) adding Bio-Rad protein assay reagent (200 µl) and PEB (1 µl). Protein standards were made up to 1ml by adding an appropriate volume of $dH_2O$. Samples were prepared with 1 µl of extract supernatant by adding equal volumes of reagent and PEB as done for the standard dilution. Absorbance was recorded at 595 nm in the NanoPhotometer (Implen P330, Schatzbogen, Germany). The concentration of unknown samples was determined by the standard curve analysis.

## 2.26 SDS-PAGE

Proteins were separated through sodium dodecyl sulphate-polyacrylamide gel electrophoresis (SDS-PAGE) technique. To the extracted protein, equal volume of 2x loading buffer (1 ml 1M Tris-HCl pH 6.8, 2 ml 10% (w/v) SDS, 4 ml 50% (v/v) Glycerol, 1 ml 0.2% bromophenol blue made up to 10 ml with $dH_2O$) was added. Proteins were denatured at 100ºC for 5 minutes except for the analysis of TIC214, for which an aliquot was incubated at 37ºC for 30 minutes as described by Kikuchi et al (2013). Denatured protein samples, ca. 20 µg and ca. 40 µg, were loaded in the stacking gel beside 8 µl of Precision Plus Protein™ Dual Colour standard ladder (10 - 250 kD) and run in the 1x TGS buffer (25 mM Tris, 250 mM glycine, 0.1% (w/v) SDS in high purity $dH_2O$, pH 8.6). An electric field of 180 volts was applied to the electrophoresis unit and proteins were resolved until the dye had reached the bottom of the gel (ca. 45 min). For every experiment two gels were run simultaneously, one of them was stained with a (ca. 20 ml) Coomassie-based solution (Instant Blue™, Expedeon, UK) for an hour to check equal loading of proteins. The other gel was used for immunoblot analysis. Stock solutions and acrylamide percentage of gels shown below were adjusted

according to the molecular weight of proteins to be analysed (Table 2.11). For example, TIC214, due to its high molecular weight, was resolved through 5% (v/v) gel.

**Table 2.11 Preparation of gels for SDS-PAGE**

| **4x Resolving buffer** | **Stock** | | **4x Stacking buffer** | **Stock** |
|---|---|---|---|---|
| 2M Tris-HCl, pH8.8 | 75 ml | | 1M Tris-HCl pH6.8 | 50 ml |
| 10% SDS (w/v) | 4 ml | | 10% SDS (w/v) | 4 ml |
| $dH_2O$ | 21 ml | | $dH_2O$ | 46 ml |

| **Resolving gel** | **10%** | | **Stacking gel** | **16.5%** |
|---|---|---|---|---|
| Acrylamide stock (30%) | 13.4 ml | | Acrylamide stock | 2.10 ml |
| 4X Resolving buffer | 10 ml | | 4X Stacking buffer | 3 ml |
| $dH_2O$ | 16.6 ml | | $dH_2O$ | 6.9 ml |
| 10% APS (w/v) | 200 µl | | 10% APS (w/v) | 150 µl |
| TEMED | 20 µl | | TEMED | 15 µl |
| Total | 40 ml | | Total | 12 ml |

## 2.27 Immunoblotting of separated proteins

Proteins separated in the SDS-PAGE gels were transferred to nitrocellulose membrane (Amersham™ Protran™ Premium 0.2 µm NC, GE Healthcare Life sciences) for immunoblot analysis. A transfer preparation was made in cold 1x transfer buffer (3 g Tris, 14.4 g glycine, 1 g SDS, 200 ml methanol made up to 1000 ml with $dH_2O$) by aligning Nitrocellulose membrane (6 x 9 cm) on the gel and both sandwiched between filter paper (7 x 10 cm) and sponge. Membrane and gel clip were immersed in the electrophoresis unit with cold 1x transfer buffer and run with 100 v of current for 60 minutes (thin gels) or 90 minutes (thick gels).

The membrane was dried and sliced with the guidance from the colour ladder according to the proteins to be analysed and blocked with Blotto (5% (w/v) dried milk powder mixed in TBS-Tween: 10 mM Tris-HCl, pH8, 150 mM NaCl, 0.05% (v/v) Tween-20) for 30 minutes at room temperature. The membrane was incubated in primary antibody (for dilutions, see appendix) diluted in Blotto (with 0.02% (w/v) Thimerosal) overnight at 4ºC. On the following day, the membrane was washed thrice every 5 minutes with TBS-Tween and incubated with secondary antibody (Anti Rabbit IgG-HRP, Abcam, UK) diluted in Blotto (1:10,000-20,000) for 1 hr at room temperature. The membrane was again washed thrice with TBS-Tween and the immobilised proteins were detected using EZ-ECL Chemiluminescence detection kit (Biological Industries) in the Image Quant ™ LAS 4000 (Fujifilm). Protein bands were analysed using Aida software (Raytest).

## 2.28 Chloroplast protein import

### 2.28.1 Chloroplast isolation

Arabidopsis seedlings (WT: 13-days, *cue8* and *soh1*: 17-days) were grown under 16-h photoperiod (100 - 130 µmol/$m^2$/s) at 20°C. About 1000 - 1500 seedlings from WT and 2500-3000 seedlings from the mutants were grown (ca. 100 per plate) to achieve a good yield of chloroplasts. Seedlings were added to (5 x 20 ml, 1x CIB) chloroplast isolation buffer (0.3 M sorbitol, 5 mM $MgCl_2$, 5 mM EGTA, 5 mM EDTA, 10 mM NaHCO3, and 20 mM HEPES-KOH, pH 8.0) and completely homogenised using Ultra-Turrax T25 Basic at low speed with 4-5 second pulses. The homogenate was filtered through double layered Miracloth (Calbiochem, Merck, Darmstadt, Germany) and pooled into a 250 ml centrifuge tube (Nalgene, Rochester, NY, USA) that was placed in the JA-14 rotor and centrifuged at 1,000 g (2,600 rpm) for 5 min (brake on) at 4°C (Beckman Coulter, Brea, CA, USA). The supernatant was poured off and the chloroplast pellet was resuspended in the leftover buffer by gently rubbing the tube on ice.

In parallel to chloroplast isolation a Percoll gradient was prepared with 13 ml of Percoll medium, 13 ml 2x CIB and dissolving 5 mg glutathione in a 30 ml tube (Nalgene). The content was centrifuged at 43,000 g for 30 min (brake off) at 4°C by setting the deceleration to 1 (JA-20 rotor, Beckman centrifuge). Chloroplast suspension was gently added (with plastic pipette) on top of the Percoll solution without disturbing the gradient and centrifuged at 7,800 g for 10 min (brake off) at 4°C in a swing-out rotor and by setting the deceleration to 1 (JS-13.1 rotor in a Beckman centrifuge). This step allowed separation of intact chloroplasts (lower green layer) from the damaged ones (upper green layer). After removing the upper layer, ca. 2 - 8 ml of intact chloroplast solution was transferred to a fresh 30 ml tube which was then filled with ice-cold 1x HMS buffer (50 mM HEPES NaOH, pH 8.0, 3 mM $MgSO_4$, and 0.3 M sorbitol). The tube was inverted a few times to wash the Percoll solution and centrifuged in a swingout rotor at 1,000 g for 5 min (brake on) at 4°C (JS-13.1 rotor in a Beckman centrifuge). The supernatant was discarded, and the pellet was resuspended in the leftover buffer by gently rubbing the tube on ice until chloroplasts were well separated from the clumps.

Chloroplasts quality and yield were determined by diluting 5 µl of chloroplast suspension in 995 µl 1x HMS buffer and visualising under the Nikon Eclipse 80*i*. Chloroplast dilution (20 µl) was added on to the haemocytometer chamber and covered with a coverslip. Quality was

confirmed by the bright green chloroplasts with their intact boundary. Counting was done in 10 different 0.25 $mm^2$ grid squares with 10x and 20x magnification using phase contrast settings. Chloroplast number per microliter was deduced by taking average count per square (*n*, obtained from 10 squares) x 25 (number of squares) x 200 (dilution factor) x $10^4$ (scaling factor, since the volume above 25 squares is 0.1 $mm^3$). For each time course, approximately $1x10^7$ chloroplasts were added to carry out import assays.

### 2.28.2 In-vitro synthesis of radiolabelled preproteins

Protein import into isolated intact chloroplasts was carried out as described in the published protocol (Aronsson, 2002) using the $T_NT^®$ T7 Quick for PCR DNA kit (Promega, USA). Plasmids with cDNA inserts encoding precursor of the small subunit of Rubisco (pSS) and plastid ribosomal protein L11 (pRPL11) downstream to T7 promoter were purified as described in section 2.28.4. The cDNA was PCR amplified using standard M13 primers and confirmed by gel electrophoresis. *In-vitro* transcription and translation reaction (40 µl $T_NT$ PCR Quick master mix, 2.5 µl of 11 µCi/µL radiolabelled [$^{35}S$] methionine, 5 µl of 100–800 ng PCR product and 2.5 µl $dH_2O$) was performed to synthesize radiolabelled preproteins.

### 2.28.3 Chloroplast preprotein import

Import of preprotein into chloroplasts was performed by modifying the procedure described in Aronsson and Jarvis, (2002). A master mix (1M k-gluconic acid, 1M $NaHCO_3$, 20% (w/v) BSA, 100 mM Mg-ATP, 250 mM methionine, 65 mM L-cysteine) was prepared for 4 reactions (time points) per genotype. According to the yield of isolated chloroplasts the 10x HMS buffer and plastid suspension were added to the mixture (Table 2.12). The precursor protein (radiolabelled) and the plastids were added just before the reaction. An import stop reagent (ice-cold 50 mM EDTA dissolved in 1x HMS buffer) was distributed in different tubes and placed on ice. Import assays were carried out in 2ml tubes placed on water bath maintained at 25ºC with a continuous white light (100 µmol $m^{-2}$ $s^{-2}$). After every time point an aliquot (140 µl) from the reaction was quickly pipetted into an equal volume of the import stop solution. The tubes were centrifuged at 10000 rpm for 1 min, the supernatant was discarded, and the chloroplast pellet was snap-frozen.

**Table 2.12 Reaction mixture for protein import assays**

| Reagent | Volume |
|---|---|
| $dH_2O$ | Up to 600 µl |
| 10x HMS | Variable |
| 1M k-gluconic acid | 12 µl |
| 1M $NaHCO_3$ | 6 µl |
| 20% BSA (w/v) | 6 µl |
| 100mM Mg-ATP | 30 µl |
| 250mM methionine | 24 µl |
| 65mM L-cysteine | 24 µl |
| Precursor | 20 µl |
| Plastids | 4 x 10^7 |
| Total (per 4 time points) | 600 µl |

### 2.28.4 Analysis of protein import

Chloroplast pellets obtained from import reaction were dissolved in ca. 20 µl 2x loading buffer (see section 2.26) mix (900 µl 2xLB and 10 µl DTT). The chloroplasts obtained from import reactions were denatured at 90ºC for 5 minutes and run through SDS-PAGE system (15% gel). A control was prepared with precursor protein (1 µl and 9 µl 2x LB mix) and loaded alongside the ladder (for SDS-PAGE and staining see section 2.25). The gels were destained for an hour and soaked on a pre-cut Whatman filter paper with pure water (removing air bubbles) and dried in the vacuum dryer set at 80ºC for 2 hours. The dried gel (filter paper) and a Storage Phosphor Screen (GE Healthcare) were aligned in the exposure cassette and stored in the dark overnight. Autoradiography results were recorded in the phosphor imager (Strom 860, Molecular imager, Amersham Biosciences)

## 2.29 Microbiology techniques

### 2.29.1 Preparation of LB media

Luria-Bertani (LB) broth was prepared to culture the *E. coli* and *Agrobacterium* cells. Ingredients used were peptone/tryptone (10 g), NaCl (10 g) and yeast extract (5 g) dissolved in 1 litre $dH_2O$ adjusted to pH 7.5 and autoclaved at 121ºC for 21 minutes. In case of solid media, the LB broth was mixed with 15 g of agar (Melford BioLaboratories Ltd.) per litre before autoclaving and poured in microbiology petri dishes.

### 2.29.2 Gateway cloning

Selective genes were transformed and expressed using Arabidopsis using Gateway® Technology (Invitrogen) following the manufacturer's protocol. Gene-specific cDNA was PCR amplified with selected primers in the first round and gel purified using QIAprep Spin Miniprep, (QIAGEN). The purified product was re-amplified using primers which also contained additional attB sequences. The cDNA was inserted into a pDONR201™ vector by recombination between the attP sites of vector and the flanked attB sites on either side of the gene. The reaction was performed using BP Clonase enzyme™ and inactivated by a proteinase K solution. Recombinant entry plasmid was transformed into One Shot® TOP10 *E. coli* competent cells (Thermo Fischer, UK). Transformants were genotyped by gel electrophoresis of PCR products and sequenced (Eurofins Genomics). Entry plasmid clones were isolated from the positive colony culture (with an appropriate antibiotic) and recombined with a destination vector pB2GW7 carrying attR sites. This reaction was catalysed by an LR Clonase enzyme™ that was inactivated by again Proteinase K solution. The final expression vector with the gene of interest was transformed first into TOP10 *E. coli* cells, confirmed by sequencing and later transformed into *Agrobacterium* with appropriate antibiotics in the culture medium. With the help of *Agrobacterium*, the gene was transferred to Arabidopsis plants. Antibiotics and concentrations for screening of transformants is listed in the appendix.

### 2.29.3 Transformation of *E. coli* competent cells

Recombinant plasmids constructed during the cloning procedure were transformed into One Shot® TOP10 *E. coli* competent cells by chemical transformation method as described in Gateway® Technology manual. Competent cells (50 µl aliquot) were thawed on ice for 20 minutes. The solution from BP and LR reaction was added to the *E. coli* cells on ice and gently mixed by flicking the tubes and incubated for 30 mins. Cells were heat-shocked at 42ºC for 30 seconds and immediately placed on ice for 2 minutes. A sterile S.O.C medium (450 µl) was added to propagate the cells for 1 hour at 37ºC. Two different volumes of mini-culture were plated on LB agar plates with appropriate antibiotics. Upon successful transformation, colonies appeared on the following day.

### 2.29.4 Plasmid isolation

Plasmids cloned in the bacterial cells (*E. coli*/*Agrobacterium*) were purified using QIAprep® Miniprep (QIAGEN) following the manufacturer's instructions. Cell pellets centrifuged from overnight bacterial cultures were lysed with the buffer also containing RNase A. The supernatant containing plasmid was loaded onto the QIAprep 2.0 spin column for the binding which was treated a couple of times with wash buffers. The plasmid was retained in the elution buffer and quantified for further use.

### 2.29.5 *Agrobacterium* transformation

Destination plasmid containing transformed insert was finally transformed into *Agrobacterium* using the Freeze-Thaw method. *Agrobacterium* competent cells were prepared by culturing (50 ml, until the $OD_{600}$ showed 0.5 to 1.0) at 28ºC for overnight (250 rpm). The culture was cooled by placing on ice and centrifuged at 3000 g for 5 mins at 4ºC. Cell pellet was resuspended in 1 ml of 20 mM ice-cold $CaCl_2$ solution and aliquoted as 100 µl competent cells and stored at -80ºC for longer use. About 1 µl plasmid (100 - 200 ng) was added to the competent cells thawed on ice and flash frozen in liquid nitrogen. The tube was thawed at 37ºC for 5 mins and incubated at 28ºC by adding 1 ml LB broth and gentle shaking for 2 - 4 hrs. The tube was centrifuged for 30 seconds at 5000 rpm, the supernatant was discarded, and the pellet was resuspended in retained liquid. About 100 µl was spread on LB agar plate containing appropriate antibiotics and incubated at 28ºC. Colonies appeared after 2 days were screened for transformants.

## 2.30 Arabidopsis transformation (Floral dip method)

Healthy growing Arabidopsis plants were trimmed to encourage more flowers a few days prior to transformation. Overnight *Agrobacterium* (200 ml) cultured at 28ºC, inoculated with a freshly grown 5 ml starter culture was centrifuged at 5000 rpm for 10 mins. Pellet was resuspended in a 5% (w/v) sucrose solution with the silwet L-77 (0.01% (v/v)). Plants with flower buds (removing siliques and opened flowers) were dipped for 30 seconds in *Agrobacterium* solution with gentle shaking. Dipped plants were covered with foil and left in the dark for 24 hrs before transfer to light. Seeds were harvested and screened with appropriate antibiotics.

## 2.31 Analysis of chloroplast quantitative data

For chloroplast compartment analysis quantitative data (cell area, mean area of 10 chloroplasts and the total number of chloroplasts) was obtained from four intact mesophyll cells per each slide. A total of 48 cells were analysed from four slides prepared out of each replicate. Statistical analysis and boxplots were performed using the R package (for codes see appendix).

**Table 2.13 Summary of various parameters and data analysis**

| Parameter | Calculation | Significance |
|---|---|---|
| Cell area | Mean area, n = 48<br>(16 x 3 replicates per section) | Expansion of mesophyll cells |
| Chloroplast area | Mean chloroplast area (n=10 in each cell) from 48 cells per section | Increase in growth of chloroplasts along the developing leaf |
| Chloroplast Count | Mean of total chloroplasts in 48 cells | Change in chloroplast number |
| Chloroplast proliferation | Slope values of chloroplast count between adjacent sections | Rate of change of chloroplast number |
| Total chloroplast area | Total chloroplast number X mean chloroplast area | Chloroplast build-up |
| Chloroplast compartment | (Total chlp. number X mean chlp. area) / cell area | Proportion of the cell occupied by chloroplasts |
| Chloroplast compartment growth rate | Slope values of chloroplast compartment between adjacent sections | Rate of change of chloroplast occupancy |
| Chloroplast ribosome investment | 16S rRNA / 18S rRNA | Cellular investment |
| Chloroplast ribosome density | 16S rRNA / Total chloroplast area | Ribosomes per chloroplast |
| Chloroplast genome copy number per cell | cpDNA / gDNA<br>Mean of triplicate samples | Chloroplast DNA replication |
| Chloroplast genome copy number per chloroplast | cpDNA / Total number of chloroplasts | Number of chlorop. DNA copies per chloroplast |
| Chlorophyll content | Chl.Tot. = $19.43*A_{646.8} + 8.05*A_{663.8}$ | Photosynthesis along the developing leaf |

# Chapter 3

# Characterisation of the molecular phenotype of *cue8* - Activation of a compensatory mechanism

## Statement of authorship

Confocal microscopy data was obtained in combined work with Zaki Ahmad (Prof. Laszlo Bogre, Royal Holloway)

The current research focuses on the *cue8* mutant (Fig. 3.1), that was identified due to its reduced expression of the *LHCB* gene and has a slow greening phenotype (Lopez-Juez et al., 1998). Seedlings of *cue8* exhibit defects in plastids prior to light exposure (Vinti et al., 2005).


**Figure 3.1** Phenotype of *cue8* mutant and pOCA108 wild type (WT). Arabidopsis plants grown for 6-weeks under 16 h photoperiod, *cue8* showing a virescent phenotype and a development delay compared to WT.

Previous research had revealed the identity of *CUE8* by map-based cloning as AT5G22640 (Maffei, 2008). The encoded protein has MORN (multiple Membrane Occupation and Recognition Nexus) motifs and is essential for embryo development, having also been identified as *EMB1211* (*Embryo defective 1211*), and for chloroplast biogenesis. Loss of EMB1211 leads to embryo lethality (Liang et al., 2010; Kikuchi et al., 2013). However, the mutant identified through forward genetics, *cue8,* suffers a point mutation in exon 6 (G ≡ C to A = T transition) and results in a single amino acid change (glycine to arginine at position 366), just outside one of the predicted MORN domains. This transition mutation has resulted in partial loss of function, hence allowing the carrying out of molecular studies. The work described in this chapter has the following objectives:

- To understand whether CUE8 plays a role in overall plant growth, cellular chloroplast distribution and chloroplast gene expression.
- To characterise the housekeeping and photosynthetic gene expression in defective chloroplasts of *cue8* mutants.
- To analyse whether the overexpression of known positive regulators of chloroplast development or the removal of chloroplast-nucleus signalling could rescue *cue8* phenotype.

### 3.1 *cue8* delays overall plant growth with poorly developed chloroplasts

Previously generated transgenic lines of pOCA108 (WT) and *cue8* containing a ds-RED reporter were used to study the plastid distribution. The ds-RED was tagged with a RecA transit-peptide that targets it to plastids (Haswell and Meyerowitz, 2006). Analysis of seedlings on 1% (w/v) sucrose media showed that loss of functional *CUE8* delays growth of both leaves and roots (Fig. 3.2 A). The analysis was done in whole-mounts of cotyledons or roots visualised by Nomarski and fluorescence microscopy. Although the fluorescence emission is a combination of both chlorophyll and ds-RED, the control image without a reporter indicates that the majority of the signal is produced from ds-RED (Fig. 3.2 B). Seedlings of *cue8* showed poorly developed chloroplasts in the shoot as well as in root cells (Fig. 3.2 C), revealed by the weak signal compared to the WT seedlings. The loss of bright fluorescence in both photosynthetic and non-photosynthetic tissues revealed *cue8* suffers a global plastid defect and impacts the overall growth of plants.

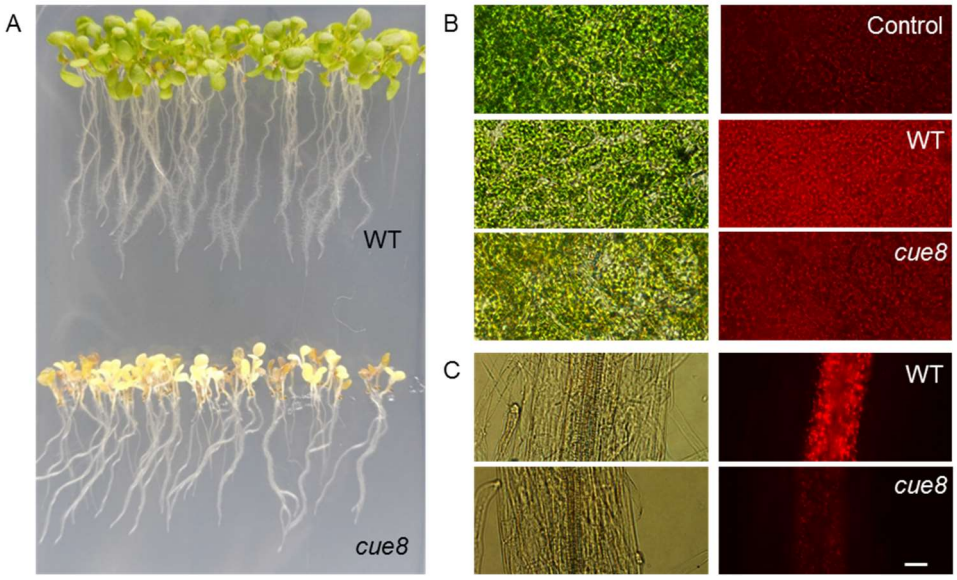


**Figure 3.2** *cue8* mutation leads to a global plastid defect. The mutation in *CUE8* delays the plastid development in both leaf and root tissues. Seedlings contain a ds-RED reporter protein that is targeted to plastids (A) Phenotypic comparison of 7-day-old pOCA108 (wild type) and *cue8* seedlings grown on 1% sucrose media. (B) Chlorophyll fluorescence in the WT cotyledons without plastid-targeted ds-Red (Control). Fluorescence emitted by the ds-RED in the WT and *cue8* cotyledons as well as in the (C) root samples. Scale bar (B and C) represents 25 µm.

Knowing the fact that sucrose supports growth of severe mutants, in order to study whether insufficient photosynthate from impaired plastids has a role in the phenotype, *cue8* seedlings were supplemented with varying sucrose concentrations (0, 20 mM, 40 mM and 60 mM). As expected, the overall growth of the mutants was severely affected in the absence of sucrose

showing no sign of growth even after 15-days of germination (Fig. 3.3 A). The difference between the roots of *cue8* and WT was 28 mm in the no-sucrose plates while 40 mM sucrose reduced this difference to 11 mm. Sucrose rescued the root phenotype, in a dose-dependent manner, to a large extent but incompletely at 40 mM concentration. Higher sucrose concentrations inhibited growth of the seedlings (Fig. 3.3 A and B). Confocal microscopy was performed on the seedlings grown for 15-days on 40 mM sucrose. Distance from the quiescent center to cells in the elongation zone was calculated based on the individual cell lengths, which allow the determination of the least distal cell division event. The data revealed that *cue8* roots have a smaller meristem (Fig. 3.3 C). The root growth studies provide evidence which demonstrates a direct role of *CUE8* in non-photosynthetic tissues.

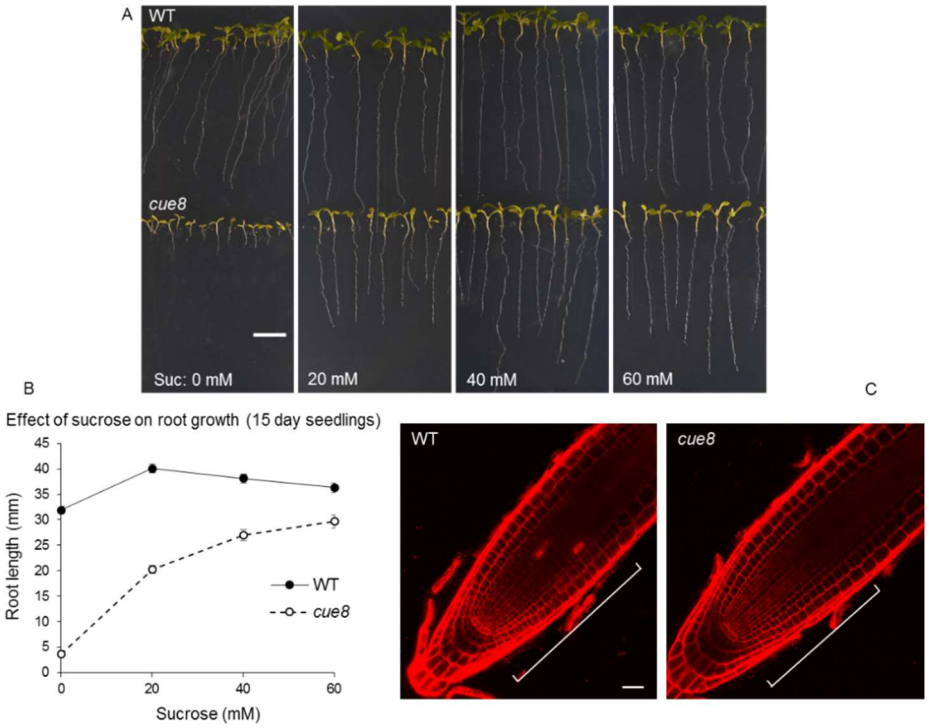


**Figure 3.3** Developmental delay of *cue8* roots is partly rescued by sucrose supplementation. (A) Seedlings of *cue8* and WT grown for 15-days on vertical plates on media containing sucrose with indicated concentrations. (B) Root length of seedlings (shown in A). Error bars represent standard error of the mean (SEM) of replicate samples, n = 30. (C) Confocal images of the meristematic zone of propidium iodide-stained representative roots of *cue8* and WT grown, on vertical plates containing 40 mM sucrose. The oblique line indicates the approximate meristematic zone, from the quiescent centre to the point at which cells of the cortical layer initiate expansion. Scale bar represents (A) 1 cm and (C) 25 µm.

### 3.2 Roots in *cue8* show smaller meristem yet larger meristematic cells

A further investigation was carried out into roots at the cellular level in the seedlings grown on 40 mM sucrose. The confocal microscopy technique showed a reduced size of the root

meristem in *cue8*, due to fewer cells, which explains the smaller roots (Fig 3.4 B). An unexpected observation in the mutants was the increase in individual meristem cell size (Fig. 3.4 C). The results were confirmed even in the *cue8*$_{col}$ line obtained by introgression of the *cue8* mutation into Columbia for 6 generations. The peculiar meristem phenotype highlights the importance of *CUE8* for cell division in the root meristem.

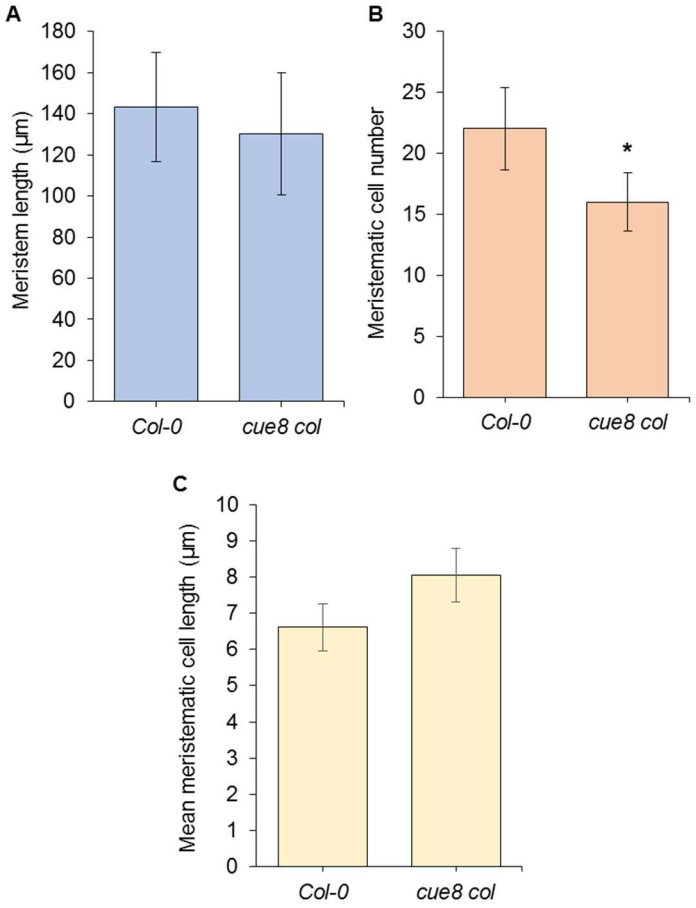


**Figure 3.4** Analysis of confocal data on root meristem of *cue8* seedlings compared to WT. (A) Length of the root meristem (µm) analysed from quiescent center to zone of elongation using imageJ software. (B) The root cells in *cue8* showing reduced meristem cell count ($p < 0.05$), and (c) increased average size of individual root meristematic cell. Error bars represent standard deviation of total replicates (n=6) of an independent experiment. Data obtained jointly with Zaki Ahmad, L. Bogre laboratory.

### 3.3 *cue8* cells have a reduced chloroplast compartment

To pursue the development of plastids in green tissues, the "chloroplast compartment" was measured in the mutant at different developmental stages. The chloroplast compartment, chloroplast coverage or cell index is referred as the ratio between the plan area of all chloroplasts in one cell and the plan area of that cell. Individual cells from cotyledons (Fig. 3.8 A), young virescent (Fig. 3.6 A), and mature rosette leaves (Fig. 3.6 A) were mounted

after fixation and cell separation, to quantify the chloroplast filling. The DIC microscopy data showed that the chloroplast number in mesophyll cells of *cue8* was slightly increased relative WT, but the size of individual chloroplasts was only 10 µm$^2$ which is reduced to 35% of the WT (Fig. 3.5 B). Therefore, the cellular chloroplast compartment was reduced in the mutant compared to similar sized mesophyll cells in the WT (Fig. 3.5C).

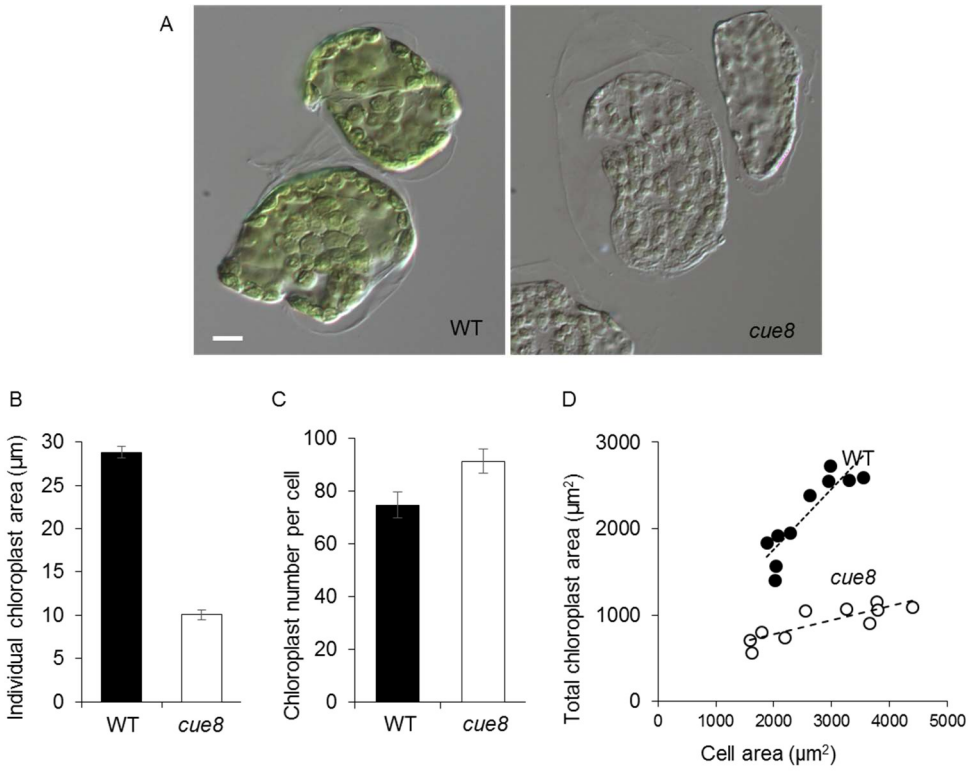


**Figure 3.5** Cellular chloroplast compartment in the cotyledon distal half. (A) Cells of WT (5-days-old) and *cue8* (6-days-old) were isolated from fixed cotyledons and separated and viewed by Nomarski optics. Scale bar: 10 µm. (B) Chloroplast area measured from 10 chloroplasts in each cell by considering 5 cells per replicate. Error bars represent standard error of the mean (SEM) of replicate samples, n=10. (C) Total number of chloroplasts in a mesophyll cell of cotyledon. (D) Total chloroplast area plotted relative to cell plan area.

The total cellular occupancy of chloroplasts, measured as plan area relative to the cell's plan area in *cue8* was indeed reduced due to smaller chloroplasts, but eventually became closer to that of the wild type (Fig. 3.5 C, 3.6 D and 3.7 D). Actually, the size difference in the chloroplasts between mutant and WT was greater in the seedlings, however this became smaller as development progressed, from 61% in young leaves to 77% in rosette leaves (Fig. 3.6 C and 3.7 C). This observation clearly matches the phenotypic gradient of slow growing *cue8* cells.

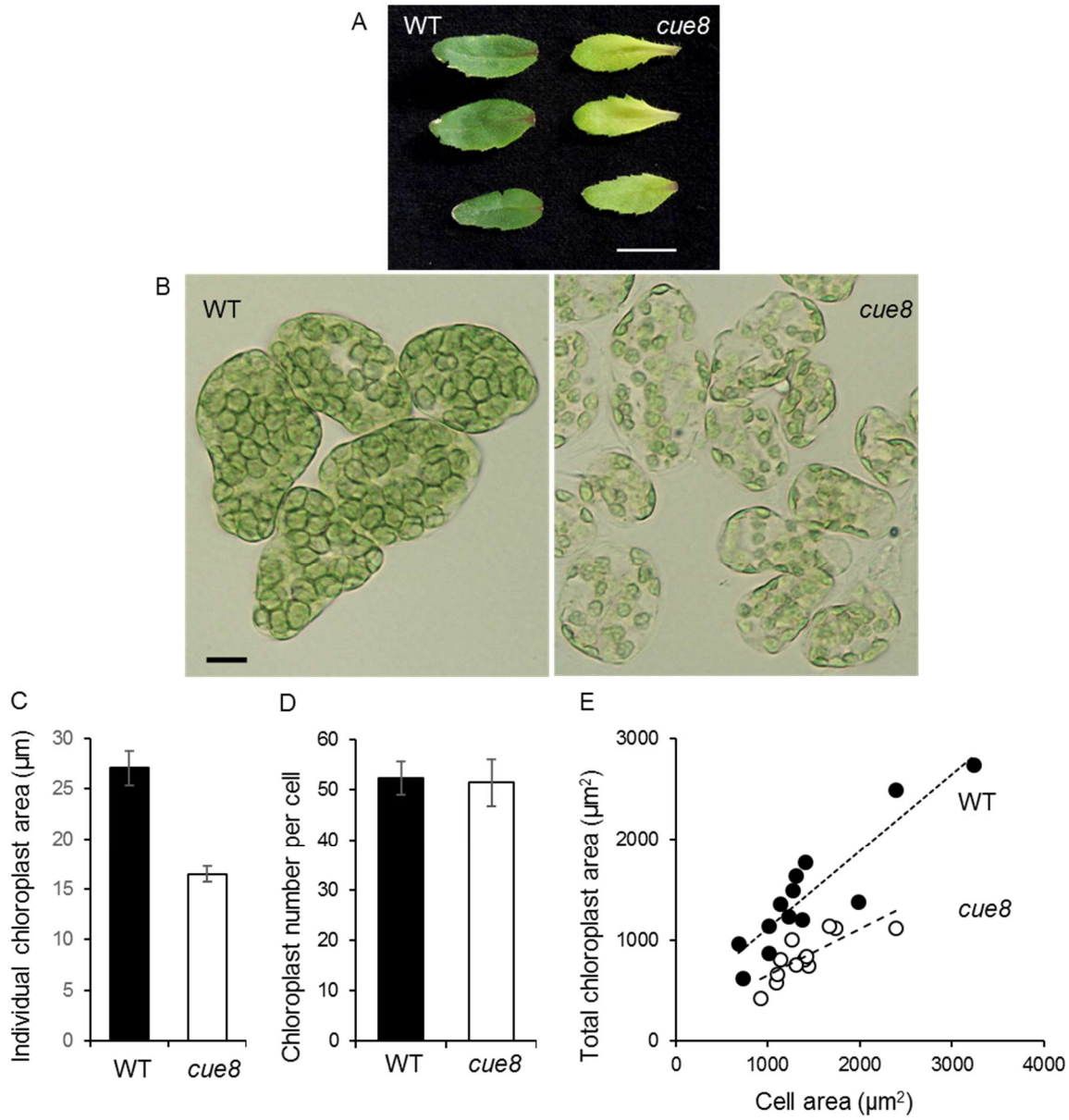


**Figure 3.6** Cellular chloroplast compartment in the young leaf distal region. (A) Image of young *cue8* (virescent) and WT leaves collected after 4-weeeks of growth in a 16h photoperiod. Scale bar represents 1 cm. (B) Mesophyll cells mounted from the distal half of fixed young leaves of *cue8* and WT, separated and viewed by Nomarski optics. Scale bar: 10 µm. (C) Chloroplast area measured with 10 chloroplasts in each cell by considering 5 cells per replicate. Error bars represent standard error of the mean (SEM) of replicate samples, n=13. (D) Total number of chloroplasts in a mesophyll cell of juvenile leaf. (E) Total chloroplast area plotted relative to cell plan area.

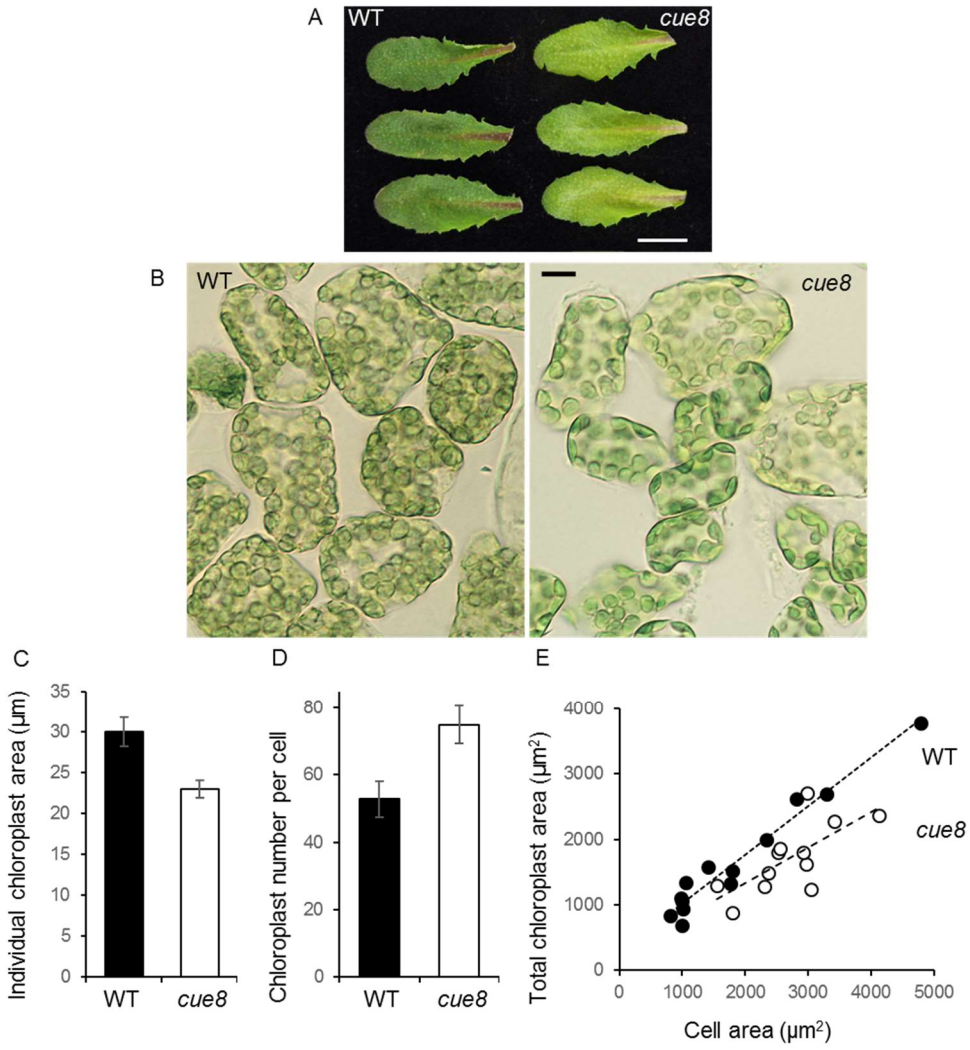


**Figure 3.7** Cellular chloroplast compartment in the mature rosette leaf distal region. (A) Image of young *cue8* (pale) and WT leaves collected after 4-weeeks of growth in a 16h photoperiod. Scale bar represents 1 cm. (B) Mesophyll cells mounted from mature leaves were separated and viewed by Nomarski optics. Scale bar: 10 µm. (C) Chloroplast area was measured with 10 chloroplasts in each cell by considering 20 cells per replicate. Error bars represent standard error of the mean (SEM) of replicate samples, n=12. (D) Total number of chloroplasts in a mesophyll cell of mature leaf. (E) Total chloroplast area plotted relative to cell plan area.

### 3.4 Molecular genetic phenotype of *cue8* chloroplasts

The cpDNA is often observed to associate with the inner membrane of the chloroplasts. Genes tightly co-expressed during development with AT5G22640 frequently contained gene ontology terms associated with early chloroplast development, particularly transcription and translation (Maffei, 2008). Therefore, further investigation was carried out to see if the CUE8 protein played any role in regulating plastid gene expression. Any peculiar phenotype would serve as a case study to learn how plastids tune their molecular processes while suffering development defects.

Chloroplast gene expression is carried out by a nucleus-encoded as well as a plastid encoded RNA polymerase. qPCR-determined gene expression analysis was performed for selected genes in 5-day old *cue8* seedlings, albeit they appeared developmentally slightly smaller compared to WT of identical age (Fig. 3.8 A). Four of the selected genes, *psaA, psbA, rbcl, ndhA* are transcribed by Plastid-Encoded Polymerase (PEP). The other four genes, *accD, rpoA, rpoC1, rps18* are transcribed by Nucleus-Encoded Polymerase (NEP), while the promoters of two genes, *clpP* and *ndhH*, are recognised by both polymerases. The *LHCB1* gene was selected as a nucleus-encoded gene. Analysis revealed a gene expression pattern among the selected genes in *cue8* showing a down-regulation of mRNA levels transcribed by PEP and yet, paradoxically, elevated NEP-driven transcript levels in the chloroplast, with the exception of *accD* (Fig. 3.8 B).

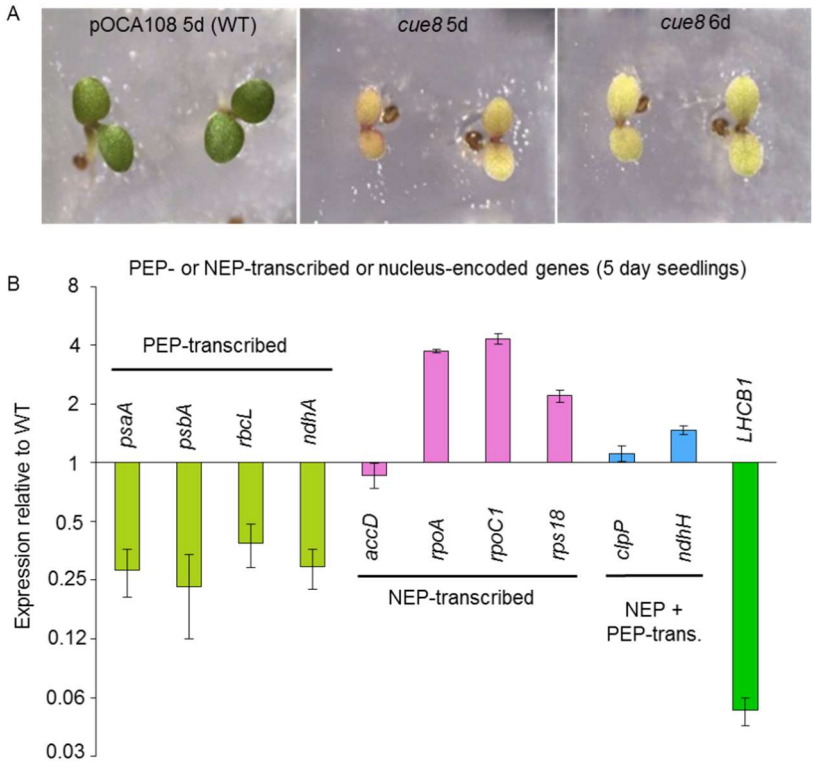


**Figure 3.8** Expression analysis of nucleus and chloroplast-encoded genes in 5-days-old *cue8* seedlings. (A) Images showing seedlings of the WT and *cue8* at different days of growth. (B) Expression of each gene was measured relative to a constitutive gene, and the values were calculated for *cue8* relative to the corresponding values of the wild type. The relative values are represented on a log2 scale, but the numbers on the scale are actual ratios, a value of 1 representing the expression in the wild type. Genes transcribed by the Plastid-encoded polymerase (PEP), the Nucleus-encoded polymerase (NEP) or both are indicated by different colours and the accompanying labels. The transcript level of the nucleus-encoded *LHCB1* gene, encoding a photosynthetic antenna protein of photosystem II, is also provided. Error bars represent standard error of the mean (SEM) of triplicate samples.

As *cue8* mutants are slow in growth, and in order to have a similar developmental stage the experiment was repeated with slightly older seedlings (6-days) compared with WT grown for 5-days (Fig. 3.8A). Relative measurement of transcripts of the above genes revealed reduced repression of PEP-driven gene expression and photosynthesis-associated nuclear gene expression (*LHCB1*) and maintenance of the elevation of NEP-driven gene expression (Fig. 3.9) over time. The results are reproducible as shown by 4 independent experiments; therefore it was concluded that *cue8* is defective in the expression of PEP-dependent genes but exhibits elevation in the expression of NEP-dependent chloroplast-encoded genes.

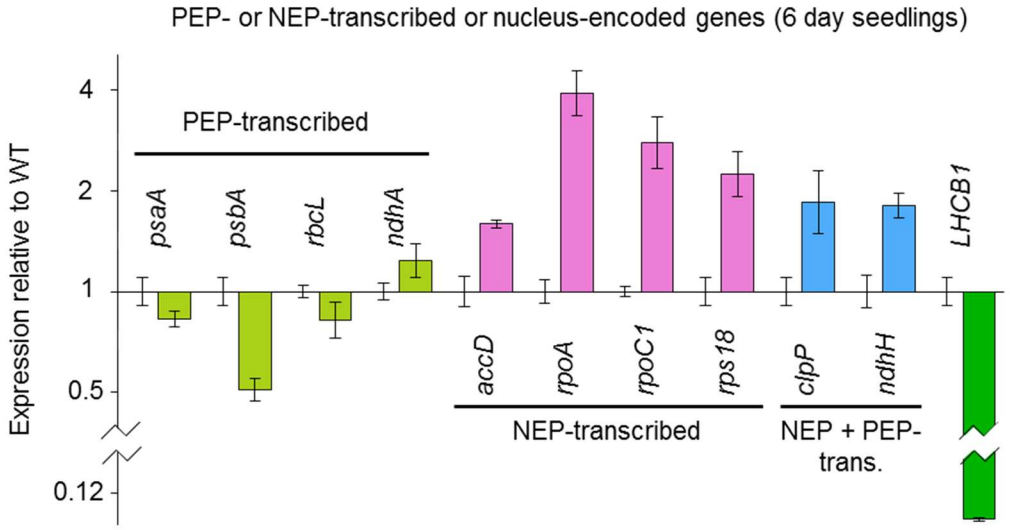


**Figure 3.9** Expression analysis of nucleus and chloroplast-encoded genes in 6-days-old *cue8* seedlings. Transcript levels, determined by quantitative real-time RT-PCR, of chloroplast-encoded genes in mutants, relative to WT (5-days-old). A value of 1 represents the corresponding transcript level in the WT. Genes transcribed by the Plastid-encoded polymerase (PEP), the Nucleus-encoded polymerase (NEP) or both are indicated by different colours and the accompanying labels. The transcript level of the nucleus-encoded LHCB1 gene, encoding a photosynthetic antenna protein of photosystem II, is also provided. Data were obtained from three independent biological samples and plotted on a log2 scale as shown in figure 3.8 B. Error bars represent standard error mean (SEM) of average of triplicate samples.

After its import into chloroplasts, NEP transcribes the genes of the multi-subunit PEP components. Two of the above selected genes transcribed by the NEP, *rpoA* and *rpoC,* are translated to subunits of PEP. It is paradoxical that while there are more transcripts of PEP components, the PEP is less active in the *cue8* chloroplasts. To understand the apparent increase of NEP activity in seedlings and decrease in the levels of PEP-driven transcripts, in spite of the elevated copies of mRNA for PEP, the gene expression analysis was carried out for the nucleus-encoded polymerases (*RPOTp, ROPTm* and *RPOTmp*) and PEP-associating

sigma factors (*SIG1-SIG6*). Indeed, the gene expression of NEPs in the *cue8* seedlings showed over 2-fold elevation, with simultaneous reduction of mRNA levels of four sigma factors *SIG1*, *SIG2, SIG4* and *SIG5* (Fig. 3.10). Meanwhile expression of *SIG3* and *SIG6* was similar to WT. The control of SIG expression could be a possible reason for the down regulation of PEP activity as part of anterograde control.

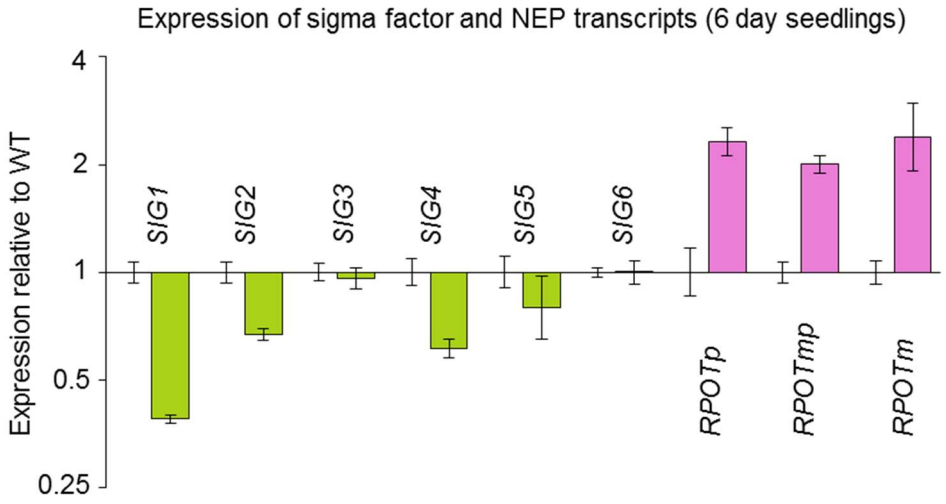


**Figure 3.10** Expression of nucleus-encoded organellar RNA polymerases and co-factors. Transcript levels of different NEPs targeted to the plastids (*RPOTp*), mitochondria (*RPOTm*) or both (*RPOTmp*) and sigma factors encoded by the nucleus, in 6-day old *cue8* relative to WT (5-day old). The values obtained were plotted on a log2 scale as shown in figure 3.8 B. Error bars represent standard error mean of the (SEM) of triplicate samples.

### 3.5 Defective *cue8* chloroplasts have densely packed plastome

In order to investigate how defective chloroplasts managed to elevate the expression of NEP-driven genes and provide the conditions for activity of the increased nucleus-encoded chloroplast proteins, a study was conducted to quantify the plastid genome copies. The absolute number of cpDNA copies was quantified by standard curve analysis using qgDNA-PCR. Sequences spanning three plastome genes covering different regions - *rbcL* (large single copy region), *ndhG* (small single copy region) and *ycf2* (inverted repeat region)- and two nuclear gene sequences, *HO1* and *CHS,* were selected. The quantitative-PCR results were shown to be robust by the fact that the plastid *ycf2* exists in two copies (both inverted repeats) and its expression values were almost doubled compared to its neighbouring plastid genes (single copy regions).

Surprisingly *cue8* maintained its number of chloroplast DNA copies regardless of the defective plastid biogenesis (Fig. 3.11 A), which helps explain the increased levels of

*RPOTp, RPOTmp* transcripts through the availability of sufficient templates for increased NEP activity. When calculated, the ratio of plastome copies per $\mu m^2$ of chloroplast area was only 27% in WT, which was raised to 58% in *cue8* seedlings (Fig. 3.11 B). This was further supported by the fluorescence microscopy of cotyledons. The DAPI stained mesophyll cells of *cue8* were densely packed with cpDNA while that of WT contained less densely packed scattered plastome (Fig. 3.11 C).

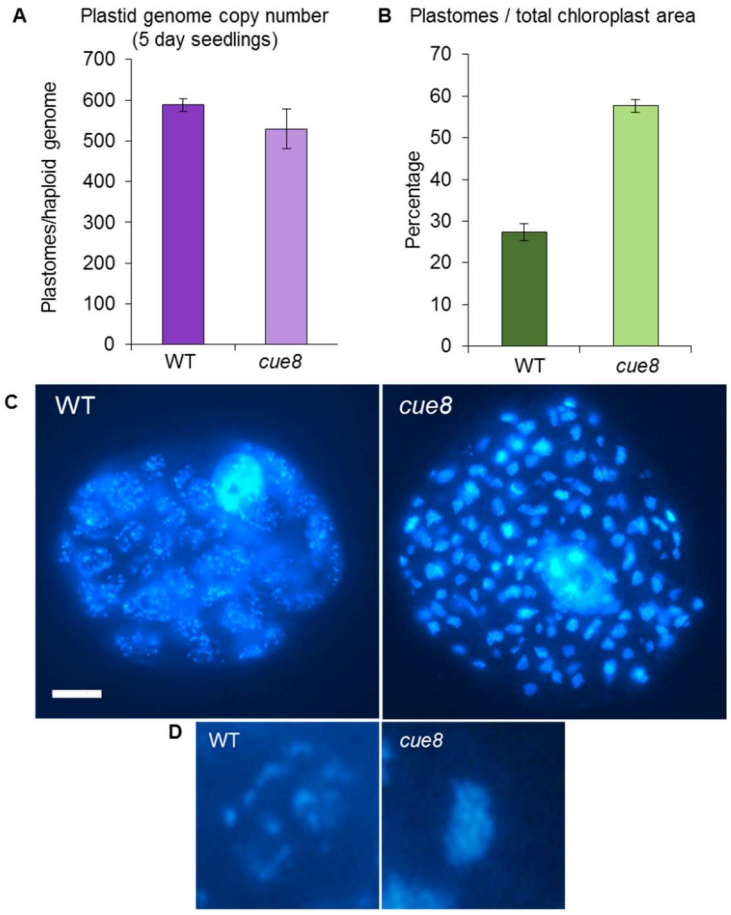


**Figure 3.11** Analysis of chloroplast DNA in *cue8* seedlings. (A) Genome copy number was quantified by real time PCR and standard curve analysis of cpDNA and genomic DNA sequences in *cue8* (6-days old) and WT (5-days old) seedlings. Bar graph represents the absolute copies of cpDNA quantified as the ratio of the mean of 3 plastid genes (*rbcL, ndhG* and *ycf2*) over the mean of 2 nuclear genes (*HO1* and *CHS*). Error bars represent standard error of the mean (SEM) of triplicate samples. (B) Percentage of cpDNA copies per total chloroplast area measured in the seedling; *cue8* maintains its genome copies in spite of the reduced chloroplast compartment (see figure 3.4C). Error bars represent standard error of the mean (SEM) of triplicate samples, the genome copy number was normalised against the total chloroplast area of the respective genotype. (C) Fluorescence microscopy of DAPI stained mesophyll cells in the cotyledons imaged with a x60 objective. Scale bar: 10 µm. (D) Individual chloroplast showing distribution of cpDNA in WT and *cue8*.

It was shown that Arabidopsis nucleotide synthesis-deficient *crinkled leaves* (*cls8*) mutant suffered developmental defects with reduced cpDNA copies in addition to reduced chloroplast compartment, pale emerging leaves and short roots (Garton et al., 2007). To address if there is any relation between chloroplast DNA replication and chloroplast compartment, a question arises as to whether a relation exists between plastid number, size and plastome copy number and size of the cell. This was addressed by analysing the *arc6* mutant (Pyke et al., 1994) defective in chloroplast division. Interestingly the 2 larger chloroplasts per cell of *arc*6 have normal coverage and showed similar amounts of plastome copies to WT that carry ca. 80 plastids per cell in cotyledons (Fig. 3.12). Taken together, despite reduced chloroplast compartment particularly in new leaves, the cells of *cue8* have maintained their cpDNA replication.

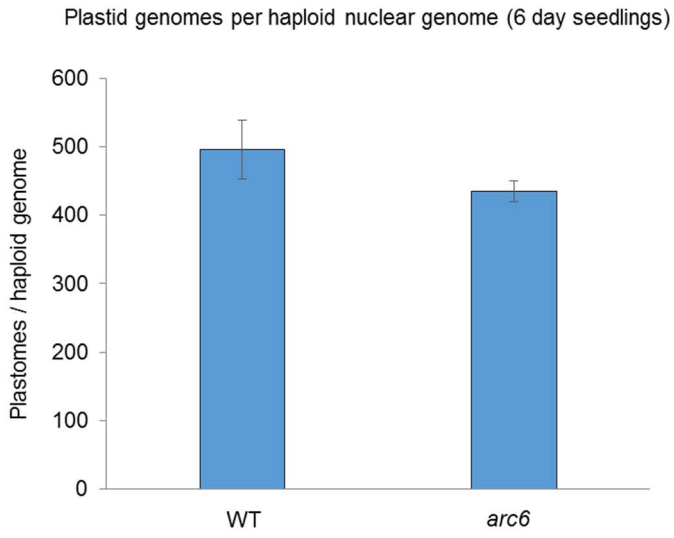


**Figure 3.12** Quantitation of cpDNA copies in *arc*6 seedlings relative to WT. Chloroplast plastome copies per haploid nuclear genome determined by quantitative real-time genomic-PCR. Quantitation was done as shown in figure 3.11 A. The ratio of plastid to nuclear genome is similar to WT in *arc*6 mutants in spite of the defective plastid division. Error bars represent standard error of the mean (SEM) of triplicate samples.

To understand chloroplast DNA replication in *cue8*, the expression of dual targeted organellar DNA polymerses (*POL IA* and *POL IB*) was quantified. There was a mild elevation in the expression of *POL IB,* possibly contributing to maintain chloroplast DNA replication (Fig. 3.13).

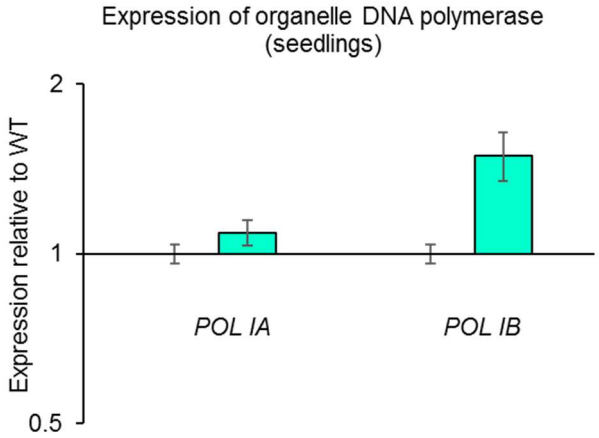


**Figure 3.13** Gene expression analysis of organelle DNA polymerases. Transcript levels determined by quantitative real-time RT-PCR in *cue8* (6-days old) relative to WT (5-days old) seedlings. The values obtained from replicate samples were plotted on a log2 scale as shown in figure 3.8 B. Error bars represent standard error of the mean (SEM) of triplicate samples.

## 3.6 Comparison of the *cue8* molecular phenotype with that of known protein import mutants

Given that *cue8* impacts on plastid biogenesis and activates a homeostatic mechanism, it was logical to ask whether the compensatory mechanism was caused by a defect in a photosynthetic or a housekeeping function. The chloroplast envelope provides specific routes that distinguish photosynthetic and housekeeping cytosolic proteins to enter through the outer membrane. Therefore, other chloroplast mutants, *ppi1* (*toc33*), defective mainly in the import of photosynthetic preproteins, and *toc132-2toc120-2/+* defective in the import of housekeeping proteins, were selected. The single homozygous *toc132-2* had no phenotype, and homozygous double mutants *toc132-2 toc120-2* were very severe and exhibited frequent seedling lethality, while hemizygous *toc132-2 toc120-2-/+* showed an intermediate phenotype, similar to that of *ppi1* and suitable for comparative gene expression studies (Table 3.1).

**Table 3.1 Comparison of known or predicted protein import in selected mutants**

| Plant | Wild type | Genetic defect | Protein import | Phenotype |
|---|---|---|---|---|
| *toc132-2* | Columbia | TOC132 | House keeping | Wild type |
| *toc132-2*<br>*toc120-2* | | TOC132<br>TOC120 | House keeping | Severe |
| *toc132-2 -/-*<br>*toc120-2-/+* | | TOC132<br>TOC120 (het.) | House keeping | Intermediate |
| *ppi1* | | TOC33 | Photosynthetic | Intermediate |
| *cue8* | Bensheim | To be confirmed | To be confirmed | Intermediate |

Given that the WT seedlings sometimes leaning on the agar media appear less green, during the initial experiments it was difficult to distinguish the hemizygous *toc132-2 toc120-2-/+* mutants and harvest sufficient plant material at 5-days. Therefore, seedlings were transferred to soil and their genotype was confirmed after they had adapted to grow on the soil. The very young juvenile leaves (<4mm) of hemizygous plants, *ppi1* and WT were examined for chloroplast gene expression.

As *ppi1* was impaired in importing photosynthetic proteins, there was a substantial reduction of nucleus-encoded *LHCB1* as well as PEP-transcribed chloroplast genes and less reduction of NEP-transcribed mRNA levels. In comparison, the *toc132-2 toc120-2-/+* mutants revealed higher amounts of mRNA transcribed by NEP (Fig. 3.14A). Additionally, the very young juvenile leaves of *cue8* continued to show down regulated PEP and upregulated NEP-dependent transcript levels (Fig. 3.14 B).

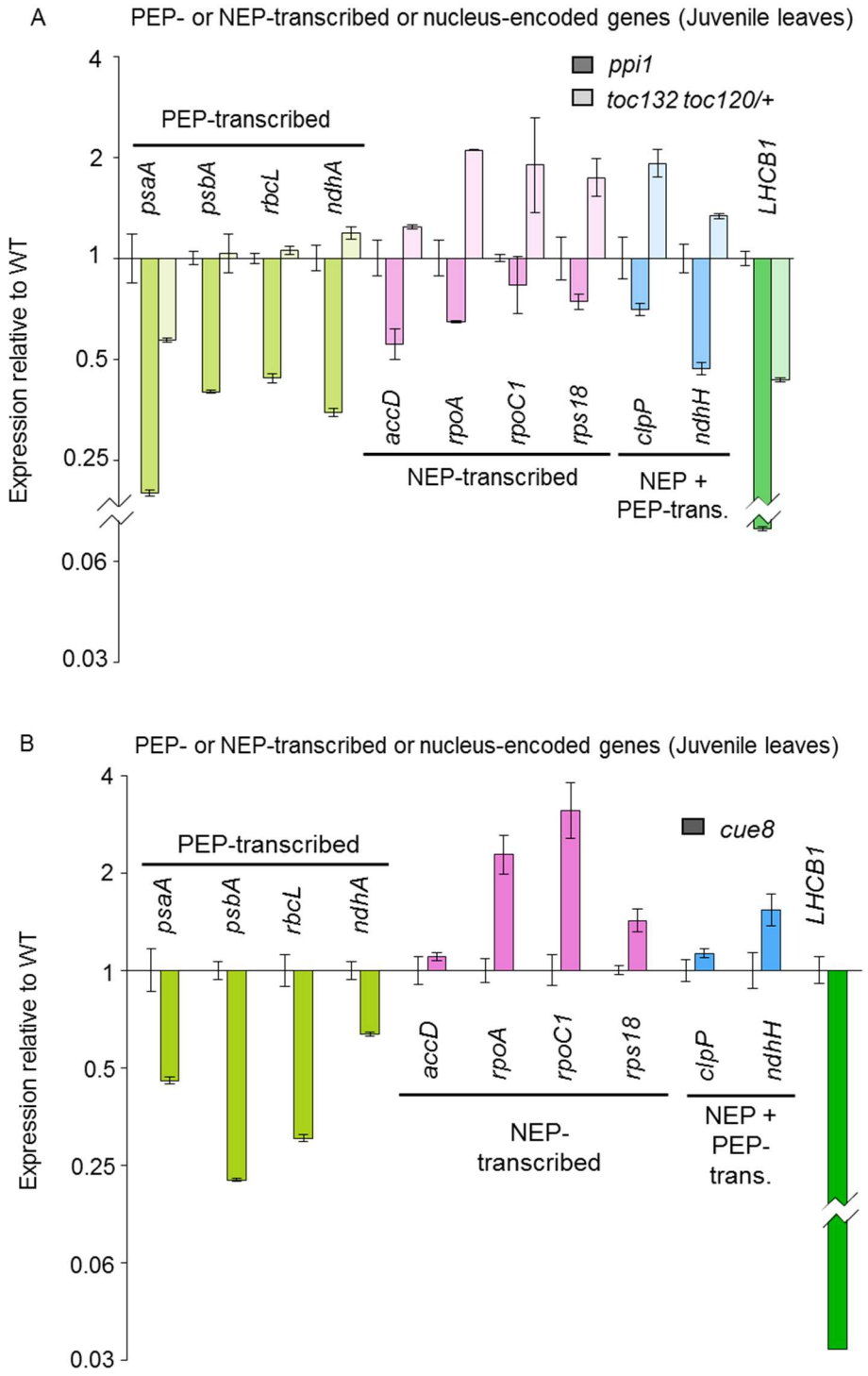


**Figure 3.14** Chloroplast gene expression in juvenile leaves for *ppi1, toc132/toc120/+* and *cue8* mutants. Transcript levels, determined by quantitative real-time RT-PCR, of chloroplast-encoded genes in very young leaves (length < 4mm) of (A) *ppi1* and *toc132 toc120/+*, relative to those of their WT (Col) and of (B) *cue8* relative to those of its WT (pOCA108). Genes transcribed by the Plastid-encoded polymerase (PEP), the Nucleus-encoded polymerase (NEP) or both are indicated by different colours and the accompanying labels. The transcript level of the nucleus-encoded *LHCB1* gene, encoding a photosynthetic antenna protein of photosystem II, is also provided. Data were obtained from three independent biological samples and plotted on a log2 scale as shown in figure 3.8 B. Error bars represent standard error of the mean (SEM) of triplicate samples.

Along with the nucleus-encoded photosynthetic genes, transcripts of SIG factors were also down regulated in *ppi1* (Fig.3.15 A). The enhanced expression of NEP-driven transcripts is due to an apparent increase in RPOTs themselves in *toc132-2 toc120-2-/+*, but to a lesser extent than in *cue8*. The figure 3.15B shows expression of nucleus-encoded factors - *SIG1*, *SIG4* and *SIG5* as reduced while others were at WT levels (*SIG2*, *SIG3* and *SIG6*) or significantly elevated (*RPOTs*) in juvenile leaves of *cue8*. The compensatory mechanism was more pronounced (over 7-fold increase in level of RPOTp) in the very young juvenile leaves.

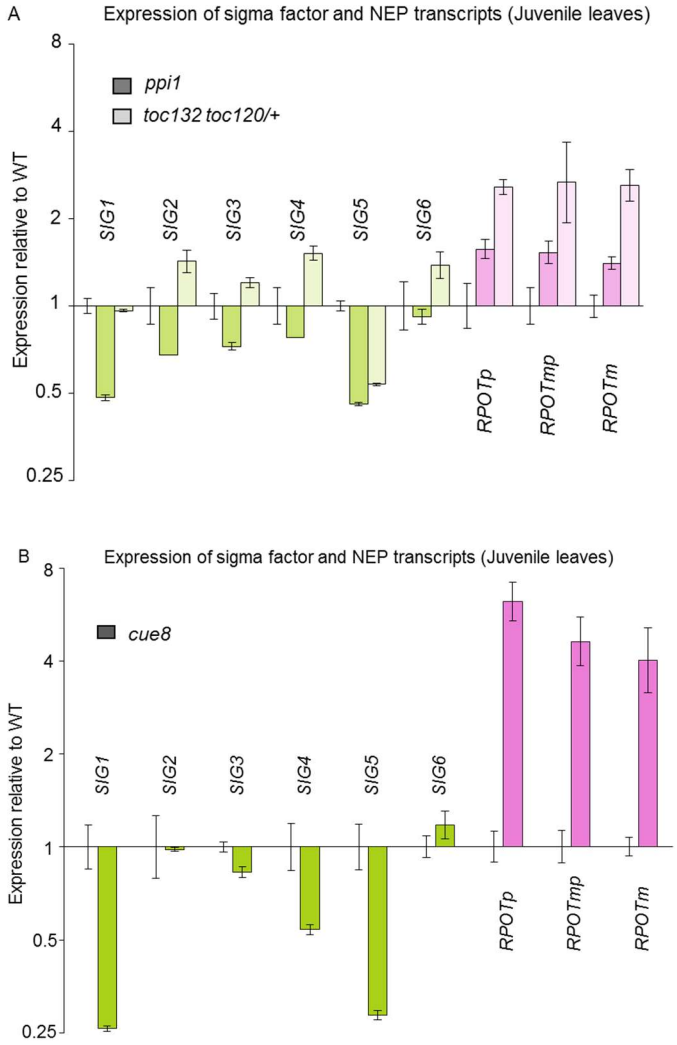


**Figure 3.15** Expression of nucleus-encoded organellar RNA polymerases and co-factors in juvenile leaves. (A) Transcript acumulation of phage-type RNA polymerases (NEP) targeted to the plastids (*RPOTp*), mitochondria (*RPOTm*) or both (*RPOTmp*) were increased in *toc132 toc120/+* while transcripts of sigma factors in *ppi1* showed lower levels. The *toc132 toc120/+* showeed decrease in only *SIG5* mRNA and increase in all the NEP levels. (B) *cue8* has clearly noticable reduction of *SIG1* and *SIG5* and increase in NEP-transcripts. Expression values were plotted on a log2 scale as shown in figure 3.8 B. Error bars represent standard error of the mean (SEM) of triplicate samples.

After subsequent trials and acquianted with the growth of the mutant plants, chloroplast gene expression was examined in 5-days old *toc132 toc120-/+* and *ppi1* seedlings (Fig. 3.16 A). The analysis was carried out for all the previously mentioned chloroplast genes. As expected *ppi1* showed reduced levels of PEP-driven gene expression, but a clear increase in the NEP-driven transcripts (Fig. 3.16B).

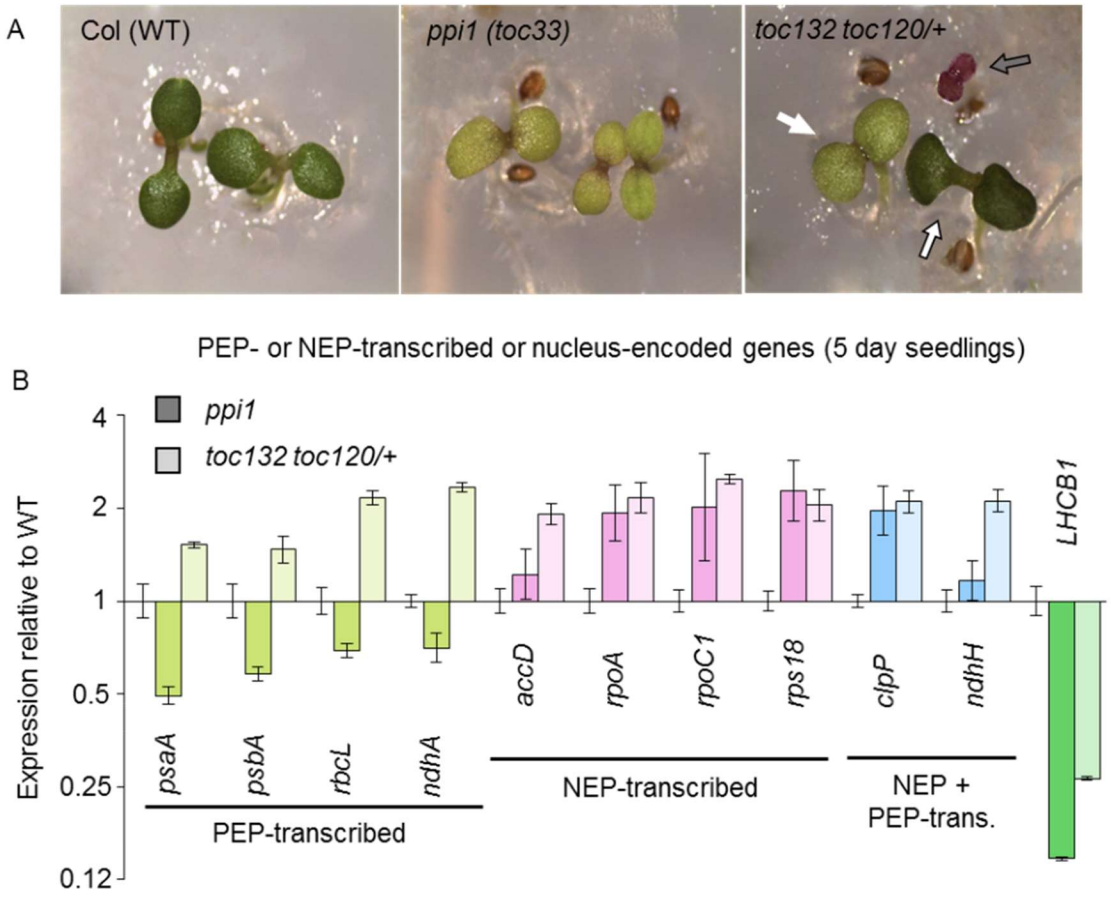


**Figure 3.16** Expression analysis of nucleus and chloroplast-encoded genes in plastid import defective mutants and their WT. (A) Images of 5-days old seedlings, of WT, *ppi1* (defective in *TOC33*) and emerging from seeds of a *toc132 toc120/+* plant (mutant for *TOC132* and heterozygous for *TOC120*). The latter seedlings are *toc132* homozygous single mutant (green seedlings, black-outlined, white arrow), *toc120/+* hemizygous seedlings (pale seedlings, large white arrow) and *toc132/ toc120* double homozygous mutant (purple small seedlings, black-outlined, grey arrow). (B) Transcript levels, determined by quantitative real-time RT-PCR, of chloroplast-encoded genes in *ppi1* and *toc132 toc120/+* seedlings, relative to the WT. Genes transcribed by the Plastid-encoded polymerase (PEP), the nucleus-encoded polymerase (NEP) or both are indicated by different colours and the accompanying labels. The transcript level of the nucleus-encoded *LHCB1* gene, encoding a photosynthetic antenna protein of photosystem II, is also provided. Reduced levels of PEP-transcribed and elevated NEP-transcribed genes in *ppi1*. Upregulation of selected PEP and NEP transcribed or both in *toc132 toc120/+*. Data were obtained from three independent biological samples and plotted on a log2 scale as shown in figure 3.8 B. Error bars represent standard error of the mean (SEM) of triplicate samples.

Additionally, the expression of nucleus-encoded NEPs and of sigma factors was elevated in both mutants (Fig. 3.17 A). The seedlings of *toc132 toc120/+* which had shown enhanced transcript levels for selected PEP-driven genes, also exhibited increase in expression of sigma factors. Both genotypes had maintained their chloroplast genome copies to provide enough templates presumably for the elevated NEP (Fig. 3.17 B). The expression of organellar DNA polymerases, in particular *POL1B*, showed enhanced levels of transcripts in *ppi1* (Fig. 3.17 C).

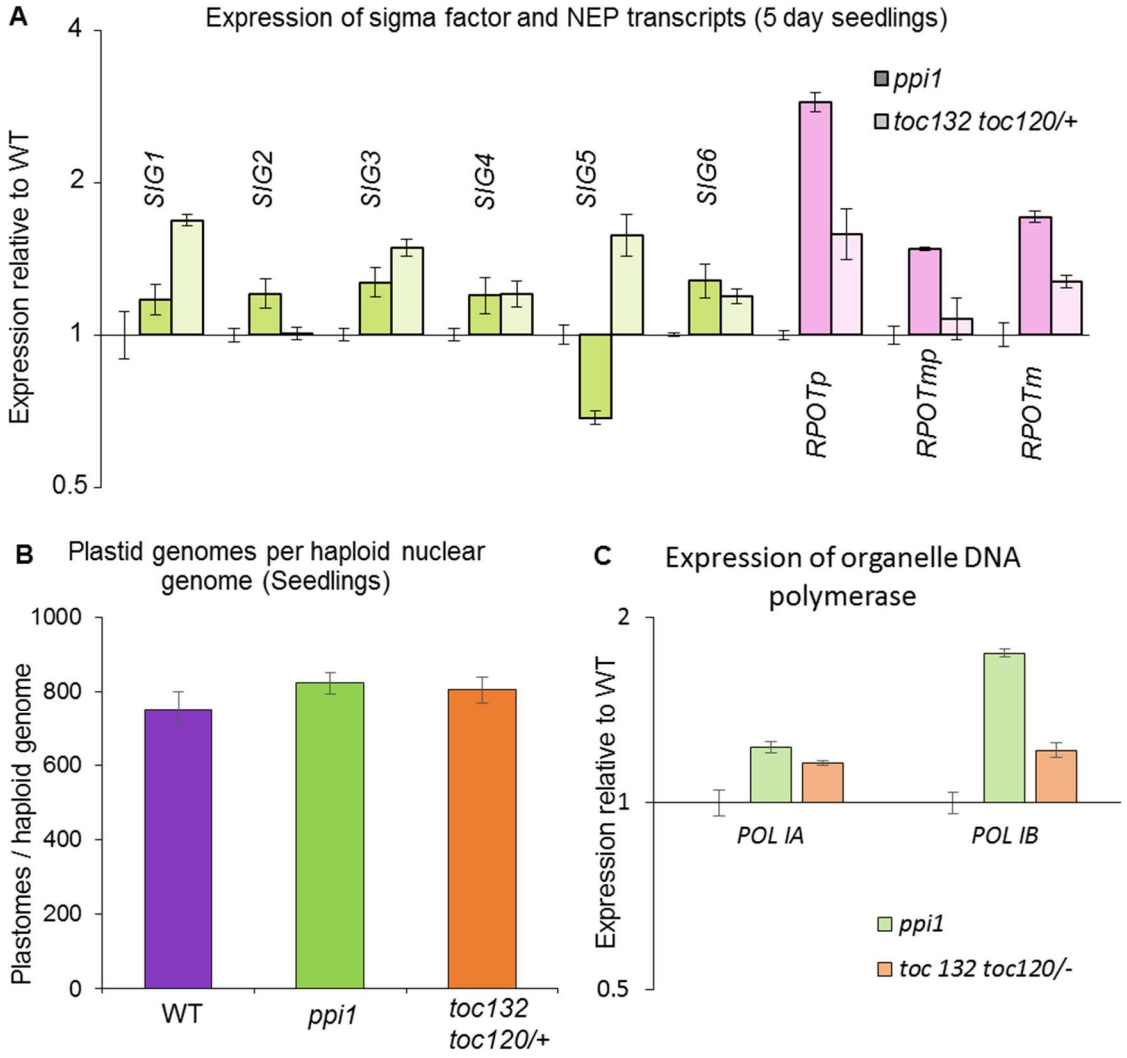


**Figure 3.17** Expression analysis of nucleus-encoded genes and plastid genome copy number in *ppi1* and *toc132 toc120/+* seedlings grown for 5days. (A) Transcript levels of nucleus-encoded sigma factors and phage-type RNA polymerases in mutants relative to WT. Seedlings of *ppi1* showed decrease in transcripts of *SIG5* mRNA levels while other *SIGs* are slightly elevated. Transcripts for NEPs are upregulated in both the mutants with an exception of *RPOTmp* in *toc132toc120/+* similar to WT. (B) Chloroplast genome copy number was quantified by real time PCR and standard curve analysis of cpDNA and genomic DNA sequences in mutants versus WT as described in figure 3.11A. (C) Expression of organellar DNA polymerases (*POLIA* or *POLIB*) in *ppi1* and *toc132 toc120/+* seedlings. Graphs shown in (A) and (C) were plotted relative to WT on a log2 scale as shown in figure 3.8 B. Error bars represent standard error of the mean (SEM) of triplicate samples.

### 3.7 Reduced expression of the photosynthetic genes in *cue8* is possibly regulated by reduction in *GLK1* and *GLK2*

The regulation of nuclear gene expression for most of the greening genes by GLK transcription factors is well established in vascular plants (Wang et al., 2013). It was reported that transcription factor GLK1 coordinates with the expression of photosynthesis associated nucleus-encoded genes (PhANGs) during impairment of protein import (*ppi2*) (Kakizaki et al., 2009).

It was worth asking whether GLKs play a role in suppression of photosynthesis related genes in *cue8*. qPCR analysis showed a dramatic reduction in the transcript levels of both *GLK1* and *GLK2* in seedlings as well as juvenile leaves of *cue8* (Fig. 3.18 A and B). Similar results were observed in *ppi1* while less reduction was seen in the *toc132 toc120/+*.

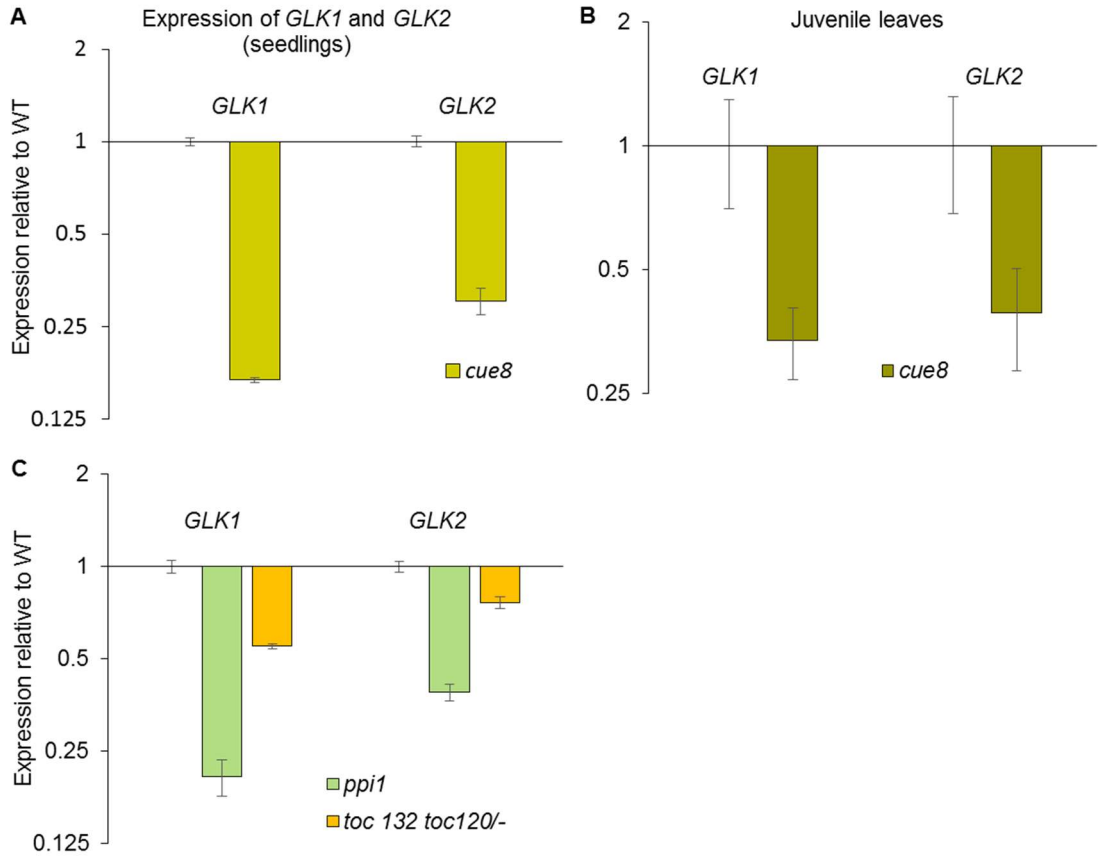


**Figure 3.18** Expression of *GLK1* and *GLK2* genes in seedlings and juvenile leaves of *cue8*. Transcript levels, determined by quantitative real-time RT-PCR, of nucleus-encoded *GLK1* and *GLK2* genes in the mutant seedlings (A) *cue8* (6-days old) relative to WT (5-days old) and (B) *cue8* juvenile leaves (<4mm) harvested from healthy grown plants and (C) seedlings of *ppi1* and *toc132 toc120/+* (5-days). Data were obtained from three independent biological samples and plotted on a log2 scale, relative to respective WT as shown in figure 3.8 B. Error bars represent standard error of the mean (SEM) of triplicate samples.

### 3.8 Overexpression of *GLK1* or *FC1* does not rescue the *cue8* phenotype

The concept of retrograde signalling is well established and led to a genetic screen for failure to normally downregulate PhANGs upon plastid impairment. Loss of function of specific genes in the tetrapyrrole synthesis pathway results in a genome uncoupled (GUN) phenotype when photobleaching occurs in the presence of norflurazon (a carotenoid inhibitor) (Mochizuki et al., 2001; Larkin et al., 2003; Koussevitzky et al., 2007; Adhikari et al., 2011; Adhikari et al., 2011). A recent finding of a *gun6-1D*, overexpression of *FC-1* (ferrochelatase-1) might led to the hypothesis that haem increase production in the developing chloroplasts might act as a positive signal for the expression of nucleus-encoded photosynthesis genes (Woodson et al., 2011). Understanding that chloroplast-encoded housekeeping genes are expressed at higher levels in *cue8*, and that the defects were associated with downregulation of photosynthetic genes, which is due to repressed GLKs, an obvious question was whether an increase in the level of GLKs or addition of a positive signal (*gun6-1D*) in *cue8* can improve the phenotype. Therefore, $cue8_{col}$ was crossed with *GLK1ox* and *gun6*-1D respectively and the double mutants were generated in the Columbia ecotype (Fig 3.19 A). Agarose gel images showing the outcome of genotyping of PCR amplified product (*GLK1ox* and *GUN6*, *gun6*-1D) and restriction digested products (*cue8*). Primers used for the PCR amplification of genomic DNA and details of restriction enzyme are provided in the appendix.

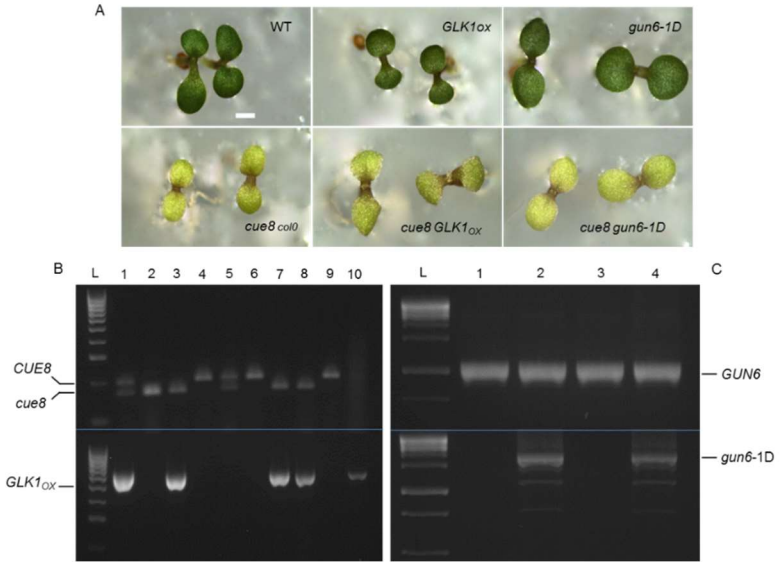


**Figure 3.19** Phenotyping and genotyping of double mutants with *cue8* combination. (A) Seedlings of $cue8_{col}$, *cue8 GLK1ox*, *cue8 GLK2ox* and *cue8 gun6-1D* along with the respective controls grown for 6-days. Scale bar represents 1mm. (B) Agarose gel images of digested (*cue8*, 164bp) and undigested (*CUE8*, 197bp) PCR amplicons (above gel). The DNA samples with both bands indicate heterozygous plants. Bands in the lower gel show presence of *GLK1ox* (625bp). Bands represent DNA obtained from individual plants from F3 generation, lane 3, 7 and 8 are *cue8 GLK1ox* double mutants (C) All

the plants carried endogenous *GUN6* (above, 1027bp) while only lane-2 and lane-4 showed the presence of *gun6-1D* (below, 1976bp).

The chlorophyll and protochlorophyllide content measured in the segregating population of 6-day old seedlings revealed that neither overexpression of *GLK* transcription factor nor *FC-1* rescues the *cue8* plastid defect (Fig. 3.20). Seedlings of double mutants *cue8 GLK1ox* exhibited severe stress during early development (Fig. 3.19 A). However, plants from both mutant combinations (*cue8 GLK1ox* and *cue8 gun6-1D*) showed a partial suppression after several weeks of growth on soil, compared to *cue8*. This probably reflected the fact that the slow developing chloroplasts of *cue8* would eventually perform better under the action of these regulators.

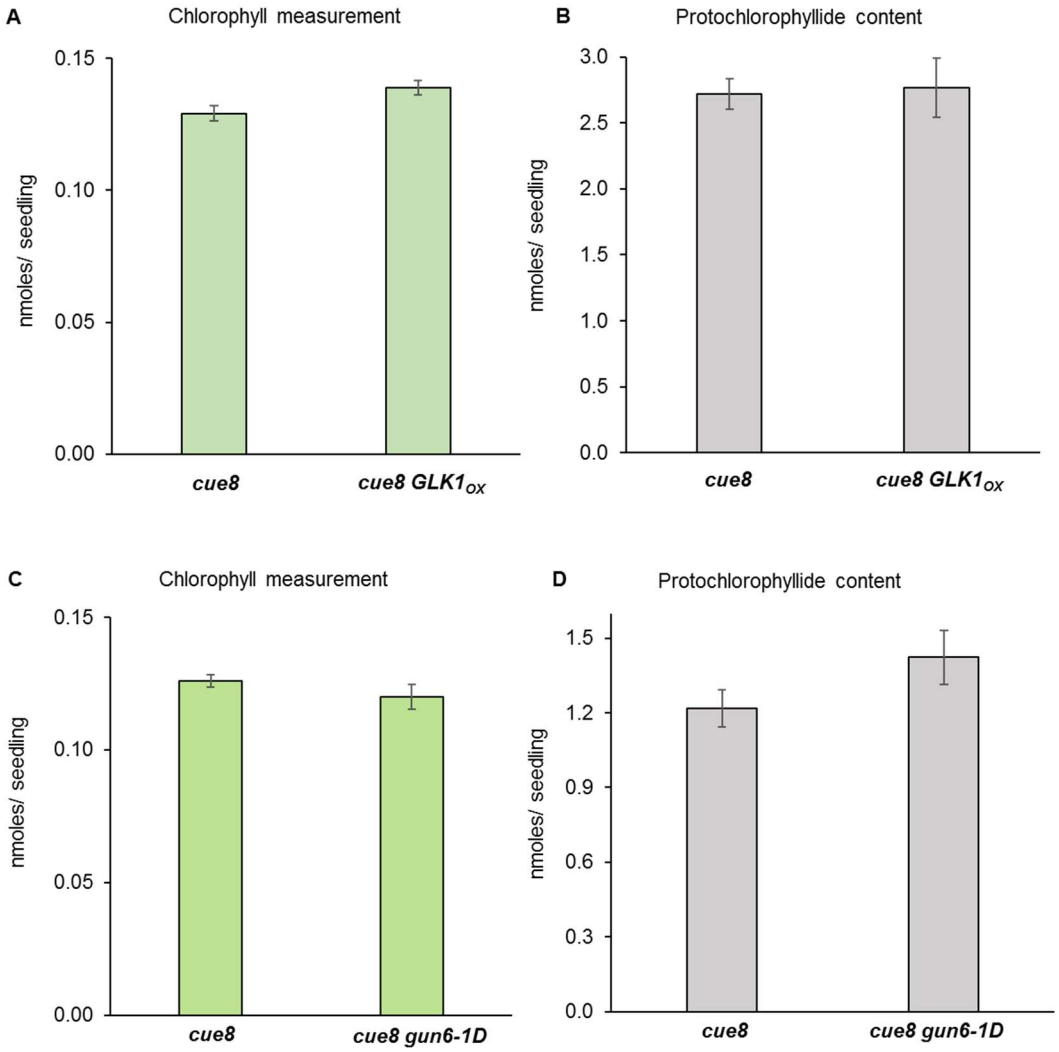


**Figure 3.20** Quantitation of plastid pigments in the dark and light grown seedlings. (A, C) Graph showing total chlorophyll content (nmoles) per seedling quantified in the light grown seedlings of *cue8*, *cue8 GLK1ox*, and *cue8 gun6-1D* (B, D) protochlorophyllide (nmoles) content quantified per seedling in dark grown etiolated seedlings of *cue8*, *cue8 GLK1ox*, and *cue8 gun6-1D*. Error bars represent standard error of the mean (SEM) of replicate samples, n=5.

### 3.9 Survival of *cue8* seedlings necessitates GUN1 activity

In an attempt to characterize retrograde signalling in the protein import mutant *ppi2* (deficient in photosynthetic protein import) it was reported that signals from import defective plastids are regulated by GUN1, which supresses the expression of GLK1 (Kakizaki et al., 2009). GUN1 is hypothesized to be a master regulator of retrograde signalling through its interaction with proteins involved in tetrapyrrole biosynthesis and plastid gene expression (Tadini et al., 2016).

To understand if chloroplast to nucleus communication in *cue8* involves the role of GUN1, *cue8* was crossed with *gun1*. Albino seedlings in the F3 generation from two different lines *cue8 gun1*/+ and *gun1 cue8*/+ were identified as homozygous *cue8 gun1* double mutants (3.21). Primers used for the PCR amplification of genomic DNA and details of restriction enzyme are provided in the appendix. Some of the seeds (3.5%) from *gun1 cue8*/+ failed to germinate, stressing the importance of at least one functional copy of *GUN1* in the presence of *cue8*. At this point it was not investigated whether loss of GUN1 has impacts on the PhANG expression in *cue8*. However, it is evident that GUN1 plays an important role in chloroplast gene expression and is necessary for survival of *cue8*.

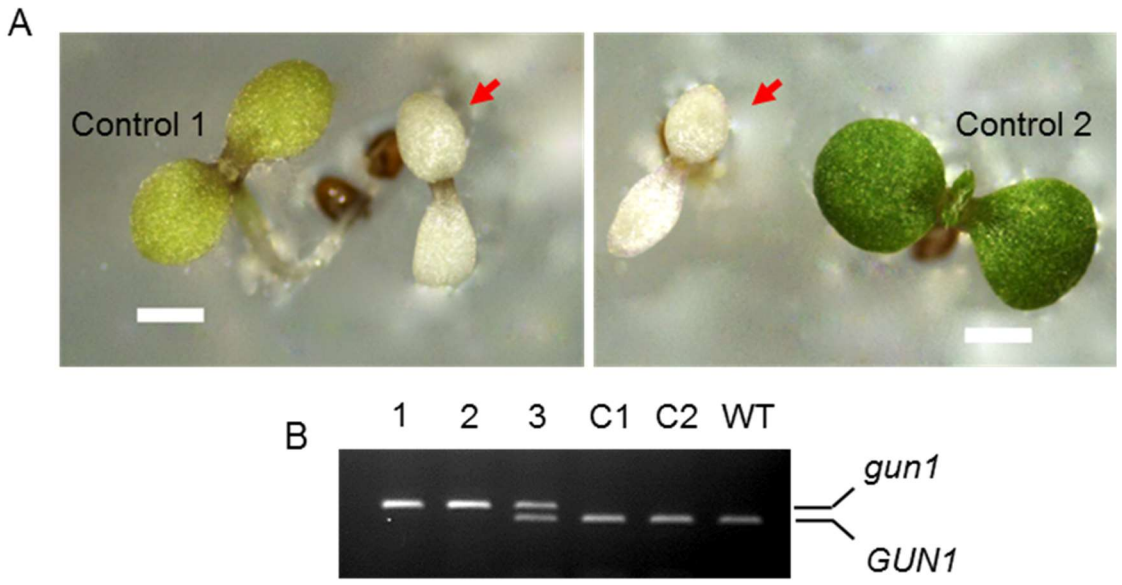


**Figure 3.21** Generation of *cue8 gun1* double mutant. (A) Image showing albino seedlings (indicated by arrows) as *cue8 gun1* obtained from *cue8 gun1*/+ (left) and *gun1 cue8*/+ (right). (B) Agarose gel analysis of digested PCR product for *GUN1* (69bp, lower band), undigested *gun1* (99bp, upper band), controls (C1, C2) and WT. Presence of both bands indicate heterozygosity.

### 3.10 Discussion

Early studies on *cue8* had shown smaller etioplasts in dark-grown seedlings in addition to reduced accumulation of protochlorophyllide, a chlorophyll precursor (Vinti et al., 2005). Taken together with reduced gene expression of PhANGs in light and dark grown seedlings, it can be concluded that *cue8* suffers a general plastid defect. The ds-RED lines show plastid development and distribution is affected globally in the absence of a fully functional CUE8. On the other hand, ds-RED results also suggest plastids are poorly distributed not only in green tissues but also in the roots. The "chloroplast compartment" correlates with the slow greening phenotype of the plant, showing reduced plastid proportion during early stages of development (pale phenotype) and it tends to rise as leaves green towards the tip.

Mutation in the *CRL* gene, which encodes a chloroplast membrane protein, affects cell division and differentiation in Arabidopsis (Asano T, 2004). Several chloroplast mutants cease development at embryonic stage (Meinke et al., 2008). The root meristem showing larger cells in *cue8* might have uncovered a link between chloroplast damage and cell division. Actively dividing cells contain undifferentiated proplastids (Jarvis and Lopez-Juez. 2013). Much of the information on plastid signalling is from differentiated chloroplasts. Therefore, what sort of signals from a defective proplastid act early during cell division is far from known. Further studies in this direction might uncover the role of *cue8* proplastids and a different dimension of plastid retrograde signalling in cell division.

As damaged chloroplasts lead to repression of PhANGs, retrograde signalling from plastids been always invoked to understand how the expression of PhANGs in the nucleus is affected. It has been previously reported that chloroplast defects lead to repression of chloroplast-encoded photosynthetic genes in addition to reduced PhANGs, and a simultaneous elevation of chloroplast-encoded housekeeping genes, yet very little is known about upregulation of chloroplast housekeeping genes. Plastid gene expression is carried out by two polymerases, NEP and PEP. The multi-subunit PEP functions as a complex and requires nucleus-encoded sigma factors which help in recognising the promoters of target genes (Allison, 2000; Lysenko, 2006). A study conducted in tobacco plants classified plastid genes, based on the promoter recognition of polymerases, into class I: PEP-transcribed genes, class II: transcribed by both PEP and NEP and class III: specifically transcribed by NEP (Hajdukiewicz et al., 1997).

Mutation in the plastid targeted NEP: RPOTp (Hricova et al., 2006) or RPOTmp, a common NEP for mitochondria and chloroplast (Baba K, 2004) induced chloroplast developmental

defects thereby reducing overall plant growth. Meanwhile deletion of *rpoB*, a subunit of PEP (Allison, 1996) or defects in PEP-associated factors, resulted in albino phenotype with downregulated PEP activity and normal or upregulated NEP function (Pfalz et al., 2006; Kindgren et al., 2012; Börner T, 2015). The barley *albostrians* mutant, with defective plastid ribosome biogenesis, is deficient in plastid proteins including PEP subunits (Hess et al., 1993), therefore gene expression was solely performed by the NEP. Interestingly, PEP elimination in these white leaf mutants activated elevation of RPOTp-dependent transcription which also included photosynthetic genes (Zhelyazkova et al., 2012). The apparent increase in NEP activity was possibly due to higher levels of expression of RPOTs themselves (Emanuel et al., 2004). Accordingly, the elevation of transcripts for NEPs (RPOTp and RPOTmp) in *cue8* might compensate the reduction of PEP and maintain the transcription of fundamental genes that are common for both the polymerases.

Plastid-to-nucleus communication is essential to synchronise plastid function with the inflow of hundreds of nucleus-encoded proteins into the chloroplasts (Hills et al., 2015). The expression of chloroplast genes is under the control of the nucleus, either directly through NEPs or indirectly by regulating the expression of SIGs in response to developmental cues. Given that loss of chloroplast translation causes altered retrograde signalling, the signals emerging from chloroplasts must be, or must depend on, products of either NEP, PEP or both. It can be reasoned that there is a stringent coordination and distribution of labour among the sigma factors to manage PEP activity. It has been shown that expression of nucleus-encoded polymerases peaks during the early stages of development, while PEP functions later during differentiation (Zhelyazkova et al., 2012). However, developing plastids in photosynthetic, as well as non-photosynthetic, tissues require expression of both polymerases during plant development (Börner T, 2015).

Sigma factors, for example SIG2 and SIG6, were shown to have partially redundant functions in maintaining gene expression and mediating retrograde signalling (Woodson et al., 2011). Comparative analysis of *sig2*, *sig6* and WT treated with norflurazon or lincomycin showed they shared a wide range of gene expression changes, highlighting the regulatory role of SIG factors in chemically-damaged plastids. It was observed that NEP-transcribed genes were either normal or elevated in *sig2* and *sig6* lines. Interestingly, *cue8* seedlings and juvenile leaves accumulated the transcripts of *SIG6* and *SIG3* to WT levels, while the expression of *SIG2* was normal in juvenile stage. Also, *ppi1* and *toc132 toc120/+* had normal or slightly elevated *SIG6* transcripts at both developmental stages. In contrast, *ppi2* revealed reduction

of *SIG6,* however certain SIG factors were either maintained or showed (*SIG*3) transcript elevation (Kakizaki et al., 2010). Mutation in *sig6* showed slow-greening phenotype with elevation of expression of NEP-dependent chloroplast genes, while the opposite was observed for PEP-dependent genes in spite of increase in PEP transcripts. Interestingly, virescent mutants like *sig6*, *yellow seedling1*, *brz-insensitive-pale green2*, and *nitric oxide-associated protein1* suppress the leaf variegation induced by *thf1* and *var2* (Hu et al., 2015). As shown by several studies, it seems that anterograde control through elevation of transcripts of NEP is a necessary step in response to plastid damage (chemical or biogenic), but the coordination is achieved by selective expression of sigma factors depending on the status of chloroplasts. Regulating expression of sigma factors according to developmental needs might be necessary to control the PEP which is required preferentially during differentiation and to promote housekeeping function by action of NEP. Given that *cue8* suffers a general plastid defect, for example dark grown seedlings also show defective etioplasts, a question arises whether the compensatory mechanism (elevation of NEP and coordinated expression of sigma factors) also occurs in the dark. This might contribute to understanding the nature of retrograde signal: observation of *cue8* reveals that this retrograde mechanism operates independently of light.

A phytochrome-defective mutant like *long hypocotyl* (*hy1*) shows reduced chloroplast compartment and in parallel also reduced cpDNA copies (He, 2018). On the other hand, fruit-specific silencing of *det1* in tomato resulted in an increased chloroplast compartment with an increase in the organelle genome copies per cell (Enfissi et al., 2010). The chloroplast division mutant *arc6,* with two larger chloroplasts, has maintained cpDNA replication. These observations evidence a close link between the “chloroplast compartment” of the cell and its amount of cpDNA. In contrast, with a reduced chloroplast compartment, cells of *cue8* have maintained their cpDNA replication. Chloroplast DNA replication is performed by two nucleus-encoded polymerases, *POL IA* and *POL IB* (Parent et al., 2011). This observation *cue8* is supported by the partial elevation of *POL IB* transcripts and increase in NEP activity. A compensatory mechanism was also evidenced in *pol1b* knockout mutants with an increase in *POL1A* transcripts (Cupp JD, 2013).

The nuclear regulation of pigment biosynthesis genes is under the control of Golden2-Like transcription factors (Waters et al., 2009). Furthermore, the promoters of SIG factors can be recognised by GLK transcription factors (Kakizaki et al., 2010). In the present study it was hypothesized that overexpression of GLKs or FC-1 might circumvent the retrograde

signalling occurred due to *cue8* defect. Although the gene expression studies in these mutants awaits testing, the *cue8 GLK1ox* and *cue8 gun6*-1D double mutants failed to show rescue of pigments in the light and dark-grown seedlings. A possible explanation is regulation of GLK1 by proteasome degradation in the presence of dysfunctional plastids (Tokumaru et al., 2017). In that study, it was reported that despite the normal transcription of *GLK1*, the *gun1-101* mutants grown either on norflurazon or on lincomycin had no detectable GLK1 proteins, demonstrating that a signal from damaged plastids also operates at the protein level. Similar results were observed even in *GLK1ox ppi2-2* double mutants. A future investigation would reveal whether overexpressed GLKs are regulated in the same manner in the presence of *cue8*. In addition, it will be interesting to understand whether overexpression of FC-1 also leads to proteasome-mediated turnover during plastid defect, or whether a separate mechanism operates in *cue8 gun6-1D*. On the other hand, whether a common retrograde signal acts at both transcription and post-translational levels, or whether there are multiple retrograde signalling mechanisms, remains to be seen. How does the compensatory mechanism operate in *cue8 GLK1ox* and *cue8 gun6*-1D and are there any changes in the expression of SIG factors? These can be considered as interesting areas of future work.

GUN1 supresses the expression of nucleus-encoded photosynthetic genes following chloroplast defects. The double mutants *gun1sig2* and *gun1sig6* recovered expression of PhANGs compared to *sig2* and *sig6* single mutants (Woodson et al., 2013). Mutation in PRPL11, a plastid ribosomal protein, results in pale green plants affected by reduction in the rate of plastid translation (Pesaresi et al., 2001). Simultaneous loss of PRPL11 and GUN1 causes severe defects with an albino phenotype (Tadini et al., 2016). Those authors have also reported a direct interaction of GUN1 with plastid-localised proteins, which included proteins of tetrapyrrole biosynthesis and of gene expression. Generation of a *cue8 gun1* also leads to albino seedlings, suggesting a vital role of GUN1 in modulating plastid homeostasis. If elevation of NEP in *cue8* occurs to compensate the chloroplast defect by enhancing housekeeping gene expression, then GUN1 might have a crucial role in this compensatory mechanism. Further study of these albino seedlings might reveal whether the elevation of NEPs is dependent on GUN1-retrograde signalling and if the maintenance of SIG6 still persists in the absence of GUN1.

The current study identifies activation of a compensatory mechanism based on a form of retrograde signalling. This mechanism primarily involves the elevation of transcripts for nucleus-encoded polymerases, an active maintenance of the number of plastid genome copies

followed by increase of NEP-dependent expression, and suppression of chloroplast photosynthetic genes by the suppression of selected SIG factors. The mechanism to enhance NEPs, thereby increasing NEP-driven transcription to compensate for the loss, and the simultaneous suppression of the action of PEP by controlling selective SIG factors, to delay expression of plastid-encoded photosynthetic genes, might be linked to delayed plastid differentiation in *cue8*.

In summary, the previously identified *CAB underexpressed* mutant (*cue8*) delays the overall growth of the plant and results in the virescent phenotype. Microscopy of seedlings with a fluorescent ds-RED protein (targeted to plastids) showed that mutants suffer a global plastid defect. The delay of chloroplast development was clearly reflected in the chloroplast compartment of *cue8* mesophyll cells with significant reduction in seedlings, while the reduction decreased as cells mature over time. Cellular microscopy of roots showed a phenotype suggesting that chloroplast biogenesis defect in *cue8* slows the process of cell division. Chloroplasts lagging in development trigger a form of retrograde signalling which in turn initiates an anterograde compensatory mechanism. Loss of *CUE8* suppresses expression of plastid-encoded photosynthetic genes by controlling the expression of sigma factors that associate with PEP subunits and elevates the expression of plastid-encoded housekeeping genes by significant upregulation of NEPs. It also promotes the cpDNA replication (which becomes disconnected from the total chloroplast compartment) to maintain the templates for enhanced NEP activity. As per the comparative gene expression analysis, the compensatory mechanism of *cue8* shares similarity either with a mutant impaired in photosynthetic protein import or housekeeping protein import, depending on the developmental stage. The current study confirms previous findings that suppression of photosynthesis associated nuclear encoded genes (PhANGs) and SIG factors is regulated by GLK transcription factors, however overexpression of *GLKs* or *FC1* does not rescue the *cue8* defect in seedlings. As shown by the albino phenotype of double mutants, *GUN1* plays an important role in allowing a delayed chloroplast differentiation in *cue8*. The upstream factors which regulate expression of NEP, and the nature of the signal from the housekeeping plastid defect that elevates NEP transcripts, are yet to be seen.

# Chapter 4

# Identification of an intragenic suppressor of *cue8* and role of TIC 1MDa complex in chloroplast protein import

## Statement of authorship

SHORE-Map computational analysis and identification of a list of candidate mutated loci in the suppressor mutant of *cue8* carried out by Sabri Ali (Prof. Paul Jarvis, Oxford University)

Recent studies conducted by Kikuchi et al. (2013) revealed a novel 1MDa chloroplast import complex in the inner membrane. The protein complex has a main channel, TIC20, and other associated proteins. The largest protein, TIC214, of the 1MDa complex, is encoded by the chloroplast genome, while TIC100, TIC56 and TIC20 are encoded by the nucleus. These findings have revealed the identity of *CUE8*, At5g22460, as *TIC100*. As discussed earlier, the knockout mutation of TIC100 leads to seedling lethality. The slow growing *cue8* mutant allows molecular studies which would otherwise be impossible in *TIC100* T-DNA mutants. An obvious question was whether the virescent phenotype of *cue8* is due to defects in import of cytoplasmic proteins. In an attempt to answer this, the Jarvis lab had found that *cue8* is defective in importing Rubisco small subunit (Bédard, López-Juez and Paul Jarvis, personal communication). In addition, the proteins of 1MDa complex in *cue8*, particularly TIC100, were significantly reduced. This evidence revealed *cue8* as an import defective mutant and provided support for the existence of the 1MDa complex. Identification of a semi-dominant suppressor of *cue8* through forward genetic screen, and the extent of suppression, is detailed in the following sections. The work described in this chapter has the following objectives:

- To understand whether CUE8 is involved in the assembly of TIC 1MDa complex.
- To examine the role of CUE8 in chloroplast protein import.
- To identify genetic suppressors of *cue8* using forward genetics and investigate whether CUE8/TIC100 is essential for importing photosynthetic or housekeeping preproteins.

### 4.1 Forward genetic screen of *cue8*

In the interest of further understanding the chloroplast TIC complex, a forward genetic screen was carried out in *cue8* (Fig. 4.1). A pool of 5000 *cue8* seeds were randomly mutagenized with EMS (Ethyl methane sulfonate) and germinated seedlings were transferred to soil in 50 trays/pools. The M2 seeds, 25% of which were homozygous for causative mutations, were screened for putative suppressor candidates with enhanced-greening phenotype. Screening was performed under white light, focussing on early development by plating on MS media.


**Figure 4.1** Schematic diagram showing screening of mutagenized *cue8*. Heterozygous M1 plants were grown in 16hr photoperiod conditions. The search for putative suppressor candidates was carried among M2 seedlings on MS media plates with 1% (w/v) sucrose.

In the mixed population, the seedlings that showed enhanced greening were scored over several days. Upon confirmation, they were transferred to soil to check the heritability of the phenotype heritability even in M3 generation before being considered as true mutants. Examples of the putative suppressor mutants (M3) with rescued growth and phenotype are shown below (Fig. 4.2).


**Figure 4.2** Phenotype of putative candidate suppressors of *cue8*. Screening of M2 seeds on MS media with 1% (w/v) sucrose identified putative suppressors of the *cue8* mutation. Images showing confirmation of putative mutants in the M3 progeny with rescued phenotype compared to unmutagenised *cue8*. Labels indicate specific seed pool from which individual plants were obtained.

## 4.2 Confirmation of *cue8* suppressors

Putative mutants ("putants"), with about two-fold enhanced levels of chlorophyll compared to the *cue8* seedlings, were considered as main candidates (Fig. 4.3). Suppressors were further confirmed by measuring protochlorophyllide levels in the dark grown (6-days) seedlings. The screen identified 9 candidate suppressors from different pools. Some of them showed peculiar phenotypes, for example seedlings of 22.1 had elongated hypocotyl along with increased pigment content. The serrated leaf margins of *cue8* were suppressed by 28.6 which showed smooth leaf margins. Interestingly, plants from three pools – 17, 18 and 19 (not shown) revealed a dramatic rescue with an increase of over 6-fold chlorophyll and over 3-fold protochlorophyllide levels compared to *cue8*. To confirm whether this was a real suppression

or a seed contamination, individual plants were genotyped for the presence of the *cue8* mutation.

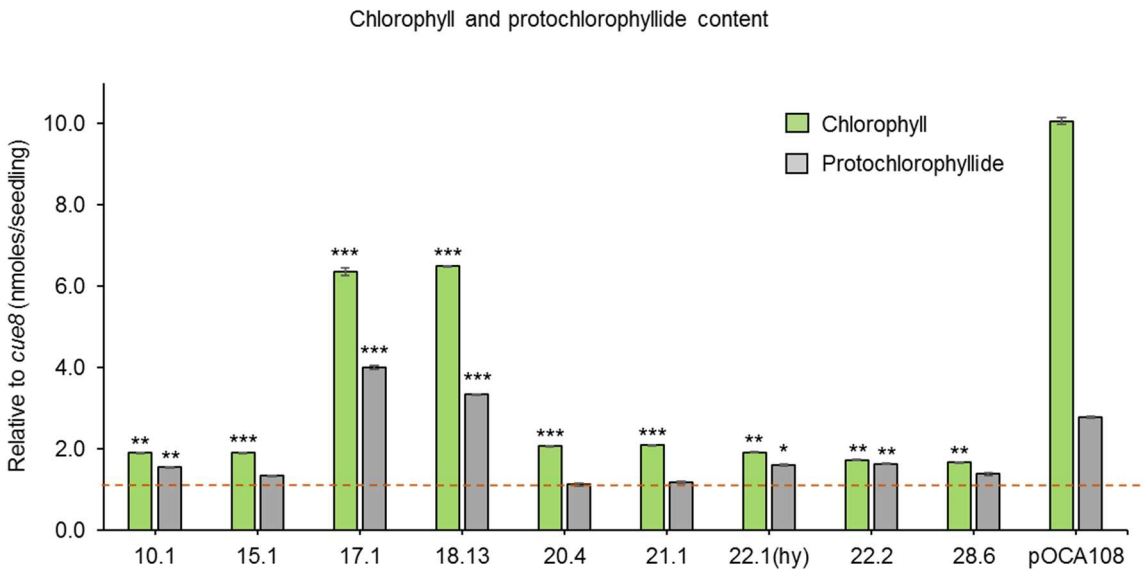


**Figure 4.3** Measurement of chlorophyll and protochlorophyllide in different suppressors and pOCA108 expressed relative to *cue8*. The value of *cue8* is indicated by dotted line as 1. Individual suppressor mutants represented by the number of their pool. Chlorophyll content was analysed per seedling and protochlorophyllide as relative fluorescence unit per seedling. Asterisk symbol is shown as significant difference at $p$ value < 0.05 (*), <0.01 (**) and <0.001 (***).

### 4.3 Identification of a semi-dominant suppressor, *soh1* (*suppressor of TIC hundred 1*)

Candidates within and among the different pools were subjected to complementation tests. To find out if the identified suppressors were non-allelic, various crosses were performed between the individual plants of the same pool (17.1-17.3, 18.1-18.15 and 19.1-19.4) and also in different pools (17, 18 and 19). Great care was taken not to mix seeds of individual plants even in the same pool. There were 15 plants from pool 18 that did not complement each other. It was found that mutants from pool 18 and 19 are allelic, probably the same mutants.

To test the zygosity, promising candidates were backcrossed into the unmutagenised parent. To make sure the cross was successful, with the obvious phenotype, *cue8* was always used as a female parent during the crosses. Several plants from pool 17, 18 and 19 were back-crossed into *cue8* to identify whether the mutation is dominant or recessive. All the F1 progeny obtained from the back-cross showed a suppressor phenotype (Fig. 4.4). When examining the F2 population, about 25% of the seedlings were *cue8*, another 25% were identical to the suppressor while 50% had an intermediate phenotype (small cotyledons compared to

suppressors) suggesting this is a semi-dominant mutation. Suppressor 18.13 was named as *soh1* (*suppressor of TIC hundred 1*) mutants.


**Figure 4.4** Semi-dominant phenotype of F1 seedling obtained from the backcross. Seedling of F1 progeny resulted from *soh1* back crossed into *cue8* showing incomplete suppressor phenotype. Image was captured after the growth 6-days of growth under continuous light. Scale bar represents 5 mm.

A punnet square below shows the outcome of the back cross. The mutant allele for *cue8* is denoted as 'c' and the *soh1* as 's'. All the seedlings contain the *cue8* mutation. There were two types of green seedlings which were grown separately, and in the F3 generation the parent with an intermediate phenotype produced a mixture of all the three phenotypes as seen in F2. Therefore, the heterozygous suppressor mutation has an intermediate phenotype.

| (F2) | c S | c s |
|---|---|---|
| c S | ccSS | ccSs |
| c s | ccSs | ccss |

**Figure 4.5** Punnett square showing genotype possible outcomes of a F2 population from a back cross of *soh1* into *cue8*. Reappearance of *cue8* (¼) confirms the suppressor mutation as dominant. The notation 'c' represents *cue8* and 's' for suppressor.

The *soh1* double mutant also appears stressed, like *cue8*, during the first two days post-germination, the suppression can be seen from day 3 and easily distinguishable by day 6. After a few days on soil the suppression is very striking with rescue of overall growth of the plant. The virescence phenotype is still seen in *soh1* but less dramatic than that of *cue8* (Fig. 4.6).


**Figure 4.6** Phenotypic comparison of WT, *cue8* and *soh1*. The plant image was captured after 30days of growth in 16hr photoperiod. *soh1* showing enhanced greening and suppression of the developmental defect in *cue8*.

### 4.4 Failed isolation of the single suppressor

In order to investigate whether the suppressor mutant has any phenotype on its own in the absence of *cue8* mutation, the *soh1* plants were crossed into pOCA108 to isolate the dominant single mutant. The size difference in cotyledons was also seen in F2 seedlings as observed in the *cue8* back-cross. All the seedlings from the F2 progeny were separated as per their size (large, average and small cotyledons). The aim was to take advantage of the *cue8* genotyping assay to remove the *cue8* mutation. According to Mendelian genetics, the F2 progeny should have three different *cue8* heterozygous plants as shown below (Fig. 4.7 A). Later the F3 seeds from these individual plants were screened to confirm the genotype of the parent.

1. CcSs: Plant heterozygous for both *cue8*/+ and *soh1*/+ is identical to its F1 parent, therefore it will produce *cue8* and *soh1* in the F3 generation.
2. CcSS: Plants heterozygous for only *cue8*/+ and has no suppressor mutation, will produce only *cue8* in the F3.
3. Ccss: Plants heterozygous for *cue8* but homozygous for *soh1* will be expected to produce *cue8* mutants only as *cue8 soh1* in the F3 generation. It is possible to obtain the single *soh1* suppressor mutant from among them by considering plants that do not carry *cue8* even in a single allele (Fig. 4.7B).

**A** (F1) CcSs

| **(F2)** | C S | C s | c S | c s |
|---|---|---|---|---|
| C S | CCSS | CCSs | CcSS | CcSs |
| C s | CCSs | CCss | CcSs | Ccss |
| c S | CcSS | CcSs | ccSS | ccSs |
| c s | CcSs | Ccss | ccSs | ccss |

**B** (F2) Ccss

| **(F3)** | C s | C s | c s | c s |
|---|---|---|---|---|
| C s | CCss | CCss | Ccss | Ccss |
| C s | CCss | CCss | Ccss | Ccss |
| c s | Ccss | Ccss | ccss | ccss |
| c s | Ccss | Ccss | ccss | ccss |

**Figure 4.7** Punnett square showing the possible genotype outcomes of a back cross of *soh1* into pOCA108 (WT). The notation 'c' represents *cue8* and 's' suppressor. (A) Various genotypes expected in the F2 population. All the *cue8* heterozygous lines are indicated in colours and the genotype of interest is shown underlined. (B) Possible outcome of F3 population from of genotype of interest isolated in the F2 (Ccss). Expected genotype of *soh1* single mutant shown in the green boxes.

A perfect comparison to the *soh1* mutant is the WT segregating in the F2 population, but this would be difficult if *soh1* has no specific phenotype. Hence, the *cue8* (CcSS) heterozygous plants could be used to compare with the *soh1* single mutant. Despite multiple attempts to isolate a single *soh1* in the F3 generation, the expected plants (with no *cue8* or *cue8*/+) always produced some segregating *cue8* phenotypes in the F4 generation.

### 4.5 Mapping-by-sequencing identified *soh1* as an intragenic suppressor of *cue8*

To identify the locus of the suppressor mutation, a mapping population was generated by back-crossing *soh1* into *cue8* and selecting recombinant *cue8* phenotypes in the F2 generation of the cross. Mapping-by-sequencing was performed by using SHOREmap software (Schneeberger et al., 2009) of Illumina sequence data of $BC_1F_2$, unmutagenised *cue8* and *soh1*. Analysis of the sequencing data produced a list of high-quality EMS-induced true SNPs in the fifth chromosome (Fig. 4.8). Surprisingly, the narrow list of candidates revealed one of the genes as *TIC100*, with a second site mutation near to *cue8* mutation (Table 4.1).

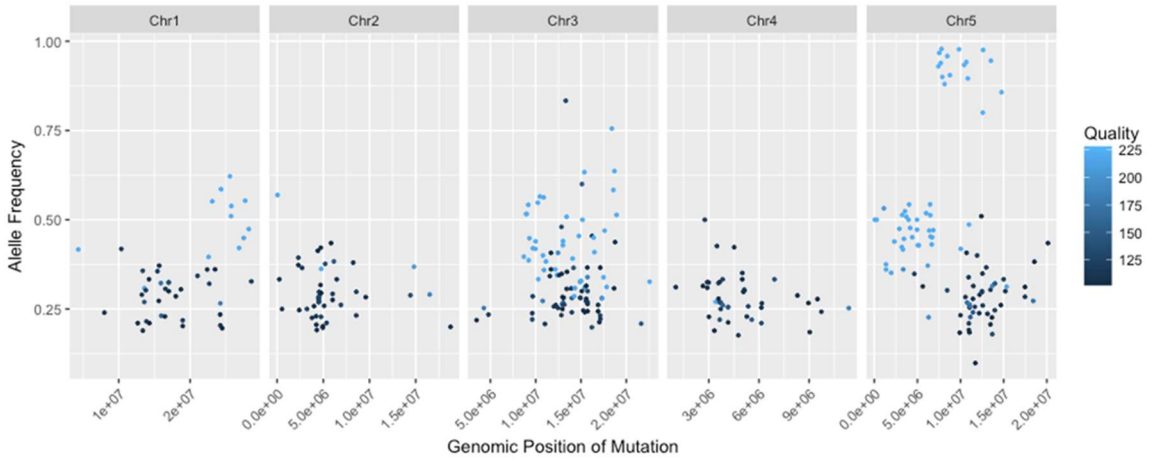


**Figure 4.8** Schematic representation of SHOREmap analysis output. Results showing polymorphisms induced by EMS mutagenesis in different chromosomes. The high-quality SNPs were identified in the 5th chromosome.

**Table 4.1. List of candidate genes with EMS induced mutations analysed by SHOREmap**

| Mutation | Gene ID | Frequency | Quality | Gene Name |
|---|---|---|---|---|
| 3' UTR | AT5G22440.1 | 0.93 | 225 | Ribosomal Protein L1p/L10e |
| | AT5G22440.2 | | | |
| R>Q | AT5G22640.1 | 0.97 | 225 | Emb1211, Embryo Defective 1211, TIC100 |
| | AT5G22640.2 | | | |
| G>S | AT5G23010.1 | 0.94 | 225 | Isopropyl malate Synthase 3 |
| A>T | AT5G23150.1 | 0.98 | 225 | Enhancer of Ag-4 2, Hua2 |
| 3' UTR | AT5G23420.1 | 0.90 | 225 | High-Mobility Group Box 6 |
| A>V | AT5G24710.1 | 0.96 | 225 | Transducin/Wd40-2 Protien, Twd40-2 |
| G>E | AT5G27720.1 | 0.98 | 225 | Emb1644, Embryo Defective 1644, Lsm4 |

The point mutation was identified in the 5th exon (G ≡ C to A = T transition) of AT5G22640 resulting in a single amino acid change from arginine to glutamine, at position 345 in the protein. The gene AT5G22640 (*TIC100*) encodes a protein of 871 amino acids and has a molecular weight of 99.95kD. There are three predicted membrane association MORN domains in TIC100 (http://mobidb.bio.unipd.it/Q8LPR8/db). The point mutation *cue8* was identified in the proximity of the third membrane-association domain, while the *soh1* is in the predicted third domain (Fig 4.9 B)

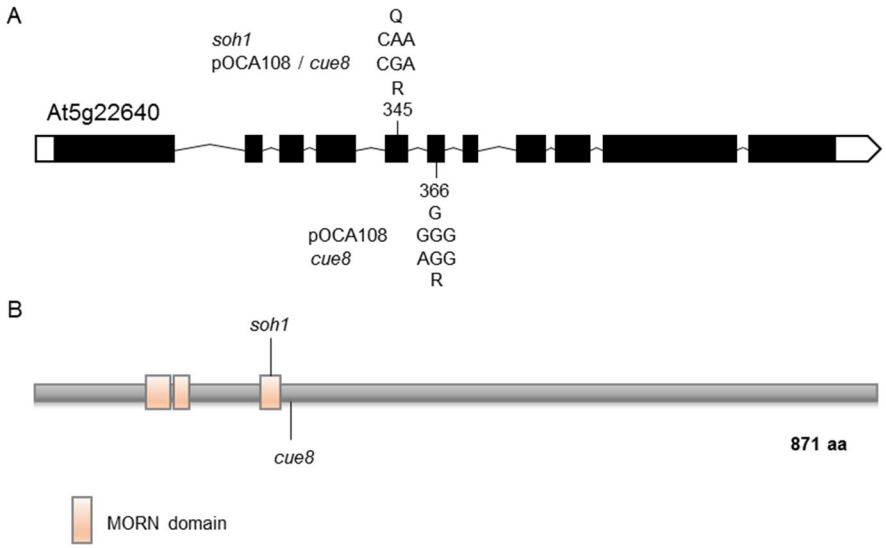


**Figure 4.9** Schematic representation of the model showing gene and protein encoded by *TIC100* (AT5G22640). (A) The point mutation in exon 6, *cue8*, results in a single amino acid change from glycine to arginine. The *soh1* mutation occurred in exon 5, changing an arginine to glutamine.

### 4.6 *soh1* has an increased chloroplast compartment

An investigation of chloroplast development was performed to examine the reason behind the apparent rescue of phenotype in *soh1*. Mesophyll cells of 6-day-old seedlings showed *soh1* cotyledons had greater chloroplast coverage compared to *cue8*. Interestingly, the individual chloroplast size was increased by 39% compared to *cue8* (Fig. 4.10 A and B). Total chloroplast area of similar-sized cells showed *soh1* has minimised the difference of chloroplast proportion between *cue8* and WT (Fig. 4.10 C)

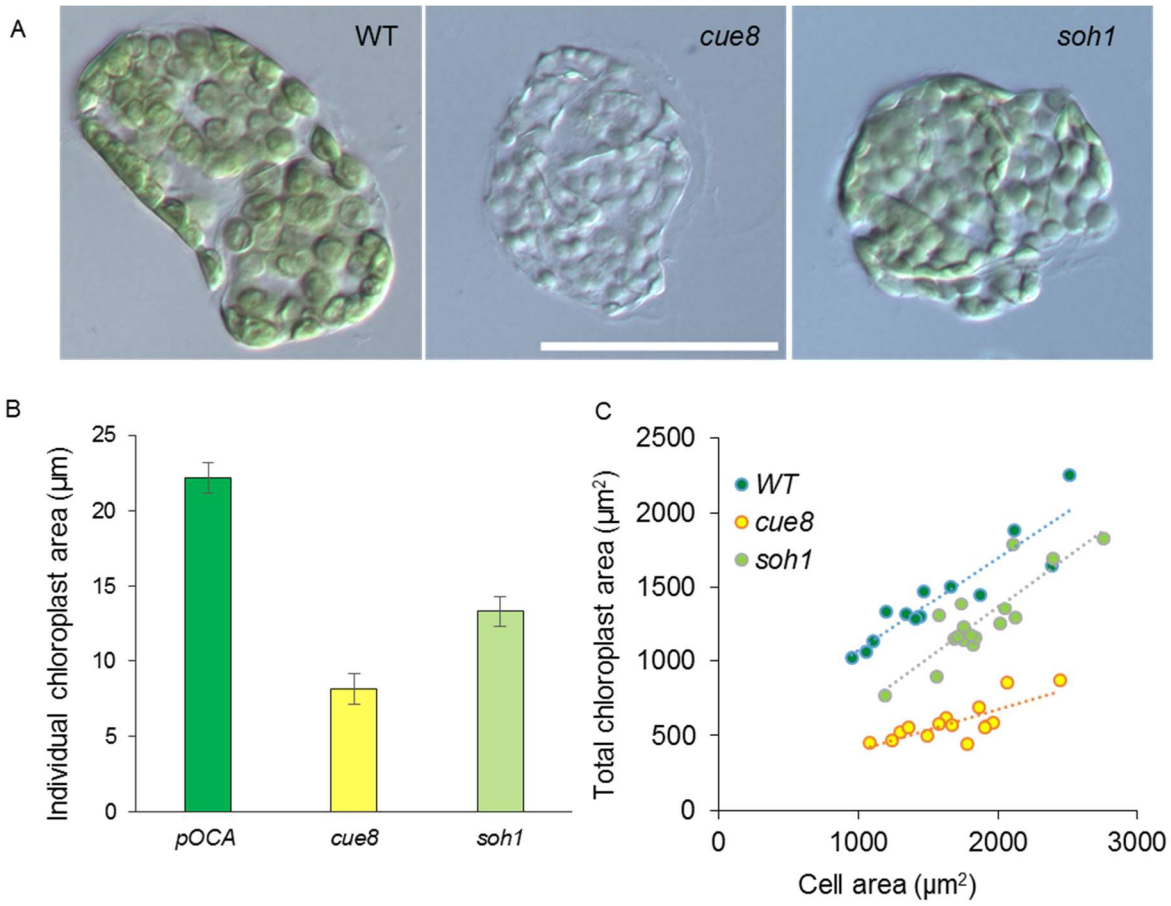


**Figure 4.10** Cellular chloroplast compartment of *cue8* and *soh1*. (A) Fixed mesophyll cells showing a difference in the chloroplast complement in WT (5-days-old), *cue8* and *soh1* (6-days-old) cells. Scale bar: 50 µm. (B) Chloroplast area measured from 10 chloroplasts in each cell by considering 20 cells per replicate. *soh1* chloroplasts are larger in size compared to *cue8*. Error bars represent standard error of the mean (SEM) of replicate samples, n=20. (C) Total chloroplast area plotted relative to cell plan area. Total chloroplast area in *soh1* is greater when compared to similar-sized cells of *cue8*.

### 4.7 *soh1* chloroplasts have less densely packed DNA

One of the striking observations in *cue8* was that the cpDNA was densely packed, DAPI stained *soh1* mesophyll cells showed suppression of this phenotype by showing more dispersed distribution of the aggregated plastome. The chloroplast DNA in the double mutant was less densely packed, showing an intermediate phenotype between WT and *cue8* (Fig. 4.11).

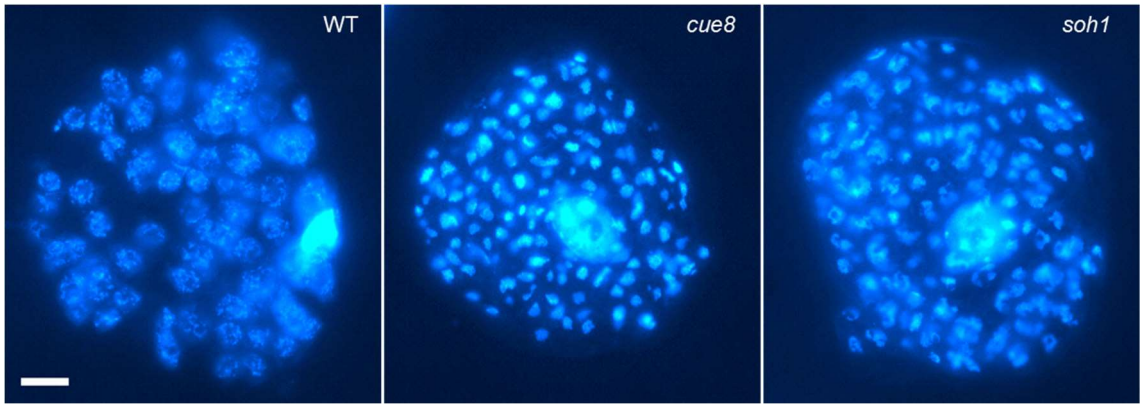


**Figure 4.11** Distribution of chloroplast DNA in *cue8* and *soh1* seedlings. Fluorescence microscopy of DAPI stained cotyledon cells showing densely packed cpDNA in *cue8*, while slightly relaxed packaging in the *soh1*. Images were captured at x60 objective. Scale bar: 10 µm.

### 4.8 *soh1* rescued import of a photosynthetic protein into chloroplasts

Previous import analysis of an *in vitro* translated preprotein of the small subunit of Rubisco (ribulose-1,5-bisphosphate carboxylase/oxygenase) demonstrated that *cue8* chloroplasts are slow in importing a photosynthetic protein (preSSU). As *soh1* showed multiple signs of suppression, import analysis was carried out to understand if the second site mutation can overcome the protein import defect of *cue8*. Considering the developmental delay, chloroplasts were isolated from 17-days old *cue8* and *soh1* seedlings and form 13-days old WT seedlings (Fig. 4.12 A). Isolation from *cue8* showed a mixed population of chloroplasts. There were multiple unusually-small to slightly-reduced chloroplasts (Fig. 4.12 B) in comparison to WT cells which had well-developed, similar-sized chloroplasts. Although there were a few smaller ones, s*oh1* also showed many larger chloroplasts compared to *cue8*.

Import of preSSU recovered in *soh1*, not fully but close to WT levels, which suggests that the *soh1* chloroplasts are able to import photosynthetic protein at faster rates compared to *cue8* (Fig. 4.13).

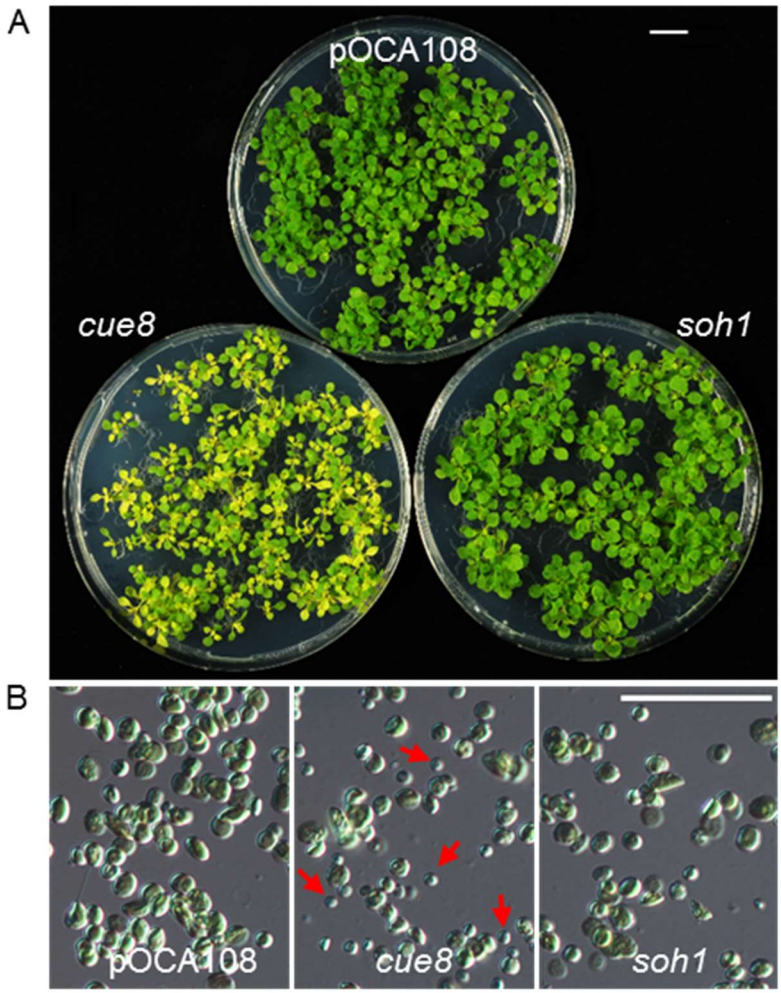


**Figure 4.12** Chloroplast isolation from seedlings of WT, *cue8* and *soh1*. (A) Seedlings grown under 16hr photoperiod conditions were collected after 13days for WT, 17-days for *cue8* and *soh1* (B) Images of isolated intact chloroplasts in different genotypes. WT showing similar sized chloroplasts, *cue8* has different sizes (arrows indicating small chloroplast). Most *soh1* chloroplasts are larger compared to those of *cue8*.

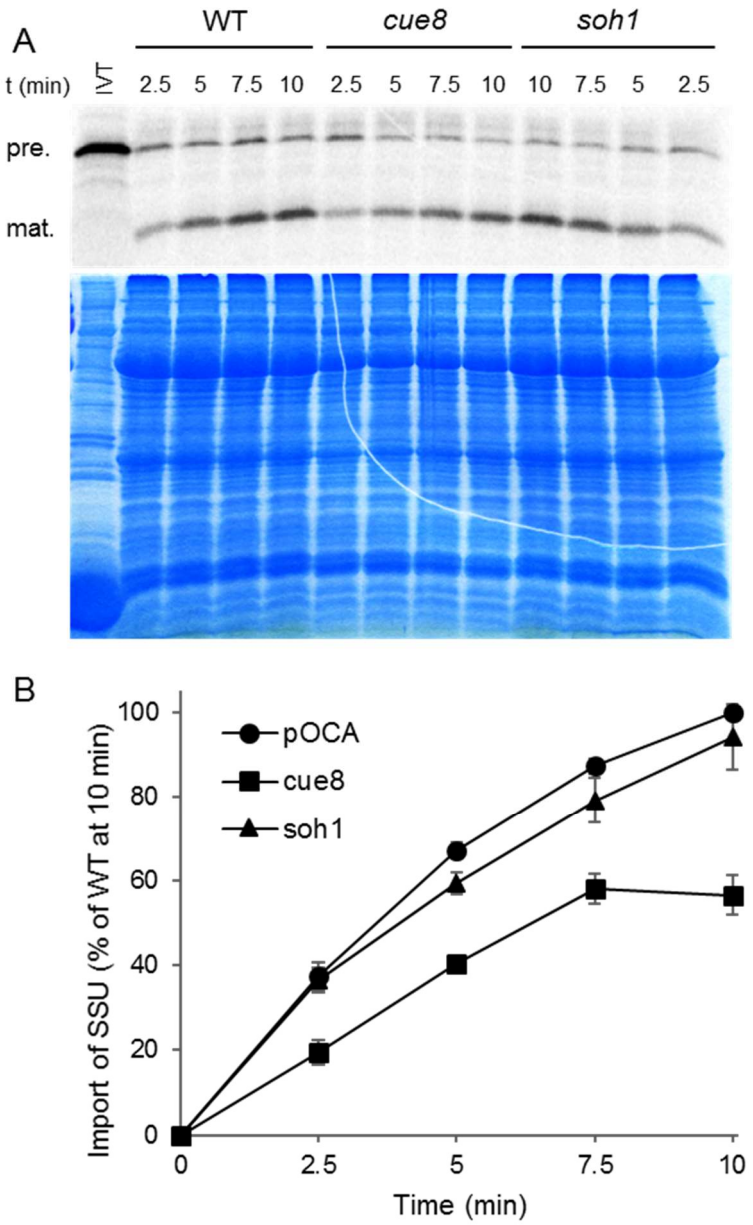


**Figure 4.13** Rate of photosynthetic protein import into chloroplasts of WT, *cue8* and *soh1*. (A) Import of radiolabelled protein at four different time points as indicated above for each genotype. A control IVT (*in vitro* translated) product run beside the samples. Gel image showing equal loading of samples. (B) Percentage of import measured from the band intensity of imported radiolabelled protein. Data in the graph represent the mean ± SEM of 3 independent experiments, expressed as percentage relative to the WT 10min import sample.

### 4.9 *cue8* also showed reduced import of a housekeeping protein

Current knowledge on TOC complexes is far advanced compared to that on the TIC machinery and provides evidence for the existence of specific import routes for photosynthetic and housekeeping proteins. However, there is no information for such a specific route in the chloroplast inner envelope. To examine whether TIC 1MDa complex acts in the import of housekeeping proteins, import of an *in vitro* translated preprotein of

ribosomal subunit PRPL11 (precursor of a 50S ribosomal protein) was tested. According to the results, *cue8* chloroplasts imported preL11 at a much lower rate. Indeed, this was again suppressed by *soh1*, importing preL11 at faster rates (Fig. 4.14). Therefore, the combined results of *cue8* and *soh1* suggest TIC 1MDa complex in the chloroplast inner membrane plays a crucial role in the import of both photosynthetic and housekeeping proteins.

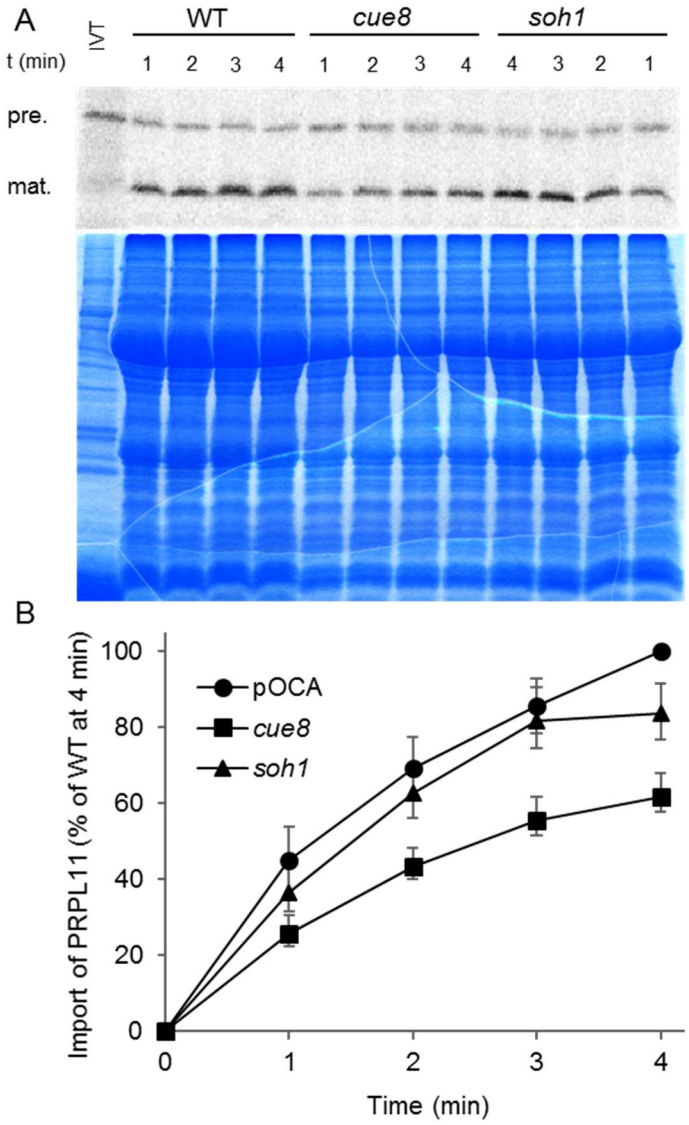


**Figure 4.14** Rate of housekeeping protein import into chloroplasts of WT, *cue8* and *soh1*. (A) Import of radiolabelled protein at four different time points as indicated above for each genotype. A control IVT (*in vitro* translated) product run beside the samples. Gel image showing equal loading of samples. (B) Percentage of import measured from the band intensity of imported radiolabelled protein. Data in the graph represent the mean of 3 independent experiments, expressed as percentage relative to the WT 10min import sample. Error bars represent standard error of the mean (SEM) of 3 independent experiments.

### 4.10 *soh1* rescued TIC 1MDa complex in *cue8*

It was previously observed that *cue8* has reduced protein abundance for 1MDa TIC complex proteins (Bédard, López-Juez and Jarvis, personal communication). Immunoblotting analysis was performed to understand what impacts the mutation has on the import machinery and whether the defects in import are due to affected levels of TIC complex. The total proteins extracted from isolated chloroplasts showed that the proteins of 1MDa TIC complex, particularly TIC100, were significantly reduced because of the *cue8* mutation, but two other tested membrane components which are not part of this complex TIC110, TIC40 and TOC75, were elevated to almost two-fold in *cue8*. The G to R substitution introduced into the TIC100 protein affects the formation of 1MDa complex (Fig. 4.15). Data shows that *soh1* accumulates more TIC100 along with other 1MDa proteins in comparison to *cue8*. Hence the second mutation that causes a R to Q substitution nearby allows re-association of the import machinery.

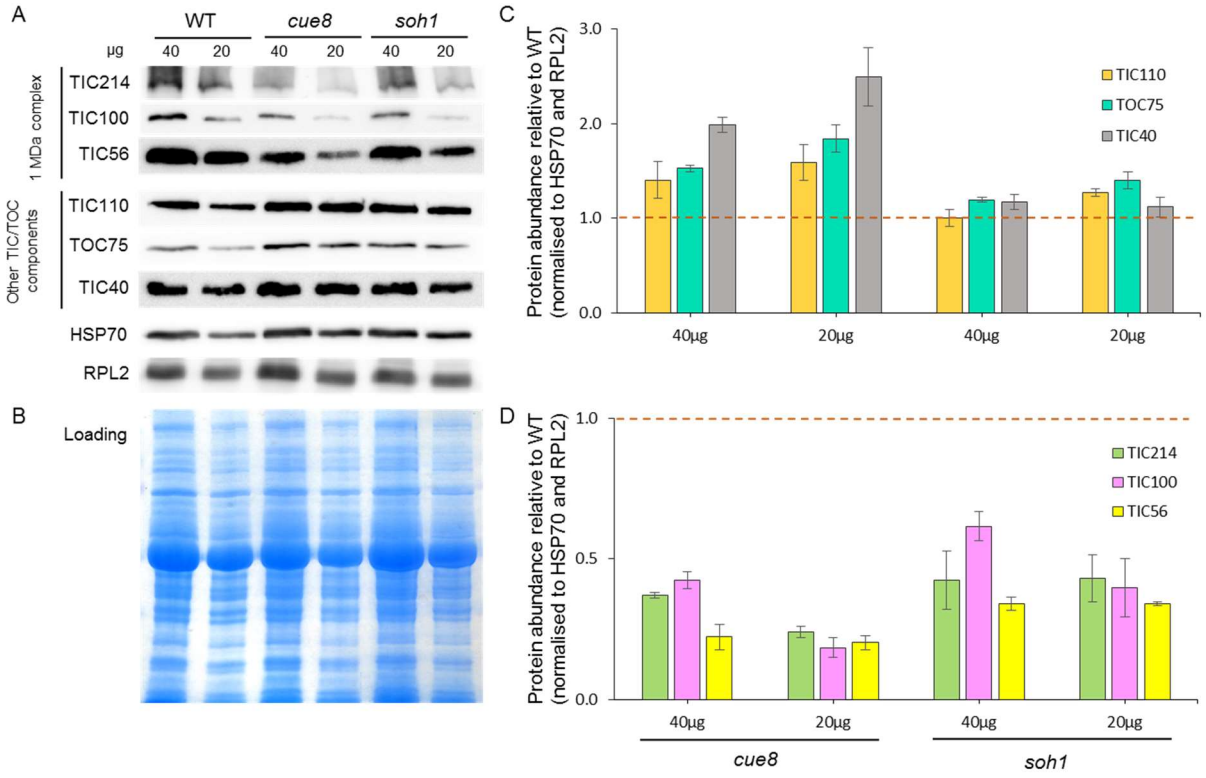


**Figure 4.15** Immunoblot analysis of import components in WT, *cue8* and *soh1*. (A) Analysis of TIC 1MDa and other membrane components (TOC/TIC) measured from total chloroplast proteins along different genotypes. Antibodies were used against nucleus-encoded TIC100, TIC56, TIC110, TOC75, TIC40, HSP70 and chloroplast encoded TIC214 and RPL2. (B) Equal loading was shown indicating 40µg and 20µg in alternate lanes. (C, D) Graphs showing quantitation of 1MDa protein (C) and other membrane-associated chloroplast protein bands (D) in A, done using Aida software and normalised to the mean of HSP70 and RPL2. Error bars represent standard error of the mean (SEM) of 3 independent experiments.

### 4.11 *cue8* shows enhanced transcript levels of chloroplast envelope proteins

The reduced level of TIC complex proteins, along with reduced expression of PhANGs, led to the hypothesis that the expression of the genes encoding TIC 1MDa proteins might be low in *cue8*. Surprisingly, the transcript levels were increased for nucleus-encoded (*TIC100*, *TIC56*, *TIC20*, *TOC159*) and for chloroplast-encoded *tic214* (Fig. 4.16). Similar results were observed in the seedlings and juvenile leaves. Therefore, the decrease of those polypeptides is not an indirect result of gene expression changes, and instead is most likely to emerge from post-translational events resulting in incomplete or de-stabilised complexes.

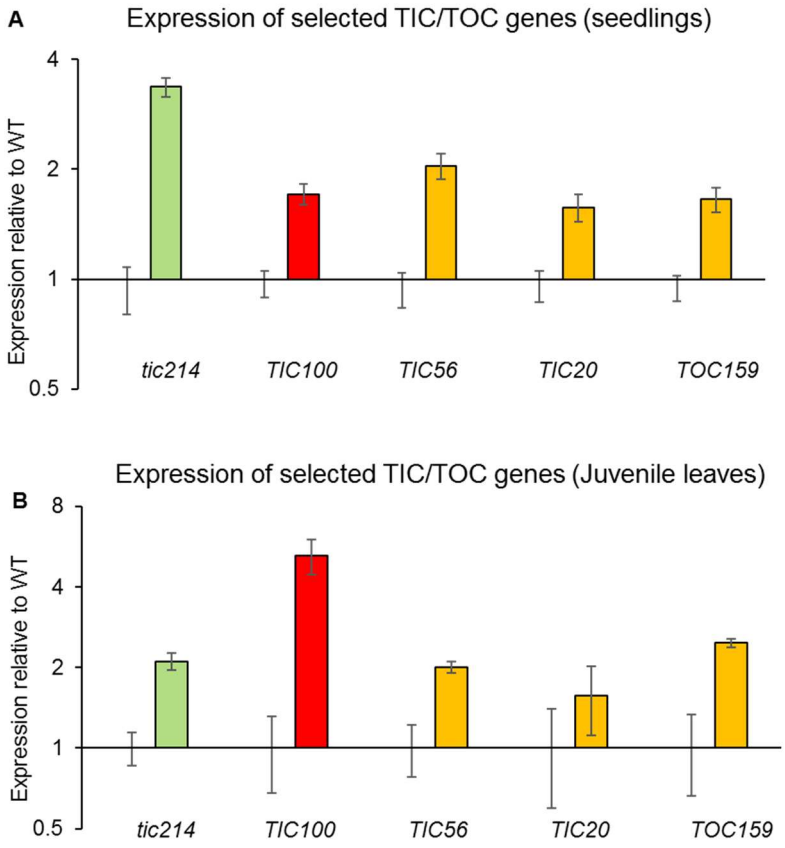


**Figure 4.16** Expression of 1MDa TIC complex and *TOC159* genes in *cue8*. Transcript levels of each gene were measured relative to a constitutive gene, *UBQ10*, and the values were calculated for *cue8* relative to the corresponding values of the wild type. The relative values are represented on a log2 scale, but the numbers on the scale are actual ratios, a value of 1 representing the expression in the wild type. (A) Elevated transcripts of nucleus-encoded *TIC100*, *TIC56*, *TIC20*, *TOC159*, and chloroplast-encoded *tic214* genes in *cue8* seedlings (6-days-old) and (B) juvenile leaves (<4mm). Error bars represent standard error of the mean (SEM) of triplicate samples.

### 4.12 Overexpression of *soh1* cDNA complements the *cue8* phenotype

Transformation of *cue8* plants with a construct overexpressing *soh1* cDNA enhanced the growth and overall development of the plant and fully mimicked the *soh1* mutant, confirming that *soh1* is an intragenic suppressor. All 11 identified positive T1 transformants showed a similar degree of phenocopy. The transformants after 3 weeks of growth were confirmed by genotyping for the presence of *35S::soh1* cDNA (Fig.4.17 C).

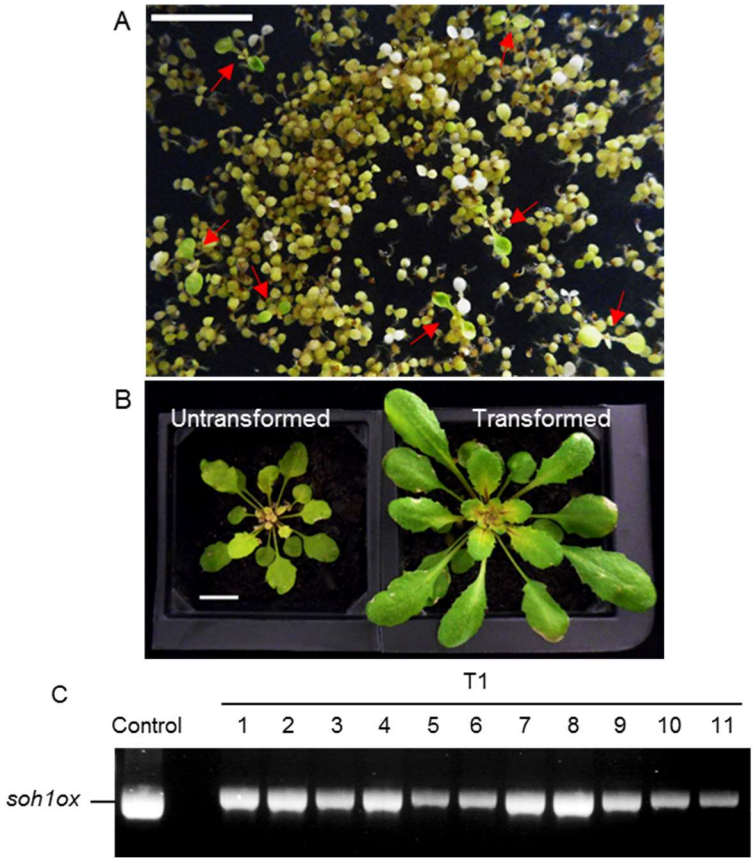


**Figure 4.17** Overexpression of *soh1* supresses the phenotype of *cue8* plants. (A) Screening of the transformants (T1) on MS media plates containing BASTA (phosphinothricin). Arrows indicate positive transformants visualised after 2-weeks of growth under 16hr photoperiod conditions. (B) Transformation of *35S::soh1* showing suppression through overall growth and enhanced greening of *cue8* grown for 30 days. Scale bar represents 1cm. (C) Confirmation of selected T1 transformants through PCR amplification of 35S promotor and 35S terminator primers of destination vector (pB2GW7). Genotyping was performed alongside the PCR amplified product of plasmid isolated from *Agrobacterium* carrying the transgene.

### 4.13 Generation of constructs for immunoprecipitation assays

To test the stability of 1MDa complex, three versions of the TIC100 open reading frame, wild type, *cue8* and *soh1*, were cloned into a modified (Jarvis lab) p2GW7 destination vector (Karimi et al., 2007) with haemagglutinin (HA) epitope-tag at the C-terminus. These

constructs are ready for protoplast transformations and the immunoprecipitation investigation would test the hypothesis that a mutated TIC100 protein is responsible for reduced interaction and dissociation of 1MDa complex in *cue8*, and that whether *soh1* helps in its reassociation.

### 4.14 A suppressor of *hy1* also supresses *cue8*

*hy1*, a phytochrome defective mutant, fails to fully perceive light and as a result exhibits defective chloroplast development, including defective *LHCB1* expression (Vinti et al., 2000). The *hy1* mutant was used in a forward genetic screen for suppressors of the low *LHCB1* expression phenotype, i.e. second mutations resulting in enhance *LHCB1* expression and increased greening were sought. This led to identification of *lynx1* (for its "ability to perceive weak light", abbreviated as *lyn1* (He, Hills and Lopez-Juez personal communication). Interestingly, *lyn1* does not act directly on the phytochrome regulatory pathway, instead this is a negative regulator of early cell differentiation. In contrast to *cue8* which has a reduced chloroplast compartment, it has been observed that loss of LYN1 enhances the chloroplast compartment beyond that of WT cells (He, unpublished). This observation brought about the question of whether *lyn1* could suppress an import defective mutant, *cue8*. The *lyn1* homozygous plants were crossed into $cue8_{col}$ obtained from introgression of *cue8* mutation in Col-0 (backcrossed three times). The plants with *cue8* phenotype from the F2 generation were individually genotyped for the presence of *lyn1* (Fig. 4.18 A). The *cue8 lyn1* double mutants were developmentally advanced compared to the segregating *cue8*, mutant seedlings, showing faster development within 24 hrs in the light. Chlorophyll content was measured at different time points in the seedlings (F3) that were transferred to light after their growth for 4-days in the dark, and there was a significant increase in chlorophyll content of *cue8 lyn1* even after 51 hrs. The difference in development continued when the plants were grown on soil (Fig. 4.18 B). However, protochlorophyllide accumulation of 6-day-old dark-grown seedlings was not different from *cue8*.

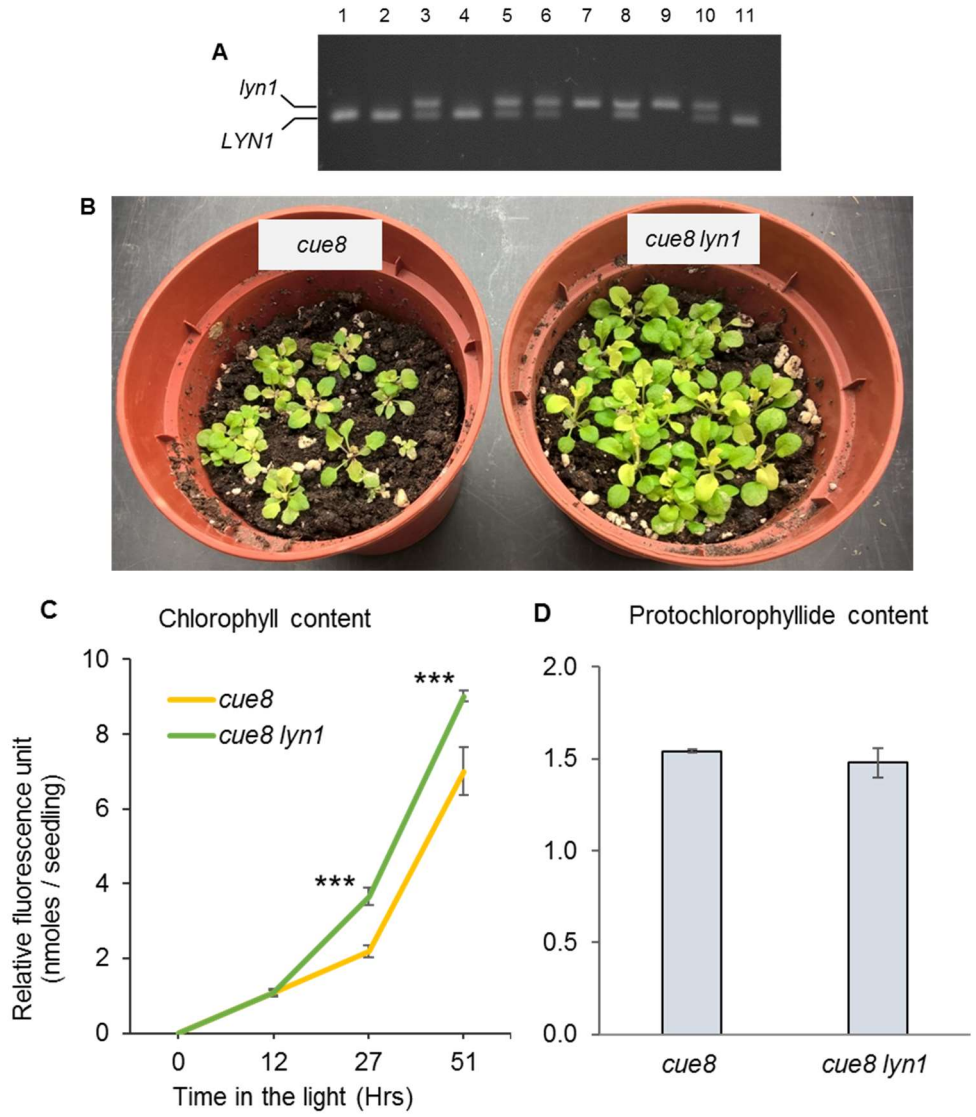


**Figure 4.18** *lyn1* is also a suppressor of *cue8*. (A) Gel image showing genotyping results of PCR amplified and restricted product. Bands represent *LYN1* (lower, 256bp), *lyn1* (upper, 285bp) and heterozygous plants in case of double bands. (B) Phenotype of plants grown for two weeks on soil. *cue8 lyn1* is developmentally ahead with leaves which are more developed and greener compared to *cue8*. (C) Chlorophyll levels quantified per seedling at different time points (as indicated) after the transfer from dark (4-days) to light. Asterisk symbol are shown as significant difference at *p* value <0.001 (***). (D) Protochlorophyllide levels in etiolated seedlings grown in the dark for 6-days.

## 4.15 Discussion

The process of plastid development requires a majority of its proteins which are nucleus-encoded to be targeted to chloroplasts (Ivanova et al., 2004; Jarvis, 2008). Import of these cytosolic proteins can be divided into three phases - directing the preproteins to the right organelle, passage of the preproteins between the two membranes of chloroplasts and targeting the final protein to internal structures (Keegstra and Cline, 1999). The double membrane envelope of chloroplast has translocon complexes embedded in both outer (TOC) and inner (TIC) membranes to facilitate protein import. The outer envelope contains a channel protein (TOC75) which allows the passage of cytoplasmic preproteins. Although the channel remains the same in different complexes, there are distinct receptor proteins that recognise different types of preproteins during the import. For example, TOC33 and TOC159 interact and look after the import of preferentially photosynthetic preproteins, while TOC34 and TOC32/TOC20 are basically involved in the import of housekeeping proteins (Jarvis et al., 1998; Bauer, 2000; Ling et al., 2012).

Formation of super-complexes between TOC and TIC components was observed to encourage successful import of chloroplast proteins (Schnell et al., 1994; Kouranov et al., 1998; Chen LJ, 2017). There are multiple TIC components identified over time (reviewed in Jarvis and Lopez-Juez., 2013) and proposals of two different channels in the inner membrane: TIC110 (Waegemann et al., 1992; Heins et al., 2002; Balsera et al., 2009) and TIC20 (Chen X, 2002), and their interaction (Kouranov et al., 1998) raised questions regarding the sorting of preproteins in the inner membrane. TIC110, TIC40 and Hsp93 were thought to be the key players in the transport of preproteins, however finding of a 1MDa complex with TIC20 as channel showed none of these three proteins to interact with the complex (Kikuchi et al., 2009). Recently, the same group identified individual proteins in the TIC 1MDa complex as TIC100, TIC56 and TIC214, that bind to the channel TIC20-I and these researchers proposed this as a general import complex. Again, there was no association of TIC110 with any of the 1MDa components, these observations challenging direct involvement of TIC110 in protein import. TIC100, TIC56 and TIC20 are nucleus-encoded while TIC214 is expressed in the chloroplast (Kikuchi et al., 2013). These proteins are conserved in dicots and most monocots and loss of the 1MDa proteins resulted in seedling lethality with severe deficiency of protein import, but somehow the grasses managed after loss of TIC100, TIC56 and TIC214, thus the role of these proteins was questioned.

This chapter focuses on characterisation of the chloroplast-defective mutant *cue8*. Findings of 1MDa components revealed the identity of *CUE8* as *TIC100,* which suggested *cue8* plastids suffer inefficient import of proteins that are required for chloroplast development. A forward genetic screen for suppressors of *cue8* has identified an intragenic suppressor, *soh1,* that shows a semi-dominant phenotype (Fig. 4.6). Overexpression of *soh1* fully suppresses the *cue8* to the same extent, confirming the suppressor role of the second-site mutation (Fig. 4.17). Because both mutations are present in the same gene, it cannot be ruled out whether overexpression of *cue8* cDNA on its own would also result in the suppression of *cue8* phenotype, however expression analysis showed the transcripts of *cue8* are elevated in the mutants (Fig. 4.16) making such a mechanism of suppression unlikely. The screening of transformants (T1) overexpressing *cue8* is ongoing, and this will act as a control for the complementation by *soh1*.

TIC100 has no known transit peptide and the immunoblotting experiments showing enhanced accumulation of *soh1* protein (still carrying *cue8*) rule out the possibility that either of the two mutations affect targeting of this protein to the chloroplast 1MDa complex. Kikuchi et al. (2013) provided evidence that lack of *TIC100* or *TIC56* reduced the formation of 1MDa complex. Interestingly this phenomenon was not seen in *tic20-I* mutants, moderate amounts of TIC214, TIC100 and TIC56 were still observed even in the absence of the proposed channel, TIC20-I. Accordingly, partial loss of function of *TIC100* (in *cue8*) also corroborated this observation showing reduction specifically in the proteins of 1MDa complex while there was less reduction in the suppressor mutant (*soh1*), an observation which fully supports the existence of the 1MDa complex. The missense *cue8* mutation introduces an arginine that gives an extra charge, potentially interfering with the folding of the protein. This could explain the disassembly of the 1MDa complex. Meanwhile *soh1* replaces another arginine (within the predicted third MORN domain and in proximity of the *cue8* transition) with a glutamine that reduces the previous charge, allowing association with other proteins in the complex (Fig. 4.9). There is a stringent coordination of gene expression between the nucleus and the chloroplast (Woodson and Chory, 2008), for example the 1MDa complex is constituted of nucleus-encoded and chloroplast-encoded proteins. It was anticipated that the expression of 1MDa complex genes could also be reduced in *cue8*; interestingly there were more transcripts of not only nucleus-encoded genes (*TIC100*, *TIC56* and *TIC20*), but surprisingly also for *tic214*, encoded in the genome of defective chloroplasts (Fig. 4.16). This suggests the accumulation of TIC 1MDa components is altered due to post translational

effects in *cue8*. The role of TIC100 and TIC56 seems fundamental in complex formation, however these proteins accumulate to normal levels even in the absence of TIC20-I (Kikuchi et al., 2013). This raises a question about the role and interaction of accumulated TIC214, TIC100 and TIC56 in TIC20-I mutants. Whether these proteins can still associate without TIC20-I, or whether they interact with other channels is not known.

A common observation among *tic100*, *tic56-1* and *tic20-I* null mutants was the absence of photosynthetic proteins, while accumulation of certain housekeeping proteins (HSP70 and HSP93) was normal. This was proposed to occur due to the elevation of a closely related TIC20-IV in the absence of TIC20-I (Hirabayashi et al., 2011). As TIC20-IV was mostly expressed in the roots, it was proposed that TIC20-IV translocon might import certain housekeeping proteins without the involvement of 1MDa proteins in the *tic20-I* mutant. Therefore, the TIC 1MDa complex was interpreted as mainly involved in the import of photosynthetic preproteins. Similar results were seen (Fig. 4.15) even in *cue8* chloroplasts, which had normal or elevated levels of housekeeping proteins (TOC75, TIC110, TIC40, HSP70 and RPL2). Kikuchi et al. (2013) interpreted the normal accumulation of HSP70 and HSP93, in severely-impaired seedlings of 1MDa component mutants, as evidence for the complex to act as a "green TIC". However, accumulation of such chaperones was observed in *ppi1* (Kubis et al., 2003). In fact, such accumulation was also observed in the *tic21/pic1-1* mutant (Kikuchi et al., 2009), which is defective in iron transport into chloroplasts (Duy et al. 2011). It is possible that such accumulation occurs as a knock-on result of import defects, as seen in *cue8*; it is compatible with the 1MDa complex acting as a "global TIC", and *cue8* being defective in import of photosynthetic and housekeeping proteins, as observed in the present study. The photosynthesis-related proteins are major contributors to the quantity of extracted total chloroplast proteins. As chloroplast-defective mutants lack these abundant photosynthetic proteins, it is important to note the loading of mutant protein (in quantity equal to WT) would involve increased amounts of envelope proteins. This could explain the greater amount of membrane proteins in the mutant, compared to WT.

Apparently-conflicting data, and conflicting interpretations, have been published in relation of mutations in a separate component of the 1MDa complex. It was shown that *tic56*-3 mutants carry a T-DNA insertion towards the end of the last exon, which results in expression of a truncated protein (Kikuchi et al., 2013), and this might be sufficient for mild accumulation of TIC214, TIC100 and TIC20. Chloroplasts show impaired import of selected proteins in this mutant, but the seedlings of *tic56*-3 mutants are pale green, compared to the

completely albino-lethal KO allele, *tic56*-1. This was challenged by very recent findings, reporting that extremely impaired seedlings of *tic56*-1 can accumulate chloroplast proteins to normal levels, while chloroplasts of *tic56*-3 can import cytosolic proteins at normal rates (Kohler et al., 2015). Data on protein import analysis of *cue8* and *soh1* demonstrated that TIC100 plays an important role in the transport of photosynthetic and housekeeping preproteins. The rate of import of photosynthetic preSSU in *cue8* chloroplasts was reduced (Fig. 4.13). The import of housekeeping protein PRPL11 (part of the chloroplast 50s ribosomal subunit) was also compromised in these mutants (Fig. 4.14). These observations are consistent with the *soh1* mutants showing less reduced import rate for selected photosynthetic as well as housekeeping proteins. These data support the notion that the 1MDa complex could act as a "global TIC". The KO *tic56*-1 seedlings examined by Kohler and collaborators may have shown comparable levels of specific proteins relative to reference proteins after many weeks of very slow growth of a near-lethal mutant, such data not reflecting import rates at all. It is also worth mentioning that elevation of nucleus-encoded polymerase activity was shown in the previous chapter of this thesis and was probably caused by elevated transcripts for NEPs, but would also require sufficient import of NEP into the chloroplast. Although the NEP proteins were not analysed, their enhanced activity is manifested by the enhanced expression of NEP-driven genes. Therefore, it is possible that other inner membrane complexes carry out housekeeping protein import in 1MDa complex mutants. To resolve between these possibilities, it would be important to examine other housekeeping chloroplast proteins.

The recently discovered SP1 was revealed to reorganise the import complexes (specifically TOC proteins) according to the developmental status of the chloroplast, as well as environmental signals (Ling et al., 2012). For example, during the etioplast to chloroplast transition, SP1 remodels the TOC complex, replacing the one that receives housekeeping proteins (atTOC132/atTOC120) with the one that prefers photosynthetic protein import (atTOC159 and atTOC33). *sp1* was identified as a suppressor of *ppi1*. In the *sp1 ppi1* double mutants the plants accumulate more photosynthetic proteins compared to *ppi1*, due to the lack of the turnover of TOC components. There is a SP1 homolog which is also targeted to the chloroplast membrane, but this doesn't show redundancy with SP1. It was observed that SP1 degrades the TOC machinery in response to stress conditions, a circumstance during which there is repression of photosynthetic proteins (Ling and Jarvis, 2015). This observation leads to an interesting question, in relation to the gene expression changes happening in *cue8*

chloroplasts: whether SP1 or its homolog play any role in reorganising the TOC complex to coordinate the import of specific proteins in response to defects of general TIC complex.

Interestingly, the *cue8 lyn1* seedlings deetiolated earlier during the dark-to-light transfer, thereby accumulating more chlorophyll in developed cotyledons (Fig. 4.18). How *lyn1* manages to induce a rapid transition of etioplast to chloroplast, in the presence of impaired TIC100, is yet to be seen. On the other hand, this sort of screen (dark to light) could also be employed to identify other candidate suppressors of *cue8* that drive the plastid transitions.

Multiple pieces of evidence suggest that *soh1* rescues the defect of chloroplast development in *cue8*. The present study of *cue8* and *soh1* fully supports the model of the novel 1MDa complex (TIC214, TIC100, TIC56 and TIC20-I). Furthermore, the observations reveal that partial loss of function in TIC100 affects the import of selected photosynthetic as well as housekeeping preproteins, hence 1MDa complex might act as a global TIC complex in the chloroplast inner membrane. It was proposed that TIC100 is facing towards the intermembrane space (Kikuchi et al., 2013) a location in which it might have an important role in recognising the preproteins crossing the TOC complexes. Future research on TIC components might reveal the precise role of TIC214, TIC100 and TIC56 and how grasses manage to develop chloroplasts without such important TIC subunits. Whether TIC110 acts as a separate translocon complex is yet to be seen.

In summary, the *cue8* plant contains a mutation in the gene that encodes TIC100, which is part of the 1MDa import complex located in the inner envelope of the chloroplast membrane. The upregulation of transcripts of nucleus-encoded (TIC100, TIC56, TIC20) and chloroplast-encoded (TIC214) proteins suggests the defects in cue8 are due to the post translational modification and turnover of TIC100 protein, in spite of the observed upregulation of transcript levels, fully consistent with the activation of the housekeeping compensatory mechanism in cue8. The forward genetic screen in cue8 has identified some interesting suppressors. This chapter focuses on soh1 (suppressor of TIC hundred 1), an intragenic suppressor of cue8. soh1 has a semi-dominant phenotype with the second nearby mutation occurring within TIC100 and the chloroplasts showing enhanced individual size and less densely packed cpDNA. With an increase in levels of 1MDa TIC complex proteins, including TIC100, a faster import of house-keeping and photosynthetic proteins was observed in soh1 compared to cue8. Given that KO mutations were previously shown to result in embryo or early seedling lethality (Liang et al, 2010, Kikuchi et al, 2013), one can conclude that the

mutation in cue8 causes a partial loss of function. The current research provides evidence that such partial loss of function in cue8 affects the accumulation of 1MDa TIC components. In addition to previous findings that TIC100 is a part of 1MDa import complex, investigation of cue8 and soh1 reveals that this TIC complex acts as a general translocon and is involved in import of housekeeping, as well as photosynthetic preproteins. cue8 causes reduced import of preproteins of both types, while soh1 rescues both defects. The mutation in cue8 introduces an extra charge (with arginine) which might interfere in the formation of the complex. On the other hand, soh1 replaces a different but nearby arginine (in a predicted membrane association domain) with glutamine, which somehow reduces the impact of the previous mutation on the complex. The precise role of TIC100, and its need for associating with the inner membrane of the chloroplast, is yet to be seen, however there is substantial data to dispel the doubts about the existence of recently proposed TIC complex in dicot plants.

# Chapter 5

# Understanding of chloroplast biogenesis along the developing wheat leaf

## Statement of authorship

Microscopy data obtained in the combined work with Priyanka Mishra

Transcriptome data analysis and Z-Score values of provided genes, involved in chloroplast development, by Kotaro Takahagi (Dr. Keiichi Mochida lab, Center for Sustainable Resource Science, Riken, Yokohama, Japan)

The monocot leaf, with its basipetal growth, serves as an ideal model to study plant development. Several studies have used developing maize and wheat seedlings to understand cellular differentiation (Boffey SA, 1979; Boffey SA, 1980; Dean and Leech, 1982; Li et al., 2010; Pick et al., 2011; Wang et al., 2014; Wang et al., 2017), however there are many gaps in understanding the process of chloroplast biogenesis. For example, most of those studies have excluded stages of cell division. Therefore, the current study focuses on exploring the fundamentals of chloroplast development, its connection with early cellular events and how individual processes change during differentiation. The aim of the research is to explore the series of events involved in plastid biogenesis and to identify the underlying regulators. The work described in this chapter has the following objectives:

- To obtain a quantitative chloroplast biogenesis dataset and examine individual organelle biological processes within it along the developmental gradient of wheat leaf.
- To generate the transcriptome data along the growing wheat leaf which could be used to identify novel candidate genes involved in the process of chloroplast development.

### 5.1 Design of a dissection strategy

A dissection strategy was designed to cover a range of cellular developmental stages from meristem to a fully mature region. Wheat seedlings grown for 6-days under continuous light were dissected along the gradient to obtain successive stages of development. At this time, the first leaf was about 170 mm showing a clear developmental gradient. Seedlings were anchored with a coleoptile of about 35 mm at the base. Sample 1 (Fig. 5.1 A) included a meristem which is enclosed in a newly developed leaf 3 primordium (<2 mm). As rapid developmental changes occur close to the meristem, the base of the first leaf was carefully dissected into consecutive 5 mm sections (samples 2 to 9) and 10mm sections (samples 10 to 14). Certain sections of leaf blade were excluded assuming their developmental stages were not different from the selected sections (Fig. 5.1 B). The leaf base was much more fragile with newly divided cells compared to sections in the mature leaf blade. Furthermore, a fully mature (but without any visible senescence) stage was also collected from the midpoint of leaf 1 (sample 15) grown under similar conditions for 14-days (Fig. 5.1 C).

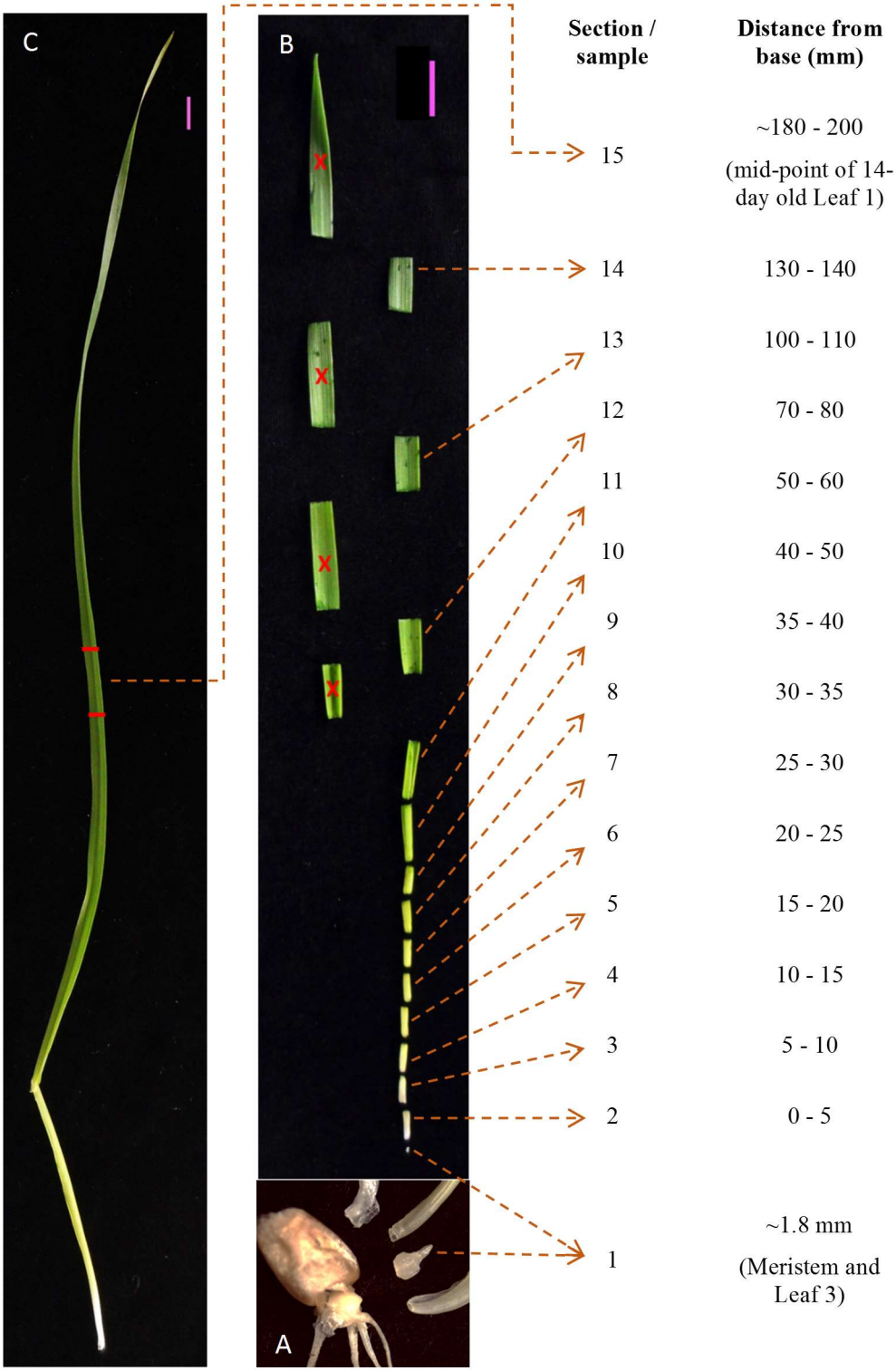


**Figure 5.1** Sample preparation along the developing wheat leaf. (A) Image showing a very young leaf 3 primordium enclosing a <1mm meristem. (B) Dissection of 6-day old leaf 1 into 14 sections covering different developmental stages. Samples 2 to 9 are of 5mm and samples 10 to 14 are of 10mm. Cross marks indicate excluded parts of the leaf. (C) Section 15 (20mm) was harvested from the midpoint of a 14-day old leaf 1. Scale bar represents 1 cm.

## 5.2 Whole genome expression analysis along the wheat leaf

The main objective of this research is to find candidate genes that are involved in chloroplast development. All the RNA samples used for gene expression studies and transcriptome sequencing were of high-quality showing RNA integrity number (RIN) above 7 (Fig 5.2). RNA samples were submitted to Dr. Keichi Mochida, Riken Institute, Yokohama, Japan for RNA sequencing. Reads were mapped against the Ref seq 1.1 IWGSC wheat genome (Appels R, 2018), normalised, averaged per stage and clustered using WGCNA (Langfelder and Horvath, 2008). Thereafter, whole-genome transcripts analysis was performed along the developing wheat leaf. Based on the differential expression, the transcriptome analysis resulted in remarkable patterns corresponding to the developmental gradient, with transcripts grouped into twelve modules or gene clusters (Fig. 5.3). Each module was tested for overrepresentation of bespoke, selected biological functions as previously carried out (López-Juez et al., 2008).

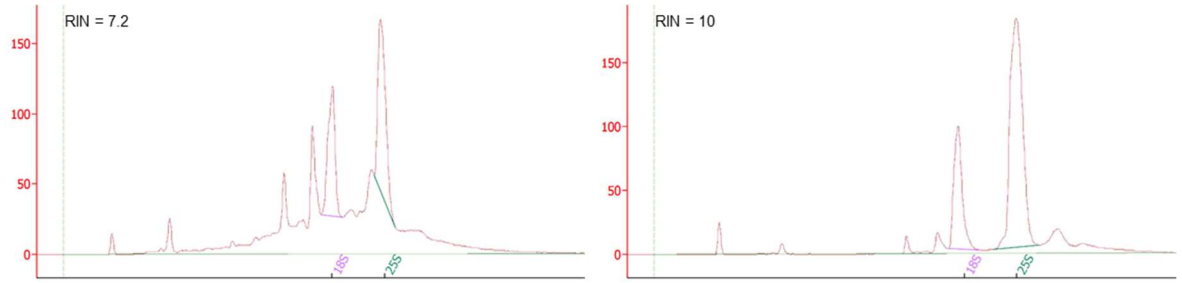


**Figure 5.2** Analysis of RNA quality using Bioanalyzer. Electropherograms showing RNA quality results plotted as fluorescence intensity versus size/migration time by Expert (Agilent) software. RNA Integrity Number (RIN) is indicated in the top left corner in each case. A RIN number above 7 represents high quality RNA.

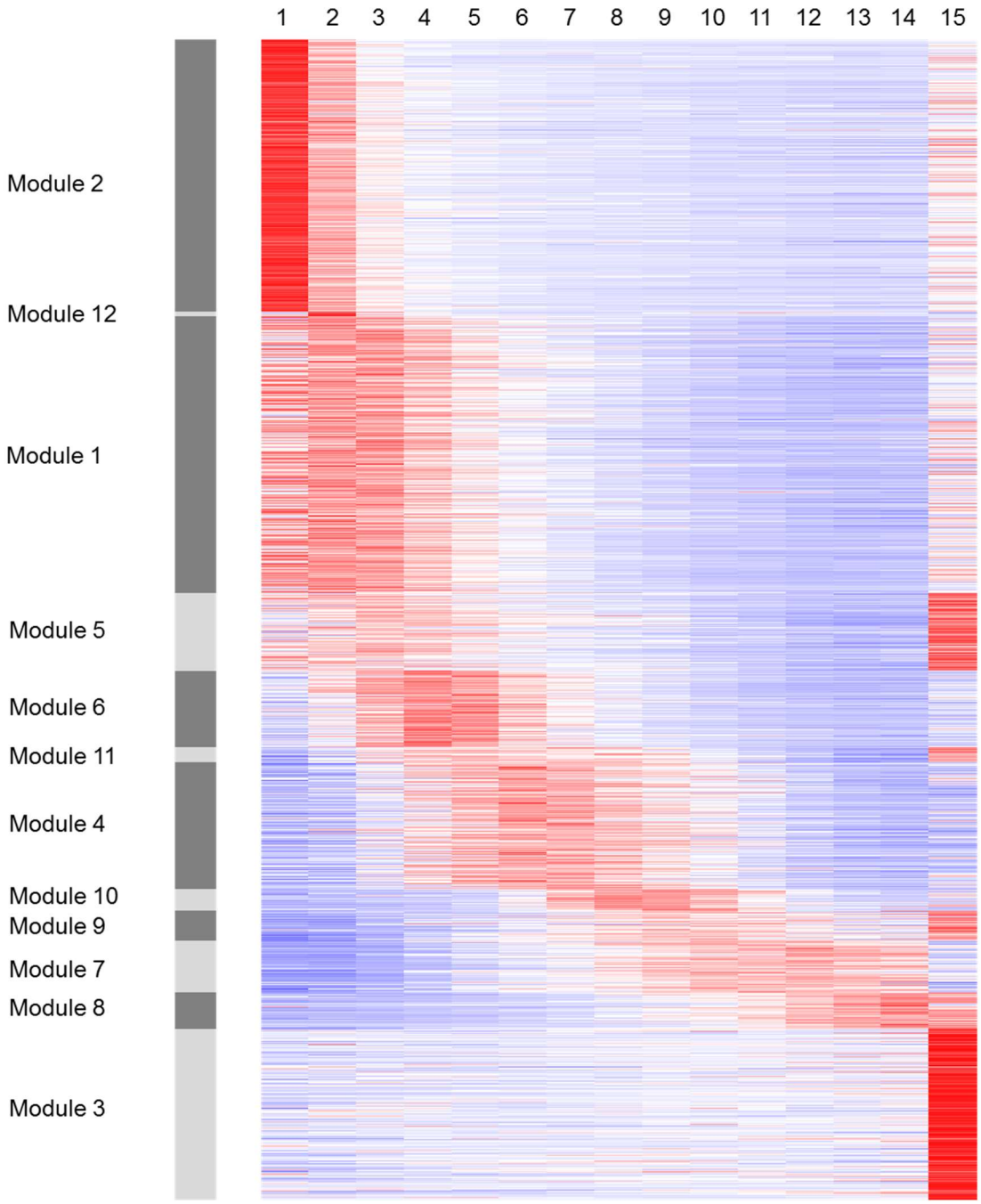


**Figure 5.3** Heat map showing clusters of differentially expressed genes along the developing wheat leaf (figure 5.1). Expression analysis resulted in 12 modules and each module represents a subset grouped according to a pattern. Samples, meristem to a mature stage, are denoted with number on top.

The analysis output showed over representation or under representation of individual function in each module (Fig. 5.4). The “overrepresented biological function” of genes in each module indicates a predominance of transcriptional regulation at the meristem region, cell cycle activity in the meristem region and leaf base (first 5 mm), generation of translation capacity (meristem and leaf basal 10 mm), cell wall building and remodelling (leaf 10 - 30 mm), primary metabolism (leaf 10 and 30 - 40 mm), the point of emergence from the coleoptile into light and photosynthetic development (gradually after 35 mm).

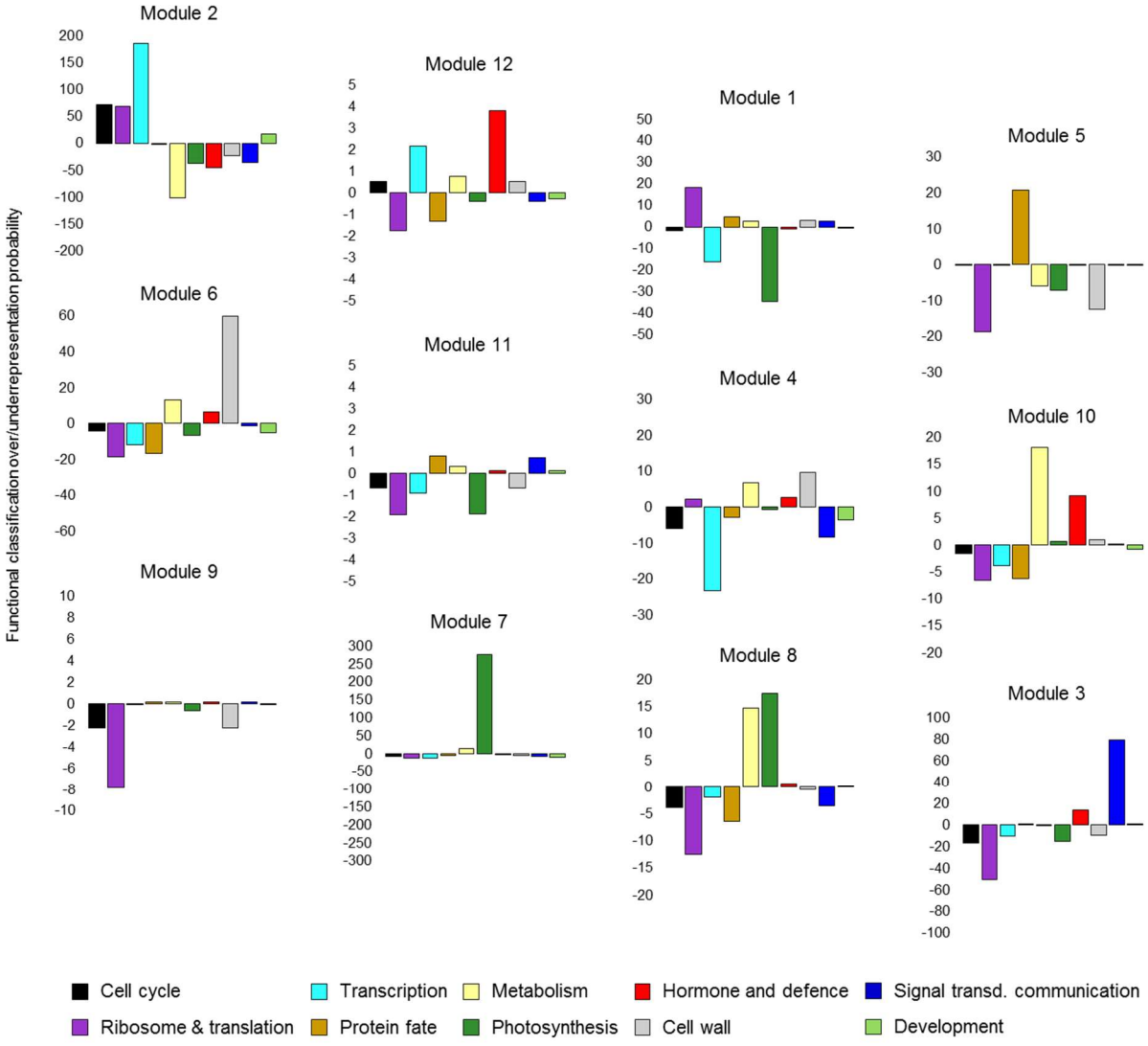


**Figure 5.4** Functional classification of differentially expressed genes along the developing wheat leaf (figure 5.3). Histogram charts show over/underrepresentation of selected functions in each module.

### 5.3 Cell proliferation occurs within and near meristem region

The cells undergoing active division share cytoplasmic organelles, hence chloroplast proliferation is closely connected to cell division. To understand how long cell division occurs in a monocot leaf, flow cytometry analysis was carried out. This quantifies the amount of DNA in individual nuclei assigning each to a 2C (G1), 4C (G2) or intermediate (DNA synthesis phase) class. Cell cycle analysis in the graph below depicts the percentage of different phases along the growing 6-days old wheat leaf (Fig. 5.5 A). As expected, rapid cell proliferation happens in the shoot apical meristem and for a very short period within the 5 mm region of the leaf base. About 30% of the cells were actively engaged in DNA synthesis (S-phase), which dropped to 10% in sample 3 (10 mm). Because DNA synthesis converts G1 nuclei into G2, and there was no increase in G2 nuclei, one can conclude that mitosis (which converts G2 nuclei to G1 nuclei) is occurring simultaneously. Noticeably, unlike Arabidopsis, there was no increase in ploidy beyond 4C, in any of the selected stages of the wheat leaf. The Retinoblastoma-related (RBR) protein acts as a repressor of cell division. Inactivation of RBR by phosphorylation is necessary for active cell division (Scofield et al., 2014). Western blot analysis using a P-RBR specific antibody shows only sample 1 and 2 contain P-RBR proteins. Therefore, cell division occurs exclusively in the meristem and to a small extent in the first 5 mm of leaf base (Fig. 5.5 B).

Having visualised these key cell cycle activities or regulators status, one can examine the transcript levels of the cell cycle-associated genes. While it has been shown that transcript levels do not always correspond to protein levels, transcript level changes indisputably represent a means by which cells alter their activity state. This was the basis for the simultaneous visualisation of selected gene expression changes, employed to help interpret cell cycle states. The same logic will be employed for other cellular processes examined in the remainder of this chapter. According to the observations above, the cell cycle genes are also expressed exclusively in the first two samples (Fig. 5.5 C). The absence of division signature in the later sections suggests the process of differentiation begins early at the leaf base.

**Table 5.1 List of genes selected representing cell cycle analysis**

| Gene ID | Name | Function | | Gene ID | Name | Function |
|---|---|---|---|---|---|---|
| TraesCS1B02G320900 | CYCB1.2 | S-phase | | TraesCS2A02G214700 | HTA2 | S-phase |
| TraesCS1D02G309400 | | | | TraesCS2B02G239600 | | |
| TraesCS3A02G333000 | | | | TraesCS2B02G239700 | | |
| TraesCS3B02G363200 | | | | TraesCS2D02G220400 | | |
| TraesCS3D02G195200 | | | | TraesCS2D02G220500 | | |
| TraesCS3D02G326600 | | | | TraesCS2A02G364000 | PCNA2 | |
| TraesCS4A02G143200 | RBR1 | | | TraesCS2B02G382000 | | |
| TraesCS4B02G162200 | | | | TraesCS2D02G361800 | | |
| TraesCS4D02G159600 | | | | TraesCS4B02G366100 | | |
| TraesCS7A02G264800 | RBR2 | | | TraesCS6A02G373400 | | |
| TraesCS7B02G162700 | | | | TraesCS6B02G411100 | | |
| TraesCS7D02G265600 | | | | TraesCS6D02G357600 | | |
| TraesCS6A02G373000 | RNR1 | | | TraesCS4A02G192300 | CDKB1.2 | Mitosis |
| TraesCS6B02G410800 | | | | TraesCS4B02G123100 | | |
| TraesCS6D02G357100 | | | | TraesCS4D02G121200 | | |
| TraesCS7A02G131200 | | | | TraesCS5A02G145500 | | |
| TraesCS7B02G031500 | | | | TraesCS5B02G144100 | | |
| TraesCS7D02G130500 | | | | TraesCS5D02G147100 | | |

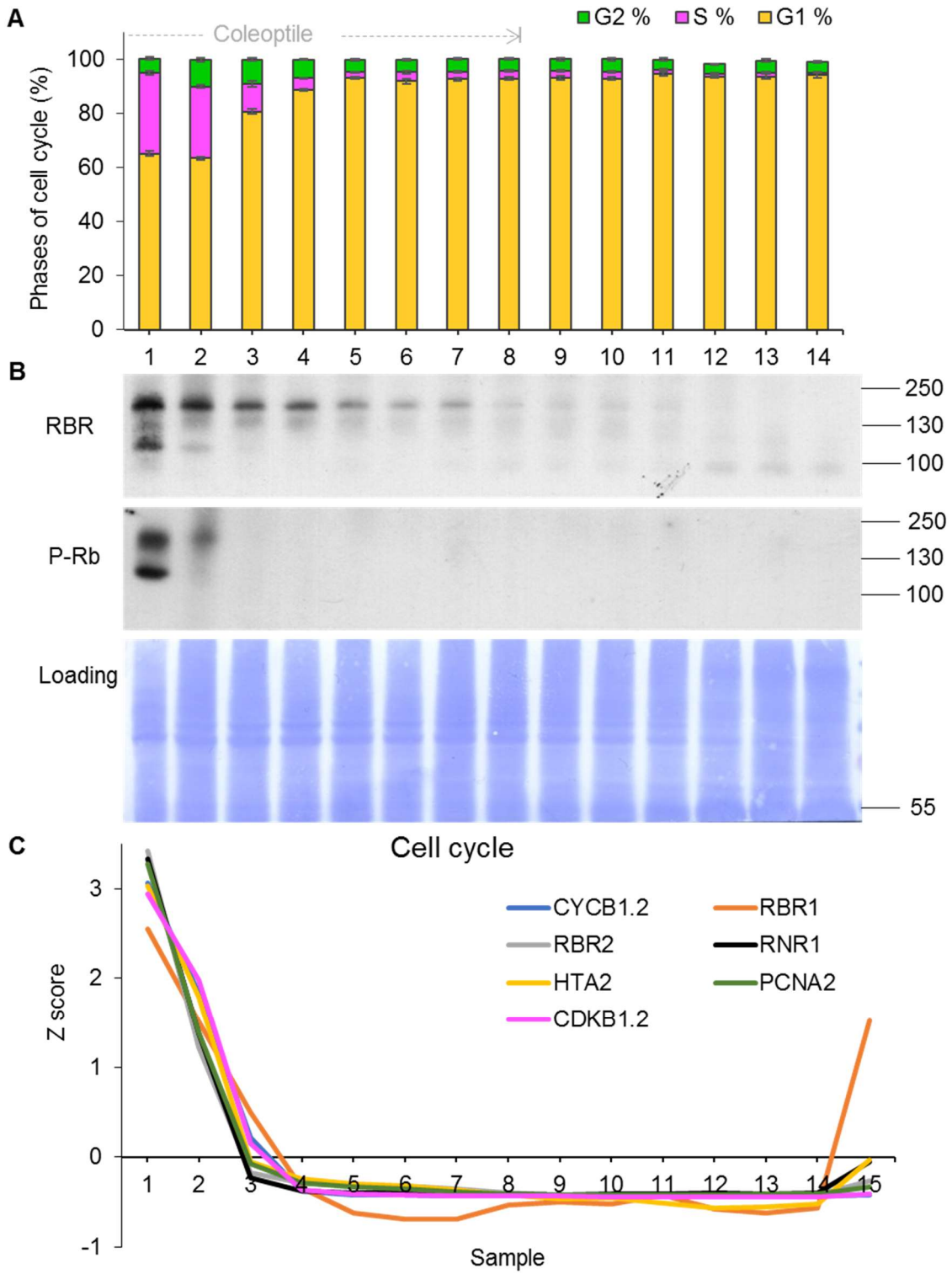


**Figure 5.5** Analysis of cell division in the developing wheat leaf. (A) Flow cytometry of DAPI stained cells at different developmental stages (see figure 5.1). Stacked bar graph represents the percentage of cell cycle phases in the meristem and along the 6-day old first leaf. Data were obtained from the mean percentages of three biological replicates and error bars show their standard error of mean (SEM) values. (B) Western blot analysis of RBR and P-Rb in developing leaf probed with the respective rice antibody. The coomassie stained membrane shows equal loading of the protein samples. (C) Transcript abundance of cell cycle genes along the developmental stages of wheat leaf presented as Z score. Each line represents the mean of Z score values of three homeologs.

### 5.4 Cellular microscopy shows a series of morphological changes

Plant growth is defined by two fundamental processes: cell division and cell expansion. As a measure of cellular expansion, growing mesophyll cells were tracked along the developing wheat leaf. Cellular and chloroplast development was quantified using differential interference contrast (DIC) microscopy. Results show that sample 1 (meristem + primordium of leaf 3) and sample 2 (0 - 5 mm), the first section at the base of leaf 1, contained undifferentiated cells which were small, quadrilateral and compactly arranged. A common characteristic of meristematic cells was a large nucleus occupying most of the cell, which sometimes had more than one nucleolus. Sample 3 (5 - 10 mm) contained undifferentiated cells that were starting to elongate and lost their straight edges. Cells at the base of the leaf grow very rapidly. Cellular lobes diverging from a cylindrical cell shape tend to appear from 15 mm and become more apparent as cells move towards the leaf blade, possibly due to growing cytoskeletal interconnections (Fig. 5.6). Localized plasma membrane shrinkage was occasionally observed, notably from section 11 (50 - 60 mm) onwards. There was clear evidence of an increase in complexity as cells grow and undergo differentiation. The technique of live microscopy counting is a remarkable tool, it requires patience but reveals a complete complement of plastids in different planes of selected cells (Pyke et al., 1994). As cells have a 3-dimensional distribution of cytoplasmic content, commonly used methods like image analysis taken from a single plane or inbuilt z-stacking microscope tool might be less accurate to exactly obtain the number of chloroplasts. As live counting technique produces the most reliable data with precision, it was used in this study. Chloroplast density was proportional to cell size, with more chloroplasts in larger cells, but also dependent on the position of the leaf section.

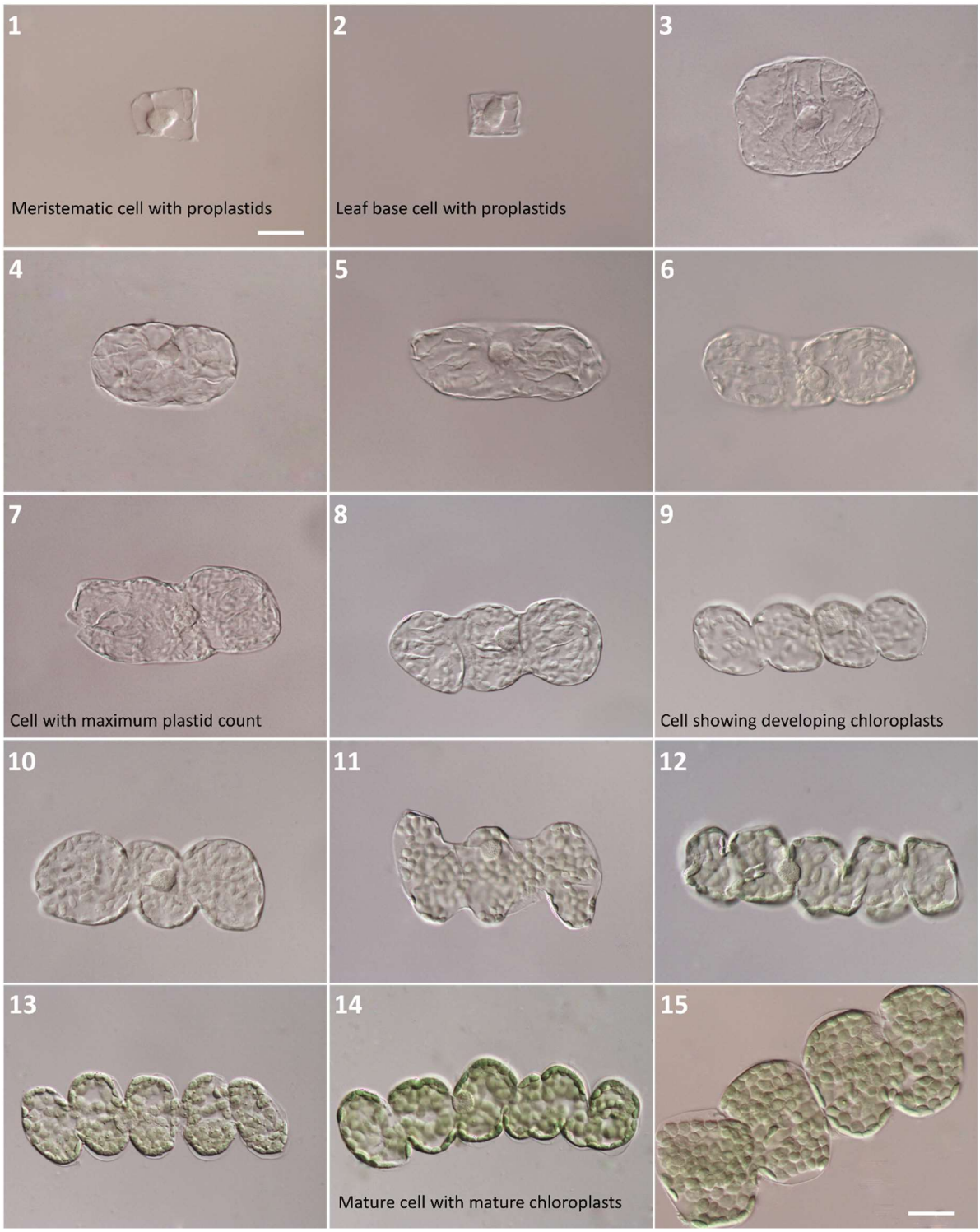


**Figure 5.6** Cellular microscopy along the greening wheat leaf. Fixed cells observed under Nomarski optics, from 6-day old leaf 1. Images are labeled as per the sample sections (see Figure 5.1). (1) Cell from a meristem and leaf 3 primordium, followed by cells from sample 2 to 14 and (15) represents a two weeks old mature leaf 1. Mesophyll cells showing developing chloroplasts. Images obtained together with Priyanka Mishra.

### 5.5 Cells grow rapidly before and after the end of division

Cell growth was measured in fixed tissue samples along the wheat leaf gradient. Looking at the cell division (Fig. 5.5) in the same batch of seedlings, cells expand rapidly before and continue to grow till 35 mm after their division. Cell expansion occurs at a constant pace until sample 8, which is the end of the coleoptile (Fig. 5.7 A). Hereafter the leaf was exposed to direct light, cell size remained unchanged between samples 9 to 12. Transcriptome analysis also showed that aquaporins, expansins, arabinogalactan, and cellulose synthesis genes are expressed mainly in the first 5 samples at the base (Fig 5.7 B and C). The second peak in cell expansion was observed in later stages of development when cells were fully mature at 100 mm. It can be concluded that cells grow rapidly before and after the end of division.

**Table 5.2 List of genes selected representing cellular growth**

| Gene ID | Name | Function | | Gene ID | Name | Function |
|---|---|---|---|---|---|---|
| TraesCS2A02G065700 | PIP3B | Aquaporins | | TraesCS1A02G116200 | CESA1 | Cellulose |
| TraesCS2B02G077700 | | | | TraesCS1B02G136200 | | |
| TraesCS2D02G063900 | | | | TraesCS1D02G117400 | | |
| TraesCS6B02G259000 | PIP2_1 | | | TraesCS6A02G077800 | | |
| TraesCS6D02G212900 | | | | TraesCS6B02G104600 | | |
| TraesCS6A02G222100 | | | | TraesCSU02G142500 | | |
| TraesCS2B02G396700 | | | | TraesCS2A02G157100 | CSLA9_1 | |
| TraesCS2D02G376000 | | | | TraesCS2B02G182700 | | |
| TraesCS2A02G379800 | | | | TraesCS2D02G163000 | | |
| TraesCS2A02G379900 | | | | TraesCS3A02G496400 | | |
| TraesCS2B02G396800 | | | | TraesCS3D02G504200 | | |
| TraesCS2D02G376100 | | | | TraesCS3B02G558400 | | |
| TraesCS5A02G481200 | EXPA4 | Expansins | | TraesCS7A02G189100 | CSLA9_3 | |
| TraesCS5B02G494400 | | | | TraesCS7D02G190000 | | |
| TraesCS2A02G393700 | EXP13_1 | | | TraesCS5B02G517500 | CESA6 | |
| TraesCS2D02G391600 | | | | TraesCS5D02G517200 | | |
| TraesCS2B02G411700 | EXP13_2 | | | TraesCS4A02G355000 | | |
| TraesCS7A02G343600 | AGP16_1 | Arabinogalactan proteins | | | | |
| TraesCS7B02G239500 | | | | | | |
| TraesCS7D02G336000 | | | | | | |
| TraesCS1A02G113100 | | | | | | |
| TraesCS1B02G133200 | | | | | | |
| TraesCS1D02G114500 | | | | | | |

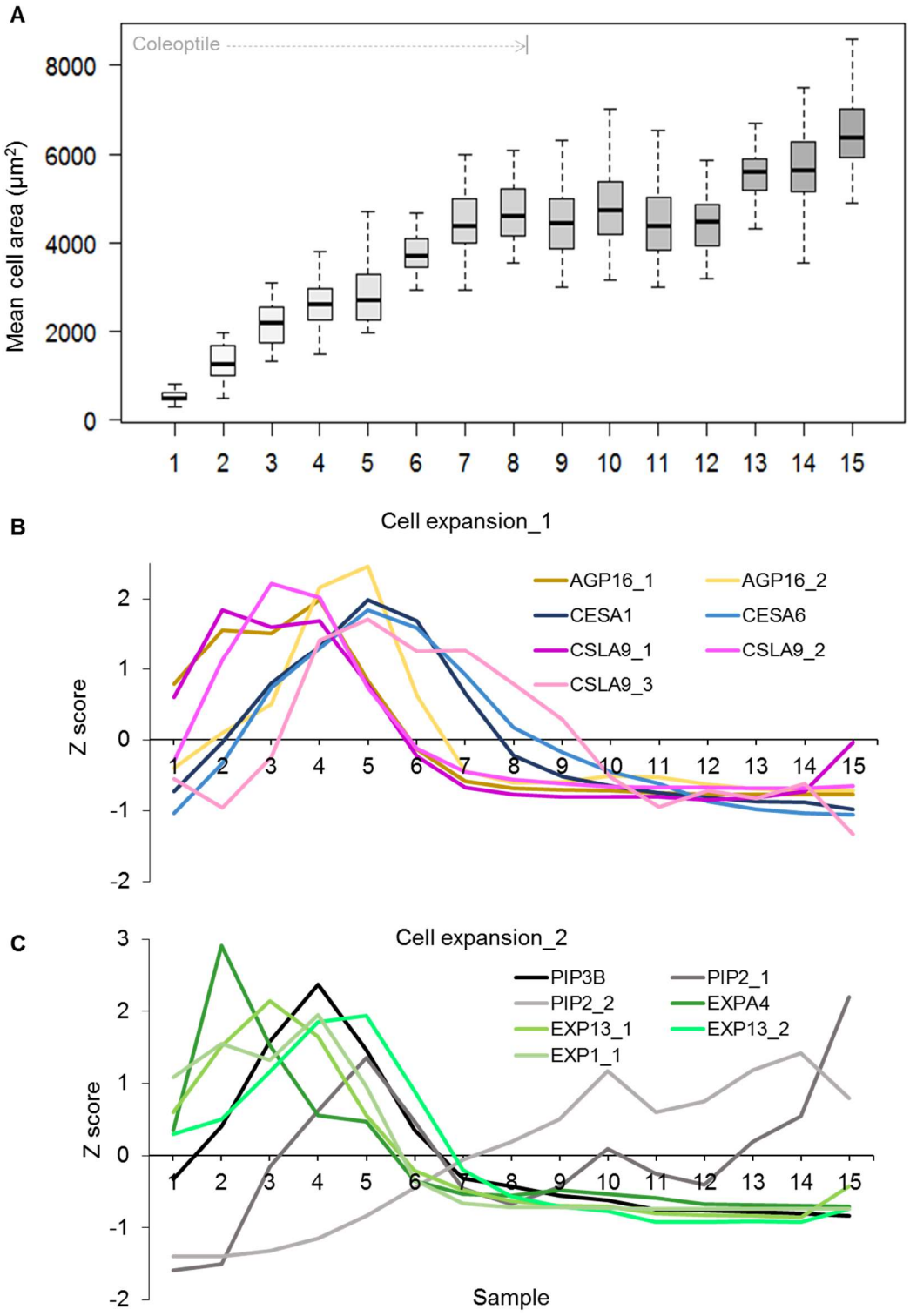


**Figure 5.7** Analysis of cell size along the developing wheat leaf. (A) Cell area was measured at different developmental stages covering the meristem to near senescence cells of leaf 1. Data collected from four biological replicates (n=48) was pooled to generate box plots. Box boundaries represent the upper and lower quartiles, horizontal lines the median, and whiskers the 5% and 95% data bins. (B), (C) Transcript abundance of selected genes along the developmental stages of wheat leaf presented as Z score. Each line represents the mean of Z score values of three homeologs.

### 5.6 Plastid proliferation occurs very early in development

Identity of the organelles counted as chloroplasts was confirmed in mesophyll cells mounted with 4',6-diamidino-2-phenylindole (DAPI) (Boffey SA, 1982). When visualized using DIC optics the leaf cells revealed clear structures of chloroplasts (Fig. 5.8 A) confirmed by the fluorescence of DAPI stained cpDNA (Fig. 5.8 B), arrows indicating multiple copies of DNA localised within each chloroplast. Wheat leaf cells are filled with a variable number of plastids depending on stage of differentiation. Following the developmental gradient, plastids became more clearly distinct in successive sections compared to the previous ones.

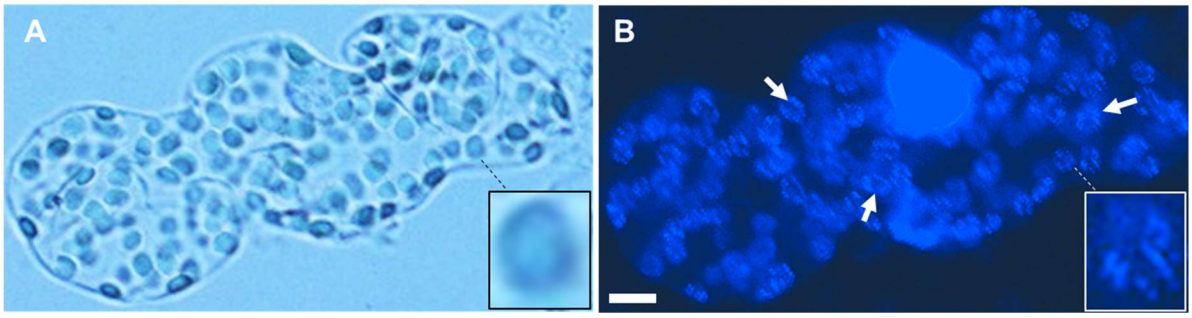


**Figure 5.8** Chloroplast distribution in a wheat mesophyll cell. Microscopy of DAPI stained mesophyll cell to confirm chloroplast count (A) visualised with Nomarsky optics, (B) DAPI fluorescence emitted by nucleus and cpDNA confirms the distribution of chloroplasts. Arrows indicate the nucleoids in the chloroplasts. (Image obtained together with Anthony Lees).

To understand chloroplast filling in growing cells, the plastid growth and number was quantified using a published protocol in the same mesophyll cells which were used for the analysis of cell expansion (along the developing wheat leaf). Plastid microscopy led to remarkable observations with distinct spatial development. Proplastids in cells near the base of the leaf, particularly in sample 1 and 2, are fewer and most difficult to count as they are very small and colourless. Therefore, quantitation was first performed in the mature sections with well-developed chloroplasts, then progressing backwards in order to accurately spot the early undifferentiated plastids.

Although plastid proliferation goes in hand with cell division at the beginning, it continues when cells cease to divide and enter differentiation. Plastid count was seen to increase rapidly in the early sections until sample 5 (20 mm), where some of the cells showed over 350 chloroplasts (Fig. 5.9 A). In the basal sections the structures of dividing plastids were clearly visible under a 40x objective. It was interesting to note the steepest division slope became flat abruptly between sample 6 and sample 7 (25 - 30 mm). Interestingly the plastid count tends to drop in sample 8 where the leaf had emerged out of the coleoptile and become exposed to

light. Observation of chloroplast decline continued and about 40% chloroplasts in total seem to be missing by the time cells had reached 75 mm (sample 12). Considering developmental time, the rate of change of plastid number (proliferation) showed a sharp increase before 15mm and declined abruptly in the following sections (Fig 5.9 B). The graph below depicts a reduction in plastid count and the rate of number change dropping to negative values in sample 8 (35 mm from the base). Consistently, the expression of chloroplast division genes was high in the proliferating cells and near base sections until sample 4 (15 – 20 mm). Previous genetic studies on *FZL* (*FZO-Like*) (Gao et al., 2006) and *GC1* (*GAINT CHLOROPLAST 1*) (Maple et al., 2004) genes in Arabidopsis reported their function in chloroplast division. It is important to note that, unlike other plastid division genes, the expression of *FZL* and *GC1* peaks later in development (samples 9 to 12) after the chloroplasts have ceased to divide (Fig. 5.9 C).

**Table 5.3 List of genes selected representing chloroplast division**

| Gene ID | Name |
|---|---|
| TraesCS3D02G157200 | PDV1 |
| TraesCS2D02G257600 | PDV2 |
| TraesCS2A02G266200 | |
| TraesCS2B02G275900 | |
| TraesCS2A02G488400 | FtsZ1 |
| TraesCS2B02G516000 | |
| TraesCS2D02G488700 | |
| TraesCS1A02G276500 | FtsZ2-1 |
| TraesCS1B02G285700 | |
| TraesCS1D02G276000 | |
| TraesCS2A02G294500 | |
| TraesCS2B02G310900 | |
| TraesCS2D02G292200 | |
| TraesCS5B02G120600 | ARC5 |
| TraesCS5D02G124800 | |
| TraesCS5A02G114600 | |
| TraesCS6A02G066200 | ARC6 |
| TraesCS6B02G089500 | |
| TraesCSU02G117700 | |
| TraesCS1A02G243700 | FZL |
| TraesCS1B02G255100 | |
| TraesCS1D02G243700 | |
| TraesCS6A02G418400 | GC1 |
| TraesCS6B02G470900 | |
| TraesCS7D02G484800 | |

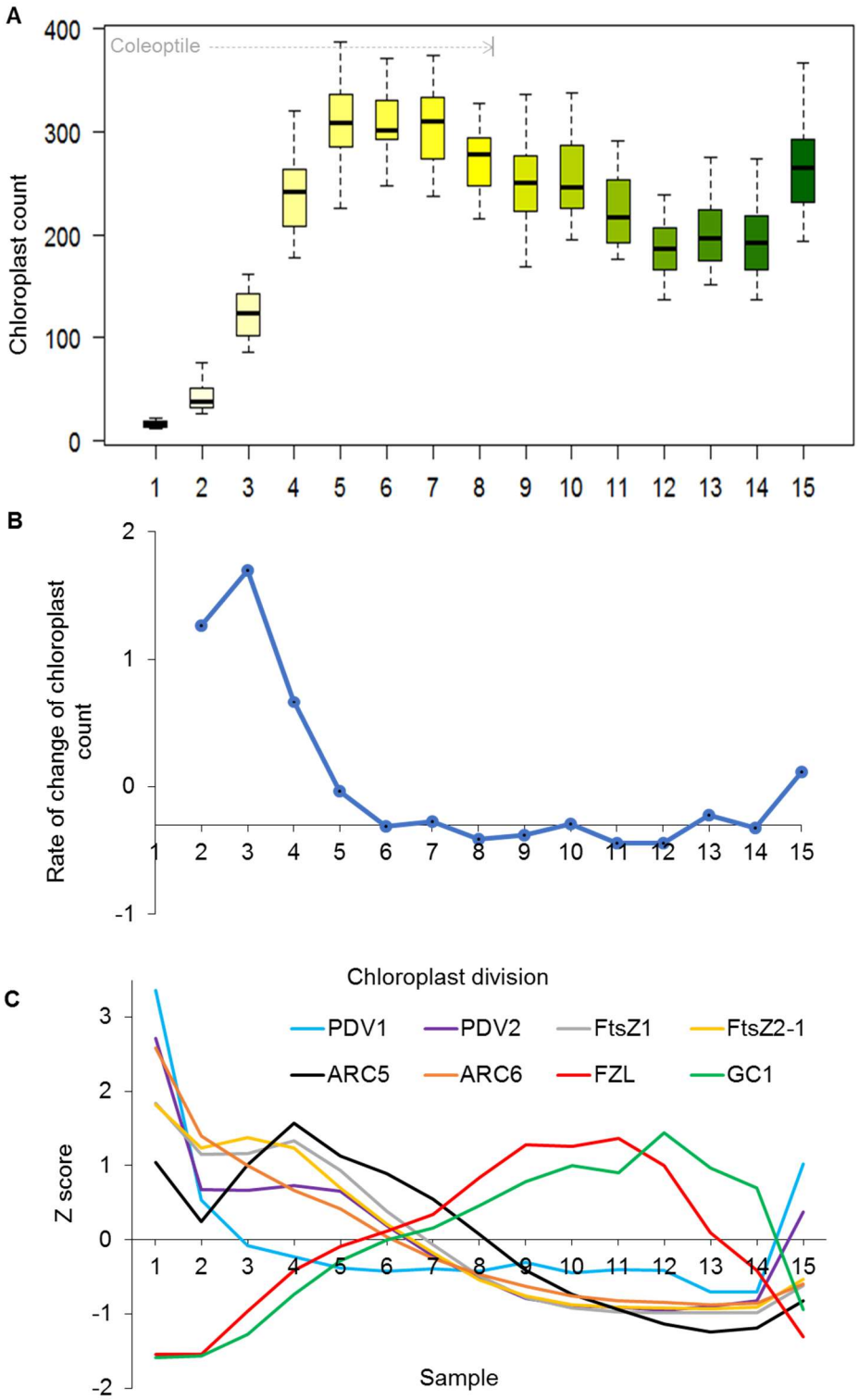


**Figure 5.9** Analysis of plastid number along the developing wheat leaf. (A) Total chloroplast count was obtained from mesophyll cells of 6-days and 14-days old leaf 1. Data collected from four biological replicates (n=48) was pooled to generate box plots as in figure 5.7. (B) The rate of change of chloroplast count was calculated with the slope values of two consecutive samples. (C) Transcript abundance of chloroplast division genes along the developmental stages of wheat leaf presented as Z score. Each line represents the mean of Z score values of three homeologs.

## 5.7 Mean and total chloroplast area increases after proliferation

The growth of chloroplasts was analysed by considering the mean chloroplast area of ten intact plastids in the same mesophyll cells used for cell size and plastid count. Proplastids grow steadily in cells near the base, their growth accelerating after they stop proliferation. Part of the acceleration can be explained by the fact that division halved the previous size of any chloroplast. A noticeable increase was observed in later sections, when plastid number declines. Chloroplasts in the 14-days old leaf section are of identical size to those in the latest sample at day 6.

Total chloroplast area was derived by considering the total plastid count and the mean plastid area in a cell. There was an increase in total chloroplast area at the leaf base within the coleoptile region and later in fully mature sections. The increase at the base occurs at the time of rapid plastid proliferation, however a greater increase was noticed in mature sections of the wheat leaf, when individual chloroplast growth is maximum. If at all, the total chloroplast area increased in cells at the time when the plastid count was dropping.

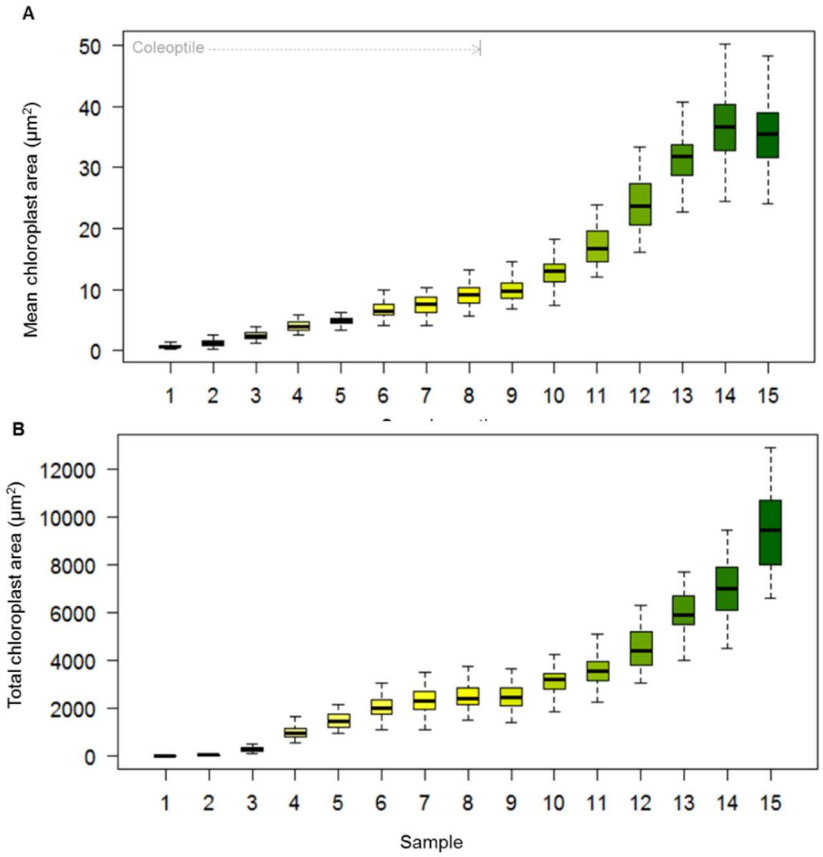


**Figure 5.10** Analysis of plastid growth along the developing wheat leaf. (A) Mean chloroplast area was obtained from 10 intact plastids in a mesophyll cell. (B) Total chloroplast area of mesophyll cells is calculated by the total number of plastids and mean chloroplast area of respective cell. Box plots are generated with the data collected from four biological replicates of a 6-days old and 14-days old leaf 1 as in figure 5.7

## 5.8 The chloroplast compartment increases most rapidly during the stages of division and individual chloroplast growth

“Cell index” or “chloroplast compartment” is the proportion of the cell occupied with plastids, therefore this parameter expresses the ratio of total chloroplast area and cell area. Proplastids cover very little space in the dividing cells, but their compartment increases to over 50% with their rapid proliferation by the time cells reach 15 mm (section 4). A stationary phase of chloroplast occupancy was observed when plastids stop dividing. Interestingly, at this phase (samples 5 to 9) both the cells and chloroplasts are growing at the same speed, this explaining the stable cell index (Fig. 5.11 A). This was followed by a second increase in chloroplast filling when cells stop expanding (40 mm). Mesophyll cells in mature sections were fully packed with chloroplasts that can be visualised even with the 20x objective. The rate of change of the chloroplast compartment was calculated similarly to proliferation rate, from the values of adjacent sections. Accordingly, cell index rate peaked at two stages in sample 3 (5 - 10 mm) during the rapid plastid division phase and in samples 12 (70 - 80 mm) with an increase in individual chloroplast size (Fig. 5.11 B).

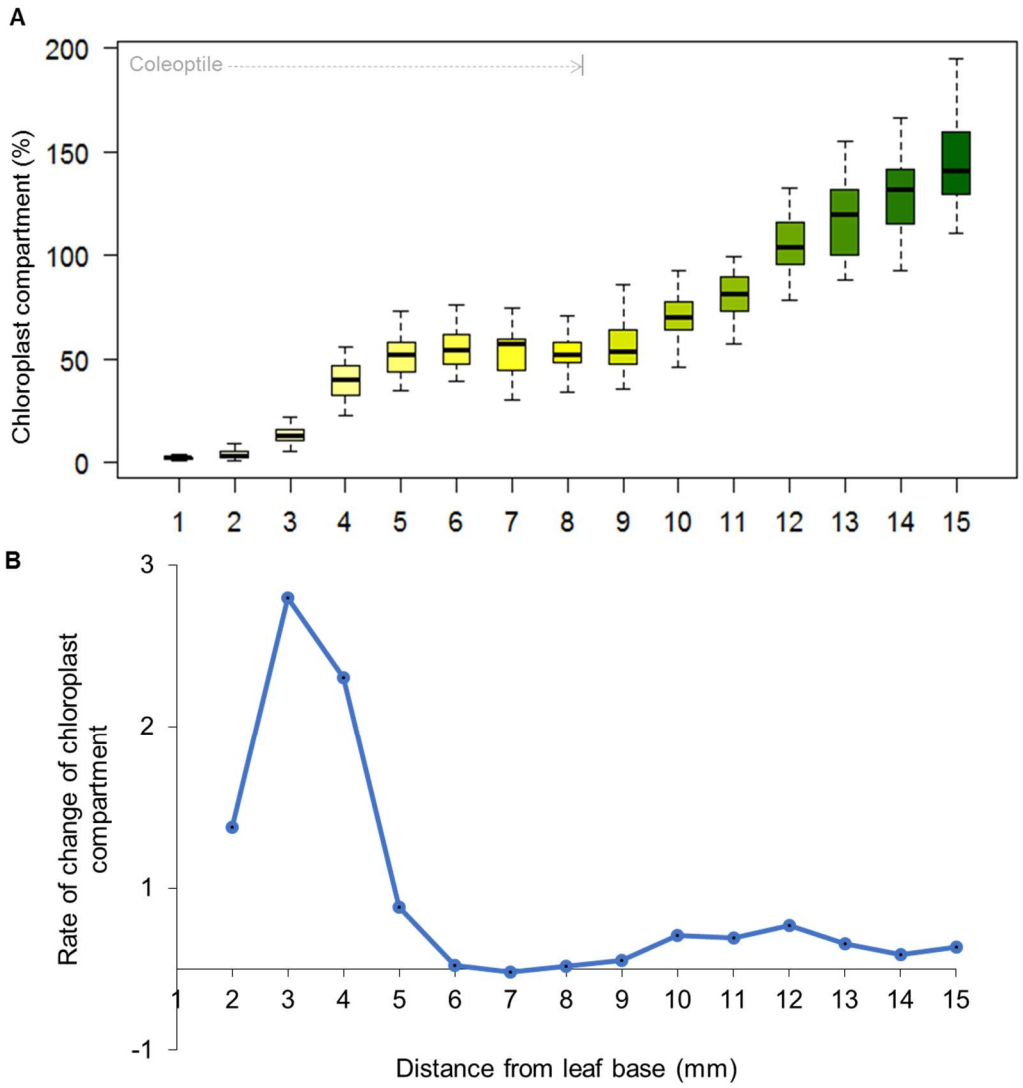


**Figure 5.11** Analysis of chloroplast compartment along the developing wheat leaf. (A) The percentage of each mesophyll cell occupied by chloroplasts was calculated using total chloroplast area and cell area. Data collected from four biological replicates of 6-days and 14-days old leaf 1 was pooled to generate box plots as in figure 5.7 (B) The rate of change of chloroplast compartment was calculated with the slope values taken from each consecutive pair of samples.

The propagation of new chloroplasts requires membrane, and eventually stromal and lamella proteins. The growth of each individual plastid is made possible by the import of nucleus-encoded cytosolic proteins. The genes encoding components of chloroplast import complexes TOC/TIC, that allow protein import, are highly expressed during early development, particularly when chloroplasts are dividing, and seems to be maintained during the proplastid-to-chloroplast transition (Fig. 5.12).

**Table 5.4 List of genes selected representing chloroplast protein import machinery**

| Gene ID | Name | | Gene ID | Name |
|---|---|---|---|---|
| TraesCS4A02G095300 | TOC75-III | | TraesCS2A02G199800 | TIC20-I |
| TraesCS4B02G209200 | | | TraesCS2B02G227100 | |
| TraesCS4D02G209900 | | | TraesCS2D02G207600 | |
| TraesCS4A02G072800 | TOC34 | | TraesCS6A02G229400 | |
| TraesCS4B02G228900 | | | TraesCS6B02G252100 | |
| TraesCS4D02G230000 | | | TraesCS6D02G205400 | |
| TraesCS1A02G208000 | TOC132 | | TraesCS1A02G165800 | TIC110 |
| TraesCS1B02G222000 | | | TraesCS1B02G182500 | |
| TraesCS1D02G211300 | | | TraesCS1D02G174900 | |
| TraesCS1A02G093900 | TOC159_1 | | TraesCS1A02G165700 | |
| TraesCS1B02G122000 | | | TraesCS1B02G182400 | |
| TraesCS1D02G102500 | | | TraesCS1D02G175000 | |
| TraesCS5B02G514000 | TOC159_2 | | TraesCS5A02G206800 | HSP21 |
| TraesCS5D02G514500 | | | TraesCS5B02G205200 | |
| TraesCS4A02G358400 | | | TraesCS5D02G213000 | |
| TraesCS2A02G138100 | SP1 | | TraesCS5A02G206900 | |
| TraesCS2B02G162000 | | | TraesCS5A02G257700 | |
| TraesCS2D02G141100 | | | TraesCS5B02G205300 | |
| TraesCS6A02G158800 | OEP80 | | TraesCS5B02G257000 | |
| TraesCS6D02G153700 | | | TraesCS5D02G213100 | |
| TraesCS6B02G192500 | | | TraesCS1A02G133100 | cpHSC70-2_1 |
| TraesCS2D02G306800 | TIC40 | | TraesCS1B02G151300 | |
| TraesCS2A02G308600 | | | TraesCS1D02G131800 | |
| TraesCS2B02G325100 | | | TraesCS5A02G106200 | cpHSC70-2_2 |
| | | | TraesCS5B02G111200 | |
| | | | TraesCS5D02G117600 | |

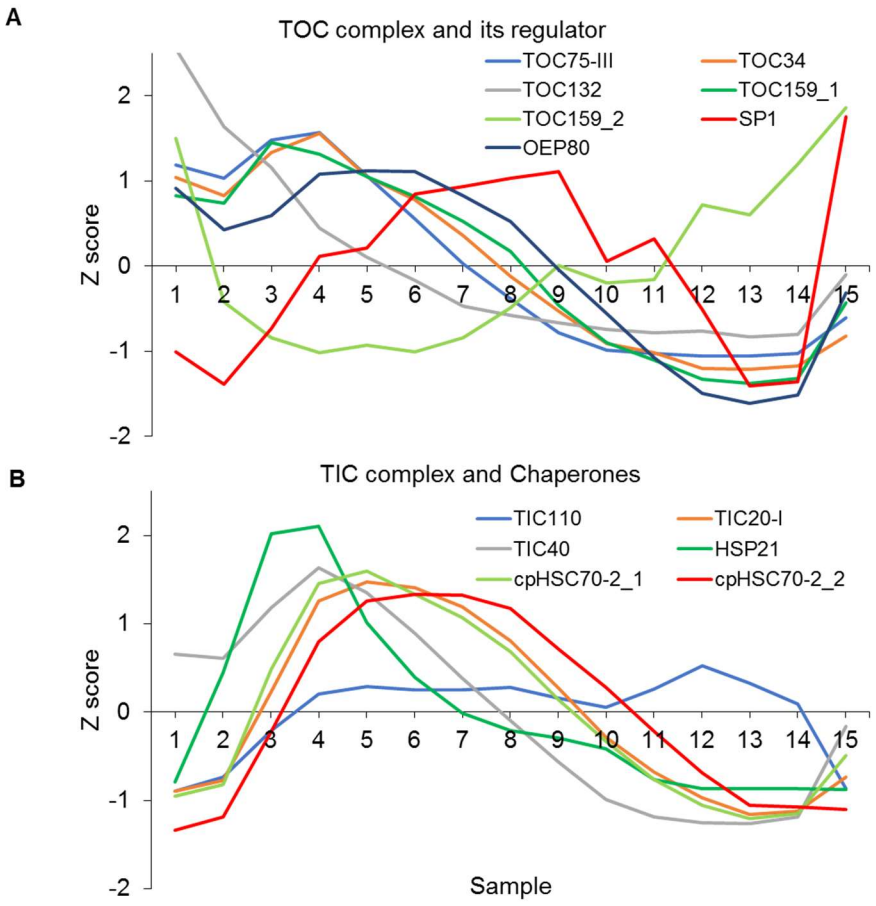


**Figure 5.12** Transcript abundance of genes encoding chloroplast protein import machinery. Data obtained along the developing wheat leaf presented as Z score. Each line represents the mean of Z score values of three homeologs.

## 5.9 Chloroplast DNA replication continues after plastid division is complete

The chloroplast genome is another important element of organelle biogenesis. An absolute number of plastome copies was quantified using qgPCR and standard curve analysis of nuclear and chloroplast DNA target sequences. The graph shown below represents plastid DNA copies accumulate as plastids divide. The number increases rapidly after the plastids have fully divided, as observed in sample 6 (25 mm) and continue to sample 11 (60 mm). A similar trend was seen when cpDNA levels were measured per unit chloroplast in mesophyll cells. Proplastids in the meristematic sample contain a dense population of replicating organellar DNA which drops in sample 2, this presumably being due to sharing of DNA copies between rapidly dividing plastids (Fig. 5.13 B). It was also noticed that before any visible onset of senescence, chloroplast DNA undergoes loss not just per cell but also per individual chloroplast. Plant organellar DNA is replicated by two known DNA polymerases (POL IA and POL IB) which are dual-targeted to chloroplasts and mitochondria.

Transcriptome analysis has shown two patterns of *POL1A*, one of them might have preferential role in mitochondrial DNA replication.

**Table 5.5 List of genes selected representing chloroplast DNA replication**

| Gene ID | Name |
|---|---|
| TraesCS7A02G295900 | POL IA_1 |
| TraesCS2A02G526000 | POL IA_2 |
| TraesCS2B02G556100 | |
| TraesCS2D02G528800 | |

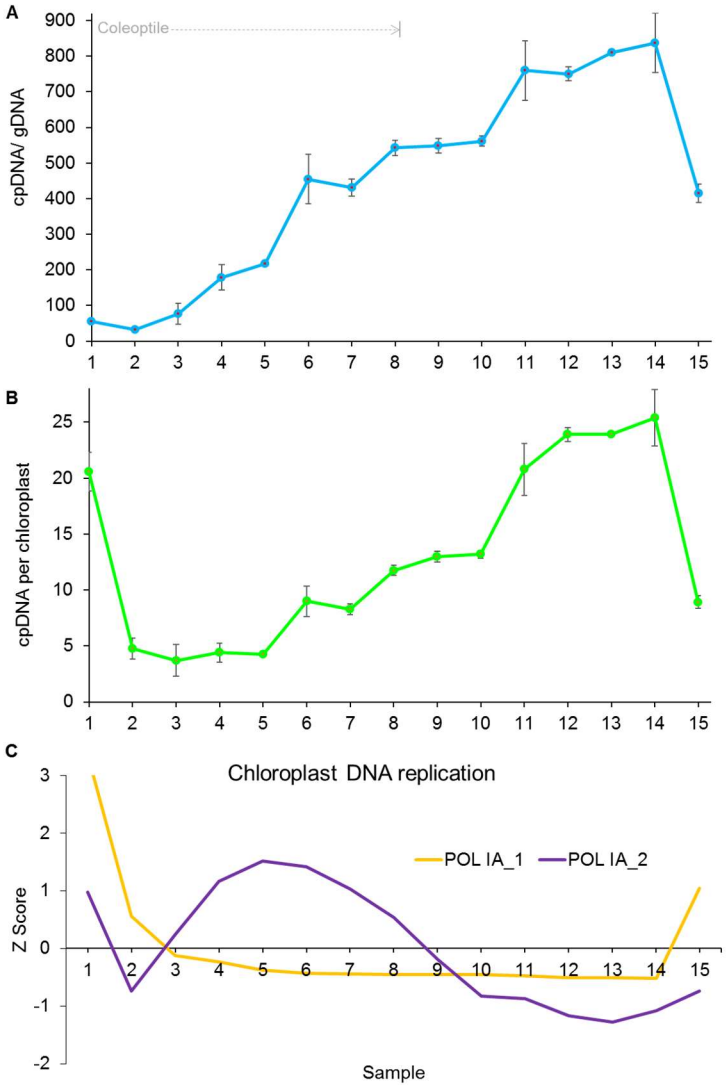


**Figure 5.13** Chloroplast DNA replication along the developing wheat leaf. (A) Genome copy number was quantified by real-time PCR and standard curve analysis of cpDNA and genomic DNA sequences from 6-day and 14-day old leaf 1. The line graph represents absolute copies of cpDNA quantified with the ratio of the mean of 3 plastid genes (*rbcL, ndhD,* and *rps7*) over the mean of 2 nuclear genes (*KO1* and *KS*) of A, B and D genomes. Error bars represent the SEM (standard error of the mean) values of triplicate samples. (B) Ratio of chloroplast genome copies per cell and total number of chloroplasts per cell along the wheat samples. Error bars represent the SEM (standard error of the mean) values of triplicate samples, the genome copy number was calculated per cell and was normalized against the total chloroplast number of the respective cell. (C) Transcript abundance of chloroplast division genes along the developmental stages of wheat leaf normalized and presented as Z score. Each line represents the mean of Z score values of three homeologs.

### 5.10 Cellular translation capacity shifts gradually towards chloroplasts

The ratio of ribosomal RNA in chloroplast (16S rRNA) and cytoplasm (18S rRNA) was calculated to follow the trend of cell investment into translation in the respective compartments. At the beginning, undifferentiated cells invest more in cell division and expansion and less in organelle development. Consequently, proplastids in early sections maintain a basal level of ribosomes just to support their biogenesis. Once the cells are filled with enough plastids, they support the growth of chloroplasts, eventually to perform vital functions like photosynthesis.

**Table 5.6 List of genes selected representing chloroplast transcription**

| Gene ID | Name | | Gene ID | Name |
|---|---|---|---|---|
| TraesCS7A02G503900 | RPOTp/SCABRA3 | | TraesCS5B02G563800 | SIG6 |
| TraesCS7B02G411000 | | | TraesCS5D02G551200 | |
| TraesCS7A02G297900 | SIG1 | | TraesCS4A02G315700 | |
| TraesCS7B02G184800 | | | TraesCS5A02G486300 | pTAC2 |
| TraesCS7D02G292000 | | | TraesCS5B02G500100 | |
| TraesCS4A02G157100 | SIG2_1 | | TraesCS5D02G500300 | |
| TraesCS4B02G163500 | | | TraesCS6A02G367100 | pTAC17 |
| TraesCS4D02G154500 | | | TraesCS6B02G402400 | |
| TraesCS4A02G095200 | SIG2_2 | | TraesCS6D02G350100 | |
| TraesCS4B02G209300 | | | TraesCS4A02G395700 | WHY3 |
| TraesCS4D02G210000 | | | TraesCS7A02G095300 | |
| TraesCS1A02G431600 | SIG3 | | TraesCS7D02G091500 | |
| TraesCS1B02G467100 | | | TraesCS5A02G085800 | GUN1 |
| TraesCS1D02G440900 | | | TraesCS5D02G097800 | |
| TraesCS1A02G426700 | SIG5 | | TraesCS5B02G091600 | |
| TraesCS1B02G461600 | | | TraesCS3A02G297500 | HEMERA |
| TraesCS1D02G436500 | | | TraesCS3B02G339200 | |
| | | | TraesCS3D02G304800 | |

**Table 5.7 List of genes selected representing chloroplast translation**

| Gene ID | Name | | Gene ID | Name |
|---|---|---|---|---|
| TraesCS4B02G347000 | PRPL11 | | TraesCS4A02G079200 | SVR7 |
| TraesCS4D02G341900 | | | TraesCS4B02G245000 | |
| TraesCS5A02G515700 | | | TraesCS4D02G244400 | |
| TraesCS5A02G404500 | RPS9 | | TraesCS3A02G275700 | W tRNA-Syn |
| TraesCS5B02G409400 | | | TraesCS3B02G309400 | |
| TraesCS5D02G414600 | | | TraesCS3D02G275600 | |
| TraesCS2A02G387000 | SCO1 | | TraesCS1A02G151500 | Y tRNA-Syn |
| TraesCS2B02G404600 | | | TraesCS1D02G148500 | |
| TraesCS2D02G383800 | | | | |

The expression of nucleus-encoded RNA polymerase (RPOTp), which transcribes most of the plastid house-keeping genes (Börner T, 2015), is high particularly during early development, in actively dividing proplastids. Interestingly, the PEP-associated sigma factors, which are

also nucleus-encoded, show distinct patterns of expression. *SIG2_1 SIG3,* peaked early, *SIG2_2* and *SIG6* were expressed during the transition of proplastids to chloroplasts and transcripts of *SIG1*, *SIG5* were abundant in samples containing fully mature chloroplasts (Fig. 5.13B). The regulatory gene of chloroplast-to-nucleus signaling (*GUN1*) is expressed mainly during the plastid to chloroplast transition. Accordingly, all the selected chloroplast translation genes were active between sample 2 to 13 (Fig. 5.14 D)

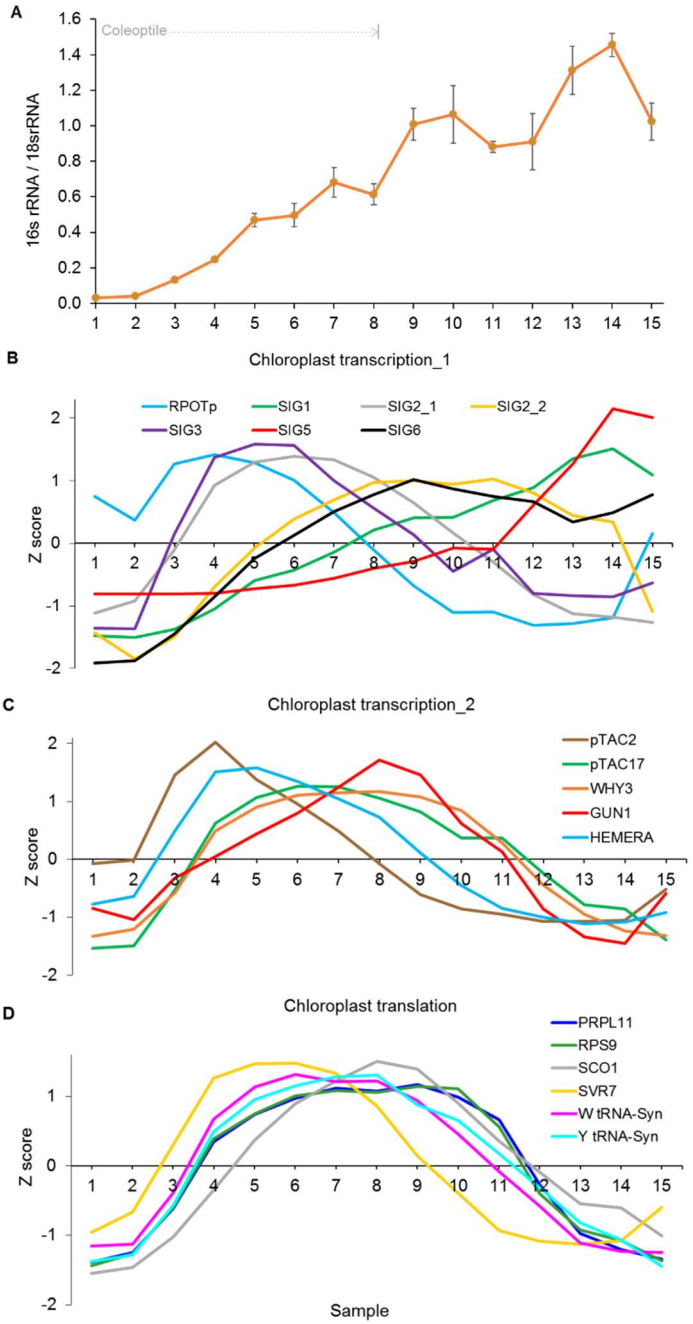


**Figure 5.14** Cellular investment and chloroplast gene expression along the growing wheat leaf. (A) Ratio of plastid and cytoplasmic ribosomal RNA. Error bars represent the SEM (standard error of the mean) values of triplicate samples. Transcript abundance of chloroplast (B, C) transcription and (D) translation genes along the developmental stages of the wheat leaf presented as Z score. Each line represents the mean of Z score values of three homeologs.

### 5.11 Chlorophyll synthesis associates with chloroplast growth

Chlorophyll concentration clearly depicts the phenotype gradient of the wheat leaf. The meristematic region embedded in the whorls of leaves 1 and 2 had almost no pigment, therefore it was completely colourless. The increase in chlorophyll content was modest in sections covered by the coleoptile, showing pale or yellow tissue. The data suggest the photosynthetic apparatus accumulation becomes rapid after chloroplasts have reached their maximum count and are exposed to light (35 mm). The rapid pigment accumulation occurs after the leaf exits from the coleoptile. Highest pigment content (1833 nmol per gram fresh weight) was observed in the leaf blade in sample 14, which has fully developed chloroplasts (Fig. 5.15 A). Congruently the genes involved in pigment biosynthesis (carotenoid and chlorophyll) are expressed gradually after chloroplast division. In addition, the expression of genes related to reaction centres, antenna proteins, electron transport and Calvin cycle also increases gradually and peaks in sample 14. In accordance to the above chloroplast parameters, chlorophyll level and transcripts of selected genes decreased in the fully mature region, before signs of senescence were apparent (sample 15) which probably reflects the initiation of the dismantling of photosynthetic apparatus.

**Table 5.8 List of genes selected representing pigment synthesis and thylakoid development**

| Gene ID | Name | Function |
|---|---|---|
| TraesCS1A02G057200 | HEMA1_1 | Chlorophyll synthesis |
| TraesCS1A02G173100 | | |
| TraesCS1B02G075200 | | |
| TraesCS1B02G191200 | | |
| TraesCS1D02G058300 | | |
| TraesCS1D02G165600 | | |
| TraesCS2A02G134000 | CHLH/GUN5 | |
| TraesCS2B02G157600 | | |
| TraesCS2D02G136200 | | |
| TraesCS3A02G506200 | CAO | |
| TraesCS3B02G574300 | | |
| TraesCS3D02G514100 | | |
| TraesCS5A02G020900 | PSY | Carotenoid synthesis |
| TraesCS5D02G026000 | | |
| TraesCS7A02G557300 | | |
| TraesCS7B02G482000 | | |
| TraesCS7D02G553300 | | |
| TraesCS5B02G017900 | | |
| TraesCS4A02G004900 | PDS3 | |
| TraesCS4B02G300100 | | |
| TraesCS4D02G299000 | | |
| TraesCS3A02G304900 | CURT1 | Thylakoid |
| TraesCS3B02G331600 | | |
| TraesCS3D02G296900 | | |

**Table 5.9 List of genes selected representing photophosphorylation, Calvin cycle and photorespiration**

| Gene ID | Name | Function |
|---|---|---|
| TraesCS2A02G247300 | PSBO 2 | Reaction centres |
| TraesCS2B02G270300 | | |
| TraesCS2D02G248400 | | |
| TraesCS5A02G482800 | PSAE 2 | |
| TraesCS5B02G496000 | | |
| TraesCS5D02G496400 | | |
| TraesCS5A02G322500 | LHCB 2.1 | Antenna |
| TraesCS5B02G322900 | | |
| TraesCS5D02G329200 | | |
| TraesCS7A02G227100 | LHCA 1 | |
| TraesCS7B02G192500 | | |
| TraesCS7D02G227300 | | |
| TraesCS4A02G499500 | PETE1 | Electron transport |
| TraesCS7A02G000400 | | |
| TraesCS7D02G000300 | | |
| TraesCS2A02G223600 | ATPC1 | ATP synthase |
| TraesCS2B02G273900 | | |
| TraesCS2D02G229600 | | |
| TraesCS2A02G066700 | RBCS | Calvin cycle |
| TraesCS2B02G078900 | | |
| TraesCS2D02G065100 | | |
| TraesCS3A02G367000 | SBPASE | Calvin cycle |
| TraesCS3B02G398300 | | |
| TraesCS3D02G359900 | | |
| TraesCS2A02G250800 | GOX1 | Photorespiration |
| TraesCS2B02G264100 | | |
| TraesCS2D02G251800 | | |
| TraesCS5B02G426500 | | |
| TraesCS5D02G432900 | | |

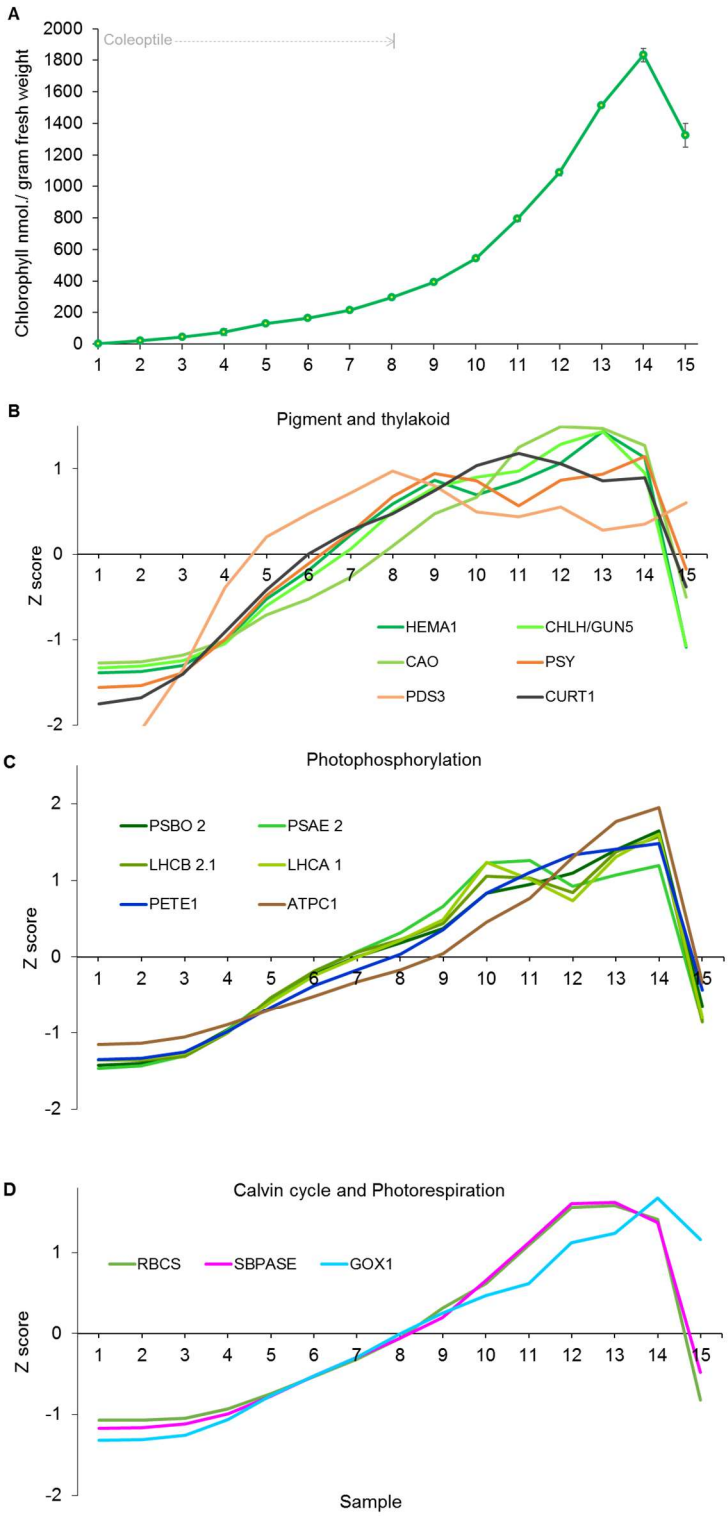


**Figure 5.15** Analysis of chlorophyll content along the developing wheat leaf. Chlorophyll concentration was measured by spectrophotometry in freshly collected samples of the developing wheat leaf. Error bars represent the SEM (standard error of the mean) values of triplicate samples. Transcript abundance of (B) pigment and thylakoid development, (C) photophosphorylation, (D) Calvin cycle and photorespiration genes along the developmental stages of wheat presented as Z score. Each line represents the mean of Z score values of three homeologs.

## 5.12 Expression of known regulators represents different stages of chloroplast development

Expression profiles of genes involved in the regulation of chloroplast development follow the pattern of individual processes (Fig. 5.16). For example, the expression of a protein import regulator (*CIA2*) is high during the plastid division and growth stages. Photomorphogenesis related gene (*HY5*) peaks after chloroplast division, in the leaf section which emerges from the coleoptile. Genes associated with pigment biosynthesis (*GLK1*) are most active in samples in which chloroplasts are most rapidly greening or fully developed.

**Table 5.10 List of genes selected representing chloroplast regulators**

| Gene ID | Name | Function |
|---|---|---|
| TraesCS7A02G422200 | CIA2_1 | Protein import |
| TraesCS7B02G322600 | | |
| TraesCS7D02G414400 | | |
| TraesCS6A02G118000 | CIA2_2 | |
| TraesCS6B02G146200 | | |
| TraesCS6D02G108000 | | |
| TraesCS7A02G339800 | GLK1_1 | Pigment synthesis |
| TraesCS7B02G251400 | | |
| TraesCS7D02G347500 | | |
| TraesCS3A02G161000 | GLK1_2 | |
| TraesCS3B02G191600 | | |
| TraesCS3D02G168200 | | |
| TraesCS7A02G363100 | GNC | Cytokinin signaling |
| TraesCS7B02G264800 | | |
| TraesCS7D02G359900 | | |
| TraesCS3A02G128900 | HY5_1 | Photomorphogenesis |
| TraesCS3D02G129800 | | |

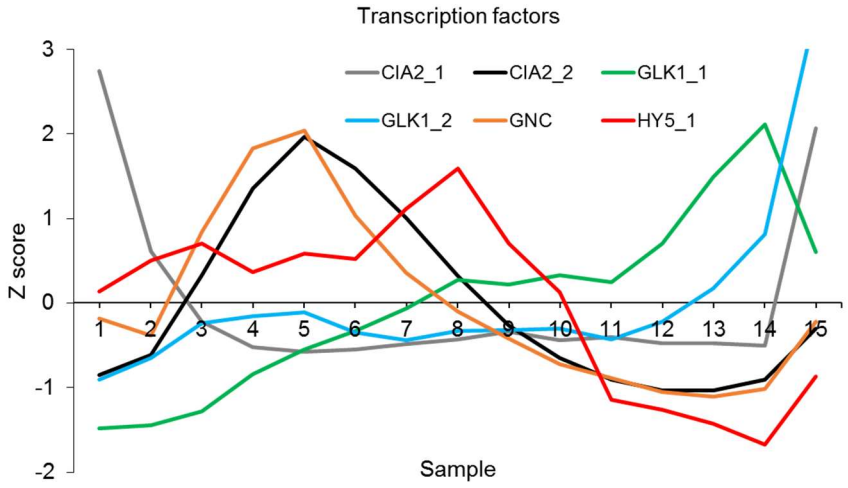


**Figure 5.16** Expression analysis of known chloroplast development regulators along the developing wheat leaf. Transcript abundance of selected genes is presented as Z score. Each line represents the mean of Z score values of three homeologs.

### 5.13 Possibility of chloroplast fusion in the wheat leaf

Multiple lines of evidence indicate that chloroplast division occurs in the first four samples at the base; however, DIC images display joint chloroplast structures even in sample 10 (40 - 50 mm). Although at first glance of the images it could be thought that some plastids are still proliferating, this hypothesis is not easily compatible with the drop of chloroplast numbers in samples 8 to 12 (70 - 80 mm, Fig. 5.9). The maximum number of plastids was seen in sample 5 (15 - 20 mm); hereafter the number continues to reduce until sample 12 (70 - 80 mm). In contrast,, the mean chloroplast area and chloroplast compartment keep increasing, if at all more in this region. In addition, cpDNA content per chloroplast also increases during this stage.

As the newly added cells move distally towards the leaf blade, to pursue whether the chloroplast count is reduced over time, an experiment was designed to follow the same cells at two different stages of development. The 6-days old leaf 1 was marked at the tip of the coleoptile (35mm) and observed again when it reached 75mm (Fig. 5.17 A). Samples were collected from those two developmental time points from unmarked seedlings of identical length. Cells isolated from point ‘x’ (35 mm), were smaller and their size slightly increased after moving to ‘y’ (75 mm). Indeed, the average chloroplast number was reduced from 300 to 230 (Fig. 5.17 B). Meanwhile the chloroplast area showed an increase in size of over 3-fold. Features of two chloroplasts joint together, “dumbbell-shape” chloroplasts, were observed at 35 mm. Fixed cells mounted on microscope slides were intentionally over-tapped to rupture the cell wall and isolate chloroplasts. Strikingly, broken cells from the 75 mm section also showed similar images of some dumbbell-shape chloroplasts (Fig. 5.17 C). This observation further highlights the fact that chloroplast number decreases during development and that of mesophyll cells show unusual joint chloroplasts in fully-differentiated mature samples.

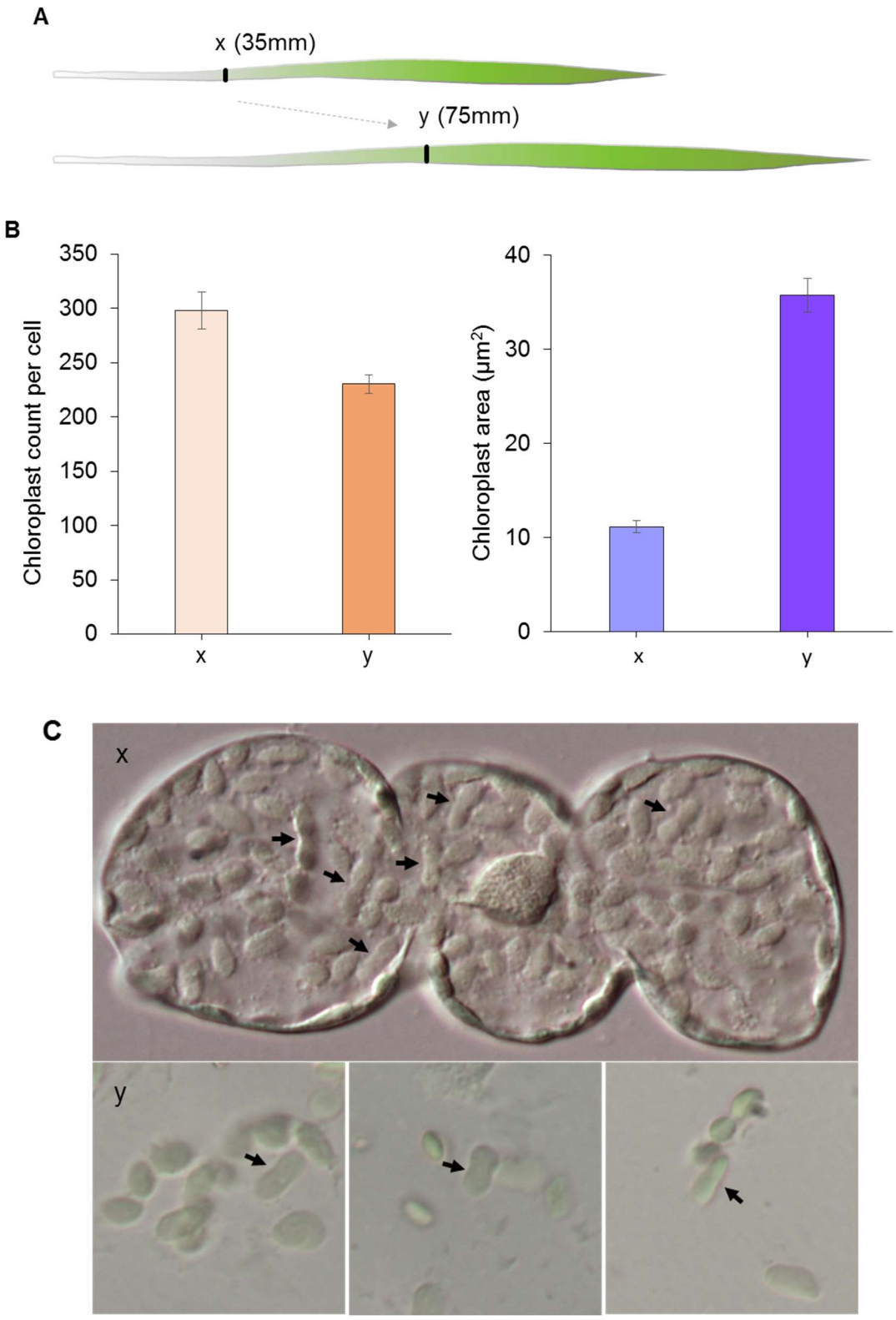


**Figure 5.17** Schematic diagram of selected samples at early and late developmental stage. Graphs showing reduced chloroplast count and increased chloroplast area as mesophyll cells move from point 'x' to 'y'. Error bars represent SEM values of the mean of the four replicates. (C) Enlarged image of a mesophyll cell from figure 5.5, captured from the 45mm section (top) and isolated chloroplasts (bottom) in samples collected at 75mm. Arrows indicate the appearance of dumbbell-shape chloroplasts.

## 5.14 Discussion

The process of cellular growth, division and pattern of differentiation is well distributed in monocot developmental stages (Langdale et al., 1989; Nelson and Langdale, 1989; Jarvis and Lopez-Juez, 2013). The cereal leaf analyses have used advanced techniques like microscopy, transcriptomics, proteomics and metabolomics which immensely contributed to the understanding of cellular differentiation. Surprisingly, so far, the understanding of chloroplast development and its regulation is incomplete. It is evident that plastid development begins early in meristematic cells (Dean and Leech, 1982), but most of the monocot studies described below were mainly interested in cell differentiation, hence they considered developmental stages after cell division. The present study has revised the dissection strategy to gather complete information about the process of chloroplast biogenesis in relation to cell development. The base of the leaf was carefully sectioned into distinct samples to distinguish closely related processes.

A cluster of differentially expressed genes along the maize leaf gradient showed that the base section was actively involved in cell cycling (Li et al., 2010). Using a more careful sampling strategy, current data showed that most of the cell cycle genes are expressed in the meristem and in the first 5mm of the leaf base. The phosphorylated-RBR1, inactivation form of the core cell cycle repressor, a marker protein form of cell division (Magyar et al., 2012) was observed only in the meristem and to a smaller extent in the first section (5 mm) of the leaf base. Like other monocots, wheat samples also showed two distinct bands for RBR protein (Lendvai et al., 2007). Although both bands were seen in the meristem section, one of them was present exclusively in material containing dividing cells, while the other was gradually reduced and disappeared after the cells emerged out of coleoptile (35 mm). The second form might have roles associated with differentiation rather than division. Rapid cell division occurs in the meristem and also in the first 5 mm of leaf base.

All the cells in the meristem were very similar in terms of their shape and size. As they moved out of the proliferation zone, a series of morphological changes and an increase in complexity were evident. Disruption of carotenoid biosynthesis with norflurazon in Arabidopsis affects the process of cell expansion, which clearly suggests that chloroplast-to-nucleus communication is necessary for cell differentiation (Andriankaja M, 2012). The cells at the base are engaged in the synthesis of cell wall and phytohormones (Li et al., 2010), the enzymes involved in formation of new cell wall components (cell elongation) being highly expressed in the first 45mm at the base of maize leaf (Majeran et al., 2010). Accordingly, cell

expansion was rapid at the base of the wheat leaf, in this case the first 35 mm. Genes involved in biosynthesis of cell wall components, for example cellulose, arabinogalactan proteins, expansins, or involved in facilitating water influx and the building of turgor (aquaporins) are abundantly expressed during this phase. Although later sections showed cytoplasmic lobes, the actual cell expansion occurred within the coleoptile covering. These lobes are common in grass leaves. It was reported that chlorenchyma cells of wheat have lobes with double the size as those in rice (Sage and Sage, 2009). Mesophyll cells in wheat carried >10 chloroplasts per each lobe pushed towards the cell membrane, while there are only 3-4 chloroplasts per lobe in rice (Evans and Loreto, 2000). Indeed, the present observation also showed an increase in the chloroplast number per lobe as cells moved towards the leaf tip.

A most important aspect of the current study was including cells of the meristem and dissecting the basal region into 5 mm sections until 40 mm. An extensive analysis of chloroplast division in wheat leaves was carried 40 years ago (Boffey SA, 1979). Interestingly this analysis did not include the first 10 mm of the leaf base, and the maximum number of detected plastids was about 150 per cell at 45 mm. It is not clear why the chloroplast count was only 150 (max.) which is less than half of present results and also significantly less than the number in fully mature cells. This could be due to the adopted technique or wheat variety. Furthermore, images of dumbbell-shaped chloroplasts were visualised until 40 mm, and it was considered that, in addition to proplastids, chloroplasts also divide after their differentiation. The identification of multiple genes, including *ACCUMULATION AND REPLICATION OF CHLOROPLASTS* 1-12 (Pyke and Leech, 1991; Pyke and Leech, 1992, 1994), and *PLASTID DIVISION* 1 and 2 (Miyagishima et al., 2006), had immensely contributed to understanding the process of chloroplast division. Most of these genes were high in expression at the base of the wheat leaf, before 20 mm, which exactly matches with the phase of increase of chloroplast count, suggesting that plastid division occurs within 20 mm of leaf base. There are other genes that are characterised to function in plastid division. For example, Gao et al. (2006) identified *FZL* (FZO-Like) gene that encodes a protein which is closely related to a mitochondrial fusion protein. Interestingly, the *fzl* mutants exhibited defects in chloroplast size as well as number. Another gene characterised as *GAINT CHLOROPLAST 1* accumulates 1-2 unusually larger chloroplasts in mesophyll cells (Maple et al., 2004). Unexpectedly, the transcripts of *FZL* and *GC1* were not expressed along with other chloroplast division genes. Instead their mRNA

levels accumulated maximally after 25 mm, when the chloroplasts cease to increase in number (Fig. 5.9 C) and were higher particularly between 40 and 80 mm. It is important to note that microscopy data has shown joint dumbbell chloroplasts even at 75 mm sections from the leaf base. Chloroplast and mitochondria, with shared endosymbiotic origin, use some related mechanisms of division (Osteryoung and Nunnari, 2003). To increase their size, for DNA recombination and to serve the high energy needs, plant mitochondria also undergo fusion in addition to fission (Arimura SI, 2004; Arimura, 2018). Chloroplast fusion was found to occur in green algae (Miyamura, 2010), but to date there is no evidence of such a phenomenon in land plants (Jarvis and Lopez-Juez, 2013). Therefore, this observation raises a question whether previous chloroplast counts in wheat mesophyll cells were misinterpreted, and leads to the hypothesis that chloroplast fusion also occurs in plants, in addition to mitochondrial fusion. This is supported by the DIC images showing intact dumbbell shaped isolated chloroplasts at the stage when there is no transcriptional evidence of chloroplast division. Further investigation is required to confirm the possibility of chloroplast fusion and the role of FZL and GC1 in land plants.

It was reasoned that multiple copies of chloroplast and mitochondrial DNA must be maintained to meet the demand of organellar translation (Bendich, 1987), also to cope with DNA damage (Shokolenko et al., 2009). Chloroplast DNA damage increased over time when assessed at the base and mature sections of leaves in maize seedlings (Kumar et al., 2014). Conversely, cpDNA remained unchanged when whole leaves were looked at different developmental stages in Arabidopsis, sugar beet, tobacco and maize (Golczyk et al., 2014). Although the selection of the whole leaf seems interesting, the sequential arrangement of developing cells in monocot makes it an ideal model, to select tissues at different developmental stages, over the mosaic pattern in dicots to study chloroplast development (Boffey SA, 1979; Nelissen et al., 2016). Boffey et al. (1979) followed cells at different developmental stages and reported that chloroplast DNA replication (through the incorporation of [3H] Thymidine) in wheat leaf occurs consistently with chloroplast division. In the present study, gene expression of chloroplast DNA polymerase and real-time PCR quantitative-analysis covering three different regions of the chloroplast genome was employed at different developmental stages of the wheat leaf. The observations revealed that cpDNA increases in dividing plastids but peaks later, even after chloroplast division has ceased. The increase in chloroplast genome copy number continued for longer (60 mm) than previously reported. Therefore, cpDNA replication is not restricted to the period of

chloroplast division, a conclusion which is consistent with earlier observations in garden pea (Bennett J, 1975) and in spinach (Rose et al., 1975). However, after 2 weeks of growth, as the onset of senescence approached, ptDNA decreased not just in the whole tissue but also per chloroplast of wheat (Boffey SA, 1982) and barley (Baumgartner BJ, 1989). This observation is consistent with the transcript levels of organellar DNA polymerases which were also decreased during the chloroplast-gerontoplast transition (Parent et al., 2011) but would, in addition, require the appearance of nuclease activities. Different cell types have different proportion of plastids, and an interesting question is to understand whether cpDNA replication (copies of the plastid genome) is regulated according to the function of plant cells.

Chloroplast gene expression is governed by a nucleus-encoded (NEP) and a plastid-encoded (PEP) RNA polymerase. Expression of NEP is higher during the early stages of development while PEP function predominates in developed chloroplasts (Zhelyazkova et al., 2012). The PEP-associated sigma factors peak differently during different stages of development (Börner T, 2015; Wang et al., 2017). Indeed, similar results were recorded in the wheat samples showing an expression pattern of sigma genes during early (*SIG1, SIG2_1*), transition (*SIG2_2, SIG6*) and mature (*SIG1, SIG5*) stages of development. Therefore, the labour of gene expression is also shared among the six sigma factors depending on the age of wheat chloroplasts. Chloroplast gene expression is tightly coordinated with nuclear gene expression and depends on the import of cytosolic preproteins. The genes encoding components of chloroplast protein import machinery and tetrapyrrole synthesis were mainly expressed during the transition from source to sink to source (Li et al., 2010). Similar results were observed while comparing the developmental gradients of rice and maize. A cluster showed highly expressed genes within the transition zone, related to tetrapyrrole metabolism and chloroplast development (Wang et al., 2014). The protein import capacity diminishes in differentiated wheat chloroplasts compared to proplastids (Dahlin and Cline, 1991). Congruently, the expression for genes encoding subunits of plastid protein import complexes (TOC/TIC) was higher particularly during stages showing high plastid division and to some extent even after the division phase. *SP1* is a ubiquitin ligase that regulates remodelling of TOC components (Ling et al., 2012), allowing the interchange of complexes favouring housekeeping or photosynthetic preproteins. Expression of *SP1* was particularly high during proplastid-to-chloroplast transition. Furthermore, during this phase, genes involved in maintenance of the chloroplast genetic machinery, ribosomal build-up and plastid-to-nucleus communication (*GUN1*) were highly expressed.

In the analysis of the maize leaf gradient, proteins involved in the process of plastid biogenesis were observed in the first 4 cm from the leaf base. In contrast, most of the photosynthetic proteins accumulated in subsequent sections. There was a gradual increase in the expression of the photosynthesis-related genes such as photoreceptors, import complexes, enzymes synthesizing tetrapyrroles and secondary cell wall components (Majeran et al., 2010). Chloroplasts are fully photosynthetic in cells situated at the distal region and chlorophyll content was reduced in the tip of the maize leaf which might be due to senescence (Li et al., 2010; Pick et al., 2011). Wheat samples also followed a gradual increase in chlorophyll concentration, thylakoid synthesis, photophosphorylation, Calvin cycle and photorespiration along the developmental gradient. Multiple pieces of evidence (chloroplast genome, pigment, transcriptome data) suggest the process of chloroplast degradation during senescence.

The ultimate aim of the research is to identify novel transcriptional factors involved in chloroplast development. For example, following the maize leaf development, Li et al. (2010) narrowed about 180 transcriptional factors in different cell types (bundle sheath and mesophyll). As proplastids in the meristem and base of leaf are dividing rapidly, most of the chloroplast division genes are highly expressed in the shoot apical meristem and continue beyond cell division. Like the function of cytokinins, the GROWTH REGULATING FACTOR 5 (GRF5) sets a connection between cell division and chloroplast proliferation. Overexpression of *GRF5* increases cell division but is also followed by enhanced chloroplast division and photosynthetic pigments (Vercruyssen et al., 2015). Other known regulators include *GATA NITRATE-INDUCIBLE CARBON-METABOLISM-INVOLVED* (GNC) and *CYTOKININ-RESPONSIVE GATA1* (CGA1) which positively regulates early plastid development and division (Hudson et al., 2011; Chiang YH, 2012). The nucleus-encoded CYTOKININ RESPONSE FACTOR 2 (CRF2) also promoted chloroplast division (Okazaki et al., 2009). Wang et al. (2014) proposed a link between a ZAT10 family transcriptional factor and chloroplast signaling based on its expression pattern. The *Chloroplast Import Apparatus 2* (CIA2) is a positive regulator of chloroplast protein import complexes (Sun et al., 2009). Well-known chloroplast regulators are the GLK transcription factors (Hall et al., 1998; Waters et al., 2009). Overexpression of a *GLK* gene converts root plastids into chloroplasts (albeit such cells will present a reduced chloroplast compartment relative to that of mesophyll cells), forming unusual green roots (Kobayashi et al., 2012). It has been argued that expression of GLK transcriptional factor occurred in differentiated cells

(photosynthetically active), therefore it is very unlikely to be a master regulator (Majeran et al., 2010).

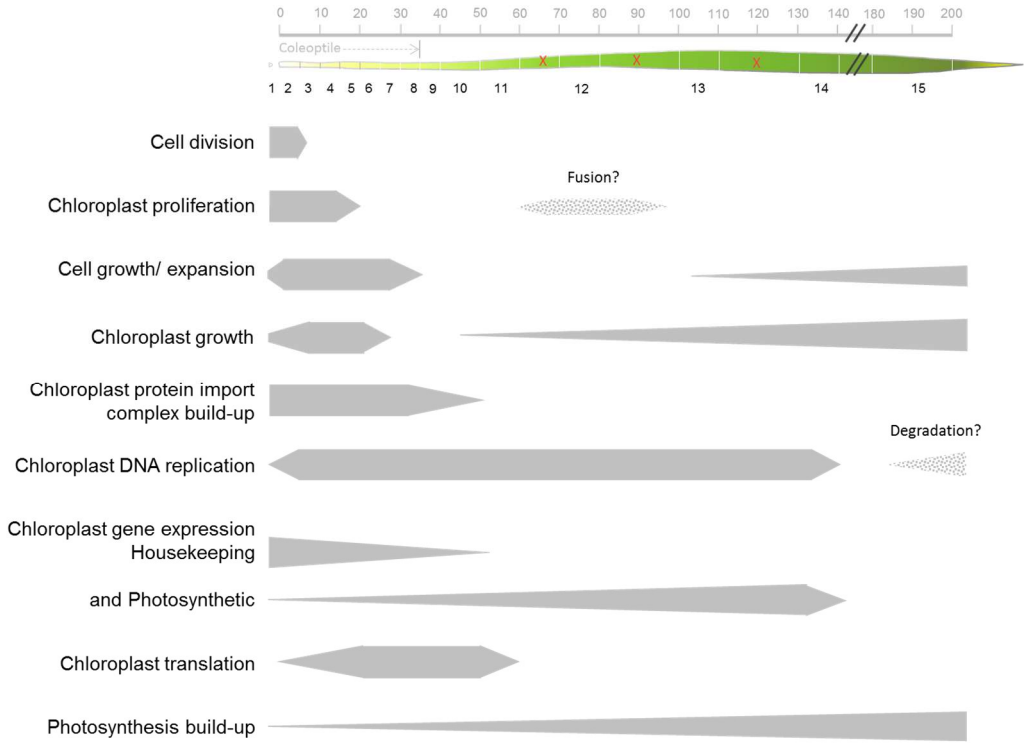


**Figure 5.18** Schematic diagram representing chloroplast biogenesis processes along the developing wheat leaf.

A thorough and revised sampling strategy in developing Chinese spring wheat has produced greater resolution for individual processes and regulatory genes of chloroplast development, like chloroplast division, cpDNA replication, protein import, retrograde signaling and photosynthesis. A combination of transcriptome and microscopy data seems a promising tool to fish out candidate genes with unknown function. Based on the expression pattern, in future work the transcriptome data will identify novel candidate regulators involved in the chloroplast biogenesis.

In summary, the current investigation has revealed that cell proliferation occurs in a narrow developmental window restricted to the meristem and base of the leaf (5 mm). Cells grow during the process of division and expand rapidly as they move away from the meristem until 35 mm. Undifferentiated plastids proliferate very rapidly during the cell division and continue to propagate (until 20 mm) after cells stop dividing. In accordance with previous studies, the present research has shown a correlation between the cell size and the total size of all chloroplasts, the chloroplast compartment. For example, during initial stages of

development, plastids fill rapidly growing cells, by rapid proliferation accompanied by growth. Once plastids stop dividing, growing cells are filled with individual chloroplasts of increased size. There is a transition phase between plastid proliferation and active photosynthesis phases when cell expansion and plastid build-up are congruent. Results suggest the possibility of chloroplast fusion in wheat cells and identify two possible candidates as FZL and GC1. This requires further investigation. Like plastid growth, the process of chloroplast gene expression is a widely spread one. Associated cellular transcription, ribosomal build-up, and translation become more active from early development to the stage of transition to chloroplasts as judged from transcripts' analysis. The membrane complexes transcripts are expressed particularly in early stages of development to promote cytosolic protein import into developing plastids. Transcripts for plastid gene expression peak during the phase of transition, between plastid division and differentiation into chloroplasts. There is strong correlation between nuclear DNA synthesis and phosphorylation level of a core, negative cell proliferation regulator. Although cpDNA replication begins during plastid proliferation, it continues for extended time until chloroplasts are fully photosynthetic, possibly to cope with the damage during light reactions. The expression of known chloroplast biogenesis regulators shows distinct patterns which correlate with individual processes and quantitative chloroplast data. The transcriptome analysis might serve to identify novel candidate regulators of chloroplast development. Taken together, the mechanism of chloroplast biogenesis has become better elucidated along the gradient of the wheat leaf. The sequence of individual processes includes: plastid division during and after cell division, early plastid growth congruent with cell expansion, which is associated with the build-up of plastid protein import complexes and gene expression, transition in chloroplast development to build-up of photosynthetic apparatus, a fully photosynthetic chloroplast and transition into gerontoplast during senescence.

# Chapter 6

# General discussion

Chloroplast biogenesis involves multiple individual processes, including DNA replication, gene expression, division and import of cytoplasmic proteins. Genetic studies in several laboratories have identified multiple genes involved in these processes. Surprisingly, very little is known about how the individual processes are regulated and whether there is any specific regulator of chloroplast development. Forward genetics, reverse genetics and activation tagging have been powerful tools to identify individual genes. However, through random mutagenesis, it takes years and a combination of different research efforts to summarise a complete process.

Chloroplast development occurs in parallel with cellular development mechanisms. For example, undifferentiated cells contain proplastids which develop into chloroplasts as cells undergo differentiation. Plastid biogenesis influences major aspects of plant growth and development, understanding its regulation therefore is an extremely important area of research (Inaba and Ito-Inaba, 2010). Some of the fundamental questions, like when do cells fill with chloroplasts, how do different cells have different number of chloroplasts (López-Juez, 2006) and what happens to the chloroplasts when plants suffer severe stress remain elusive.

In a flowering plant like Arabidopsis, the development of chloroplasts from proplastids occurs very early in the L2 and L3 layers of the shoot apical meristem (Charuvi, 2012). Although knowledge gained from knockout mutants and genetic screens in a dicot model plant is substantial, one main limitation is its small size, it is extremely difficult to prepare samples to study series of developmental processes. Even for a larger leaf size, the transition to greening occurs extremely early, the earliest observable leaf primordia showing almost complete greening. As an alternative, the monocot leaf provides a well distributed pattern of cellular developmental stages. For example, through the process of cell proliferation new daughter cells are added at the base of the leaf, thereby pushing the mature cells upwards to the leaf apex, this forming a developmental gradient (Avramova et al., 2015). The knowledge of chloroplast development and cell differentiation using cereal leaf models has accumulated substantially over time and provided evidence for the identification of candidate regulatory genes (Boffey SA, 1979; Boffey SA, 1980; Boffey SA, 1982; Li et al., 2010; Majeran et al., 2010; Pick et al., 2011; Wang et al., 2014; Wang et al., 2017). However, a better sampling strategy is required to separate the cellular processes in a cereal leaf model. The current study on the developmental gradient of the wheat leaf has shown a fine distribution of overall

chloroplast development. The sequential events occurring during plastid biogenesis can be divided into different phases.

The first phase of chloroplast development involves plastid division. Proplastids begin to divide during the process of cell division. Initially very few plastids are shared among the newly divided daughter cells. Depending on the function of cells and need for chloroplast development, plastids are distributed differently in various cell types (Charuvi, 2012). For example, mesophyll cells have a maximum number of chloroplasts as they are actively engaged in photosynthesis (reviewed by Jarvis and Lopez-Juez, 2013). How the regulation of differentiation is achieved among different cells or how the decision of a varying degree of chloroplast filling is made among cell types is far from known. The *CLUMPED CHLOROPLASTS 1* (*CLMP1*) is essential for chloroplast distribution. Loss of function of this gene results in clustered chloroplasts (Yang et al., 2011). Wheat transcriptome data shows that expression of *CLMP1* follows a pattern similar to that of the chloroplast division machinery. Therefore, this gene might be functioning in parallel to plastid division. It seems the plastid number does not affect overall plant development, for instance the *arc6* Arabidopsis plastid division mutant shows no distinct visible whole-plant phenotype. As the plastid division occurs during cell division, it will be interesting to see if defects in chloroplast division are communicated or have any impact on cell division. Transcriptome data obtained in the wheat leaf might identify candidate genes which regulate plastid number in green cells. Contrary to a previous observation that reported cpDNA replication ceases before plastid division (Boffey SA, 1982), the results presented here have shown that plastid DNA replication continues even in fully developed chloroplasts. In addition, the plastid division-defective *arc6* mutants contain the same number of plastid genome copies compared to wild type, which confirms that cpDNA replication can occur independent of plastid division. The replication of plastid DNA, expression of NEP and early sigma factors and the making of plastid protein import complexes are also active during the first phase of chloroplast biogenesis.

The second phase of chloroplast development is a preparatory or transition phase. At the beginning, newly divided cells and proplastids grow congruently, but subsequently plastid growth continues alone, if at all plastid growth is rapid when cells stop growing. The concept of a predetermined “chloroplast compartment” reflects the observation that there seems to be a correlation between cell size and the total chloroplast content of those cells. As the chloroplast compartment changes towards its set-point, smaller cells contain a lower

proportion of the cellular space taken by plastids while mature cells have more chloroplast coverage, which is mostly due to increase in size of individual plastids (Ellis and Leech, 1985). Plastid growth mainly involves import of thousands of nucleus-encoded proteins. The formation of import complexes continues even during the transition phase to facilitate import of cytosolic proteins, thereby promoting plastid growth. The process of thylakoid biogenesis happens after plastid proliferation and peaks in the transition phase. Notably, the expression of genes involved in chloroplast-to-nucleus signalling, like *GUN1*, or its downstream targets *SIG2* and *SIG6*, is also higher during this phase (post plastid division). Plastids in this phase are enriched with processes including the maintenance of their genetic machinery, ribosomal build-up, import of cytoplasmic proteins and formation of tetrapyrrole compounds. As mentioned above the number of plastids in *arc6* is reduced, yet the overall plastid proportion is maintained with 2-3 giant chloroplasts (Pyke et al., 1994). On the other hand, the *REDUCED CHLOROPLAST COVERAGE* (*REC*) quadruple mutants have only 50% cellular plastid proportion and this severely affects plant growth (Larkin et al., 2016). Therefore, unlike plastid number, it seems that the proportion or chloroplast coverage is an important factor for plant development. Are there any other chloroplast compartment regulators? How do these mechanisms work together? This is poorly understood.

Chloroplast defects in housekeeping functions, like synthesis of nucleic acids (Morley and Neilson. 2016), amino acids or vitamins, arrest plant growth at the embryonic stage; however plants manage to survive with defects in photosynthesis or pigment synthesis genes (Bryant N, 2011). The *EMB1211* gene is essential for embryogenesis and chloroplast development (Liang et al., 2010). *EMB1211* / *TIC100* encodes a protein associated to 1MDa TIC complex that mediates protein import at the inner chloroplast membrane (Kikuchi et al., 2013). The present research has demonstrated that chloroplasts of *cue8* (with a partial loss of function of *TIC100*) suffer from defective import of photosynthetic as well as housekeeping proteins. This was confirmed by the rescue of the import defect to near-wild type levels in the identified suppressor of *cue8*, *soh1*. The *cue8* virescent phenotype depicts a delay in chloroplast development which is very similar to a stage in the gradient of the developing wheat leaf. The gradual greening in the wheat leaf provides a better understanding of the slow-greening *cue8* mutant. Results have shown that the defect in *cue8* does not affect plastid division. Therefore, with partial loss of protein import function, the cells of *cue8* have completed the phase of plastid division normally. However, the root meristem phenotype suggests a general plastid protein import is necessary for cell division. Reduction in

individual size and overall chloroplast compartment suggests that growth of plastids has been slowed down in the transition phase. Interestingly, a compensatory mechanism (discovered in this study) is developed to prolong and upregulate the expression of nucleus-encoded polymerase (NEP) and maintain the expression of *SIG2* and *SIG6* to normal levels. In addition, the transcripts of TOC and TIC (1MDa) components are also elevated in an attempt to overcome the plastid defect. The wheat analysis showed that cpDNA replication occurs until chloroplasts are fully differentiated. In contrast, in *cue8*, despite of the import defect and delayed development, the plastids have maintained (i.e., have prematurely achieved) normal numbers of copies of the genome. This made the upregulation of housekeeping gene expression possible, by providing sufficient templates to the elevated NEP in *cue8* chloroplasts. Taken together, the results suggest *cue8* plastids remain in the transition phase for longer than WT chloroplasts. As shown by the *cue8 gun1* double mutants, the role of GUN1 seems crucial for the process of slow greening in *cue8* to take place, and it is a reasonable hypothesis that GUN1 action is the cause of such modification of the normal course of chloroplast development. It is not clear whether the import defect is initiated by the reduced action of SIG6/ SIG2 factors or by reduced levels of tetrapyrrole compounds, both of which may be communicated by GUN1. Retrograde signalling was proposed to involve several signal sources, gene expression, metabolites, reactive oxygen species. A consensus about how the defects in chloroplast development are communicated to the nucleus could be achieved by analysing the spatial distribution of multi-level signals along the development of the monocot leaf. Some other examples of genes whose mutation also leads to a gradual greening phenotype include the PEP-associated *SIGMA FACTOR 2* and *SIGMA FACTOR 6* (Woodson et al., 2013), *SLOW GREENING 1* which encodes a chloroplast targeted tetratricopeptide repeat protein (Hu et al., 2014), and *DELAYED PALE-GREENING1*, a predicted chloroplast membrane protein, Interestingly *DPG1* is absent in monocot plants (Liu et al., 2016). It is important to note that loss of function of any of these genes also leads to elevated expression of NEP-dependent genes in the chloroplast, which is consistent to the observation in *cue8*. Given the fact that *ppi1* and *toc132 toc120/+* also show enhanced NEP expression, this type of plastid development homeostatic mechanism displayed by *cue8* could be a common phenomenon underlying the slow greening/virescent or pale mutants. The wheat transcriptome data might help in identifying the regulators of NEP and TOC/TIC membrane component expression of chloroplasts.

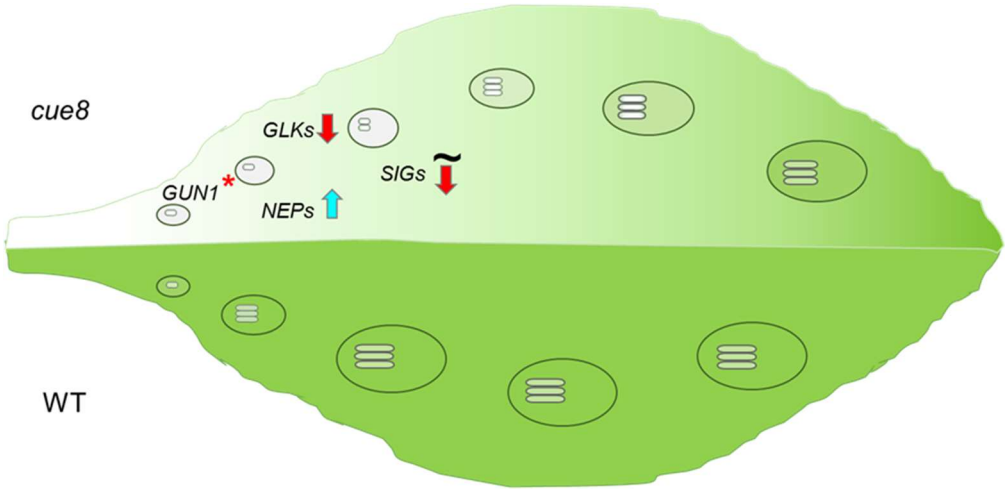


**Figure 6.1** Schematic representation of the compensatory mechanism in *cue8*. NEP is elevated to promote plastid-encoded housekeeping genes, while suppression of nucleus-encoded and chloroplast-encoded photosynthetic genes occurs by reduced expression of *GLKs* and selective sigma factors respectively. A functional *GUN1* is necessary for the slow greening phenotype of *cue8*. The activation of plastid homeostasis mechanism and prolongation of proplastids-to-chloroplast transition phase appears to be linked to the virescent phenotype.

The last phase of plastid biogenesis is the formation of fully differentiated chloroplasts. During this phase the chloroplasts occupy most of the available space in mesophyll cells. The enzyme synthesising tetrapyrrole compounds, and other genes involved in pigment biosynthesis are highly expressed. The well-developed thylakoid membrane structures with antenna proteins and accumulated pigments become actively engaged in the process of photosynthesis. The transcription factors GLK1 and GLK2, associated with the regulation of pigment biosynthesis are higher in expression after the plastids stop dividing, indicating that GLKs are involved in the differentiation of chloroplasts rather than in early plastid biogenesis. Consistent with other pale mutants, the expression of *GLK1* and *GLK2* is down-regulated in *cue8*, resulting in delayed proplastid to chloroplast transition. This is in contrast to the expression of NEP, plastid protein import complexes (TOC/TIC), and chloroplast DNA replicase (POL1A, POL1B). Therefore, it is evident that none of these genes are regulated by GLK transcription factors. A known regulator of TOC/TIC and plastid ribosomal genes in green tissues of Arabidopsis is *CHLOROPLAST IMPORT APPARATUS 2* (*CIA2*). The analysis of *cia2* mutants revealed that most of the downregulated genes were involved in chloroplast import complexes and gene expression (Sun et al., 2009).

Furthermore, the fact that *cue8* shows normal plastid division suggests GLKs are not required for that process during early plastid biogenesis (division). This supports the observations in the wheat transcriptome analysis that show *GLK* expression is limited during early plastid

development. Recently, the overexpression of maize *GLK* into rice plants enhanced the proportion of chloroplasts in bundle sheath cells (Wang et al., 2017). Further insight is required to understand if GLK transcription factors promote plastid growth in land plants. Given the fact that *glk1 glk2* does not show a severe phenotype (embryo lethality) and accumulates reduced levels of photosynthesis-related proteins (Fitter et al., 2002), it is very unlikely to be a master regulator of plastid development. As proposed for *sig6* mutants, the slow growth of *cue8* might also be compensated by selected sigma factors expressed at a later stage of development, and help in the accumulation of chlorophyll over time (Woodson and Chory, 2012; Liu et al., 2016). Interestingly, the promoter regions of *SIG1*, *SIG2* and *SIG6* were shown to have GLK recognition motifs (Kakizaki et al., 2010). Further investigation is needed to resolve whether the sigma factors are under the control of GLKs, something which can be tested in the *glk1 glk2* double mutants.

Kikuchi et al. (2013) reported that *TIC100* is part of a green TIC complex that resides only in the photosynthetic tissues. Notably, had there been no role of CUE8 in the roots, the ds-RED fluorescence of *cue8* might have showed a bright signal similar to that in WT roots. Taken together, plastid distribution, root meristem phenotype and reduced root growth suggest *CUE8* is also important for root development. The absence of *TIC100*, *TIC56* and *TIC214* in grasses raised doubts about their role in land plants (Paila et al., 2015; Bolter, 2016). The near-WT accumulation of TIC100 and TIC56 proteins in *tic20-I* mutants suggests these proteins might have other roles in the absence of TIC20-I. Most importantly, the level of TIC110 is also enhanced in parallel to the proposed alternative import translocon, TIC20-IV. The argument of increased chloroplast housekeeping protein (HSP93, HSP70) import following disruption of 1MDa TIC complex, taking place through TIC20-IV, needs further investigation with housekeeping proteins that are themselves not directly related to protein import. The defects in TOC components or general plastid defects also result in elevated chaperone proteins (Kubis et al., 2003). Current results of *cue8* also show what could be somewhat enhanced levels of the HSP70 protein (see Fig. 4.15, when compared to total protein), suggesting this might also be part of the compensatory mechanism. The identification of intragenic suppressor *soh1*, together with the analysis of its phenotype, has confirmed that *CUE8* plays an essential role in the import of photosynthetic as well as housekeeping proteins.

The rate of growth of individual chloroplasts is maximum during the last phase of chloroplast development. There is no evidence for plastid division at 75 mm from the base of the leaf,

therefore it can be ruled out that the images of joint dumbbell-shape chloroplasts in wheat cells represent organelle division. It is reasonable to question the accuracy of the data showing a reduction of plastid count in mature leaf sections: as the chloroplasts have increased in size, they might mask others in the background. This is where various approaches like chloroplast DNA replication, translational capacity and gene expression patterns of known chloroplast processes provided supporting evidence for the possibility of chloroplast fusion. Should it eventually be demonstrated, a biological significance for chloroplast fusion might be to promote less traffic and free movement according to the light during active photosynthesis, in addition to coping with cpDNA damage by allowing the exchange of genomes for recombination-based repair as proposed for mitochondria (Arimura, 2018).

The wheat samples grown for two weeks show a fully mature chloroplast; at this stage there was limited expression of most chloroplast-related genes. In fact, a slight reduction in the expression of PhANGs and in the number of cpDNA copies was observed, which might be a sign of the beginning of senescence and its associated nutrient recycling (Avila-Ospina et al., 2014). The importance of a cereal leaf model system in understanding chloroplast development is accurately highlighted by the expression pattern of various genes that correlate with the quantitative data. Research on Arabidopsis and wheat leaf models has provided answers to fundamental questions in the field of plastid biology. The combination of quantitative, molecular and transcriptome data of the wheat leaf has detailed the process of chloroplast development in a unique way and holds the basis for the future search of novel chloroplast biogenesis regulators.

## 6.1 Conclusions of this work

Through this work it has been revealed that partial loss of *TIC100* slows the process of chloroplast differentiation in *cue8* resulting in a virescent phenotype. A 'retro-anterograde control' mechanism is initiated to increase expression of chloroplast-encoded housekeeping genes, maintain cpDNA replication, and supresses chloroplast-encoded photosynthetic genes by selective expression of sigma factors. As a consequence, the proplastid to chloroplast transition phase is prolonged to cope with the defect and turn green over time. GUN1 seems to play an important role in communicating the defects to nucleus. Overexpression of the positive regulators like GLK1 or FC1 does not rescue plastid defects in *cue8*, however loss of function of a negative regulator (*lyn1*) partly suppresses the *cue8* phenotype.

It has also been confirmed through loss of the *CUE8/ TIC100* gene, which encodes a protein involved in the formation of the novel 1MDa TIC complex, that this complex is necessary for the import of nucleus-encoded proteins into plastids, specifically that it mediates the import of a housekeeping as well as a photosynthetic protein into plastids. Identification of a semidominant intragenic suppressor, *soh1*, confirms the role of *CUE8* in the formation of the 1MDa TIC complex, import of proteins through the inner membrane, maintenance of chloroplast compartment in mesophyll cells and cpDNA distribution within the chloroplasts.

The detailed study along the gradient of growing wheat leaf has uncovered fundamental aspects of chloroplast biogenesis with special emphasis on how proplastids develop into mature chloroplasts. The underlying sequential processes are well resolved and allowed to distinct phases of plastid development. This study provides preliminary evidence for the occurrence of chloroplast fusion in plants. The combination of quantitative chloroplast data and transcriptome data along the developing wheat leaf confirms the resolved chloroplast biogenesis processes which can be used for the future search of novel chloroplast regulators.

## 6.2 Future prospects

Some of the suppressors of *cue8* might reveal novel genes possibly interacting with the components of import complexes and regulating chloroplast protein import. SP1 is one such regulator which reorganises chloroplast import complex (TOC) and plays a crucial role during abiotic stress conditions (Ling et al., 2012).

The detailed analysis of chloroplast biogenesis in the wheat leaf serves as a knowledge resource for understanding various genes involved in chloroplast development. This will also

contribute to a better understanding of chloroplast mutants, for example to identify defects in specific developmental stages of chloroplasts in those mutants. The current study helps to distinguish and specify the role of previously identified genes in chloroplast development. For example, looking at the phenotype of cellular chloroplasts, the *fzl* and *gc1* mutants are considered as defective in chloroplast division. A thorough analysis of the wheat leaf shows these genes are highly expressed independently of the major chloroplast division genes.

The identification of novel chloroplast regulators will contribute in the following areas of plant research:

(1) Addressing fundamental questions like how cells develop and maintain their chloroplast proportion and regulating the process of photosynthesis or developing photosynthetically efficient crops. Unlike maize and sorghum, the rice crop uses a C3 pathway which is a disadvantage during hot conditions due to photorespiration. Using genetic approach researchers are trying to generate the C4 rice to enhance photosynthetic yield (Hibberd et al., 2008; Sage and Zhu, 2011). A key investigation includes use of single gene regulators (Golden2-Like transcriptional factor) to develop C4 rice (Wang et al., 2013). The present study shows this regulator might be crucial during the phase of active photosynthesis and less important for the early events of chloroplast biogenesis and extends the possibility of identifying potential candidate regulators of chloroplast development.

(2) Growing plants on less nutrient resources. Recent findings have shown that Growth-regulating factor4 (GRF4) plays an important role in growing plants with a more efficient use of fertilisers, and increases the production (Li et al., 2018). This minimises the use of fertilisers thereby reducing the environmental damage caused by the energy demand of their production, and by the loss of nitrates and the evolution of nitrous oxides to the atmosphere.

(3) The regulators of fruit ripening and the production of high nutritional value foods. The tissue-specific silencing of the *DET1* gene produced tomatoes rich in carotenoid and flavonoid contents (Enfissi et al., 2010). Such foods are sources of increased antioxidants that will benefit human health by neutralising the oxidative free radicals in the cells, therefore reducing the risk of various diseases (Fraser and Bramley, 2004).

These are only some of the multiple benefits which an ability to modulate the extent of chloroplast development in cells of different plant tissues could bring. The number of doors towards further applications that it would open is very substantial.

# References


**Adhikari ND, Froehlich JE, Strand DD, Buck SM, Kramer DM, Larkin RM** (2011) GUN4-Porphyrin Complexes Bind the ChlH/GUN5 Subunit of Mg-Chelatase and Promote Chlorophyll Biosynthesis in Arabidopsis. Plant Cell **23:** 1449-1467

**Allison LA.** (2000) The role of sigma factors in plastid transcription. Biochimie **82:** 537-548

**Allison LAS, L. D. Maliga, P.** (1996) Deletion of rpoB reveals a second distinct transcription system in plastids of higher plants. EMBO Journal **15:** 2802-2809

**Andriankaja M DS, De Bodt S, Vanhaeren H, Coppens F, De Milde L, Mühlenbock P, Skirycz A, Gonzalez N, Beemster GT, Inzé D.** (2012) Exit from proliferation during leaf development in Arabidopsis thaliana: a not-so-gradual process. Developmental cell **22:** 64-78

**Appels R EK, Feuillet C, Keller B, Rogers J, Stein N, Pozniak CJ, Choulet F, Distelfeld A, Poland J, Ronen G.** (2018) Shifting the limits in wheat research and breeding using a fully annotated reference genome. Science **361:** eaar7191

**Arimura S** (2018) Fission and fusion of plant mitochondria, and genome maintenance. Plant physiology **176:** 152-161

**Arimura SI YJ, Aida GP, Nakazono M, Tsutsumi N.** (2004) Frequent fusion and fission of plant mitochondria with unequal nucleoid distribution. Proceedings of the National Academy of Sciences **101:** 7805-7808

**Aronsson HJ, P** (2002) A simple method for isolating import-competent Arabidopsis chloroplasts. Febs Letters **529:** 215-220

**Asano T YY, Kurei S, Sakamoto W, Sodmergen, Machida Y. A** (2004) A mutation of the CRUMPLED LEAF gene that encodes a protein localized in the outer envelope membrane of plastids affects the pattern of cell division, cell differentiation, and plastid division in Arabidopsis. The Plant Journal **38:** 448-459

**Avila-Ospina L, Moison M, Yoshimoto K, Masclaux-Daubresse C** (2014) Autophagy, plant senescence, and nutrient recycling. Journal of Experimental Botany **65:** 3799-3811

**Avramova V SK, Beemster GT.** (2015) The maize leaf: another perspective on growth regulation. Trends in plant science **20:** 787-797

**Avramova V, Sprangers K, Beemster GTJTips** (2015) The maize leaf: another perspective on growth regulation. Trends in plant science **20:** 787-797

**Baba K SJ, Espinosa-Ruiz A, Villarejo A, Shiina T, Gardeström P, Sane AP, Bhalerao RP.** (2004) Organellar gene transcription and early seedling development are affected in the rpoT; 2 mutant of Arabidopsis. The Plant Journal **38:** 38-48

**Balsera M, Goetze TA, Kovács-Bogdán E, Schürmann P, Wagner R, Buchanan BB, Soll J, Bölter B** (2009) Characterization of Tic110, a channel-forming protein at the inner envelope membrane of chloroplasts, unveils a response to Ca2+ and a stromal regulatory disulfide bridge. Journal of Biological Chemistry **284:** 2603-2616

**Balsera M GT, Kovács-Bogdán E, Schürmann P, Wagner R, Buchanan BB, Soll J, Bölter B.** (2009) Characterization of Tic110, a channel-forming protein at the inner envelope membrane of chloroplasts, unveils a response to Ca(2+) and a stromal regulatory disulfide bridge. Journal of Biological Chemistry **284:** 2603-2616

**Bauer JC, K. Hiltbunner, A. Wehrli, E. Eugster, M. Schnell, D. Kessler, F.** (2000) The major protein import receptor of plastids is essential for chloroplast biogenesis. Nature **403:** 203-207

**Baumgartner BJ RJ, Mullet JE.** (1989) Plastid transcription activity and DNA copy number increase early in barley chloroplast development. Plant physiology **89:** 1011-1018

**Bédard J TR, Wu F, Ling Q, Flores-Pérez Ú, Töpel M, Nawaz F, Jarvis P.** (2017) Suppressors of the chloroplast protein import mutant tic40 reveal a genetic link between protein import and thylakoid biogenesis. The Plant Cell **29:** 1726-1747

**Bedard JJ, P.** (2005) Recognition and envelope translocation of chloroplast preproteins. Journal of Experimental Botany **56:** 2287-2320

**Bendich A** (1987) Why do chloroplasts and mitochondria contain so many copies of their genome? BioEssays **6:** 279-282

**Bendich A** (2013) DNA abandonment and the mechanisms of uniparental inheritance of mitochondria and chloroplasts. Chromosome Research. **21:** 287-296

**Bennett J RC** (1975) Plastid DNA replication and plastid division in the garden pea. FEBS letters **56:** 222-225

**Boffey SA EJ, Selldén G, Leech RM.** (1979) Chloroplast Division and DNA Synthesis in Light-grown Wheat Leaves. Plant Physiol **64:** 502-505

**Boffey SA LR** (1982) Chloroplast DNA levels and the control of chloroplast division in light-grown wheat leaves. Plant Physiology **69:** 1387-1391

**Boffey SA SG, Leech RM.** (1980) Influence of cell age on chlorophyll formation in light-grown and etiolated wheat seedlings. Plant Physiology **65:** 680-684

**Bolter BS, J.** (2016) Once upon a Time - Chloroplast Protein Import Research from Infancy to Future Challenges. Molecular Plant **9:** 798-812

**Börner T AA, Zubo YO, Kusnetsov VV.** (2015) Chloroplast RNA polymerases: Role in chloroplast biogenesis. Biochimica et Biophysica Acta (BBA)-Bioenergetics. **1847:** 761-769

**Bruce B** (2001) The paradox of plastid transit peptides: conservation of function despite divergence in primary structure. Biochimica et Biophysica Acta (BBA)-Molecular Cell Research. **1541:** 2-21

**Bryant N LJ, Sweeney C, Myouga F, Meinke D.** (2011) Identification of nuclear genes encoding chloroplast-localized proteins required for embryo development in Arabidopsis. Plant physiology **155:** 1678-1689

**Buchanan BB GW, Jones RL.** (2000) Biochemistry & molecular biology of plants. American Society of Plant Physiologists, Rockville, Md

**Chan KX, Phua SY, Crisp P, McQuinn R, Pogson BJ** (2016) Learning the languages of the chloroplast: retrograde signaling and beyond. Annual review of plant biology **67:** 25-53

**Charuvi DK, V. Nevo, R. Shimoni, E. Adam, Z. Reich, Z.** (2012) Gain and Loss of Photosynthetic Membranes during Plastid Differentiation in the Shoot Apex of Arabidopsis. Plant Cell **24:** 1143-1157

**Chen C MJ, Ducat DC, Osteryoung KW.** (2018) The molecular machinery of chloroplast division. Plant physiology **176:** 138-151

**Chen LJ LH** (2017) Stable megadalton TOC–TIC supercomplexes as major mediators of protein import into chloroplasts. The Plant Journal **92:** 178-188

**Chen Lj, Li Hm** (2017) Stable megadalton TOC–TIC supercomplexes as major mediators of protein import into chloroplasts. The Plant Journal **92:** 178-188

**Chen X SM, Fitzpatrick L, Schnell DJ.** (2002) In vivo analysis of the role of atTic20 in protein import into chloroplasts. Plant Cell **14:** 641-654

**Chiang YH ZY, Tapken W, Kim HJ, Lavanway AM, Howard L, Pilon M, Kieber JJ, Schaller GE.** (2012) Functional characterization of the GATA transcription factors GNC and CGA1 reveals their key role in chloroplast development, growth, and division in Arabidopsis. Plant physiology **160:** 332-348

**Chotewutmontri P BA** (2016) Dynamics of Chloroplast Translation during Chloroplast Differentiation in Maize. PLOS Genetics **12:** e1006106

**Colombo M TL, Peracchio C, Ferrari R, Pesaresi P.** (2016) GUN1, a jack-of-all-trades in chloroplast protein homeostasis and signaling. Frontiers in plant science **7:** 1427

**Cupp JD NB** (2013) Arabidopsis thaliana organellar DNA polymerase IB mutants exhibit reduced mtDNA levels with a decrease in mitochondrial area density. Physiologia plantarum **149:** 91-103

**Dahlin C, Cline K** (1991) Developmental regulation of the plastid protein import apparatus. The Plant Cell **3:** 1131-1140

**Dean C, Leech RM** (1982) Genome expression during normal leaf development: I. Cellular and chloroplast numbers and DNA, RNA, and protein levels in tissues of different ages within a seven-day-old wheat leaf. Plant Physiology **69:** 904-910

**Deng X-W, Matsui M, Wei N, Wagner D, Chu AM, Feldmann KA, Quail PH** (1992) COP1, an Arabidopsis regulatory gene, encodes a protein with both a zinc-binding motif and a Gβ homologous domain. Cell **71:** 791-801

**Driever SM, Simkin AJ, Alotaibi S, Fisk SJ, Madgwick PJ, Sparks CA, Jones HD, Lawson T, Parry MA, Raines CA** (2017) Increased SBPase activity improves photosynthesis and grain yield in wheat grown in greenhouse conditions. Phil. Trans. R. Soc. B **372:** 20160384

**Edwards K, Johnstone C, Thompson C** (1991) A simple and rapid method for the preparation of plant genomic DNA for PCR analysis. Nucleic acids research **19:** 1349

**Egea I, Barsan C, Bian W, Purgatto E, Latché A, Chervin C, Bouzayen M, Pech J-C** (2010) Chromoplast differentiation: current status and perspectives. Plant and Cell Physiology **51:** 1601-1611

**Ellis J, Leech R** (1985) Cell size and chloroplast size in relation to chloroplast replication in light-grown wheat leaves. Planta **165:** 120-125

**Emanuel C, Weihe A, Graner A, Hess WR, Borner T** (2004) Chloroplast development affects expression of phage-type RNA polymerases in barley leaves. The Plant Journal **38:** 460-472

**Enfissi EMA, Barneche F, Ahmed I, Lichtle C, Gerrish C, McQuinn RP, Giovannoni JJ, Lopez-Juez E, Bowler C, Bramley PM, Fraser PD** (2010) Integrative Transcript and Metabolite Analysis of Nutritionally Enhanced DE-ETIOLATED1 Downregulated Tomato Fruit. Plant Cell **22:** 1190-1215

**Evans JR, Loreto F** (2000) Acquisition and diffusion of CO 2 in higher plant leaves. *In* Photosynthesis. Springer, pp 321-351

**Fellerer C, Schweiger R, Schongruber K, Soll J, Schwenkert S** (2011) Cytosolic HSP90 cochaperones HOP and FKBP interact with freshly synthesized chloroplast preproteins of Arabidopsis. Mol Plant **4:** 1133-1145

**Fitter DW, Martin DJ, Copley MJ, Scotland RW, Langdale JA** (2002) GLK gene pairs regulate chloroplast development in diverse plant species. The Plant Journal **31:** 713-727

**Flores-Pérez Ú, Jarvis P** (2013) Molecular chaperone involvement in chloroplast protein import. Biochimica et Biophysica Acta (BBA)-Molecular Cell Research **1833:** 332-340

**Fraser PD, Bramley PM** (2004) The biosynthesis and nutritional uses of carotenoids. Progress in Lipid Research **43:** 228-265

**Fujiwara M, Nagashima A, Kanamaru K, Tanaka K, Takahashi H** (2000) Three new nuclear genes, sigD, sigE and sigF, encoding putative plastid RNA polymerase σ factors in Arabidopsis thaliana. FEBS letters **481:** 47-52

**Gao H, Sage TL, Osteryoung KW** (2006) FZL, an FZO-like protein in plants, is a determinant of thylakoid and chloroplast morphology. Proceedings of the National Academy of Sciences **103:** 6759-6764

**Garton S, Knight H, Warren GJ, Knight MR, Thorlby GJ** (2007) crinkled leaves 8–a mutation in the large subunit of ribonucleotide reductase–leads to defects in leaf development and chloroplast division in Arabidopsis thaliana. The Plant Journal **50:** 118-127

**Glynn JM, Froehlich JE, Osteryoung KW** (2008) Arabidopsis ARC6 coordinates the division machineries of the inner and outer chloroplast membranes through interaction with PDV2 in the intermembrane space. The Plant Cell **20:** 2460-2470

**Golczyk H, Greiner S, Wanner G, Weihe A, Bock R, Borner T, Herrmann RG** (2014) Chloroplast DNA in Mature and Senescing Leaves: A Reappraisal. Plant Cell **26:** 847-854

**Gutensohn M, Pahnke S, Kolukisaoglu U, Schulz B, Schierhorn A, Voigt A, Hust B, Rollwitz I, Stockel J, Geimer S, Albrecht V, Flugge UI, Klosgen RB** (2004) Characterization of a T-DNA insertion mutant for the protein import receptor atToc33 from chloroplasts. Mol Genet Genomics **272:** 379-396

**Hajdukiewicz PT, Allison LA, Maliga P** (1997) The two RNA polymerases encoded by the nuclear and the plastid compartments transcribe distinct groups of genes in tobacco plastids. The EMBO Journal **16:** 4041-4048

**Hall LN, Rossini L, Cribb L, Langdale JA** (1998) GOLDEN 2: a novel transcriptional regulator of cellular differentiation in the maize leaf. Plant Cell **10:** 925-936

**Hanaoka M, Kanamaru K, Takahashi H, Tanaka K** (2003) Molecular genetic analysis of chloroplast gene promoters dependent on SIG2, a nucleus-encoded sigma factor for the plastid-encoded RNA polymerase, in Arabidopsis thaliana. Nucleic acids research **31:** 7090-7098

**Haswell ES, Meyerowitz EM** (2006) MscS-like proteins control plastid size and shape in Arabidopsis thaliana. Current Biology **16:** 1-11

**He J** (2018) Role of the chromatin modifier *LYN1* gene in chloroplast development. PhD thesis. University of London.

**Heins L, Mehrle A, Hemmler R, Wagner R, Kuchler M, Hormann F, Sveshnikov D, Soll J** (2002) The preprotein conducting channel at the inner envelope membrane of plastids. Embo Journal **21:** 2616-2625

**Heldt H-W, Heldt F** (2005) Plant biochemistry, Ed An update and translation of the German third edition., Amsterdam ; Boston Elsevier Academic Press,

**Hess WR, Prombona A, Fieder B, Subramanian AR, Borner T** (1993) Chloroplast rps15 and the rpoB/C1/C2 gene cluster are strongly transcribed in ribosome-deficient plastids: evidence for a functioning non-chloroplast-encoded RNA polymerase. EMBO J **12:** 563-571

**Hibberd JM, Sheehy JE, Langdale JA** (2008) Using C4 photosynthesis to increase the yield of rice—rationale and feasibility. Current opinion in plant biology **11:** 228-231

**Hills AC, Khan S, Lopez-Juez E** (2015) Chloroplast Biogenesis-Associated Nuclear Genes: Control by Plastid Signals Evolved Prior to Their Regulation as Part of Photomorphogenesis. Frontiers in Plant Science **6**

**Hirabayashi Y, Kikuchi S, Oishi M, Nakai M** (2011) In Vivo Studies on the Roles of Two Closely Related Arabidopsis Tic20 Proteins, AtTic20-I and AtTic20-IV. Plant and Cell Physiology **52:** 469-478

**Hricová A, Quesada V, Micol JLJPp** (2006) The SCABRA3 nuclear gene encodes the plastid RpoTp RNA polymerase, which is required for chloroplast biogenesis and mesophyll cell proliferation in Arabidopsis. Plant physiology **141:** 942-956

**Hu Z, Xu F, Guan L, Qian P, Liu Y, Zhang H, Huang Y, Hou S** (2014) The tetratricopeptide repeat-containing protein slow green1 is required for chloroplast development in Arabidopsis. Journal of experimental botany **65:** 1111-1123

**Hudson D, Guevara D, Yaish MW, Hannam C, Long N, Clarke JD, Bi Y-M, Rothstein SJ** (2011) GNC and CGA1 modulate chlorophyll biosynthesis and glutamate synthase (GLU1/Fd-GOGAT) expression in Arabidopsis. PLoS One **6:** e26765

**Inaba T, Ito-Inaba Y** (2010) Versatile Roles of Plastids in Plant Growth and Development. Plant and Cell Physiology **51:** 1847-1853

**Inaba T, Li M, Alvarez-Huerta M, Kessler F, Schnell DJ** (2003) atTic110 functions as a scaffold for coordinating the stromal events of protein import into chloroplasts. Journal of Biological Chemistry**:** 38617-38627

**Inskeep WP, Bloom PR** (1985) Extinction coefficients of chlorophyll a and b in N, N-dimethylformamide and 80% acetone. Plant physiology **77:** 483-485

**Ishizaki Y, Tsunoyama Y, Hatano K, Ando K, Kato K, Shinmyo A, Kobori M, Takeba G, Nakahira Y, Shiina T** (2005) A nuclear-encoded sigma factor, Arabidopsis SIG6, recognizes sigma-70 type chloroplast promoters and regulates early chloroplast development in cotyledons. The Plant Journal **42:** 133-144

**Ivanova Y, Smith MD, Chen K, Schnell DJ** (2004) Members of the Toc159 import receptor family represent distinct pathways for protein targeting to plastids. Molecular Biology of the Cell **15:** 3379-3392

**Jarvis P** (2008) Targeting of nucleus-encoded proteins to chloroplasts in plants. New Phytologist **179:** 257-285

**Jarvis P, Chen LJ, Li HM, Pete CA, Fankhauser C, Chory J** (1998) An Arabidopsis mutant defective in the plastid general protein import apparatus. Science **282:** 100-103

**Jarvis P, Lopez-Juez E** (2013) Biogenesis and homeostasis of chloroplasts and other plastids. Nat Rev Mol Cell Biol **14:** 787-802

**Jarvis P, Robinson C** (2004) Mechanisms of protein import and routing in chloroplasts. Curr Biol **14:** R1064-1077

**Johnson CB, Tang LK, Smith AG, Ravichandran A, Luo Z, Vitha S, Holzenburg A** (2013) Single particle tracking analysis of the chloroplast division protein FtsZ anchoring to the inner envelope membrane. Microscopy and Microanalysis **19:** 507-512

**Kakizaki T, Inaba TJPs, behavior** (2010) New insights into the retrograde signaling pathway between the plastids and the nucleus. Plant signaling & behavior **5:** 196-199

**Kakizaki T, Matsumura H, Nakayama K, Che FS, Terauchi R, Inaba T** (2009) Coordination of Plastid Protein Import and Nuclear Gene Expression by Plastid-to-Nucleus Retrograde Signaling. Plant Physiology **151:** 1339-1353

**Karimi M, Depicker A, Hilson P** (2007) Recombinational cloning with plant gateway vectors. Plant Physiol **145:** 1144-1154

**Keegstra K, Cline K** (1999) Protein import and routing systems of chloroplasts. Plant Cell **11:** 557-570

**Kessler F, Schnell D** (2009) Chloroplast biogenesis: diversity and regulation of the protein import apparatus. Current Opinion in Cell Biology **21:** 494-500

**Kikuchi S, Bedard J, Hirano M, Hirabayashi Y, Oishi M, Imai M, Takase M, Ide T, Nakai M** (2013) Uncovering the protein translocon at the chloroplast inner envelope membrane. Science **339:** 571-574

**Kikuchi S, Oishi M, Hirabayashi Y, Lee DW, Hwang I, Nakai M** (2009) A 1-Megadalton Translocation Complex Containing Tic20 and Tic21 Mediates Chloroplast Protein Import at the Inner Envelope Membrane. Plant Cell **21:** 1781-1797

**Kindgren P, Kremnev D, Blanco NE, Lopez JDB, Fernandez AP, Tellgren-Roth C, Small I, Strand A** (2012) The plastid redox insensitive 2 mutant of Arabidopsis is impaired in PEP activity and high light-dependent plastid redox signalling to the nucleus. Plant Journal **70:** 279-291

**Kobayashi K, Baba S, Obayashi T, Sato M, Toyooka K, Keranen M, Aro EM, Fukaki H, Ohta H, Sugimoto K, Masuda T** (2012) Regulation of root greening by light and auxin/cytokinin signaling in Arabidopsis. Plant Cell **24:** 1081-1095

**Kohler D, Montandon C, Hause G, Majovsky P, Kessler F, Baginsky S, Agne B** (2015) Characterization of Chloroplast Protein Import without Tic56, a Component of the 1-Megadalton Translocon at the Inner Envelope Membrane of Chloroplasts. Plant Physiology **167:** 972-+

**Konieczny A, Ausubel FM** (1993) A procedure for mapping Arabidopsis mutations using co-dominant ecotype-specific PCR-based markers. The Plant Journal **4:** 403-410

**Kouranov A, Chen X, Fuks B, Schnell DJ** (1998) Tic20 and Tic22 are new components of the protein import apparatus at the chloroplast inner envelope membrane. J Cell Biol **143:** 991-1002

**Koussevitzky S, Nott A, Mockler TC, Hong F, Sachetto-Martins G, Surpin M, Lim IJ, Mittler R, Chory J** (2007) Signals from chloroplasts converge to regulate nuclear gene expression. Science **316:** 715-719

**Kruger NJ, von Schaewen A** (2003) The oxidative pentose phosphate pathway: structure and organisation. Current Opinion in Plant Biology **6:** 236-246

**Kubis S, Baldwin A, Patel R, Razzaq A, Dupree P, Lilley K, Kurth J, Leister D, Jarvis P** (2003) The Arabidopsis ppi1 mutant is specifically defective in the expression, chloroplast import, and accumulation of photosynthetic proteins. Plant Cell **15:** 1859-1871

**Kubis S, Patel R, Combe J, Bedard J, Kovacheva S, Lilley K, Biehl A, Leister D, Rios G, Koncz C, Jarvis P** (2004) Functional specialization amongst the Arabidopsis Toc159 family of chloroplast protein import receptors. Plant Cell **16:** 2059-2077

**Kumar RA, Oldenburg DJ, Bendich AJ** (2014) Changes in DNA damage, molecular integrity, and copy number for plastid DNA and mitochondrial DNA during maize development. Journal of Experimental Botany **65:** 6425-6439

**Kuroiwa T, Misumi O, Nishida K, Yagisawa F, Yoshida Y, Fujiwara T, Kuroiwa H** (2008) Vesicle, mitochondrial, and plastid division machineries with emphasis on dynamin and electron-dense rings. International review of cell and molecular biology **271:** 97-152

**Landoni M, De Francesco A, Bellatti S, Delledonne M, Ferrarini A, Venturini L, Pilu R, Bononi M, Tonelli C** (2013) A mutation in the FZL gene of Arabidopsis causing alteration in chloroplast morphology results in a lesion mimic phenotype. Journal of experimental botany **64:** 4313-4328

**Langdale JA, Lane B, Freeling M, Nelson T** (1989) Cell lineage analysis of maize bundle sheath and mesophyll cells. Developmental biology **133:** 128-139

**Langfelder P, Horvath S** (2008) WGCNA: an R package for weighted correlation network analysis. BMC bioinformatics **9:** 559

**Larkin RM, Alonso JM, Ecker JR, Chory J** (2003) GUN4, a regulator of chlorophyll synthesis and intracellular signaling. Science **299:** 902-906

**Larkin RM, Stefano G, Ruckle ME, Stavoe AK, Sinkler CA, Brandizzi F, Malmstrom CM, Osteryoung KW** (2016) REDUCED CHLOROPLAST COVERAGE genes from Arabidopsis thaliana help to establish the size of the chloroplast compartment. Proceedings of the National Academy of Sciences of the United States of America **113:** E1116-E1125

**Lee DW, Jung C, Hwang I** (2013) Cytosolic events involved in chloroplast protein targeting. Biochim Biophys Acta **1833:** 245-252

**Lendvai Á, Pettkó-Szandtner A, Csordás-Tóth É, Miskolczi P, Horváth GV, Györgyey J, Dudits D** (2007) Dicot and monocot plants differ in retinoblastoma-related protein subfamilies. Journal of experimental botany **58:** 1663-1675

**Li HM, Culligan K, Dixon RA, Chory J** (1995) Cue1 - a Mesophyll Cell-Specific Positive Regulator of Light-Controlled Gene-Expression in Arabidopsis. Plant Cell **7:** 1599-1610

**Li HM, Teng YS** (2013) Transit peptide design and plastid import regulation. Trends Plant Sci **18:** 360-366

**Li P, Ponnala L, Gandotra N, Wang L, Si Y, Tausta SL, Kebrom TH, Provart N, Patel R, Myers CR, Reidel EJ, Turgeon R, Liu P, Sun Q, Nelson T, Brutnell TP** (2010) The developmental dynamics of the maize leaf transcriptome. Nat Genet **42:** 1060-1067

**Li S, Tian Y, Wu K, Ye Y, Yu J, Zhang J, Liu Q, Hu M, Li H, Tong YJN** (2018) Modulating plant growth–metabolism coordination for sustainable agriculture. **560:** 595

**Liang QJ, Lu XD, Jiang L, Wang CY, Fan YL, Zhang CY** (2010) EMB1211 is required for normal embryo development and influences chloroplast biogenesis in Arabidopsis. Physiologia Plantarum **140:** 380-394

**Ling Q, Huang W, Baldwin A, Jarvis P** (2012) Chloroplast biogenesis is regulated by direct action of the ubiquitin-proteasome system. Science **338:** 655-659

**Ling QH, Jarvis P** (2015) Functions of plastid protein import and the ubiquitin-proteasome system in plastid development. Biochimica Et Biophysica Acta-Bioenergetics **1847:** 939-948

**Liu D, Li W, Cheng J** (2016) The novel protein DELAYED PALE-GREENING1 is required for early chloroplast biogenesis in Arabidopsis thaliana. Scientific reports **6:** 25742

**Long SP, Marshall-Colon A, Zhu X-G** (2015) Meeting the global food demand of the future by engineering crop photosynthesis and yield potential. Cell **161:** 56-66

**López-Juez E** (2006) Plastid biogenesis, between light and shadows. Journal of experimental botany **58:** 11-26

**López-Juez E, Bowyer JR, Sakai T** (2007) Distinct leaf developmental and gene expression responses to light quantity depend on blue-photoreceptor or plastid-derived signals, and can occur in the absence of phototropins. Planta **227:** 113-123

**López-Juez E, Dillon E, Magyar Z, Khan S, Hazeldine S, de Jager SM, Murray JA, Beemster GT, Bögre L, Shanahan H** (2008) Distinct light-initiated gene expression and cell cycle programs in the shoot apex and cotyledons of Arabidopsis. The Plant Cell **20:** 947-968

**López-Juez E, Hills A** (2011) Screening or Selection for Chloroplast Biogenesis Mutants of Arabidopsis, Following Chemical or Insertional Mutagenesis. *In* Chloroplast Research in Arabidopsis. Springer, pp 3-18

**Lopez-Juez E, Jarvis RP, Takeuchi A, Page AM, Chory J** (1998) New Arabidopsis cue mutants suggest a close connection between plastid- and phytochrome regulation of nuclear gene expression. Plant Physiol **118:** 803-815

**Lopez-Juez E, Pyke KA** (2005) Plastids unleashed: their development and their integration in plant development. Int J Dev Biol **49:** 557-577

**Lysenko E** (2006) Analysis of the evolution of the family of the Sig genes encoding plant sigma factors. Russian Journal of Plant Physiology **53:** 605-614

**Maffei D** (2008) Identification of Genes Affecting Plastid Biogenesis and Plastid nuclear Signalling. PhD thesis. University of London.

**Magyar Z, Horvath B, Khan S, Mohammed B, Henriques R, De Veylder L, Bakó L, Scheres B, Bögre L** (2012) Arabidopsis E2FA stimulates proliferation and endocycle separately through RBR-bound and RBR-free complexes. The EMBO journal **31:** 1480-1493

**Majeran W, Friso G, Ponnala L, Connolly B, Huang M, Reidel E, Zhang C, Asakura Y, Bhuiyan NH, Sun Q** (2010) Structural and metabolic transitions of C4 leaf development and differentiation defined by microscopy and quantitative proteomics in maize. The Plant Cell**:** 3509–3542

**Maple J, Fujiwara MT, Kitahata N, Lawson T, Baker NR, Yoshida S, Møller SG** (2004) GIANT CHLOROPLAST 1 is essential for correct plastid division in Arabidopsis. Current Biology **14:** 776-781

**Martin W, Rujan T, Richly E, Hansen A, Cornelsen S, Lins T, Leister D, Stoebe B, Hasegawa M, Penny D** (2002) Evolutionary analysis of Arabidopsis, cyanobacterial, and chloroplast genomes reveals plastid phylogeny and thousands of cyanobacterial genes in the nucleus. Proceedings of the National Academy of Sciences **99:** 12246-12251

**May T, Soll J** (2000) 14-3-3 proteins form a guidance complex with chloroplast precursor proteins in plants. Plant Cell **12:** 53-64

**Meinke D, Muralla R, Sweeney C, Dickerman A** (2008) Identifying essential genes in Arabidopsis thaliana. Trends in plant science **13:** 483-491

**Middleton CP, Senerchia N, Stein N, Akhunov ED, Keller B, Wicker T, Kilian B** (2014) Sequencing of chloroplast genomes from wheat, barley, rye and their relatives provides a detailed insight into the evolution of the Triticeae tribe. PLoS One **9:** e85761

**Miyagishima S-y, Froehlich JE, Osteryoung KW** (2006) PDV1 and PDV2 mediate recruitment of the dynamin-related protein ARC5 to the plastid division site. The Plant Cell **18:** 2517-2530

**Miyagishima S-y, Nakanishi H, Kabeya Y** (2011) Structure, regulation, and evolution of the plastid division machinery. *In* International review of cell and molecular biology, Vol 291. Elsevier, pp 115-153

**Miyamura S** (2010) Cytoplasmic inheritance in green algae: patterns, mechanisms and relation to sex type. Journal of plant research **123:** 171-184

**Mochizuki N, Brusslan JA, Larkin R, Nagatani A, Chory J** (2001) Arabidopsis genomes uncoupled 5 (GUN5) mutant reveals the involvement of Mg-chelatase H subunit in plastid-to-nucleus signal transduction. Proceedings of the National Academy of Sciences of the United States of America **98:** 2053-2058

**Mueller O, Lightfoot S, Schroeder A** (2004) RNA integrity number (RIN)–standardization of RNA quality control. Agilent application note, publication**:** 1-8

**Mullet JE** (1988) Chloroplast development and gene expression. Annual Review of Plant Physiology and Plant Molecular Biology **39:** 475-502

**Murashige T, Skoog F** (1962) A revised medium for rapid growth and bio assays with tobacco tissue cultures. Physiologia plantarum **15:** 473-497

**Nakamura H, Muramatsu M, Hakata M, Ueno O, Nagamura Y, Hirochika H, Takano M, Ichikawa H** (2009) Ectopic overexpression of the transcription factor OsGLK1 induces chloroplast development in non-green rice cells. Plant Cell Physiology **50:** 1933-1949

**Neff MM, Turk E, Kalishman M** (2002) Web-based primer design for single nucleotide polymorphism analysis. TRENDS in Genetics **18:** 613-615

**Nelissen H, Gonzalez N, Inze D** (2016) Leaf growth in dicots and monocots: so different yet so alike. Current opinion in plant biology **33:** 72-76

**Nelson T, Langdale JA** (1989) Patterns of leaf development in C4 plants. The Plant Cell **1:** 3

**Neuhaus H, Emes MJAropb** (2000) Nonphotosynthetic metabolism in plastids. Annual review of plant biology **51:** 111-140

**Nomura H, Komori T, Uemura S, Kanda Y, Shimotani K, Nakai K, Furuichi T, Takebayashi K, Sugimoto T, Sano S, Suwastika IN, Fukusaki E, Yoshioka H, Nakahira Y, Shiina T** (2012) Chloroplast-mediated activation of plant immune signalling in Arabidopsis. Nature Communications **3:** 926

**Ogihara Y, Isono K, Kojima T, Endo A, Hanaoka M, Shiina T, Terachi T, Utsugi S, Murata M, Mori N** (2002) Structural features of a wheat plastome as revealed by complete sequencing of chloroplast DNA. Molecular Genetics and Genomics **266:** 740-746

**Okazaki K, Kabeya Y, Suzuki K, Mori T, Ichikawa T, Matsui M, Nakanishi H, Miyagishima S-y** (2009) The PLASTID DIVISION1 and 2 components of the chloroplast division machinery determine the rate of chloroplast division in land plant cell differentiation. The plant cell **21:** 1769-1780

**Ort DR, Merchant SS, Alric J, Barkan A, Blankenship RE, Bock R, Croce R, Hanson MR, Hibberd JM, Long SP** (2015) Redesigning photosynthesis to sustainably meet global food and bioenergy demand. Proceedings of the national academy of sciences **112:** 8529-8536

**Osteryoung KW, Nunnari J** (2003) The division of endosymbiotic organelles. Science **302:** 1698-1704

**Osteryoung KW, Pyke KA** (2014) Division and dynamic morphology of plastids. Annual Review of Plant Biology **65:** 443-472

**Paila YD, Richardson LG, Schnell DJ** (2015) New insights into the mechanism of chloroplast protein import and its integration with protein quality control, organelle biogenesis and development. J Mol Biol **427:** 1038-1060

**Parent JS, Lepage E, Brisson N** (2011) Divergent roles for the two PolI-like organelle DNA polymerases of Arabidopsis. Plant Physiol **156:** 254-262

**Pesaresi P, Varotto C, Meurer J, Jahns P, Salamini F, Leister D** (2001) Knock-out of the plastid ribosomal protein L11 in Arabidopsis: effects on mRNA translation and photosynthesis. Plant J **27:** 179-189

**Pfalz J, Liere K, Kandlbinder A, Dietz KJ, Oelmuller R** (2006) pTAC2, -6, and -12 are components of the transcriptionally active plastid chromosome that are required for plastid gene expression. Plant Cell **18:** 176-197

**Pick TR, Bräutigam A, Schlüter U, Denton AK, Colmsee C, Scholz U, Fahnenstich H, Pieruschka R, Rascher U, Sonnewald U** (2011) Systems analysis of a maize leaf developmental gradient redefines the current C4 model and provides candidates for regulation. The Plant Cell **The Plant cell:** 4208-4220

**Pogson BJ, Ganguly D, Albrecht-Borth V** (2015) Insights into chloroplast biogenesis and development. Biochimica Et Biophysica Acta-Bioenergetics **1847:** 1017-1024

**Porra R, Thompson W, Kriedemann P** (1989) Determination of accurate extinction coefficients and simultaneous equations for assaying chlorophylls a and b extracted with four different solvents: verification of the concentration of chlorophyll standards by atomic absorption spectroscopy. Biochimica et Biophysica Acta (BBA)-Bioenergetics **975:** 384-394

**Pyke K** (2011) Analysis of plastid number, size, and distribution in Arabidopsis plants by light and fluorescence microscopy. *In* Chloroplast Research in Arabidopsis. Springer, pp 19-32

**Pyke KA, Leech RM** (1991) Rapid Image-Analysis Screening-Procedure for Identifying Chloroplast Number Mutants in Mesophyll-Cells of Arabidopsis-Thaliana (L) Heynh. Plant Physiology **96:** 1193-1195

**Pyke KA, Leech RM** (1992) Chloroplast division and expansion is radically altered by nuclear mutations in Arabidopsis thaliana. Plant physiology **99:** 1005-1008

**Pyke KA, Leech RM** (1994) A genetic analysis of chloroplast division and expansion in Arabidopsis thaliana. Plant Physiology **104:** 201-207

**Pyke KA, Rutherford SM, Robertson EJ, Leech RM** (1994) arc6, A Fertile Arabidopsis Mutant with Only Two Mesophyll Cell Chloroplasts. Plant Physiol **106:** 1169-1177

**Qi Y, Liu X, Liang S, Wang R, Li Y, Zhao J, Shao J, An L, Yu F** (2016) A putative chloroplast thylakoid metalloprotease VIRESCENT3 regulates chloroplast development in Arabidopsis thaliana. Journal of Biological Chemistry **291:** 3319-3332

**Raines CA** (2003) The Calvin cycle revisited. Photosynthesis Research **75:** 1-10

**Rashotte AM, Mason MG, Hutchison CE, Ferreira FJ, Schaller GE, Kieber JJ** (2006) A subset of Arabidopsis AP2 transcription factors mediates cytokinin responses in concert with a two-component pathway. Proceedings of the National Academy of Sciences **103:** 11081-11085

**Raynaud C, Perennes C, Reuzeau C, Catrice O, Brown S, Bergounioux C** (2005) Cell and plastid division are coordinated through the prereplication factor AtCDT1. Proceedings of the National Academy of Sciences **102:** 8216-8221

**Reyes-Prieto A, Moustafa A** (2012) Plastid-localized amino acid biosynthetic pathways of Plantae are predominantly composed of non-cyanobacterial enzymes. Scientific Reports **2:** 955

**Rolland N, Bouchnak I, Moyet L, Salvi D, Kuntz M** (2018) The Main Functions of Plastids. Methods Mol Biol **1829:** 73-85

**Rolland N, Curien G, Finazzi G, Kuntz M, Marechal E, Matringe M, Ravanel S, Seigneurin-Berny D** (2012) The Biosynthetic Capacities of the Plastids and Integration Between Cytoplasmic and Chloroplast Processes. Annual Review of Genetics, Vol 46 **46:** 233-264

**Rose R, Cran D, Possingham J** (1975) Changes in DNA synthesis during cell growth and chloroplast replication in greening spinach leaf disks. Journal of cell science **17:** 27-41

**Rudella A, Friso G, Alonso JM, Ecker JR, Van Wijk KJ** (2006) Downregulation of ClpR2 leads to reduced accumulation of the ClpPRS protease complex and defects in chloroplast biogenesis in Arabidopsis. The Plant Cell **18:** 1704-1721

**Sage RF, Zhu X-G** (2011) Exploiting the engine of C4 photosynthesis. **62:** 2989-3000

**Sage TL, Sage RF** (2009) The functional anatomy of rice leaves: implications for refixation of photorespiratory CO2 and efforts to engineer C4 photosynthesis into rice. Plant and Cell Physiology **50:** 756-772

**Sakamoto W, Miyagishima S-y, Jarvis P** (2008) Chloroplast biogenesis: control of plastid development, protein import, division and inheritance. The Arabidopsis book/American Society of Plant Biologists **6**

**Sato S, Nakamura Y, Kaneko T, Asamizu E, Tabata S** (1999) Complete structure of the chloroplast genome of Arabidopsis thaliana. DNA Res **6:** 283-290

**Schneeberger K, Ossowski S, Lanz C, Juul T, Petersen AH, Nielsen KL, Jørgensen J-E, Weigel D, Andersen SUJNm** (2009) SHOREmap: simultaneous mapping and mutation identification by deep sequencing. Nature methods **6:** 550

**Schneeberger K, Ossowski S, Lanz C, Juul T, Petersen AH, Nielsen KL, Jorgensen JE, Weigel D, Andersen SU** (2009) SHOREmap: simultaneous mapping and mutation identification by deep sequencing. Nature Methods **6:** 550-551

**Schnell DJ, Kessler F, Blobel G** (1994) Isolation of components of the chloroplast protein import machinery. Science **266:** 1007-1012

**Scofield S, Jones A, Murray JA** (2014) The plant cell cycle in context. Journal of experimental botany **65:** 2557-2562

**Shiina T, Tsunoyama Y, Nakahira Y, Khan MS** (2005) Plastid RNA polymerases, promoters, and transcription regulators in higher plants. Int Rev Cytol **244:** 1-68

**Shokolenko I, Venediktova N, Bochkareva A, Wilson GL, Alexeyev MF** (2009) Oxidative stress induces degradation of mitochondrial DNA. Nucleic acids research **37:** 2539-2548

**Simkin AJ, Lopez-Calcagno PE, Davey PA, Headland LR, Lawson T, Timm S, Bauwe H, Raines CA** (2017) Simultaneous stimulation of sedoheptulose 1, 7-bisphosphatase, fructose 1, 6-bisphophate aldolase and the photorespiratory glycine decarboxylase-H protein increases CO 2 assimilation, vegetative biomass and seed yield in Arabidopsis. Plant biotechnology journal **15:** 805-816

**Smith AM** (2010) Plant biology. Garland Science, New York, NY

**Soll J, Schleiff E** (2004) Protein import into chloroplasts. Nature Reviews Molecular Cell Biology **5:** 198–208

**South PF, Cavanagh AP, Lopez-Calcagno PE, Raines CA, Ort DR** (2018) Optimizing photorespiration for improved crop productivity. Journal of Integrative Plant Biology **60:** 1217-1230

**Stephenson PG, Fankhauser C, Terry MJ** (2009) PIF3 is a repressor of chloroplast development. Proceedings of the National Academy of Sciences **106:** 7654-7659

**Sun C-W, Huang Y-C, Chang H-Y** (2009) CIA2 coordinately up-regulates protein import and synthesis in leaf chloroplasts. Plant physiology **150:** 879-888

**Susek RE, Ausubel FM, Chory JJC** (1993) Signal transduction mutants of Arabidopsis uncouple nuclear CAB and RBCS gene expression from chloroplast development. Cell **74:** 787-799

**T. B** (2017) The discovery of plastid-to-nucleus retrograde signaling—a personal perspective. Protoplasma **254:** 1845-1855

**Tadini L, Pesaresi P, Kleine T, Rossi F, Guljamow A, Sommer F, Mühlhaus T, Schroda M, Masiero S, Pribil M** (2016) GUN1 controls accumulation of the plastid ribosomal protein S1 at the protein level and interacts with proteins involved in plastid protein homeostasis. Plant physiology**:** 1817-1830

**Teng Y-S, Su Y-s, Chen L-J, Lee YJ, Hwang I, Li H-m** (2006) Tic21 is an essential translocon component for protein translocation across the chloroplast inner envelope membrane. The Plant Cell **18:** 2247-2257

**Terry MJ, Smith AG** (2013) A model for tetrapyrrole synthesis as the primary mechanism for plastid-to-nucleus signaling during chloroplast biogenesis. Frontiers in Plant Science **4:** 1-14

**Tokumaru M, Adachi F, Toda M, Ito-Inaba Y, Yazu F, Hirosawa Y, Sakakibara Y, Suiko M, Kakizaki T, Inaba T** (2017) Ubiquitin-Proteasome Dependent Regulation of the GOLDEN2-LIKE 1 Transcription Factor in Response to Plastid Signals. Plant Physiol **173:** 524-535

**Vercruyssen L, Tognetti VB, Gonzalez N, Van Dingenen J, De Milde L, Bielach A, De Rycke R, Van Breusegem F, Inzé D** (2015) Growth regulating factor 5 stimulates Arabidopsis chloroplast division, photosynthesis, and leaf longevity. Plant physiology**:** pp. 114.256180

**Vinti G, Fourrier N, Bowyer JR, Lopez-Juez E** (2005) Arabidopsis cue mutants with defective plastids are impaired primarily in the photocontrol of expression of photosynthesis-associated nuclear genes. Plant Molecular Biology **57:** 343-357

**Vinti G, Hills A, Campbell S, Bowyer JR, Mochizuki N, Chory J, Lopez-Juez E** (2000) Interactions between hy1 and gun mutants of Arabidopsis, and their implications for plastid/nuclear signalling. Plant Journal **24:** 883-894

**Waegemann K, Eichacker S, Soll J** (1992) Outer envelope membranes from chloroplasts are isolated as right-side-out vesicles. Planta **187:** 89-94

**Wang L, Czedik-Eysenberg A, Mertz RA, Si Y, Tohge T, Nunes-Nesi A, Arrivault S, Dedow LK, Bryant DW, Zhou W** (2014) Comparative analyses of C 4 and C 3 photosynthesis in developing leaves of maize and rice. Nature biotechnology **32:** 1158-1165

**Wang L, Czedik-Eysenberg A, Mertz RA, Si Y, Tohge T, Nunes-Nesi A, Arrivault S, Dedow LK, Bryant DW, Zhou WJNb** (2014) Comparative analyses of C 4 and C 3 photosynthesis in developing leaves of maize and rice. Nature biotechnology **32:** 1158

**Wang P, Fouracre J, Kelly S, Karki S, Gowik U, Aubry S, Shaw MK, Westhoff P, Slamet-Loedin IH, Quick WP** (2013) Evolution of GOLDEN2-LIKE gene function in C 3 and C 4 plants. Planta **237:** 481-495

**Wang P, Khoshravesh R, Karki S, Tapia R, Balahadia CP, Bandyopadhyay A, Quick WP, Furbank R, Sage TL, Langdale JA** (2017) Re-creation of a key step in the evolutionary switch from C3 to C4 leaf anatomy. Current Biology **27:** 3278-3287

**Waters MT, Moylan EC, Langdale JA** (2008) GLK transcription factors regulate chloroplast development in a cell-autonomous manner. The Plant Journal **56:** 432-444

**Waters MT, Wang P, Korkaric M, Capper RG, Saunders NJ, Langdale JA** (2009) GLK transcription factors coordinate expression of the photosynthetic apparatus in Arabidopsis. The Plant Cell **21:** 1109-1128

**Wilson Z** (2000) Arabidopsis: a practical approach, Vol 223. OUP Oxford

**Woodson JD, Chory J** (2008) Coordination of gene expression between organellar and nuclear genomes. Nat Rev Genet **9:** 383-395

**Woodson JD, Chory J** (2012) Organelle Signaling: How Stressed Chloroplasts Communicate with the Nucleus. Current Biology **22:** 690-692

**Woodson JD, Perez-Ruiz JM, Chory J** (2011) Heme Synthesis by Plastid Ferrochelatase I Regulates Nuclear Gene Expression in Plants. Current Biology **21:** 897-903

**Woodson JD, Perez-Ruiz JM, Schmitz RJ, Ecker JR, Chory J** (2013) Sigma factor-mediated plastid retrograde signals control nuclear gene expression. Plant Journal **73:** 1-13

**Yang Y, Sage TL, Liu Y, Ahmad TR, Marshall WF, Shiu S-H, Froehlich JE, Imre KM, Osteryoung KW** (2011) CLUMPED CHLOROPLASTS 1 is required for plastid separation in Arabidopsis. Proceedings of the National Academy of Sciences**:** 18530–18535

**Yoshida Y, Miyagishima SY, Kuroiwa H, Kuroiwa T** (2012) The plastid-dividing machinery: formation, constriction and fission. Curr Opin Plant Biol **15:** 714-721

**Zhang M, Chen C, Froehlich JE, TerBush AD, Osteryoung KW** (2016) Roles of Arabidopsis PARC6 in coordination of the chloroplast division complex and negative regulation of FtsZ assembly. Plant physiology **170:** 250-262

**Zhang XP, Glaser E** (2002) Interaction of plant mitochondrial and chloroplast signal peptides with the Hsp70 molecular chaperone. Trends Plant Sci **7:** 14-21

**Zhelyazkova P, Sharma CM, Forstner KU, Liere K, Vogel J, Borner T** (2012) The Primary Transcriptome of Barley Chloroplasts: Numerous Noncoding RNAs and the Dominating Role of the Plastid-Encoded RNA Polymerase. Plant Cell **24:** 123-136

# Appendix

**Primers used for chloroplast genome copy number in Arabidopsis**

| Gene | Locus | Forward / Reverse | Primer sequence |
|---|---|---|---|
| HO1 | AT2G26670 | AtHO1-F | CCCCAACTCTCAAGATTCCA |
| | | AtHO1-R | CCGCAACCACCACTAAAGAC |
| CHS | AT5G13930 | AtCHS-F | TGAGATCAGACAGGCTCAGAGA |
| | | AtCHS-R | ACTGTTGGTGATGCGGAAGT |
| *rbcL* | ATCG00490 | AtrbcL-F | TTCGGTGGAGGAACTTTAGG |
| | | AtrbcL-R | GCAAGATCACGTCCCTCATT |
| *ndhG* | ATCG01080 | AtndhG-F | GGGAATGGGATTACTTCGTTGG |
| | | AtndhG-R | ACCCCGTACCATGACGTATC |
| *ycf2* | ATCG00860 | AtYcf2-F | TGGAAAAGGCCCGTCTCAAT |
| | | AtYcf2-R | CCACCGCACGAAGAAAATGT |

**Primers used for genotyping various T-DNA insertion mutants or transformants**

| Gene / vector | Locus | Forward / Reverse | Sequence |
|---|---|---|---|
| TOC120 | AT3G16620 | toc120-2_F | CAAAAGTGGAGCAGCACGAC |
| | | toc120-2_R | AACCAGGTTAGATTCTCGCCA |
| | | FISH1-2 | CTGGGAATGGCGAAATCAAGG |
| | | | |
| | T-DNA | p35S_F | AGATGCCTCTACCGACAGTG |
| GLK1ox | AT2G20570 | GLK1OX_R | GTCACCGTCATAAGTCACCGT |
| GLK2ox | AT5G44190 | GLK2OX_R | ACACCAACGTCTCTCTCCGA |
| | | | |
| | T-DNA | pSKI015_F | GTGGCGAGAAAGGAAGGGAA |
| GUN6-1D (FC1) | AT5G26030 | gun6D_gD_F | ACTGTTTACGTGGCACCAAC |
| | | gun6D_gD_R | TAGGCACGGGTCCAGGTAAT |
| | | | |
| pB2GW7 (DESTINATION) | - | 35S_P_F | ACGCACAATCCCACTATCCT |
| | | 35S_T_R | CAACACATGAGCGAAACCCT |

**Primers used for gene expression quantitation (RT-qPCR) of nucleus-encoded genes**

| Gene | Locus | Forward / Reverse | Primer sequence |
|---|---|---|---|
| UBQ10 | AT4G05320 | UBQ10-F | GGAGGATGGTCGTACTTTGG |
| | | UBQ10-R | TCCACTTCAAGGGTGATGGT |
| LHCB1.2 | AT1G29910 | LHCB1-F | CCGATCCAGTCAACAACAAC |
| | | LHCB1-R | TCAAACCATCACATACAACCTTC |
| RPOTp | AT2G24120 | RPOTp -F | CTTGGTGATTGTGCAAAGATAATT |
| | | RPOTp -R | GGGAGGAAATGCAGTTCTTTGTT |
| RPOTm | AT1G68990 | RPOTm-F | GGAGCCAGTATATGAGGCTTA |
| | | RPOTm-R | CTCTTCTGGAATGGGTACATCTT |
| RPOTmp | AT5G15700 | RPOTmp-F | CATATGATGATGACTGCGGTTG |
| | | RPOTmp-R | TATCCACATCACACGCATGC |
| SIG1 | AT1G64860 | SIG1-F | AACTAAAACACGCAGCGAGGA |
| | | SIG1-R | TCTTAAGGATCATTGCCTCCATTT |
| SIG2 | AT1G08540 | SIG2-F | TTGGACAAAGTGTTGGACTCGT |
| | | SIG2-R | CTTCATTCTCCCATCCTCCATC |
| SIG3 | AT3553920 | SIG3-F | CCCACATACCCTGCCTGAA |
| | | SIG3-R | TGTAGAGATGAACTGGTGAAAAGCA |
| SIG4 | AT5G13730 | SIG4-F | CGGGGACCAGATGAAACAA |
| | | SIG4-R | GCCCAAAGTAAAGTCCCAATACAC |
| SIG5 | AT5G24120 | SIG5-F | TGGAGCTAATAACAGCAGACAGC |
| | | SIG5-R | TCGGCTTCAATGAATCGAGCAC |
| SIG6 | AT2G36990 | SIG6-F | CTTATTGCAGGAAGGAAGCATGGG |
| | | SIG6-R | TCTGCATCCGGATTGCGGTTTG |
| TIC56 | AT5G01590 | TIC56-F | AGGAGTGTCATGAGGCTATTCCG |
| | | TIC56-R | AGCTTCTGGCCTACTCGAACAC |
| TOC159 | AT4G02510 | TOC159-F | AGAGGCGATTTAGCCCTTGGAG |
| | | TOC159-R | CCTGCACGAAGCGCAATCTTTG |

| | | | |
|---|---|---|---|
| POL IA | AT1G50840 | POL IA-F | TTCCGGCGTCAAAGTCACGTGC |
| | | POL IA-R | TGCACTTCCCTGGACTGGAGTGT |
| POL IB | AT3G20540 | POL IB-F | CCTGAATACCGTTCACGTGCCCA |
| | | POL IB-R | AGCCGCACTTCCCTGAACAGGA |
| TIC20 | AT1G04940 | TIC20_F | CGTTTGTCTGTGATGCTGCC |
| | | TIC20_R | GAGGAGTCATAACGATCCAATGT |
| TIC100 | AT5G22640 | TIC100_F | GAGATGATACAGCAAGAACT |
| | | TIC100_R | AATTCTTCATCCATATCTTC |
| GLK1 | AT2G20570 | GLK1_F | TTGGGTCTCCGATTCTCCCTAT |
| | | GLK1_R | GCAACTGGCGGTGCTCTAAAT |
| GLK2 | AT5G44190 | GLK2_F | ACCGTACTGGCATCAGCAAC |
| | | GLK2_R | TGAATGTCGATGGGAGGATT |

**Primers used for gene expression quantitation (RT-qPCR) of chloroplast-encoded genes**

| *Gene* | Locus | Forward / Reverse | Primer sequence |
|---|---|---|---|
| *psaA* | ATCG00350 | psaA-F | GCCAAGAAATCCTGAATGGA |
| | | psaA-R | CATCTTGGAACCAAGCCAAT |
| *psbA* | ATCG00020 | psbA-F | GAGCAGCAATGAATGCGATA |
| | | psbA-R | CCTATGGGGTCGCTTCTGTA |
| *rbcL* | ATCG00490 | rbcL-F | AGGAACTTTAGGCCACCCTTGG |
| | | rbcL-R | TGCTTCCAGAGCTACTCGGTTG |
| *ndhA* | ATCG01100 | ndhA-F | GGATGGAATTTGTGGCGTCAACC |
| | | ndhA-R | ACGGTAACCTCTCGCATTCTGC |
| *clpP* | ATCG00670 | clpP-F | GTCGGAGGAGCAATTACCAA |
| | | clpP-R | GTGATGGTTTCGCGAAGTTT |
| *ndhH* | ATCG01110 | ndhH-F | ATGGGAAATTCAATGGCAAA |
| | | ndhH-R | TCAAAGCCCCTGCTTTCTAA |
| *accD* | ATCG00500 | accD-F | TGTGGATTCAATGCGACAAT |
| | | accD-R | TTTTGCGCAGAGTCAATACG |
| *rpoA* | ATCG00740 | rpoA-F | GCGATGCGAAGAGCTTTACT |
| | | rpoA-R | CCAGGACCTTGGACACAAAT |
| *rpoC1* | ATCG00180 | rpoC1-F | CTCGGTGATTGTCGTTGGACCTTC |
| | | rpoC1-R | ATTTCGCGAGGCAATCCACAGC |
| *rpS18* | ATCG00650 | rpS18-F | CAAGCGATCTTTTCGTAGGC |
| | | rpS18-R | AAAGTCACTCTATTCACCCGTCT |
| *tic214* | ATCG01130 | TIC214-F | AGAATCGGCCGGTCAAGTAGAAC |
| | | TIC214-R | AATCGAGCTGCTTCGGGATTTC |

**Primers used for genotyping point mutations by dCAPS**

| Primer name | Sequence | Enzyme digestion | Result (band size) |
|---|---|---|---|
| cue8-dCaps2-F<br>cue8-dCaps2-R | ACATCTTAATGGTAACGCAGGGTAGATTCTACCT<br>TCCGCCAAACCAGAATGCAGCTG | *DdeI*<br>(*cue8*) | *CUE8* (197bp)<br>*cue8* (164bp) |
| lyn1-dCaps2-F<br>lyn1-dCaps2-R | GCAGAAGCGTGTGCAGATGG<br>ATCCCCTTCTAGAGCTCTGACCAGTGG | *HaeIII*<br>(*LYN1*) | *LYN1* (256bp)<br>*lyn1* (285bp) |
| gun1-dCaps2-F<br>gun1-dCaps2-R | TAACTATTGCTAAGAGGATTTTCGAAACAG<br>CACTTCTCCCATAAGCGCTGA | *AluI*<br>(*GUN1*) | *GUN1* (69bp)<br>*gun1* (99bp) |

**List of vector constructs and antibiotic selection used in the cloning**

| Vector construct | Transformation organism | Antibiotic | Stock | Final concentration (selection) |
|---|---|---|---|---|
| pDONR201™<br>(ENTRY) | *Escherichia coli* | Kanamycin | 50 mg/ml | 50 µg/ml |
| pB2GW7<br>(DESTINATION) | *Escherichia coli* | Spectinomycin | 10 mg/ml | 100 µg/ml |
| pB2GW7<br>(DESTINATION) | *Agrobacterium tumefaciens* | Spectinomycin<br>+<br>Gentamycin | 10 mg/ml<br><br>25 mg/ml | 100 µg/ml<br><br>50 µg/ml |
| p2GW7-HA<br>(DESTINATION) | *Escherichia coli* | Ampicillin<br>(or)<br>Carbenicillin | 100 mg/ml | 100 µg/ml |
| - | Arabidopsis<br>(T1 seeds) | Phosphinothricin<br>+<br>Cefotaxime | 10 mg/ml<br><br>100 mg/ml | 5 - 10 µg/ml<br><br>100 µg/ml |

**Primers used for chloroplast genome copy number in wheat**

| Region | Forward / Reverse | Primer sequence |
|---|---|---|
| Nucleus | Ta_KO1_F | TGCTACATGTGACTATGGTGAC |
| | Ta_KO1_R | AGCAGAAGAACCCAACAAACC |
| | Ta_KS_F | CAAGGAGCTGTTCTGGAAGA |
| | Ta_KS_R | TCGTTGATAACAGCATTCACCG |
| Chloroplast (Large single copy) | Ta_rbcL_F | AGCAGGTGTTGGATTTAAAGCTG |
| | Ta_rbcL_R | ACTCGGAATGCTGCCAAGAT |
| Chloroplast (Small single copy) | Ta_ndhD_F | GTTCTCGTGGTCCAGAATCCA |
| | Ta_ndhD_R | TGTTACGCCAGATGTTCTATGGA |
| Chloroplast (Inverted repeat) | Ta_rps7_F | TCTGCCATTCTATGAGTCGCT |
| | Ta_rps7_R | TCCGAATTAGTAGATGCTGCCA |

**Primers used for the reverse transcription (RT), and RT qPCR of 18S rRNA and 16S rRNA in wheat**

| Region | Oligo Name | Function | Sequence |
|---|---|---|---|
| 18S rRNA and 16S rRNA | Ta_rRNA_RT_F | RT | ACCTTGTTACGACTTC |
| 18S rRNA | Ta_18SrRNA _F | qPCR | TGAAAGACGAACAACTGCGAAAG |
| | Ta_18SrRNA _R | qPCR | TGGTTGAGACTAGGACGGTATCT |
| 16S rRNA | Ta_16SrRNA _F | qPCR | CATCGGCTAACTCTGTGCCA |
| | Ta_16SrRNA _R | qPCR | GGTTGAGCCCTGGGATTTGA |

**Antibody dilution used in the immunoblotting**

| Antibody | Dilution |
|---|---|
| TIC214 | 1:5,000 |
| TIC110 | 1:5,000 |
| TIC100 | 1:5,000 |
| TIC56 | 1:5,000 |
| TIC40 | 1:1,000,000 |
| TOC75 | 1:1,000 |
| HSP70 | 1:2,000 |
| RPL2 | 1:2,000 |
| Rice RBR | 1:1,000 |
| RBR-P | 1:500 |

**List of R package codes used for the box plots**

| |
|---|
| #Grey<br>• colour<-colorRampPalette(c("white", "light grey", "dark grey")) |
| • colour(15) |
| • boxplot(Cell_area$Cell_area~Cell_area$Sample, outline=FALSE, col=colour(15), names=c("1", "2", "3", "4", "5", "6", "7", "8", "9", "10", "11", "12", "13", "14", "15"), las=1, boxwex=0.5, cex.axis=1.1) |
| # Colour<br>• colour<-colorRampPalette(c("white", "yellow", "dark green"))<br>• colour(15) |
| • boxplot(Chloroplast_count$Chloroplast_count~Chloroplast_count$Sample, outline=FALSE, col=colour(15), names=c("1", "2", "3", "4", "5", "6", "7", "8", "9", "10", "11", "12", "13", "14", "15"), las=1, boxwex=0.5, cex.axis=1.1) |
| • boxplot(Mean_chloroplastarea$Mean_chloroplast_area~Mean_chloroplastarea$Sample, outline=FALSE, col=colour(15), names=c("1", "2", "3", "4", "5", "6", "7", "8", "9", "10", "11", "12", "13", "14", "15"), las=1, boxwex=0.5, cex.axis=1.1) |
| • boxplot(Total_chloroplastarea$Total_chloroplast_area~Total_chloroplastarea$Sample, outline=FALSE, col=colour(15), names=c("1", "2", "3", "4", "5", "6", "7", "8", "9", "10", "11", "12", "13", "14", "15"), las=1, boxwex=0.5, cex.axis=1.1) |
| • boxplot(Chloroplast_compartment$Chloroplast_compartment~Chloroplast_compartment$Sample, outline=FALSE, col=colour(15), names=c("1", "2", "3", "4", "5", "6", "7", "8", "9", "10", "11", "12", "13", "14", "15"), las=1, boxwex=0.5, cex.axis=1.1, ylim=c(0,200)) |